CRANFIELD INSTITUTE OF TECHNOLOGY

COLLEGE OF AERONAUTICS

AERODYNAMICS DIVISION

Ph.D. THESIS

Gareth D. Padfield

The Application of Perturbation Methods to Nonlinear Problems in Flight Mechanics

Supervisor: P.A.T. Christopher

September 1976

SUMMARY

Analytical techniques are developed for deriving approximate solutions to a class of problems that arise in nonlinear flight mechanics typically when an aeroplane is flying close to a stability boundary. The techniques are based on perturbation methods and the method of multiple scales is used to correct for nonuniformities otherwise present in the asymptotic expansions. Applications are mainly concerned with the lateral dynamics of slender aircraft flying at high incidence. Approximations are derived for both linear and nonlinear lateral motions that serve to illustrate the importance of particular parameters in the problem. For the linear theory the approximations are achieved by reducing the fourth order system to two weakly coupled second order systems. The nonlinear theory is mainly concerned with the effect of aerodynamic nonlinearity on the lateral oscillation when the latter has marginal stability or instability, as predicted by the linear theory.

The analytic approximations are extended for use in the problem of estimating damping moments on aircraft in oscillatory motion. For this purpose approximations are constructed for the logarithmic decrement of a nonlinear oscillation that can be used to fit experimental measurements. Some thought is given to the issue of memory effects in the representation of aerodynamic forces and moments.

CONTENTS

TABLES

FIGURES

NOTATION

CHAPTER 2

$A(\nu)$ - system matrix (2.1).

A_{ij} - submatrices (2.54).

$A_0(\tau)$ - amplitude for strongly nonlinear oscillations.

B_{11}, B_{22} - non-critical and critical subsystem matrices (2.73).

C - transformation matrix (2.102).

$K(\mu), E(\mu)$ - elliptic integrals of first and second kind.

R_0 - Routhian (2.110).

R_2 - nonlinear coefficient in bifurcation approximation (2.110).

T_η - period in

$\underset{\sim}{U}$ - matrix of eigenvectors of companion matrix (2.101).

$\underset{\sim}{Y}_{1c}(\eta)$ - principal matrix solution (2.89).

a_0 - amplitude (2.6).

a_{0L} - limit cycle amplitude (2.31).

$a_{1c}(\tau), b_{1s}(\tau)$ - $\cos\eta$ and $\sin\eta$ components of $z_{1c}(\eta,\tau)$ (2.66).

$a_{20}(\eta)$ - $\cos\eta$ component of $z_{2c}(\eta,\tau)$ (2.65).

a_1, b_1, c_1, d_1 - linear coefficients in nonlinear companion problem (2.95).

b_3, c_3, d_3 - nonlinear coefficients in nonlinear companion problem (2.95).

c_1, c_3 - also stiffness parameters (2.3).

$\underset{\sim}{g}(\underset{\sim}{x}, \nu; \varepsilon)$ - nonlinear vector function (2.1).

$\underset{\sim}{g}_1, \underset{\sim}{g}_2$ - components of $\underset{\sim}{g}(\underset{\sim}{x})$ (2.54).

h_0, h_2 - damping parameters (2.3).

$h(y, \dot{y}, \varepsilon)$ - damping function (2.34).

$\underset{\sim}{h}_1, \underset{\sim}{h}_2$	–	non-critical and critical nonlinear vector functions (2.73).
h_{ij}	–	scalar coefficients in expansion of $\underset{\sim}{h}_1, \underset{\sim}{h}_2$
$p(A_0), q_1(A_0)$	–	amplitude functions (2.42).
p_i, q_i	–	scalar coefficients in (2.106).
$r_c(A_c)$	–	amplitude function for strongly nonlinear equation (2.51).
t	–	time.
$V(x,y)$	–	function arising in decomposition of $Z(t)$ (2.77).
V_i	–	i th order form in expansion of $V(x,y)$ (2.80).
$X(t)$	–	state vector (2.1).
$\underset{\sim}{X}_1, \underset{\sim}{X}_2$	–	partitioned state vectors (2.54).
$\underset{\sim}{X}_F$	–	periodic vector function.
x, y, z	–	scalar functions in (2.76).
$y(t)$	–	dependant variable in (2.3).
y_i	–	i th order approximation to $y(t)$ (2.4).
$y_1(t), y_2(t)$	–	non-critical and critical state vectors (2.73).
$z(\eta,\tau;\varepsilon)$	–	equivalent to $y(t;\varepsilon)$
z_{1i}, z_{2i}	–	i th order approximations in (2.63).
$\Phi(A_0)$	–	approximate amplitude function (2.35).
$\Psi(A_0)$	–	approximate frequency function (2.36).
α_i, β_i	–	coefficients in coupled equations (2.57), (2.58).
$\bar{\alpha}(x_1), \bar{\beta}(x_1)$	–	nonlinear functions in (2.60), (2.61).
γ	–	$\frac{\varepsilon_3}{\varepsilon_1} A_0^2$
ε	–	small parameter (dummy).
η	–	fast time scale (2.8).
θ	–	amplitude (2.119).

λ - $\frac{c_1}{c_3}\frac{h_2}{4h_4}$

λ_1, λ_2 - non-critical eigenvalues of B_{11}

μ - damping.

μ_e - modulus of Jacobian elliptic functions (2.46).

ν - a parameter in , ν_f - critical value of ν , (2.1).

ξ - function in decomposition of $z(t)$ (2.77).

τ - εt , slow time scale.

ω_c - basic frequency (2.6).

ω_1 - frequency correction (2.9).

CHAPTERS 3, 4 and APPENDIX A.

(NOTE: in Appendix A a bar above a quantity denotes that it has been normalized, although in the main text the bars are omitted for clarity).

C_{ij} - submatrices (3.6).

C_L - lift coefficient.

$C_{y\beta}$, C_{e_β} etc. - aerodynamic derivatives (normalized) in American notation.

I_{xx}, I_{yy}, I_{zz} - moments of inertia about body X, Y, Z axes respectively.

I_{xz} - product of inertia about X , Z. axes.

L, N - Rolling and Yawing moments about X, Z. axes.

R_{V_0}, I_{V_0} - real and imaginary parts of (V_0/V) ratio for oscillatory mode (3.20).

R_2 - denominator of limit cycle function.

S - wing area.

V_R - flight reference speed.

Y - sideforce.

$q_0(\tau)$ - amplitude of zeroth order solution (4.8).

a_1, b_1, c_1, d_1 – linear coefficients in 4th order sideslip equation (4.18).

b_3, c_3, d_3 – nonlinear coefficients in 4th order sideslip equation (4.18).

$\bar{c}$ – mean chord.

e_x, e_y, e_z – normalized product of inertia parameters (4.63-4.65).

g – gravitational constant.

g_1 – normalized gravitational constant (Appendix A).

g_y, g_z – components of gravitational force along Y and Z axes.

i_{xx}, i_{yy}, i_{zz} – normalized values of I_{xx}, I_{yy}, I_{zz}.

i_{Ac} – normalized moment of inertia about principal X axis of inertia (3.15).

$\ell_v, \ell_p, \ell_r, \ell_{\dot{v}}$ – normalized rolling moment derivatives.

ℓ_{vc}, ℓ_{v_2} – rolling moment coefficients (4.3).

m – vehicle mass.

m_d, m_q – normalized pitching moment derivatives.

$n_v, n_p, n_r, n_{\dot{v}}$ – normalized yawing moment derivatives.

n_{vc}, n_{v_2} – yawing moment coefficients (4.2).

p – roll rate about X axis.

q – pitch rate about Y axis.

r – yaw rate about Z axis.

s – wing semi-span.

V – sideslip velocity.

V_c – sideways velocity (3.2).

V_L – limit cycle sideslip velocity.

V_i – sideslip velocity about displaced axis.

W – heave velocity along Z axis.

y_v, y_p, y_r – normalized sideforce derivatives.

z_0 – distance along z axis.

z_α – normalized heave force derivative.

Δ – $a_{1c}(b_{1c}^2 + c_{1c}a_{1c} - 4d_{1c})$

α, α' – incidence angles.

α_i, β_i – coefficients in sideways/sideslip equations (3.3).

$\alpha_3(v), \beta_3(v)$ – nonlinear functions of v (4.4, 4.5).

β – sideslip angle.

γ_2 – ρ_{v2}/n_{v2}

θ_0 – angle between x axis and flight velocity vector (incidence for straight and level flight).

λ – an eigenvalue.

λ_1, λ_2 – non-critical eigenvalues (4.21).

μ^* – approximate damping (3.17).

μ_2 – relative density.

ρ – air density.

σ_L – limit cycle function $(\frac{3}{4} n_{v2} v_L^2)$

ϕ – roll angle.

ω – a frequency.

ω^* – approximate frequency.

ω_0 – linear frequency.

ω_L – limit cycle frequency.

CHAPTER 5

$A_0(T)$ – amplitude

$C_{\ell}(H), C_k(H)$ – aerodynamic moments.

$C_{kq\beta}, C_{k\dot{\alpha}}$
$C_{kr\beta}, C_{k\dot{\beta}}$ – coefficients functions in the representation of aerodynamic moments (5.103).

$F(A^2), K(A^2)$ - amplitude functions (5.45, 5.46).

$F(A_0)$ - integral of $C(x)$

$H(\nu)$ - frequency response function.

$H_e(\nu), H_i(\nu)$ - in phase and quadrature components of $H(\nu)$

L, N - rolling and yawing moments about model axes.

L' - rolling moment about sting axis.

L_v, L_p, L_r - rolling derivatives about model fixed axes.

N_v, N_p, N_r - yawing derivatives about model fixed axes.

T_2 - period in 2

V_R - resultant velocity.

Y - sideforce on model.

Y_v, Y_p, Y_r - model sideforce derivatives.

C_1, C_3 - stiffness parameters (5.51).

$C(\phi'), C(y)$ - stiffness functions (5.13, 5.14).

$f(y)$ - damping function (5.41).

h, k - distance to model c.g. from point on sting axis.

$h(t)$ - impulse response function (5.90).

h_0, h_2, h_4 - damping coefficients.

$h(y, \dot{y}; \varepsilon)$ - damping function (5.14).

ℓ - representative length (5.103).

p - roll rate of model, about model axis.

$p(A_0), q(A_0)$ - amplitude functions (5.16, 5.17).

$p_0^{(i)}, q_0^{(i)}$ - amplitude functions in elliptic function approximations.

r - yaw rate of model, about model axis.

u, v, w - model velocities.

$V(H)$ - motion variable (5.90).

$y(t)$ - amplitude response (5.14).

y_n, y_{n+1} - adjacent max. or min. points on oscillation.

y_m^2 - $(y_{n+1}^2 + y_n^2)/2$

$z_0(\gamma,\tau)$ - zeroth order solution.

Δ - $h\sin\delta - R\cos\delta$

$\psi_0^{(1)}$ - approximate logarithmic decrement functions.

α - incidence of model.

$\hat{\alpha}, \hat{\beta}$ - incidence and sideslip angles (5.103).

γ - $(c_3/c_1)\, y_m^2$

δ - $\alpha - \theta$

δ_m - $|y_{n+1}/y_n|$

ε - a small parameter.

θ - incidence of sting.

η - fast time scale.

$\Delta\eta$ - interval in η between max. or min. points.

λ - $\frac{h_2}{4h_0}\left|\frac{c_1}{c_3}\right|$

σ_m - logarithmic decrement approximation (5.34).

τ - slow time scale.

$\Delta\tau$ - interval in τ

ϕ - roll angle of model.

ω_0 - basic frequency.

ω_1 - frequency correction.

CHAPTER 1 - GENERAL INTRODUCTION

The dynamic behaviour of a rigid aeroplane in flight is characterised by the interaction of the resultant aerodynamic, gravitational and inertial forces and moments acting on and about the vehicle's centre of gravity. A mathematical representation of these three contributions can always be linearised about some reference condition and the nature of free or stimulated 'small' motions relative to this reference condition determined by solving the linearised equations of motion. The results of this linear model have provided and will continue to provide the bulk of the information required on an aircraft's stability and control characteristics. However, there are a number of flight situations where the linear analysis fails to predict or explain aircraft behaviour for the simple reason that linearisation is not valid. Examples are numerous and include the stall, spin and spin entry, wing rocking, deep stalling, roll coupling and control surface buzz. Such motions can generally be associated with the aerodynamic gravitational or inertial forces and moments having a nonlinear dependance on the motion they generate and hence can only be fully explained by solving the resultant nonlinear equations of motion.

Now the nonlinear problems of flight mechanics are not generally amenable to exact analytic techniques and there is therefore a requirement for the development of sound approximations that can be justified for a number of reasons. One important reason is that the range of validity of a linear theory can be readily established if a nonlinear theory is also available. Another is that an analytic approximation is more suitable for a parametric study of a problem than are numerical solutions. Of great significance is the effect of any nonlinearities on the stability characteristics of an aircraft, particularly when the linear theory predicts marginal stability or instability. In such situations the nonlinear terms in the equations of motion can have a profound effect on even small motions about the equilibrium flight condition. As will be shown in this thesis, approximate analytic solutions are capable of revealing these effects.

The amount of published material on nonlinear problems in flight mechanics is quite small which must reflect, surprisingly, the requirements of the aircraft designers. We mention here only a few of these works. In the early fifties Sternfield (REF. 1.1) examined the effect of nonlinearities in the yawing derivatives with a view to explaining the lateral 'snaking' motions experienced on some aircraft at that time. Later Rhoads and Schuler made an extensive study of the rolling pull out manoeuver, summarised in (REF. 1.2), comparing results from various approximations and identifying simple models for certain types of behaviour. The roll coupling problem, in which inertial nonlinearities play an important roll, has been given serious attention over the years. A discussion of this problem can be found in (REF. 1.3), where the authors extend previous work using a perturbation method to include the effects of gravity and control variations. Another nonlinear problem that has been investigated in some depth is the deep stall phenomenon where the nonlinear aerodynamic pitching moment causes the trouble (REF. 1.4, 1.5). Approximate analytic solutions for the lateral oscillations of slender aircraft at high angle of attack (a problem discussed in this thesis) are developed in (REF. 1.6).

Undoubtedly, one of the main reasons for the relative scarcity of nonlinear aircraft motion studies in the literature is the somewhat more complex mathematical technique required to solve these problems. Aircraft stability and control engineers are often sagacious individuals who steer clear of 'heavy' mathematics through a lack of familiarity. However, the extreme flight conditions in which some craft operate, such as re-entry vehicles and high performance fixed wing and rotary wing military aircraft, necessitate the use of more sophisticated theoretical techniques in the early design stage. Unfortunately, 'practical' mathematical methods for nonlinear systems are also scarce and unavoidably of an approximate nature, leading to nonunique answers, a situation which can often replace simple ignorance with confusion.

An analytic approximate technique, which has probably found more applications in the physical sciences than any other, is the small parameter perturbation method. Basically, one starts with a problem with a known solution and tries to find the solution of similar problem, differing from the known one by only a small amount, by expressing the solution as an asymptotic expansion in a small parameter that characterises this difference. The expansion scheme is based on an order of magnitude analysis and thus has an intrinsically rational flavour and allows improvements to be made systematically by including higher order successive approximations. It is sometimes said that the mark of a good approximate method is that it works well where it isn't supposed to; at least in a perturbation method it is clear where the approximation isn't supposed to work well. The perturbation method is clearly well suited to problems in which the nonlinearities are in some sense small so that the nonlinear problem can be treated as a perturbation of a linear problem. This thesis is concerned with the application of perturbation methods to aircraft stability problems where the linear theory predicts that the aircraft is flying close to a stability boundary; the main substance is contained in the following four chapters.

Chapter two introduces the mathematical techniques used extensively in the thesis. After defining the basic problem, second order systems are investigated in some detail. It is shown that a straightforward perturbation scheme breaks down and the source of the nonuniformity is revealed; uniformly valid solutions are constructed using the method of multiple scales. The techniques are then extended to fourth order problems characteristic of the nonlinear problems of flight mechanics.

In Chapter three approximations are derived for the lateral modes of motion of aircraft within the framework of the linear theory in order to glean an understanding of the important aspects of this linear problem. The main emphasis is on constructing approximations for the modes of slender configurations at high incidence where stability problems might be expected. For more conventional configurations a different set of approximations ~~are~~ 15 required to reveal the classical spiral, dutch roll and roll modes.

The techniques developed in Chapter 2 are applied in Chapter 4 to the lateral motion of slender aircraft at high incidence with aerodynamic nonlinearity. In particular, when an aircraft is flying close to the oscillatory stability boundary, the analysis reveals how the stability characteristics can be significantly changed by only a small amount of nonlinearity. The effect of the longitudinal short period response on this motion is also investigated.

Finally, Chapter 5 deals with some aspects of the representation and estimation of aerodynamic forces and moments when nonlinear effects are present. It is shown here how the logarithmic decrement concept can be extended to nonlinear oscillations and used to estimate damping parameters. A review of techniques for, and the author's views on, the representation of aerodynamic forces, when memory effects are apparent, is also included in this chapter.

The general discussion in Chapter 6 completes the thesis.

CHAPTER 2 - MATHEMATICAL PRELIMINARIES

In order to provide a framework for the approximation schemes used extensively in the later chapters of this thesis, it is appropriate to introduce and develop, in this chapter, some important mathematical concepts and results. For the most part the techniques outlined are applicable to weakly nonlinear autonomous systems and are based on perturbation methods and the attendant techniques of asymptotic expansions. Under certain conditions it will be shown that the methods can be extended to 'strongly' nonlinear autonomous systems. The meaning of the terms weakly and strongly will become clearer in what follows. It should be pointed out at this stage that the author relies heavily on heuristic arguments in the development of some of the results, the rigorous proofs being either too involved to warrant inclusion or plainly non-existent. In the former situation appropriate references will, of course, be given when necessary.

The problems discussed in detail in Chapters 3 and 4 are distinguished by the following characteristics.

2.1 Statement of the Problem

A nonlinear autonomous system, the solution of which depends on parameters ν and ε, is described by the differential equation,

$$\frac{d\underset{\sim}{X}}{dt} - A(\nu)\underset{\sim}{X} = \varepsilon \underset{\sim}{g}(\underset{\sim}{X}, \nu ; \varepsilon) \qquad (2.1)$$

Where $X(t ; \nu ; \varepsilon)$ is an n-vector containing the components of the state of the system; $A(\nu)$ is an $(n \times n)$ t-invariant matrix; $g(\underset{\sim}{X}, \nu ; \varepsilon)$ is a nonlinear function of $X(t, \nu ; \varepsilon)$, continuous and analytic in $\underset{\sim}{X}$ and satisfying the nonlinearity condition. (REF. 2.1 p.132).

$$\lim_{\underset{\sim}{X} \to \underset{\sim}{0}} \frac{|\underset{\sim}{g}(\underset{\sim}{X}, \nu ; \varepsilon)|}{|\underset{\sim}{X}(t, \nu ; \varepsilon)|} = 0 \qquad (2.2)$$

ε is a 'small' parameter not necessarily having physical significance. Suppose that at some value of ν, say ν_F, the unique linear part of (2.1) when $\varepsilon = 0$, exhibits a periodic solution $\underset{\sim}{X}_F(t, \nu_F ; 0)$. At this condition $A(\nu_F)$ is referred to as critical. It is then appropriate to ask the following questions for $\varepsilon \neq 0$.

Q.1. For small non-zero values of ε, are there any periodic solutions of (2.1) that bifurcate or branch off the linear solution $\underset{\sim}{X}_F$ and if so how do we approach determining these solution curves and ones nearby?

Q.2. How is the geometry of the state space modified close to the equilibrium point $\underset{\sim}{X}(t;\nu;\varepsilon) = \underset{\sim}{0}$? As will be shown this last question is intimately connected with the stability characteristics of the zero and periodic solution of (2.1) when $\varepsilon \neq 0$. (Note that when $A(\nu)$ is critical the linear part of the system is no longer responsible for the stability of the equilibrium).

Using a perturbation method we can develop quantitative answers to these questions in an approximate form, although the systematic nature of the perturbation method allows us to increase the order of accuracy without limit.

The condition that $A(\nu_F)$ is critical is crucial to the resolution of these questions. Any attempt to generate an approximate solution of (2.1), at $\nu = \nu_F$, via a straight forward asymptotic expansion in powers of ε , will fail due to the presence of so called secular terms in the higher order approximations. These unbounded terms can be corrected for, in the search for <u>periodic</u> solutions, by noting that the frequency of the solution depends on the amplitude and thus requires, itself, an asymptotic expansion form. It is in the elimination of these secular terms that we obtain the conditions necessary for periodic solutions to exist.

Before proceeding to answer Q.1. and Q.2. above in some detail it is useful to pose a further question at this stage.

Q.3. Can we continue a solution, obtained for $\varepsilon \neq 0$, as a function of ν , for small variations in ν about $\nu = \nu_F$, so as to include the areas in which the linear approximation predicts asymptotic stability (REF. 2.1 p.130) and instability? The answer to this question would indicate whether the instability is mild (stability boundary safe) or catastrophic (stability boundary dangerous) and will be sought after by transforming (2.1) into an equivalent though somewhat artificial system.

We begin by relating those ideas to some familiar second order problems.

2.2. <u>Periodic Solutions for Second Order Systems</u>

Later on in this section we will generalise some of the results obtained but to begin with we examine a particular example. Consider the autonomous equation,

$$\ddot{y} + \varepsilon(h_0 + h_2 y^2)\dot{y} + c_1 y + \varepsilon c_3 y^3 = 0 \qquad (2.3)$$

where $y(0) = a$, $\dot{y}(0) = 0$. A dot above a quantity denotes differentiation with respect to time, t . ε is a dummy small parameter; in actuality the combinations εh_0 , εh_2 , εc_3 are to be regarded as small since in the final analysis the physical parameters h_0, h_2, c_3 will be free and ε fixed. To expose the

origin of the non-uniformity in a straightforward expansion of the solution of (2.3) in powers of ε we begin by setting,

$$y(t;\varepsilon) = y_0(t) + \varepsilon y_1(t) + \varepsilon^2 y_2(t) + O(\varepsilon^3) \qquad (2.4)$$

Substituting (2.4) into (2.3) and equating coefficients of ε , we obtain to $O(\varepsilon^2)$,

$$O(1) \qquad \ddot{y}_0 + c_1 y_0 = 0 \qquad (2.5a)$$

$$O(\varepsilon) \qquad \ddot{y}_1 + c_1 y_1 = -(h_0 + h_2 y_0^2)\dot{y}_0 - c_3 y_0^3 \qquad (2.5b)$$

From (2.5a) we can write,

$$y_0(t) = a_0 \cos w_0 t \quad , \qquad w_0 = c_1^{1/2} \qquad (2.6)$$

and hence, (2.5b) becomes,

$$\ddot{y}_1 + c_1 y_1 = w_0 \left(h_0 + \frac{1}{4} h_2 a_0^2 \right) a_0 \sin w_0 t$$

$$- \frac{3}{4} c_3 a_0^3 \cos w_0 t + \frac{1}{4} a_0^3 (w_0 h_2 \sin 3 w_0 t - c_3 \cos 3 w_0 t) \qquad (2.7)$$

The presence of terms in $\sin w_0 t$, $\cos w_0 t$ on the right side of (2.7) will give rise to terms of the form $t \sin w_0 t$, $t \cos w_0 t$ in the general solution of $y_1(t)$. These secular terms are the source of the non-uniformity in the expansion since they grow unbounded with time. The expansion is of no practical use for large time since $\varepsilon y_1(t)$ soon dominates $y_0(t)$ and a similar behaviour is to be expected for $y_2(t)$, $y_3(t)$ etc.

If we restrict our search to periodic solutions of (2.3) we can make more progress. In particular we wish to determine those periodic solutions for $\varepsilon \neq 0$ that bifurcate from the solution $\cos \omega_c t$. In general we must expect that the frequency will depend on ε and we incorporate this variation into the problem by introducing a new time scale η, so that,

$$\frac{d}{dt} = \frac{d\eta}{dt}\frac{d}{d\eta} \tag{2.8}$$

The dependence of the frequency on ε can then be expressed in the expansion,

$$\frac{d\eta}{dt} = \omega_0 + \varepsilon \omega_1 + O(\varepsilon^2) \tag{2.9}$$

Using (2.8), (2.9), (2.3) can be transformed to,

$$\omega_c^2 y'' + \varepsilon (2\omega_0 \omega_1 + \varepsilon \omega_1^2) y'' +$$

$$+ \varepsilon (h_0 + h_2 y^2)(\omega_0 + \varepsilon \omega_1) y' + c_1 y + \varepsilon c_3 y^3 = O(\varepsilon^3) \tag{2.10}$$

Where a prime denotes differentiation with respect to η. We are now in a position to expand $y(\eta;\varepsilon)$ in the form,

$$y(\eta;\varepsilon) = y_0(\eta) + \varepsilon y_1(\eta) + O(\varepsilon^2) \tag{2.11}$$

Once again we substitute (2.11) into (2.10), equate coefficients of ε and obtain to $O(\varepsilon^2)$

$$O(1) \qquad \omega_0^2 y_0'' + c_1 y_0 = 0 \tag{2.12a}$$

$$O(\varepsilon) \qquad \omega_0^2 y_1'' + c_1 y_1 = -2\omega_0\omega_1 y_0'' - \omega_0(h_0 + h_2 y_0^2) y_0' - c_3 y_0^3 \tag{2.12b}$$

Since we are seeking periodic solution of (2.10) we must take a different approach to solving (2.12). The problem is now, strictly speaking, of the nature of a boundary value problem since we are going to force every $y_i, i = 1,1...$, to repeat itself every 2π . The initial values must be regarded as unknowns and will in general be shared by, to increasingly higher order, the functions $y_i(\eta)$.

The solution of (2.12a) can be written as,

$$y_0(\eta) = a_0 \cos\eta \tag{2.13}$$

Hence (2.12b) takes the form,

$$w_0^2 y_1'' + c_1 y_1 = \left(2 a_0 w_0 w_1 - \frac{3}{4} c_3 a_0^3\right)\cos\eta +$$

$$+ w_0 a_0 \left(h_0 + \frac{1}{4} h_2 a_0^2\right)\sin\eta + \frac{1}{4} a_0^3 \left(w_0 h_2 \sin 3\eta - c_3 \cos 3\eta\right) \tag{2.14}$$

Now the function $y_1(\eta)$ can only be periodic if the right side of (2.14) is free from terms in $\cos\eta$ and $\sin\eta$. This condition requires that the following bifurcation equations are satisfied,

$$2 w_0 w_1 - \frac{3}{4} c_3 a_0^2 = 0 \tag{2.15}$$

$$h_0 + \frac{1}{4} h_2 a_0^2 = 0 \tag{2.16}$$

The outcome is that the periodicity conditions (2.15) and (2.16) for the function $y_1(\eta)$ predict the amplitude and frequency correction of the zeroth order solution $y_0(\eta)$. Hence,

$$a_0^2 = -4 h_0 / h_2 \tag{2.17}$$

$$w_1 = \frac{3}{8 w_0} c_3 a_0^2 \tag{2.18}$$

A similar procedure is adopted with the right side of the second order perturbation equation in $y_2(\tau)$, to determine a_1 and ω_2 . In the phase plane (y_c, y_c') the zeroth order solution appears as a generating circle for the exact oval periodic solution, The orbital stability (REF. 2.1, p.130) of this particular solution can be indicated using the Poincaré Method of sections (REF. 2.1 p.218) and reduces to,

$h_c < 0 \; ; \; h_2 > 0$ orbital stability

$h_c > 0 \; ; \; h_2 < 0$ orbital instability

The results obtained are seen to go a long way in providing answers to Q.1. and Q.2. in Section 2.1. We now focus our attention on the initial value problem for trajectories in the vicinity of the periodic solution of (2.3).

2.3 The Method of Multiple Scales

In tackling the initial value problem we employ a technique known as the method of multiple scales; in fact the two time scale version. To prepare the ground for the method we make two important observations concerning the analysis in section (2.2). The use of a straightforward expansion predicted a non-uniformity in the solution that manifested itself for $t = O(1/\varepsilon)$; the non-uniformity appeared in εy_1 through the presence of terms in εt . This suggests that $y(t;\varepsilon)$ depends explicitly on t and εt as well as, perhaps, $\varepsilon^2 t, \varepsilon^3 t, \ldots$. The time scale εt is, for small ε , much slower than t and it is not unreasonable to imagine that any slowly varying function of t will actually depend on εt . Trajectories close to a periodic solution of (2.3) should, for small εh_0 and εh_2 be slowly varying functions of t . By imbedding the scale εt in the problem of determining periodic solutions, it may be possible to approximate nearby trajections. This is the procedure we are going to adopt. The method of multiple scales was, it seems, first discovered by Kuzmak (REF. 2.2) but a good, up to date, description of the various techniques involved can be found in the book by Nayfeh (REF. 2.3).

We begin by redefining the function $y(t;\varepsilon)$ as a function of two time scales η and τ , so that,

$$y(t;\varepsilon) \equiv z(\eta, \tau; \varepsilon) \tag{2.19}$$

and

$$\frac{d}{dt} = \frac{d\eta}{dt}\left(\frac{\partial}{\partial \eta}\right) + \varepsilon \frac{\partial}{\partial \tau} \tag{2.20}$$

where we write,

$$\frac{d\eta}{dt} = \omega(\tau) + \varepsilon\omega_1(\tau) + O(\varepsilon^2) \quad \text{and} \quad \tau = \varepsilon t \tag{2.21}$$

In (2.19) the variables η and τ are to be regarded formally as independent so that (2.20) becomes a partial differential operator. To $O(\varepsilon^2)$ (2.3) can therefore be written,

$$\omega_0^2 \frac{\partial^2 z}{\partial \eta^2} + c_1 z + \varepsilon\left\{ 2\omega_0\omega_1 \frac{\partial^2 z}{\partial \eta^2} + 2\omega_0 \frac{\partial^2 z}{\partial \eta \partial \tau} + \right.$$

$$\left. + \frac{\partial z}{\partial \eta}\left(\frac{d\omega_0}{d\tau} + h_0 + h_2 z^2 \right) + c_3 z^3 \right\} = O(\varepsilon^2) \tag{2.22}$$

We proceed as before by expanding $z(\eta, \tau ; \varepsilon)$ as an asymptotic sequence in ε ,

$$z(\eta, \tau ; \varepsilon) = z_0(\eta, \tau) + \varepsilon z_1(\eta, \tau) + O(\varepsilon^2) \tag{2.23}$$

The zeroth and first order perturbation equationsthus become,

$$O(1) \qquad \omega_0 \frac{\partial^2 z_0}{\partial \eta^2} + c_1 z_0 = 0 \tag{2.24}$$

$$O(\varepsilon) \qquad \omega_0^2 \frac{\partial^2 z_1}{\partial \eta^2} + c_1 z_1 = -2\omega_0 \frac{\partial^2 z_0}{\partial \eta \partial \tau} - 2\omega_0\omega_1 \frac{\partial^2 z_0}{\partial \eta^2}$$

$$- \omega_0 (h_0 + h_2 z_0^2) \frac{\partial z_0}{\partial \eta} - c_3 z_0^3 \tag{2.25}$$

Since the variable τ does not appear in the differential operator of (2.24) and (2.25) the solutions to those equations can be written as though they were ordinary differential equations in η with all integration constants now becoming functions of τ .

The solution of (2.24) is therefore,

$$z_0(\eta,\tau) = a_0(\tau)\cos\eta \qquad (2.26)$$

The functions $a_0(\tau)$ and $\omega_1(\tau)$ are determined by requiring that $z_1(\eta,\tau)$ be periodic in η with period 2π. As before, this condition amounts to setting to zero the terms in $\cos\eta$ and $\sin\eta$ on the right side of (2.25). The two conditions can be written as,

$$2\frac{da_0}{d\tau} + h_0 a_0 + \frac{1}{4} h_2 a_0^3 = 0 \qquad (2.27)$$

$$\omega_1(\tau) = \frac{3}{8\omega_0} c_3 a_0^2 \qquad (2.28)$$

The solution to (2.27) takes the form,

$$a_0(\tau) = \frac{e^{-h_0\tau/2}}{\left(k_0 - \frac{h_2}{4h_0} e^{-h_0\tau}\right)^{1/2}} \qquad (2.29)$$

The form of $\omega_1(\tau)$ given by (2.28) enables us to express the scale η in terms of real time t through the relation (2.21). Hence, upon integrating $a_0(\tau)^2$ we obtain,

$$\eta = \omega_0 t + \frac{3c_3}{2\omega_0 h_2} \log_e\left\{k_1\left(k_0 - \frac{1}{4}\frac{h_2}{h_0} e^{-\varepsilon h_0 t}\right)\right\} \qquad (2.30)$$

The quantities k_0 and k_1 are constants of integration and can be chosen to satisfy given initial conditions. Note that even for zero initial velocity we require that $\eta \neq 0$ at $t = 0$.

From (2.27) the limiting value of $a_c(\tau)$ as $t \to \infty$ can easily be obtained and agrees with (2.17), i.e.

$$\lim_{\tau \to \infty} a_c(\tau)^2 = a_{c_L}^2 = -\frac{4h_c}{h_2} \tag{2.31}$$

The stability of the periodic orbit obtained can be determined from (2.27) by constructing the equation of first variation about the point $a_0 = a_{cL}$. Thus, setting

$$a_c(\tau) = a_{cL} + \delta a_c(\tau) \tag{2.32}$$

(2.27) can be written,

$$\frac{d\delta a_c}{d\tau} + \frac{1}{2}\left(h_c + \frac{3}{4}h_2 a_{cL}^2\right)\delta a_c = 0 \tag{2.33}$$

Using (2.31) we can therefore conclude that trajectories will spiral in or out toward a_{cL} if $h_c < 0$ and away from a_{cL} if $h_c > 0$. These conclusions are consistant with the orbital stability characteristics predicted in section (2.2).

The techniques outlined above can readily be extended to the more general equation,

$$\ddot{y} + c_1 y + \varepsilon h(y, \dot{y}; \varepsilon) = 0 \tag{2.34}$$

Where the function $h(y, \dot{y}; \varepsilon)$ is continuous in each of its arguments. In this case it can be shown that the bifurcation equations, with imbedded slow time scale $\tilde{\tau}$ becomes,

$$\frac{da_0}{d\tau} = \frac{1}{2\pi\omega_0}\int_0^{2\pi} h(a_c\cos\eta, -\omega_c a_c \sin\eta; 0)\sin\eta\, d\eta = \Phi(a_0) \tag{2.35}$$

$$\omega_1(\tau) = \frac{1}{2\pi a_c \omega_c} \int_0^{2\pi} h(a_c \cos\eta, -\omega_c a_c \sin\eta ; 0) \cos\eta \, d\eta = \Psi(a_c) \qquad (2.36)$$

The orbital stability of the periodic solutions of (2.34), approximated by the real roots of the equation $\Phi(a_c) = 0$, say a_{ci}, $i = 1,2 \ldots$, will be reflected in the sign of the function $d\Phi / da_c$ evaluated at a_{ci}, $i = 1,2 \ldots$. Thus if $(d\Phi / da_c)_{a_c = a_{ci}} < 0$ we have orbital stability and if $(d\Phi / da_c)_{a_c = a_{ci}} > 0$ we have orbital instability. If $(d\Phi / da_c) = 0$ at $a_c = a_{ci}$, then a_{ci} can no longer be regarded as an approximation to a periodic solution of (2.34) since in this case the equation of first variation of (2.35) with respect to a_{ci} becomes degenerate (REF. 2.1 p.216).

Fig. 2.1 shows a comparison between the approximate solution represented by (2.26), (2.29) and (2.30) and a numerical solution using Merson's method. The amplitude envelope is predicted fairly well; the growth of the limit cycle is accompanied by an ever increasing phase shift between approximate and numerical solution.

In Chapter 5 we shall return to the type of approximation outlined above to examine its usefulness in predicting system characteristics.

2.4 Strongly nonlinear Second Order Systems

In special circumstances we can generate useful zeroth order approximations to the more general equation,

$$\ddot{y} + c(y) + \varepsilon h(y, \dot{y} ; \varepsilon) = 0 \qquad (2.37)$$

With $c(y)$ a general nonlinear function of y such that when $\varepsilon = 0$ (2.37) admits a known periodic solution. An approximate solution of (2.37) expressed as a asymptotic expansion in ε was, it appears, first analysed by Kuzmak (REF. 2.2) who also seems to be the first author to exploit the idea of two time scales. The procedure follows in much the same manner as when $c(y)$ was a linear function i.e. the introduction of two time scales, η and τ ; the definition of the function $Z(\eta, \tau ; \varepsilon)$ and the asymptotic expansion of $Z(\eta, \tau ; \varepsilon)$ and $d\eta / dt$ in powers of ε ; up to the point where the zeroth and first order equations are set down the analysis is the same. These can be written,

$$O(1) \qquad \omega_0^2 \frac{\partial^2 z_0}{\partial \eta^2} + c(z_0) = 0 \qquad (2.38)$$

$$\omega_0^2 \frac{\partial^2 z_1}{\partial \eta^2} + \left(\frac{\partial c(z)}{\partial z}\right)_{z=z_0} z_1 = -\left\{ 2\omega_0\omega_1 \frac{\partial^2 z_0}{\partial \eta^2} + \right.$$

$$O(\varepsilon) \qquad \left. + 2\omega_0 \frac{\partial^2 z_0}{\partial \eta \partial \tau} + \frac{d\omega_0}{d\tau}\frac{\partial z_0}{\partial \eta} + h\left(z_0, \omega_0 \frac{\partial z_0}{\partial \eta}; 0\right)\right\} \qquad (2.39)$$

For $z_1(\eta, \tau)$ to be periodic in η with the same period as $z_0(\eta, \tau)$ bifurcation equations can still be set down, but the arguments are of a more general character than the elimination of secular terms as in (2.25), (2.27) and (2.28). The conditions are applicable to constant or periodic systems and can be stated (REF. 2.4 p.359) as applicable to (2.39) as follows. If the adjoint homogeneous form of (2.39) admits one or more periodic solutions, then the solution $z_1(\eta, \tau)$ of the inhomogeneous equation will be similarly periodic if, and only if, the inhomogeneous term is orthogonal to every periodic solution of the adjoint homogeneous equation i.e. the integral of the product of the two functions, integrated over the period, vanishes. Now an obvious periodic solution to the homogeneous form of (2.39) (Note that the differential operator is self-adjoint) is the function $\partial z_0 / \partial \eta$ and hence a bifurcation equation for the zeroth order amplitude reads,

$$\int_0^{T_2} \left\{ 2\omega_0\omega_1 \frac{\partial^2 z_0}{\partial \eta^2} + 2\omega_0 \frac{\partial^2 z_0}{\partial \eta \partial \tau} + \frac{d\omega_0}{d\tau}\frac{\partial z_0}{\partial \eta} + h\left(z_0, \omega_0 \frac{\partial z_0}{\partial \eta}; 0\right)\right\} \frac{\partial z_0}{\partial \eta} d\eta$$

$$= 0 \qquad (2.40)$$

Noting that the first term in the integral in (2.40) vanishes for periodic $z_0(\eta, \tau)$, the bifurcation equation can be written in the simpler form,

$$\frac{\partial}{\partial \tau}\left\{\int_0^{T_\eta} w_c\left(\frac{dz_0}{d\eta}\right)^2 d\eta\right\} = -\int_0^{T_\eta} h\left(z_0, w_c\frac{dz_0}{d\eta}; 0\right)\frac{\partial z_0}{\partial \eta}\, d\eta \qquad (2.41)$$

(2.41) can be written in the equivalent form,

$$\frac{\partial}{\partial \tau}\, \phi(A_0(\tau)) = -\, q(A_0(\tau)) \qquad (2.42)$$

where the integrals in (2.41) are replaced by the functions $\phi(A_0)$ and $q(A_0)$, where $A_c(\tau)$ is the amplitude of the oscillation; (2.42) can be replaced by,

$$\frac{dA_0}{d\tau} = -\, q(A_0) \Big/ \frac{d\phi}{dA_0} \qquad (2.43)$$

With the functions $\phi(A_c)$ and $q(A_c)$ known explicitly the equation (2.43) will, in general, only yield solution by quadrature methods, and the solution will then be of the form $\tau = \tau(A_c)$. To demonstrate the more general technique we examine (2.3) again but with c_3 no longer regarded as small.

$$\ddot{y} + c_1 y + c_3 y^3 + \varepsilon(h_0 + h_2 y^2)\dot{y} = 0 \qquad (2.44)$$

The zeroth order solution can be written in terms of the Jacobian Elliptic functions $C_n(\gamma,\mu)$, $S_n(\gamma,\mu)$, $D_n(\gamma,\mu)$ etc. with period $4K(\mu)$ where $K(\mu)$ is the complete elliptic integral of the first kind. (REF. 2.5 App.1). For the case $c_1 > 0$ $c_3 > 0$ the appropriate solution for $0 \leq \mu \leq 1$ is given by,

$$z_c(\gamma,\tau) = A_0(\tau)\, C_n(\gamma, \mu_c(\tau)) \qquad (2.45)$$

and,

$$w_0^2 = c_1 + c_3 A_0^2 \qquad \mu_c^2 = \frac{\frac{1}{2} c_3 A_c^2}{c_1 + c_3 A_0^2} \tag{2.46}$$

The derivative $\partial z_0 / \partial \eta$ is then given by

$$\partial z_0 / \partial \eta = -A_0(\tau)\, S_n(\eta, \mu_c)\, D_n(\eta, \mu_c) \tag{2.47}$$

The various integrals involved in determining the functions $\phi(A_c)$ and $q(A_c)$ can be extracted from tables (REF. 2.6 pp. 211-212), giving,

$$\phi(A_0) = \frac{4 w_c A_0^2}{3 \mu_0^2} \left\{ (2\mu_c^2 - 1) E(\mu_c) + (1 - \mu_c^2) K(\mu_c) \right\} \tag{2.48}$$

$$q(A_0) = h_0 \phi(A_c) + h_2 \frac{4 w_0 A_0^4}{15 \mu_c^4} \left\{ (1-\mu_c^2)(\mu_c^2 - 2) K(\mu_c) + 2(\mu_0^4 + 1 - \mu_0^2) E(\mu_c) \right\} \tag{2.49}$$

Where $E(\mu_0)$ is the complete elliptic integral of the second kind.

The derivative $\partial \phi / d A_0$ can be readily obtained and simplifies to

$$d\phi / dA_c = 4 w_0 A_c K(\mu_c) \tag{2.50}$$

Using (2.48), (2.49) and (2.50), the bifurcation equation with embedded slow time scale τ , (2.43), can be written in the form.

$$\frac{dA_0}{d\tau} = -\frac{A_0 h_0}{3\mu_0^2}\left\{(2\mu_0^2-1)\frac{E}{K} + (1-\mu_0^2) + \right.$$

$$\left. + \frac{h_2}{h_0}\frac{A_0^2}{5\mu_0^2}\left[(1-\mu_0^2)(\mu_0^2-2) + 2(\mu_0^4+1-\mu_0^2)\frac{E}{K}\right]\right\} = \Gamma_0(A_0) \qquad (2.51)$$

for $\mu_0^2 << 1$ we can expand $E(\mu)$ and $K(\mu)$ in powers of μ^2 (REF. 2.6 p.297) and hence deduce the limiting result as $\mu \to 0$. Hence we obtain,

$$\Gamma_0(A_0)_{\mu^2 \to 0} = -\frac{h_0 A_0}{2} - h_2\frac{A_0^3}{8}$$

This result is see to agree with the result obtained when εC_3 is small (Cff. (2.27)).

Writing,

$$\gamma = \frac{C_3}{C_1}A_0^2 \quad , \quad \mu_0^2 = \frac{1}{2}\gamma/_{1+\gamma} \quad , \quad \lambda = \frac{C_1}{C_3}\frac{h_2}{4h_0}$$

Eqn. (2.51) can be expressed in the alternative form for quadrature.

$$h_0\tau = \int_{\gamma(0)}^{\gamma}\frac{d\gamma}{\bar{\Gamma}_0(\gamma,\lambda)} \qquad (2.52)$$

where

$$\bar{\Gamma}_0(\gamma,\lambda) = -\frac{4(1+\gamma)}{3}\left\{(2\mu_0^2-1)\frac{E}{K} + (1-\mu_0^2) + \right.$$

$$\left. + \frac{\lambda 8(1+\gamma)}{5}\left[(1-\mu_0^2)(\mu_0^2-2) + 2(\mu_0^4+1-\mu_0^2)\frac{E}{K}\right]\right\} \qquad (2.53)$$

For $\lambda = -0.1$ the approximate function $h_0 \tau$ is plotted with Y in Fig. 2.2, together with the function $1/\bar{\tau}_c(\gamma, \lambda)$. Some numerical results are shown for comparison which are extremely good. Note that the limit cycle is predicted at the second singularity in the function $1/\bar{\tau}_c(\gamma, \lambda)$. We will return to demonstrate an important use of the foregoing approximation in Chapter 5.

Before progressing to a discussion of fourth order systems it is appropriate at this stage to briefly review the enormous quantity of past effort with regard to second order equations. For weakly non-linear equations the results obtained in section 2.3, utilising the two time scale method, could have been obtained by a method known as the averaging method of Krylov and Bogoliubov (REF. 2.3 p.165). In Ref. 2.3 Nayfeh endeavours to show the equivalence of the various techniques for obtaining uniformly valid approximations to this type of equation. The present author feels that, because of the systematic and rational nature of the perturbation method, where possible such a method of successive approximations, based on a well defined ordering scheme, should be favoured. For strongly nonlinear equations, such as those discussed in (2.4), the situation, not surprisingly, is very sparse with regard to available results. The early work of Kuzmak (REF. 2.2) still remains one of the few systematic approaches to the problem. The use of Jacobian Elliptic functions as generating solutions has received some attention in the recent past. In a series of papers, Barkham and Soudack (REF. 2.7), try to develop an averaging method using these functions and in a later series of papers, Christopher (REF. 2.8) improved this approach and obtained good agreement with numerical results. Rasmussen (REF. 2.9) presents a successful approximation technique to equation of the form (2.37), using the two time variable method coupled with a novel transformation process reducing the equation to first order form.

Since the Jacobian Elliptic functions usually arise in non-linear oscillation problems as the inverse of the Elliptic integrals then it seems possible that some progress may be made with more general forms of $c(y)$ in (2.37) using Hyperelliptic integrals (REF. 2.6 p.252). This possibility is not explored any further in this thesis.

2.5 Extension to Fourth Order Systems

It is now appropriate to extend the ideas and techniques outlined in the previous three sections to the construction of approximate solutions for higher order autonomous systems. With the forthcoming applications in mind we restrict the analysis to fourth order problems with, to begin with, the nonlinearity confined to a single variable and its derivatives. We return therefore to (2.1) and the question posed regarding the behaviour of its solutions in the vicinity of the oscillatory stability boundary. In order to exploit directly the results developed for second order systems, we begin with a suitable form of (2.1) that allows us to readily approximate the fourth order system by a pair of 'weakly coupled' second order systems. Consider, then, the partitioned system,

$$\frac{d}{dt}\begin{bmatrix} \underset{\sim}{X}_1 \\ \underset{\sim}{X}_2 \end{bmatrix} - \begin{bmatrix} A_{11} & A_{12} \\ A_{21} & A_{22} \end{bmatrix} \begin{bmatrix} \underset{\sim}{X}_1 \\ \underset{\sim}{X}_2 \end{bmatrix} = \varepsilon \begin{bmatrix} \underset{\sim}{g}_1(\underset{\sim}{X}_2;\varepsilon) \\ \underset{\sim}{g}_2(\underset{\sim}{X}_2;\varepsilon) \end{bmatrix} \qquad (2.54)$$

where we have assumed the nonlinearity to be confined to the vector $\underset{\sim}{X}_2(t)$. Here A_{11} and A_{22} are (2×2) constant matrices and we assume for the linear problem, $\varepsilon = 0$, that these subsystems are weakly coupled (REF. 2.10). The necessary conditions for weak coupling between the partitioned linear subsystems can be expressed in the following terms (REF. 2.10).

(a) The eigenvalue sets of the matrices A_{11} and A_{22} should be widely separated in the complex plane. If the eigenvalues of A_{11} lie on or within the circle of radius r and the eigenvalues of A_{22} on or outside the circle of radius R then this condition can be expressed more precisely as

$$r/R \ll 1$$

(b) The coupling matrices A_{12}, A_{21} should be small in the following sense. If γ_m and ℓ_m are the maximum elements of A_{12} and A_{21} respectively, then we require that

$$2\gamma_m \ell_m / R^2 \ll 1$$

We have assumed here that the eigenvalues of A_{11} are smaller in modulus. With these conditions for weak coupling satisfied, the solution of (2.54) with $\varepsilon = 0$ can be approximated by a combination of the modified subsystems.

$$\frac{d\,\underset{\sim}{X}_1}{dt} - \left[A_{11} - A_{12}A_{22}^{-1}A_{21}\right]\underset{\sim}{X}_1 = \underset{\sim}{0} \qquad (2.55)$$

and

$$\frac{d\,\underset{\sim}{X}_1}{dt} - A_{22}\,\underset{\sim}{X}_2 = \underset{\sim}{0} \qquad (2.56)$$

In fact, with (a) and (b) satisfied the eigenvalues of the sub-matrices $[A_{11} - A_{12} A_{22}^{-1} A_{21}]$ and A_{22} will approximate the eigenvalue sets of A of low and high modulus respectively. This result will be used later in Chapter 4 in connection with the lateral modes of motion of aircraft. Details of how the complete solution of (2.54) with $\varepsilon = 0$ can be approximated by combination of the solutions of (2.55) and (2.56) will not be discussed here but can be found in REF. 2.10. For the present study we wish to explore the following situation when $\varepsilon \neq 0$. Suppose the matrix A has, for the value ν_F of some parameter ν (Cff. 2.1), a pair of imaginary eigenvalues and that, with conditions (a) and (b) satisfied, these eigenvalues are approximated by the eigenvalues of the matrix A_{22}. For the nonlinear problem it would be very convenient if the answers to the question posed in section 2.1 could be adequately answered by examining the reduced nonlinear system obtained by replacing the zero on the right hand side of (2.56) with the function $\underset{\sim}{g}_2(\underset{\sim}{x}_2 ; \varepsilon)$. That this scheme does not, in general, provide adequate answers will be demonstrated in the following example, where, as will be seen, realistic approximations to the nonlinear problem can only be achieved by considering the nonlinear coupling term $\underset{\sim}{g}_1(\underset{\sim}{x}_2 ; \varepsilon)$ in a perturbation approach.

For convenience we choose to analyse the example in second order form rather than the first order form of (2.54). With nonlinearity further restricted to the 'displacement' term in $\underset{\sim}{x}_1(t)$, a pair of coupled second order systems takes the form

$$\ddot{x}_1 - \alpha_2 \dot{x}_1 - \alpha_1 x_1 - \alpha_3(x_2)\, x_2 - \alpha_4 \dot{x}_2 = 0 \qquad (2.57)$$

$$\ddot{x}_2 - \beta_4 \dot{x}_2 - \beta_3(x_2) x_2 - \beta_1 x_1 - \beta_2 \dot{x}_1 = 0 \qquad (2.58)$$

Comparing with the vector form (2.54) we have

$$\{\underset{\sim}{x}_1 \; \underset{\sim}{x}_2\} = \{x_1 \; \dot{x}_1 \; x_2 \; \dot{x}_2\}$$

The functions $\alpha_3(x_2)$, $\beta_3(x_2)$ are assumed to be symmetric functions of x_2.

We now introduce a parameter ε to denote the smallness of a quantity and rewrite (2.57) and (2.58) in the form

$$\ddot{x}_1 - \alpha_2 \dot{x}_1 - \alpha_1 x_1 - (\alpha_{20} + \bar{\alpha}_3(x_2)) x_2 - \alpha_4 \dot{x}_2 = 0 \qquad (2.60)$$

$$\ddot{x}_2 - \beta_{30} x_2 = \varepsilon(\beta_4 \dot{x}_2 + \bar{\beta}_3(x_2) x_2 + \beta_1 x_1 + \beta_2 \dot{x}_1) \qquad (2.61)$$

When $\varepsilon = 0$ (2.61) now represents the approximate sub-system given by (2.56). For $\varepsilon \neq 0$ we approach the problem in a similar fashion to the two time scale method of section 2.4. Introducing the time scales η and τ, as in (2.21).

$$\begin{aligned} \frac{d\eta}{dt} &= \omega_0 + \varepsilon \omega_1(\tau) + O(\varepsilon^2) \\ \tau &= \varepsilon t \end{aligned} \tag{2.62}$$

Expanding the function $X_1(t)$ and $X_2(t)$ as powers of ε,

$$X_1(t) \equiv Z_1(\eta, \tau; \varepsilon) = Z_{10}(\eta, \tau) + \varepsilon Z_{11}(\eta, \tau) + O(\varepsilon^2) \tag{2.63a}$$

$$X_2(t) \equiv Z_2(\eta, \tau; \varepsilon) = Z_{20}(\eta, \tau) + \varepsilon Z_{21}(\eta, \tau) + O(\varepsilon^2) \tag{2.63b}$$

we obtain the zeroth and first order equation for $Z_2(\eta, \tau; \varepsilon)$ and the zeroth order equation for $Z_1(\eta, \tau; \varepsilon)$ by substituting (2.62), (2.63a), (2.63b) into (2.60) and (2.61).

$$O(1) \quad \omega_0^2 Z_{10}'' - \alpha_2 \omega_0 Z_{10}' - \alpha_1 Z_{10} = \alpha_4 \omega_0 Z_{20}' + (\alpha_{30} + \bar{\alpha}_3(Z_{20})) Z_{20} \tag{2.64a}$$

$$O(1) \quad \omega_0^2 Z_{20}'' - \beta_{30} Z_{20} = 0 \tag{2.64b}$$

$$\begin{aligned} O(\varepsilon) \quad \omega_0^2 Z_{21}'' - \beta_{30} Z_{21} = -\varepsilon \Big\{ & 2\omega_0 \frac{\partial^2 Z_{20}}{\partial \eta \partial \tau} + 2\omega_0 \omega_1 \frac{\partial^2 Z_{20}}{\partial \eta^2} \\ & - \bar{\beta}_3(Z_{20}) Z_{20} - \beta_4 \omega_0 Z_{20}' - \beta_1 Z_{10} - \beta_2 \omega_0 Z_{10}' \Big\} \end{aligned} \tag{2.64c}$$

The zeroth order solution for $Z_2(\eta, \tau; \varepsilon)$ can therefore be written as

$$Z_{20}(\eta, \tau) = a_{20}(\tau) \cos \eta \tag{2.65}$$

Once again we require that the right hand side of (2.64c) be free from $\cos\eta$ and $\sin\eta$ terms in order that $z_{21}(\eta,\tau)$ be periodic in η. To construct the bifurcation equation for $a_{2c}(\tau)$ we require also, in this case, the zeroth order contribution to $z_1(\eta,\tau;\varepsilon)$. From (2.64a), after some simplification, we can write,

$$z_{1c}(\eta,\tau) = a_{1c}(\tau)\cos\eta + b_{1c}(\tau)\sin\eta + (\cos 3\eta, \sin 3\eta \text{ terms}) \quad (2.66)$$

where

$$a_{1c}(\tau) = -\left\{\frac{(w_c^2+\alpha_1)(\alpha_{3c}+\bar{\alpha}_3(a_{2c})) + \alpha_2\alpha_4 w_c^2}{(w_c^2+\alpha_1)^2 + \alpha_2^2 w_c^2}\right\} a_{2c}(\tau) \quad (2.67a)$$

and

$$b_{1c}(\tau) = w_c\left\{\frac{(w_c^2+\alpha_1)\alpha_4 - \alpha_2(\alpha_{3c}+\bar{\alpha}_3(a_{2c}))}{(w_c^2+\alpha_1)^2 + \alpha_2^2 w_c^2}\right\} a_{2c}(\tau) \quad (2.67b)$$

Where $\bar{\alpha}_3(a_{2c})a_{2c}$ is the $\cos\eta$ component in the Fourier expansion of $\bar{\alpha}_3(z_{2c})z_{2c}$. Hence the bifurcation equations read,

$$(\sin\eta) \quad 2w_c\frac{da_{2c}}{d\tau} - \beta_4 w_c a_{2c} + \beta_1 b_{1c} - \beta_2 w_c a_{1c} = 0 \quad (2.68a)$$

$$(\cos\eta) \quad 2w_c w_1 a_{2c} + \bar{\beta}_3(a_{2c})a_{2c} + \beta_1 a_{1c} + \beta_2 w_c b_{1c} = 0 \quad (2.68b)$$

Where $\bar{\beta}_3(a_{2c})\,a_{2c}$ is the $\cos\eta$ component in the Fourier expansion of $\bar{\beta}_3(z_{2c})\,z_{2o}$.

Finally (2.68a) and (2.68b) can be written in the form,

$$\frac{da_{2o}}{d\tau} = \frac{1}{2}\left\{\beta_4 + \left[\frac{\alpha_{3c}(\beta_1\alpha_2 - \beta_2(\omega_c^2+\alpha_1)) - \alpha_4(\beta_2\alpha_2\omega_c^2 + \beta_1(\omega_c^2+\alpha_1))}{(\omega_c^2+\alpha_1)^2 + \alpha_2^2\omega_c^2}\right] + \right.$$

$$\left. + \bar{\alpha}_2(a_{2o})\left[\frac{\beta_1\alpha_2 - \beta_2(\omega_c^2+\alpha_1)}{(\omega_c^2+\alpha_1)^2+\alpha_2^2\omega_c^2}\right]\right\} a_{2o} \qquad (2.69)$$

and

$$\omega_1(\tau) = -\frac{1}{2\omega_c}\left\{\bar{\beta}_3(a_{2c}) - \left[\frac{\alpha_{3c}(\beta_1(\omega_c^2+\alpha_1)+\beta_2\omega_c^2\alpha_2) + \alpha_4(\beta_1\alpha_2\omega_c^2 - \beta_2\omega_c^2(\omega_c^2+\alpha_1))}{(\omega_c^2+\alpha_1)^2+\alpha_2^2\omega_c^2}\right]\right.$$

$$\left. - \bar{\alpha}_3(a_{2o})\left[\frac{\beta_1(\omega_c^2+\alpha_1)+\beta_2\omega_c^2\alpha_2}{(\omega_c^2+\alpha_1)^2+\alpha_2^2\omega_c^2}\right]\right\} \qquad (2.70)$$

A significant deduction can be made from (2.69). The periodic solutions will be given by

$$\bar{\alpha}_3(a_{2o_L}) =$$

$$-\left\{\frac{\beta_4((\omega_c^2+\alpha_1)^2+\alpha_2^2\omega_c^2) + \alpha_{3c}(\beta_1\alpha_2 - \beta_2(\omega_c^2+\alpha_1)) - \alpha_4(\beta_2\alpha_2\omega_c^2 + \beta_1(\omega_c^2+\alpha_1))}{\beta_1\alpha_2 - \beta_2(\omega_c^2+\alpha_1)}\right\} \qquad (2.71)$$

This result is identical to that obtained by setting to zero the $O(\varepsilon)$ term in the nonlinear Routhian for (2.60), (2.61) given by,

$$R(a_{2c}) = [\alpha_2 + \varepsilon\beta_4][\alpha_1 + \beta_{3c} + \varepsilon\bar{\beta}_3(a_{2c}) + \varepsilon(\alpha_2\beta_4 - \alpha_4\beta_2)][\alpha_2(\beta_{3c} +$$

$$+ \varepsilon\bar{\beta}_3(a_{2c}) + \varepsilon(\alpha_1\beta_4 - \beta_1\alpha_4 - (\alpha_{3c} + \bar{\alpha}_3(a_{2c}))\beta_2] - [\alpha_2(\beta_{3c} + \varepsilon\bar{\beta}_3(a_{2c})) +$$

$$+ \varepsilon(\alpha_1\beta_4 - \beta_1\alpha_4 - \beta_2(\alpha_{3c} + \bar{\alpha}_3(a_{2c})))]^2$$

$$- [\alpha_2 + \varepsilon\beta_4]^2[\alpha_1(\beta_{3c} + \varepsilon\bar{\beta}_3(a_{2c})) - \varepsilon\beta_1(\alpha_{3c} + \bar{\alpha}(a_{2c}))] \qquad (2.72)$$

This rather meaningful result will be shown later to have a more general range of application and in particular to be valid even when two equations of the form (2.57), (2.58) are not weakly coupled. For the present problem the results depicted in (2.69), (2.70) serve to illustrate some important aspects of coupled systems. Even for the linear problem $\bar{\alpha}_3(x_2) = \bar{\beta}_3(x_2) = 0$ we can see that (2.69) generates an addition to the damping of the higher order mode. For the nonlinear problem we see that the coupling term $\bar{\alpha}_3(x_2)x_2$ can lead to a limit cycle condition for the whole system. The stability of these limit cycles (solution of (2.71)) can be determined by examining the behaviour of solutions to the equation of first variation of (2.69). In the proceeding analysis we have implicitly answered question 3 of section 2.1. By allowing $\beta_1, \beta_2, \beta_4$ to have non-zero values as above we continue the solution $a_{2c}\cos\gamma$ into the region where the equilibrium point is a focus and the envelope of trajectories is given by (2.69). In Chapter 4 we will apply the above analysis to a weakly coupled form of the lateral equations of motion of slender aircraft with aerodynamic nonlinearity.

We return now to the more general problem defined by (2.1). With regard to the stability properties of the equilibrium of (2.1) it is known that at the critical condition ($\nu = \nu_F$) the terms in the function $\underset{\sim}{g}(\underset{\sim}{x}, \nu; \varepsilon)$ become important. Assuming we can expand $\underset{\sim}{g}(\underset{\sim}{x})$ as a Taylor series in $\underset{\sim}{x}$ about $\underset{\sim}{x} = 0$, then a useful definition of stability in critical cases relates to the stability in the N th approximation. Here, N is the degree to which terms in $\underset{\sim}{g}(\underset{\sim}{x})$ have been included. Much of the work on the stability of these critical cases has been formulated by Malkin (REF. 2.11 Chapter IV) and the important theorems developed are applicable to systems in which the

stability properties in the N th approximation can be determined from the stability properties of a reduced form of (2.1) in which only the 'critical variables' appear. In the following practical technique, we base the analysis on a similar though less extensive decomposition of (2.1) into a 'critical' and 'non-critical' pair of sub-systems. However, as stated at the beginning of this chapter, no attempt is made to find an entirely rigorous justification for the analysis.

By a suitable transformation of co-ordinates, $\underset{\sim}{X} = C\,\underset{\sim}{y}$, (2.1) can always be written in the alternative form

$$\frac{d\,\underset{\sim}{y_1}}{dt} - B_{11}\,\underset{\sim}{y_1} = \varepsilon\,\underset{\sim}{h_1}(\underset{\sim}{y_1}, \underset{\sim}{y_2}\,;\varepsilon) \qquad (2.73a)$$

$$\frac{d\,\underset{\sim}{y_2}}{dt} - B_{22}\,\underset{\sim}{y_2} = \varepsilon\,\underset{\sim}{h_2}(\underset{\sim}{y_1}, \underset{\sim}{y_2}\,;\varepsilon) \qquad (2.73b)$$

Where, when $\nu = \nu_F$, $\underset{\sim}{y_1}(t;\varepsilon)$ and $\underset{\sim}{y_2}(t;\varepsilon)$ are the two-dimensional sub-vectors of $\underset{\sim}{y}(t;\varepsilon)$ composed of the non-critical and critical variables respectively, such that,

$$B_{11} = \begin{bmatrix} 0 & 1 \\ -\lambda_1\lambda_2 & \lambda_1+\lambda_2 \end{bmatrix} \qquad (2.74a)$$

and

$$B_{22} = \begin{bmatrix} 0 & 1 \\ -\omega_0^2 & 0 \end{bmatrix} \qquad (2.74b)$$

Here, λ_1 and λ_2 are the eigenvalues of A with negative real part and $\pm i\omega_0$ are the purely imaginary eigenvalues of A . It is assumed at the outset that $Re(\lambda_1)$ and $Re(\lambda_2)$ are negative so that, when $\varepsilon = 0$, the equilibrium of (2.73a) is asymptotically stable in the first approximation.

The periodic solutions of (2.73a), (2.73b) when $\varepsilon = o$ are thus restricted to the sub-vector $\underset{\sim}{y}_2(t)$, i.e.

$$\underset{\sim}{y}_1(t) = \underset{\sim}{0} \tag{2.75a}$$

$$\underset{\sim}{y}_2(t) = \underset{\sim}{y}_{2c}(t) \tag{2.75b}$$

We will assume that when ε is non-zero the periodic solutions can be approximated, for small ε, by (2.75) with the bifurcation amplitude and frequency correction for this zeroth order approximation obtained by solving the periodicity conditions for the first order perturbation form of (2.73b). Hence, for small ε the problem reduces to one in two dimensions. For this approximation to be truly valid it is clear that there should be more restrictive conditions on the non-critical sub-system matrix β_{11} and the vector $\underset{\sim}{h}_1$. For example, if the non-critical mode is oscillatory with small damping and frequency close to an integer multiple of ω_c, then at some stage in the perturbation scheme to develop successive approximations, the response in the non-critical mode will be $\varepsilon\, O(1/\varepsilon) = O(1)$. If $\lambda_1\lambda_2 \simeq +(3\omega_c)^2$ and $(\lambda_1+\lambda_2) = O(\varepsilon)$ then the first order response in $\underset{\sim}{y}_1(t)$ will be $O(1)$, contradicting the initial assumptions. In such cases it is necessary to include a component of $\underset{\sim}{y}_1(t)$ in the zeroth order approximation, hence destroying the simpler two-dimensional result obtained above. The conditions on the form of $\underset{\sim}{h}_1(\underset{\sim}{y}_1, \underset{\sim}{y}_2 ; \varepsilon)$ for the above approximation to be valid are somewhat more elaborate and if not realised in a particular example can lead to erroneous results. Malkin (REF. 2.11 p.386) has shown that the 'abbreviated' system given by (2.73b) with $\underset{\sim}{y}_1(t)$ set to zero will only reproduce the stability nature of the equilibrium of the complete system in the N th approximation when the following condition is satisfied. The resolution of the vector function $\underset{\sim}{h}_1(0, \underset{\sim}{y}_2 ; \varepsilon)$ must begin with terms or order greater than N. If this is not the case then a suitable transformation of $\underset{\sim}{y}_1(t)$ can be devised to eliminate terms in $\underset{\sim}{y}_2(t)$ of order $\leq \tilde{N}$. An example will help to clarify this point. Consider the three dimensional system

$$\frac{dx}{dt} = -y + \alpha xz + \beta x^3 \tag{2.76a}$$

$$\frac{dy}{dt} = x + \alpha yz \tag{2.76b}$$

$$\frac{dz}{dt} = -z + x^2 + y^2 \tag{2.76c}$$

So in this case we have that $y_1(t)$ is the one dimensional system $\{z\}$ and $y_2(t)$ is the two dimensional system $\{y, x\}$. Now if we ignore completely the effect of z. in the critical system given by (2.76a) and (2.76b) and analyse the effect of the third order term βx^3 we could arrive at a false conclusion regarding the stability of the complete system because of the presence of the second order terms in (2.76c). We require to eliminate these by defining the new variable,

$$z = \xi + V(x, y) \tag{2.77}$$

so that (2.76c) can be written in the form,

$$\frac{d\xi}{dt} + (-y + \alpha x(\xi + V) + \beta x^3)\frac{\partial V}{\partial x} + (x + \alpha y(\xi + V))\frac{\partial V}{\partial y}$$

$$= -(\xi + V) + x^2 + y^2 \tag{2.78}$$

The function $V(x, y)$ can now be determined by setting to zero the aggregate of those terms in (2.78) which do not depend on the new non-critical variable ξ (REF.2.11 p.154)., i.e.

$$(-y + \alpha xV + \beta V^3)\frac{\partial V}{\partial x} + (x + \alpha yV)\frac{\partial V}{\partial y} = -V + x^2 + y^2 \tag{2.79}$$

To determine $V(x, y)$ it is necessary to expand in forms of increasing order and to equate forms of equal order. Thus we set,

$$V(x, y) = V_1(x, y) + V_2(x, y) + \cdots \tag{2.80}$$

where $V_i(x, y)$ are forms of the i th order.

By substituting (2.80) into (2.79) and equating forms of the same order we can therefore derive equations for V_1 and V_2 .

$$-y\frac{\partial V_1}{\partial x} + x\frac{\partial V_1}{\partial y} = -V_1 \tag{2.81a}$$

$$-y\frac{\partial V_2}{\partial x} + x\frac{\partial V_2}{\partial y} = -V_2 + x^2 + y^2 - \alpha y V_1\frac{\partial V_1}{\partial y} - \alpha x V_1\frac{\partial V_1}{\partial x} \tag{2.81b}$$

From which it can fairly easily be shown that

$$V_1 = 0 \tag{2.82a}$$

$$V_2 = x^2 + y^2 \tag{2.82b}$$

The new abbreviated critical system can be obtained by replacing z by V in (2.76a) and 2.76b), i.e.

$$\frac{dx}{dt} + y = \alpha x(x^2+y^2) + \beta x^3 + \text{higher order terms} \tag{2.83a}$$

$$\frac{dy}{dt} - x = \alpha y(x^2+y^2) + \text{higher order terms} \tag{2.83b}$$

It is clear from the additional terms in (2.83a) and (2.83b) that the stability nature of the abbreviated system could be completely changed by the presence of the terms premultiplied by α . Indeed, the change could be from a state of asymptotic stability to instability according to the 3rd approximation.

In the examples which comprise chapter 4 of this thesis, for the most part the elaborate procedure outlined above will not be required. This is because the nonlinear terms will be of the same order both in $\underset{\sim}{h}_1(\underset{\sim}{y}_1, \underset{\sim}{y}_1; \varepsilon)$ and $\underset{\sim}{h}_2(\underset{\sim}{y}_1, \underset{\sim}{y}_1; \varepsilon)$ and the function

$V(x,y)$ introduced above will only lead to higher order terms than those being considered. For example, if $\underset{\sim}{h}_1$ and $\underset{\sim}{h}_2$ are entirely third order nonlinear functions then it can be shown that the function V will start with V_3 and hence the additional terms in the abbreviated system will be at least 5th order.

For convenience we assume that the nature of the problem allows us to assume that the family of periodic solutions of (2.73a), (2.73b) bifurcate off the vector defined by (2.75). The two dimensional system then takes the form,

$$\frac{d\underset{\sim}{y}_2}{dt} - B_{22}\underset{\sim}{y}_2 = \varepsilon \underset{\sim}{h}_2(\underset{\sim}{0}, \underset{\sim}{y}_2 ; 0) \qquad (2.84)$$

Transforming the system into two time scales η and τ as defined

$$\frac{d\eta}{dt} = \omega_0 + \varepsilon\omega_1 + O(\varepsilon^2) \quad , \quad \tau = \varepsilon t \qquad (2.85)$$

and expressing the vector $\underset{\sim}{y}_2(t)$, in terms of η and τ, as an asymptotic expansion in powers of ε, i.e.

$$\underset{\sim}{y}_2(t) \equiv \underset{\sim}{z}_2(\eta,\tau;\varepsilon) = \underset{\sim}{z}_{20}(\eta,\tau) + \varepsilon\,\underset{\sim}{z}_{21}(\eta,\tau) + O(\varepsilon^2) \qquad (2.86)$$

we obtain the zeroth and first order perturbation equations as

$$O(1) \qquad \frac{\partial \underset{\sim}{z}_{20}}{\partial\eta} - B_{22}^{*}\underset{\sim}{z}_{20} = \underset{\sim}{0} \qquad (2.87a)$$

$$O(\varepsilon) \qquad \frac{\partial \underset{\sim}{z}_{21}}{\partial\eta} - B_{22}^{*}\underset{\sim}{z}_{21} = -\frac{1}{\omega_0}\left\{\omega_1\frac{\partial \underset{\sim}{z}_{20}}{\partial\eta} + \frac{\partial \underset{\sim}{z}_{20}}{\partial\tau} + \underset{\sim}{h}_2(0, \underset{\sim}{z}_{20}; 0)\right\} \qquad (2.87b)$$

$$B_{22}^{*} = \begin{bmatrix} 0 & 1/\omega_0 \\ -\omega_0 & 0 \end{bmatrix}$$

The zeroth order solution is given by

$$\underset{\sim}{z}_{20}(\eta,\tau) = Y_{2c}(\eta)\ \underset{\sim}{a}_{20}(\tau) \qquad (2.88)$$

where the principal matrix solution $Y_{2c}(\eta)$ is given by

$$Y_{2c}(\eta) = \begin{bmatrix} \cos\eta & \sin\eta \\ -\omega_c \sin\eta & \omega_c \cos\eta \end{bmatrix} \qquad (2.89)$$

Without loss of generality we can set the second component in $\underset{\sim}{a}_{2c}(\tau)$ to zero and denote the first element by $a_c(\tau)$. The bifurcation equation for $a_c(\tau)$ and $\omega_1(\tau)$ are found from the periodicity condition for the function $z_{21}(\eta,\tau)$ in (2.87b). i.e. that the right hand side of (2.87b) must be orthogonal tc the two periodic solution of the adjoint homogeneous form of (2.87b). Now the principal matrix solution for the adjoint homogeneous form of (2.87b) is given by the inverse of (2.89). The bifurcation equations can therefore be written in the vector form

$$\int_0^{2\pi} Y_{20}^{-1}(\eta)\left\{-\omega_1 \frac{\partial \underset{\sim}{z}_{20}}{\partial \eta} - \frac{\partial \underset{\sim}{z}_{20}}{\partial \tau} + \underset{\sim}{h}_2(\underset{\sim}{0}, \underset{\sim}{z}_{20}; 0)\right\} d\eta = \underset{\sim}{0} \qquad (2.90)$$

If we denote the upper and lower components of $\underset{\sim}{h}_2$ by the functions h_1^* and h_2^* respectively then, after some reduction, the bifurcation equation take the scalar form,

$$\frac{da_0}{d\tau} = -\frac{1}{2\pi\omega_c}\int_0^{2\pi}(h_2^* \sin\eta - \omega_c h_1^* \cos\eta)\, d\eta. \qquad (2.91a)$$

$$\omega_1(\tau) = \frac{-1}{2\pi\omega_c a_c}\int_0^{2\pi}(h_2^* \cos\eta + \omega_c h_1^* \sin\eta)\, d\eta \qquad (2.91b)$$

If the functions $h_1^*(u,v)$, $h_2^*(u,v)$ have the general cubic form,

$$h_1^*(u,v) = h_{11}u + h_{12}v + h_{13}uv^2 + h_{14}u^2v + h_{15}u^3 + h_{16}v^3 \qquad (2.92a)$$

$$h_2^*(u,v) = h_{21}u + h_{22}v + h_{23}uv^2 + h_{24}u^2v + h_{25}u^3 + h_{26}v^3 \qquad (2.92b)$$

where (u,v) denote the upper and lower components of z_{3c} ; then (2.91a) and (2.91b) take the form

$$\frac{dq_0}{d\tau} = \frac{q_0}{2}\left\{h_{11}+h_{22}+\left[\frac{3(h_{15}+w_0^2h_{26})+h_{24}+w_0^2h_{13}}{4}\right]q_0^2\right\} \qquad (2.93a)$$

$$w_1(\tau) = -\frac{1}{2w_0}\left\{h_{21}-w_0^2h_{12}+\left[\frac{3(h_{25}-w_0^4h_{16})+w_0^2(h_{23}-h_{14})}{4}\right]q_0^2\right\} \qquad (2.93b)$$

We have included linear terms in the expansion of $h_1(u,v)$ and $h_2(u,v)$ so that we may investigate the behaviour of trajectories away from the critical point $\nu = \nu_F$.

The orbital stability characteristics of the periodic solution, defined by the right side of (2.91a) being set to zero, can be determined from the equation of first variation of (2.91a) with respect to the amplitude of the periodic solutions. For the cubic system (2.93c) the conditions read,

orbital stability - $(h_{11}+h_{22})>0$; $(3(h_{15}+w_0^2h_{26})+h_{24}+w_0^2h_{13})<0$

equilibrium unstable.

orbital instability - $(h_{11}+h_{22})>0$; $(3(h_{15}+w_0^2h_{26})+h_{24}+w_0^2h_{13})>0$

equilibrium stable.

2.6 The Nonlinear Companion Problem

An interesting example of a fourth order nonlinear system, and one that is pertinent to the problems studied in Chapters 3 and 4, is afforded by the equation,

$$\frac{d^4x}{dt^4} + a_1\frac{d^3x}{dt^3} + \frac{d^2b(x)}{dt^2} + \frac{dc(x)}{dt} + d(x) = 0 \qquad (2.95)$$

where the functions $b(x)$, $c(x)$ and $d(x)$ are assumed to be anti-symmetric functions of x of the form

$$b(x) = b_1 x + \varepsilon b_3 x^3 + \ldots \text{ etc.} \qquad (2.96)$$

Setting $x_1 = x$, $x_2 = \frac{dx}{dt}$, $x_3 = \frac{d^2x}{dt^2}$, $x_4 = \frac{d^3x}{dt^3}$ and denoting by $-\varepsilon g_4(x_1, x_2, x_3, x_4)$ the nonlinear part of (2.95), the first order matrix form of (2.95) can be written as,

$$\frac{d}{dt}\begin{bmatrix} x_1 \\ x_2 \\ x_3 \\ x_4 \end{bmatrix} - \begin{bmatrix} 0 & 1 & 0 & 0 \\ 0 & 0 & 1 & 0 \\ 0 & 0 & 0 & 1 \\ -d_1 & -c_1 & -b_1 & -a_1 \end{bmatrix}\begin{bmatrix} x_1 \\ x_2 \\ x_3 \\ x_4 \end{bmatrix} = \varepsilon\begin{bmatrix} 0 \\ 0 \\ 0 \\ g_4(\underset{\sim}{x}) \end{bmatrix} \qquad (2.97)$$

where $\underset{\sim}{x} = \{x_1, x_2, x_3, x_4\}$

In such a form the linear system matrix is known as a companion matrix.

Once again we assume that the coefficients a_i, b_i, c_i, d_i are functions of some parameter ν and at $\nu = \nu_F$ a pair of purely imaginary eigenvalues of the 'companion matrix' in (2.97) appear. With eigenvalues $\lambda_1, \lambda_2, \pm i\omega_c$ it can be easily shown that,

$$\omega_c^2 = \frac{c_1}{a_1} \quad ; \quad \lambda_1\lambda_2 = b_1 - \frac{c_1}{a_1} = \frac{d_1 a_1}{c_1} \quad ; \quad \lambda_1 + \lambda_2 = -a_1 \qquad (2.98)$$

and hence the Routhian vanishes,

$$a_1 b_1 c_1 - c_1^2 - a_1^2 d_1 = 0 \qquad (2.99)$$

Bearing in mind that we would like to investigate the behaviour of trajectories either side of the point $\nu = \nu_F$, it is appropriate to take some of the linear terms from the left side of (2.97) to the right side in order that the companion matrix retains its critical condition. Which terms we should take over is actually quite arbitrary. We could allow three of the coefficients a_1, b_1, c_1, d_1 to vary naturally with ν and fix the fourth to satisfy (2.99) for small variations in ν about ν_F. However, we will choose a particular method that allows the most accurate representation of the linear part of the system for varying ν. By requiring that the coefficients in the companion matrix satisfy (2.98) for all values of ν in the range of interest we will preserve the eigenvalues of the non-critical modes (λ_1, λ_2) and the frequency of the near critical oscillatory mode as they vary with ν. The damping in the latter will now appear as perturbed values of a_1, b_1, c_1, d_1 on the right side of (2.97). We will thus have what we referred to as an artificial system in Q.3. of section 2.1. This artifice is of course necessary to deem the problem amenable to the foregoing analytic techniques.

We thus rewrite the coefficients in the form,

$$a_1 = a_{1c} + \varepsilon a_{11} \quad , b_1 = b_{1c} + \varepsilon b_{11} \quad , c_1 = c_{1c} + \varepsilon c_{11} \quad , d_1 = d_{1c} + \varepsilon d_{11} \qquad (2.100)$$

where a_{1c}, b_{1c} etc. are the required values to satisfy (2.98).

For the companion matrix, the similarity transformation C required to bring (2.97) into the decomposed form given by (2.78), (2.79) has a relatively simple form. Let U be the matrix of eigenvectors of the companion matrix so that,

$$U = \begin{bmatrix} U_{11} & U_{12} \\ U_{21} & U_{22} \end{bmatrix} = \begin{bmatrix} 1 & 1 & 1 & 1 \\ \lambda_1 & \lambda_2 & i\omega_0 & -i\omega_0 \\ \lambda_1^2 & \lambda_2^2 & -\omega_0^2 & -\omega_0^2 \\ \lambda_1^3 & \lambda_2^3 & -i\omega_0^3 & i\omega_0^3 \end{bmatrix} \qquad (2.101)$$

Then the required similarity transformation can be written,

$$\underset{\sim}{X} = \begin{bmatrix} X_1 \\ X_2 \\ X_3 \\ X_4 \end{bmatrix} = \begin{bmatrix} I & U_{12}U_{22}^{-1} \\ U_{21}U_{11}^{-1} & I \end{bmatrix} \begin{bmatrix} y_1 \\ y_2 \\ y_3 \\ y_4 \end{bmatrix} = C \underset{\sim}{y} \qquad (2.102)$$

where

$$U_{12}U_{22}^{-1} = \begin{bmatrix} -1 & 0 \\ 0 & -1 \end{bmatrix} \frac{a_{10}}{c_{10}} \quad ; \quad U_{21}U_{11}^{-1} = \begin{bmatrix} -\frac{a_{10}d_{10}}{c_{10}} & -a_{10} \\ \frac{a_{10}^2 d_{10}}{c_{10}} & a_{10}^2 - \frac{a_{10}d_{10}}{c_{10}} \end{bmatrix} \qquad (2.103)$$

The inverse of C can be written as

$$C^{-1} = \begin{bmatrix} I + D_{11} & \frac{a_{10}}{c_{10}} D_{22} \\ \frac{c_{10}}{a_{10}} D_{11} & D_{22} \end{bmatrix}$$

$$D_{11} = \begin{bmatrix} \left(1 - \frac{a_{10}^2 d_{10}}{c_{10}^2}\right) \frac{a_{10}^2 d_{10}}{c_{10}^2 \delta} & \frac{a_{10}^2}{c_{10}\delta} \\ -\frac{a_{10}^3 d_{10}}{c_{10}^2 \delta} & -\frac{a_{10}}{c_{10}\delta}\left(a_{10}^2 - \frac{a_{10}d_{10}}{c_{10}}\left(1 - \frac{a_{10}^2 d_{10}}{c_{10}^2}\right)\right) \end{bmatrix}$$

$$D_{22} = \frac{1}{\delta} \begin{bmatrix} 1 + \frac{a_{10}^2}{c_{10}}\left(a_{10} - \frac{d_{10}}{c_{10}}\right) & \frac{a_{10}^2}{c_{10}} \\ -\frac{a_{10}^2 d_{10}}{c_{10}^2} & 1 - \frac{a_{10}^2 d_{10}}{c_{10}^2} \end{bmatrix}$$

$$\delta = \frac{a_{10}^3}{c_{10}} + \left(1 - \frac{a_{10}^2 d_{10}}{c_{10}^2}\right)^2 \qquad (2.104)$$

Note that we actually only require the last column in C^{-1} since the elements $g_i(x_1, x_2, x_3, x_4)$, $i = 1,2,3$ are zero. The function $g_4(x_i)$ can be converted to $g_4(y_i)$ using (2.102).

We can write, including the linear perturbed terms, that

$$g_4^*(x_i,\dots) = -a_{11}x_4 - b_{11}x_3 - c_{11}x_2 - d_{11}x_1 -$$

$$- 3b_3(2x_1x_2^2 + x_1^2x_3) - 3c_3x_1^2x_2 - d_3x_1^2 +$$

$$+ \text{(odd terms of higher degree)} \qquad (2.105)$$

By transforming (2.97) in terms of y_i, $i = 1,\dots 4$ using (2.102) we are able to extract from the new system, the reduced second order critical system in terms of the variables $\{y_2, y_4\}$. For reference we write down the full equation in terms of y_i, $i = 1,\dots 4$.

$$\frac{dy_1}{dt} - y_2 =$$

$$= \varepsilon q_1(p_1y_1 + p_2y_2 + p_3y_3 + p_4y_4 + g_4(y_1,y_2,y_3,y_4)) \qquad (2.106a)$$

$$\frac{dy_2}{dt} + \frac{d_{10}}{c_{10}}a_{10}y_1 + a_{10}y_2 =$$

$$= \varepsilon q_2(p_1y_1 + p_2y_2 + p_3y_3 + p_4y_4 + g_4(y_1,y_2,y_3,y_4)) \qquad (2.106b)$$

$$\frac{dy_3}{dt} - y_4 =$$

$$= \varepsilon q_3(p_1y_1 + p_2y_2 + p_3y_3 + p_4y_4 + g_4(y_1,y_2,y_3,y_4)) \qquad (2.106c)$$

$$\frac{dy_4}{dt} + \frac{c_{10}}{a_{10}}y_3 =$$

$$= \varepsilon q_4(p_1y_1 + p_2y_2 + p_3y_3 + p_4y_4 + g_4(y_1,y_2,y_3,y_4)) \qquad (2.106d)$$

where the final column in C^{-1}, $\{q_1, q_2, q_3, q_4\}$, is given by (2.104).

and

$$p_1 = -a_{11}\frac{q_{10}^2 d_{10}}{c_{10}} + b_{11}\frac{q_{10} d_{10}}{c_{10}} - d_{11}$$

$$p_2 = -a_{11}\left(q_{10}^2 - \frac{q_{10} d_{10}}{c_{10}}\right) + b_{11} q_{10} - c_{11}$$

$$p_3 = -b_{11} + d_{11}\frac{q_{10}}{c_{10}} \qquad p_4 = -a_{11} + c_{11}\frac{q_{10}}{c_{10}} \tag{2.107}$$

The expanded expression for $g_4(y_1, y_2, y_3, y_4)$ is extremely lengthy and is not needed for the present analysis. The two dimensional critical system can therefore be extracted from (2.106), as,

$$\frac{dy_3}{dt} - y_4 = \varepsilon q_3\left(p_3 y_3 + p_4 y_4 + g_4(0,0,y_3,y_4)\right) \tag{2.108a}$$

$$\frac{dy_4}{dt} + \omega_c^2 y_3 = \varepsilon q_4\left(p_3 y_3 + p_4 y_4 + g_4(0,0,y_3,y_4)\right) \tag{2.108b}$$

where the nonlinear function $g_4(y_3, y_4)$ can be written as,

$$g_4(y_3, y_4) = \frac{1}{\omega_c^4}\left\{\left(\frac{d_3}{\omega_c^2} - 3b_3\right)y_3^3 + \frac{6b_3}{\omega_c^2} y_3 y_4^2 + 3c_3 y_3^2 y_4\right\} \tag{2.109}$$

The bifurcation equation for the zeroth order solution of (2.108) can be obtained using (2.92) ~~and~~ at (2.93). After some lengthy manipulation we arrive at,

$$\frac{da_0}{d\tau} = -\frac{1}{2}\left\{\frac{R_0 + \frac{R_2 a_0^2}{\omega_c^4}}{a_{1c}(b_{1c}^2 + c_0 a_{1c} - 4d_{10})}\right\} a_0 \tag{2.110}$$

where $a_c(\tau)$ is the amplitude function for the zeroth order solution of (2.108)

$$\begin{bmatrix} y_{3c}(t;\varepsilon) \\ \\ y_{4c}(t;\varepsilon) \end{bmatrix} = \begin{bmatrix} z_{3c}(\eta,\tau) \\ \\ z_{4c}(\eta,\tau) \end{bmatrix} \begin{bmatrix} \cos\eta & \sin\eta \\ \\ -w_c\sin\eta & w_c\cos\eta \end{bmatrix} \begin{bmatrix} a_c(\tau) \\ \\ 0 \end{bmatrix} \tag{2.111}$$

and,

$$R_0 = a_{10}(b_{10}c_{11} + c_{10}b_{11}) - 2c_{10}c_{11} - a_{10}^2 d_{11} \tag{2.112}$$

$$R_2 = \frac{3}{4}\left(a_{10}c_{10}b_3 + a_{10}b_{10}c_3 - a_{10}^2 d_3 - 2c_{10}c_3\right) \tag{2.113}$$

Hence we arrive at the result that the amplitude of the periodic solutions for (2.95) that branch off the linear solution in the critical mode only can be determined by setting to zero the $O(\varepsilon)$ term in the expanded modified Routhian given by

$$\left(a_{10}+\varepsilon a_{11}\right)\left(b_{10}+\varepsilon\left(b_{11}+\frac{3}{4}b_3 a_0^2\right)\right)\left(c_{10}+\varepsilon\left(c_{11}+\frac{3}{4}c_3 a_0^2\right)\right) -$$

$$-\left(c_{10}+\varepsilon\left(c_{11}+\frac{3}{4}c_3 a_0^2\right)\right)^2$$

$$-\left(a_{10}+\varepsilon a_{11}\right)^2\left(d_{10}+\varepsilon\left(d_{11}+\frac{3}{4}d_3 a_0^2\right)\right)$$

$$= 0 + \varepsilon\left(R_0 + \frac{3}{4}\frac{R_2}{w_c^4}a_0^2\right) + O(\varepsilon^2) \tag{2.114}$$

The ω_0^4 term multiplying (2.110) disappears when we transform back to the X co-ordinates, (2.102). The limit cycles are therefore given by,

$$a_{cL}^2 = -\frac{R_0 \omega_0^4}{\frac{3}{4} R_2} \tag{2.115}$$

The frequency correction can be obtained from the second bifurcation equation for (2.108) and takes the form,

$$W_1(\tau) = \frac{1}{2 a_0}\left\{(2\omega_c^2 - b_{1c})\frac{da_c}{d\tau} + \frac{3}{4} C_3 a_0^2\right\} \tag{2.116}$$

Hence in the limit as $a_0 \to a_{cL}$ we obtain,

$$W_1(\alpha) = \frac{3}{8}\frac{C_3}{a_{1c}} a_{cL}^2 \tag{2.117}$$

The initial value problem for (2.95) can be solved in the zeroth order approximation by forming a linear combination of the linear non-critical mode and nonlinear critical 'mode' with initial values distributed appropriately. If it is required to improve the approximation by including higher order terms then at, say the m th stage, the bifurcation equations for the amplitude and frequency correction are obtained by satisfying the periodicity conditions for the $(m+1)$ th approximation.

The result given by (2.114), (2.115) for cubic systems has a similar form when anti-symmetric terms of higher degree are included. In this case the coefficients in the generalised Routhian become,

$$(a_{1c} + \varepsilon a_{11}) \quad , \quad b_{1c} + \varepsilon\left(b_{11} + \sum_{j=1}^{N} b_{2j+1}\, \sigma_j\, a_0^{2j}\right)$$

$$c_{10} + \varepsilon\left(c_{11} + \sum_{j=1}^{N} c_{2j+1}\, \sigma_j\, a_0^{2j}\right) \quad , \quad d_{10} + \varepsilon\left(d_{11} + \sum_{j=1}^{N} d_{2j+1}\, \sigma_j\, a_0^{2j}\right)$$

where $$\sigma_j = \frac{(2j+1)!}{2^{2j}\, j!\,(j+1)!} \tag{2.118}$$

It should be pointed out here that the linear terms on the right side of (2.106) are actually superfluous apart from a damping term in the critical equation. This is because the additional terms in the eigenvector matrix (2.101) due to the damping of the critical mode are of $O(\varepsilon)$ and $O(\varepsilon^2)$ i.e. the term $i\omega_c$ would be replaced by $\varepsilon\mu + i\omega_c + O(\varepsilon^2)$ where μ is the damping. The inverse of the matrix C in (2.102) would, therefore, only be affected by an $O(\varepsilon)$ term and on multiplying the vector $\varepsilon g(\underline{X})$ would give additional $O(\varepsilon^2)$ terms. To $O(\varepsilon)$ we omit these and hence (2.106) can be replaced by a system with $p_i = 0$, $i = 1,\dots 4$ and an additional term $-\lambda\varepsilon\mu y_4$ on the right side of (2.106d). The result has been developed in its present form to illustrate the close connection with the $O(\varepsilon)$ change in the Routhian, but this could have been achieved by noting that

$$\mu = \frac{R_0}{a_{1c}(b_{1c}^2 + c_{1c}a_{1c} - 4d_{1c})} + O(\varepsilon)$$

In a practical application of the technique we therefore require a full knowledge of the linear system eigenvalues.

The essential feature of the foregoing technique is the decomposition of the system into the critical and non-critical modes by a suitable transformation. However, if one takes a different viewpoint the same results can be obtained without resorting to vector form at all. Applying the perturbation scheme to the fourth order form (2.95) directly a sequence of approximations can be determined each having the same fourth order differential operator with zero Routhian. Once again, the bifurcation equation for the amplitude and frequency correction at the m th stage are determined by setting to zero the $\cos\eta$ and $\sin\eta$ terms on the right hand side of the $(m+1)$th perturbation equation. Using a similar approach, though not based on a perturbation method, the authors of Ref. 2.12 obtain a result of an apparently more general nature. Writing the unknown $x(t)$ and its derivatives in the form,

$$x(t) = \theta\cos\varphi \quad , \quad \frac{dx}{dt} = -\omega\theta\sin\varphi \quad , \quad \frac{d^2x}{dt^2} = -\omega^2\theta\cos\varphi \quad , \text{etc.}$$

Substituting these forms into (2.95) and balancing the harmonics, $\cos\eta$, $\sin\eta$, $\cos 3\eta$, $\sin 3\eta$ etc. they obtain the result,

$$a_1\left(b_1 + \tfrac{3}{4}b_3\theta^2\right)\left(c_1 + \tfrac{3}{4}c_3\theta^2\right) - \left(c_1 + \tfrac{3}{4}c_3\theta^2\right)^2 - a_1^2\left(d_1 + \tfrac{3}{4}d_3\theta^2\right) = 0 \qquad (2.119)$$

There is no rational basis for this result as obtained in Ref. 2.12. Nevertheless, it might be true that if we went on to obtain the higher order approximations in (2.114) the result given by (2.119) would be obtained in the limit. Now (2.119) is a bi-quadratic in θ^2 and if it is assumed that θ^2 is small an approximation to (2.119) can be written by neglecting terms in θ^4, i.e.

$$\theta^2 = - \frac{a_1 b_1 c_1 - c_1^2 - a_1^2 d_1}{\frac{3}{4}\left(a_1(b_1 c_3 + c_1 b_3) - 2c_1 c_3 - a_1^2 d_3\right)} \qquad (2.120)$$

For small changes in the coefficients a_1, b_1, c_1, d_1 the numerator in (2.120) is practically the same as R_4 in (2.110). The denominator in (2.120) would only be equal to R_2 in (2.110) if, of the coefficients a_1, b_1, c_1, d_1, it is assumed that only d_1 varies to preserve a zero Routhian.

$$\text{i.e.} \qquad d_{10} = \frac{a_1 b_1 c_1 - c_1^2}{a_1^2} \qquad (2.121)$$

This could well lead to a negative value for d_{10} and hence one of the non-critical modes of the complete system would be unstable. This situation would not be acceptable from the perturbation approach and it therefore seems that the use of (2.120) must be regarded as suspect. A comparison of the various forms of the modified Routhian result will be presented for the examples of Chapters 3 and 4.

AIRCRAFT LATERAL MOTION

A feature of the lateral motion of inertially slender aircraft is the marked reduction in the damping of the oscillatory mode that occurs as the flight incidence is increased. At high enough incidences this mode can become unstable and we can expect that, in the vicinity of this critical condition, large excursions in this mode can take place. This situation can arise in the landing configuration and also in tight manoeuvring situations and in both cases it is clearly more satisfactory if the aircraft remains steady and fairly insensitive to disturbances. The actual physical mechanism responsible for this loss of stability, in terms of the variation in applied forces and moments, will obviously depend upon aircraft configuration and flight condition. In the following two chapters we are going to examine both small amplitude linear and large amplitude nonlinear oscillatory motion of aircraft with a view to obtaining approximations that go some way in explaining these motions. The approximations serve to describe and explain the motions from an essentially phenomenological point of view. No detailed attempt is made to relate particular aircraft behaviour to particular flow conditions. The aerodynamic data used in the examples is, through necessity, obtained from experiments in wind tunnels and flight. Sound theoretical methods for obtaining the lateral unsteady forces on aircraft at high incidence are, generally speaking, not yet available.

CHAPTER 3 - APPROXIMATIONS FOR THE LINEARISED THEORY

3.1 Introduction

The uncontrolled lateral motion of an aircraft in flight usually consists of an oscillatory mode and two aperiodic modes, or, in some cases, two oscillatory modes. The character of these modes, in terms of their stability and modal content, depends, very strongly, on aircraft configuration and flight condition. That this is indeed the case is demonstrated in an illustrative manner by Pinsker (REF.3.1), who pays particular attention to the oscillatory mode, showing clearly the contrast between the yaw/sideslip motion of high aspect ratio aircraft at low incidence and the almost purely rolling motion of low aspect ratio configurations at high incidence.

This situation of great variety is discouraging from the point of view of finding approximations with a wide range of validity, although this challenge has produced some very useful and now established results. The successful early work of Thomas and Neumark (REF. 3.2) concentrated on approximate factorisation of the characteristic equation and this technique was later used by Ross (REF. 3.3) to predict, amongst other things, the critical angle of incidence at which the lateral oscillation of various flying models became unstable. Pinsker (REF.3.1) takes a different viewpoint and derives quite simple expressions for mode damping and frequencies by omitting degrees of freedom and hence reducing the order and simplifying the equations of motion. Using C_L as a parameter he proceeds to show how, for slender configuration, two distinct approximations are valid over different ranges of C_L with a region of mid C_L values where neither is applicable.

In this section we will construct approximations to the lateral modes based on a consideration of the aircraft as a weakly coupled system. (REF. 3.4). This consideration is made possible by a judicious choice of coordinate transformation which recasts the equations of motion in terms of motion variables that have more significance in the natural modes. The essence of the technique is then to partition the system equations into lower order subsystems and hence to generate approximations to the modes of the complete system. The conditions necessary for the approximation scheme to be valid are reviewed briefly in section 2.5.

In REF. 3.4, Milne showed that by introducing the aircraft vertical velocity into the longitudinal equations of motion, a successful partitioning and hence approximation could be achieved for the phugoid and short period modes. Similarly, for aircraft lateral motion, it will be shown here that by introducing the aircraft 'sideways' velocity the equations can be partitioned to reveal the lateral modes for two distinct situations. The two situations can be summarised as follows:

(i) High incidence flight conditions where oscillation and other modes are dominated by rolling. Geometric body axes used to define motion.

(ii) Low incidence flight conditions with conventional spiral, dutch roll, roll subsidence modes. Stability axes used to define motion.

In both cases the oscillation will be approximated by a sideslipping mode. However, as will be shown, the damping associated with this mode is not predicted too well, and, generally speaking, it is necessary to include the effect of the sideways modes using a perturbation analysis. This result is consistent with the observation that in general the lateral oscillation of an aeroplane takes place about some axis displaced in translation and rotation from the body axes passing through the centre of gravity.

As already pointed out, but worthy of further emphasis, the main attraction of such approximations is that they can lead to a better understanding of the character of the natural modes of aircraft; some numerical examples are given for particular aircraft to illustrate the utility of the technique and the validity of the hypothesis. We consider the two situations separately.

3.2 High Incidence Approximation - Sideways and Sideslip Motions.

The analysis presented here relates particularly to the flight of slender aircraft at high incidence. It is now well known (REF. 3.1) that the oscillatory mode in such cases takes the form of an almost pure rolling motion about the aircraft fuselage axis and that the damping of this mode can often be very low or even negative. Also the remaining modes, which may form another oscillation, can no longer enjoy the simple spiral and roll subsidence titles and become more complicated functions of rolling and sideslipping. Yawing motion is practically absent from all of the modes.

An inspection of the makeup of typical eigenvectors for such configurations reveals that the oscillation contains very little lateral motion of the aircraft centre of gravity while the other modes contain very little sideslip motion. In simple terms the oscillation takes place mainly about the body reference axis whereas the remaining modes are composed of rolling and a sideways motion of the c.g., combined to produce little sideslip. Based on this evidence we will derive a co-ordinate transformation to recast the equation of motion into a necessary form for the application of the approximation.

The linearised equation of lateral motion referred to a body axes system can be written in the general first order matrix form. (Appendix A).

$$\frac{d}{dt}\begin{bmatrix} v \\ p \\ r \\ \phi \end{bmatrix} - \begin{bmatrix} y_v' & y_p'+w_0 & y_r'-u_0 & g_1 \\ \ell_v' & \ell_p' & \ell_r' & 0 \\ n_v' & n_p' & n_r' & 0 \\ 0 & 1 & \tan\theta_e & 0 \end{bmatrix}\begin{bmatrix} v \\ p \\ r \\ \phi \end{bmatrix} = \underset{\sim}{0} \qquad (3.1)$$

The motion variables $\{ v , p , r , \phi \}$, the aerodynamic derivatives y_v' , ℓ_p' , n_r' etc., the trim velocities w_c , u_c and the gravitational coefficient g, are all assumed to be normalized. No reference is made at this stage to any particular normalising scheme or the precise location of the body X axis except to say that the latter should lie close to the principal axes of inertia, (see Appendix A for normalising scheme). When the product of inertia I_{xz} is non zero, the rolling and yawing derivatives will be modified as shown in Appendix A.

Let the sideslip velocity v be divided into two parts; a contribution due entirely to rolling $(w_c \phi)$ and the remainder v_c. With only a small amount of yaw involved in the motion the velocity v_o is mainly associated with a translational sideways motion of the aircraft centre of gravity. Hence we can write,

$$v = v_o + w_c \phi \qquad (3.2)$$

We wish now to transform (3.1) into a similar equation in terms of the state vector $\{ v_c , \dot{v}_o , v , \dot{v} \}$ where a dot above a quantity denotes differentiation with respect to t. This can be achieved by expressing p in terms of ϕ, eliminating r and finally relating ϕ to v_o and v as given by (3.2). Details are given in Appendix A. The required equations can be written in the partitioned form,

$$\frac{d}{dt} \left[\begin{array}{c} v_c \\ \dot{v}_o \\ \hdashline v \\ \dot{v} \end{array}\right] - \left[\begin{array}{cc:cc} 0 & 1 & 0 & 0 \\ \alpha_1 & \alpha_2 & \alpha_3 & \alpha_4 \\ \hdashline 0 & 0 & 0 & 1 \\ \beta_1 & \beta_2 & \beta_3 & \beta_4 \end{array}\right] \left[\begin{array}{c} v_c \\ \dot{v}_c \\ \hdashline v \\ \dot{v} \end{array}\right] = \underset{\sim}{0} \qquad (3.3)$$

Where, $$\alpha_1 = \frac{g_1}{w_0} \left\{ \frac{n_r^* (y_r^* - u_c^*) + y_p^* \ell_r^*}{y_r^* - u_c^*} \right\} \qquad (3.4a)$$

$$\alpha_2 = \frac{1}{W_0}\left\{ -g_1 + \frac{y_r^*}{y_r^* - u_c^*}\left(\rho_r^*(y_p^* + W_c) - \rho_p^*(y_r^* - u_c^*)\right)\right.$$

$$\left. - n_p^*(y_r^* - u_c^*) + n_r^*(y_p^* + W_c)\right\} \qquad (3.4b)$$

$$\alpha_3 = \frac{y_p^*}{y_r^* - u_c^*}\left(\rho_v^*(y_r^* - u_c^*) - \rho_r^*\left(y_v^* + \frac{g_1}{W_c}\right)\right) +$$

$$+ n_v^*(y_r^* - u_c^*) - n_r^*\left(y_v^* + \frac{g_1}{W_c}\right) \qquad (3.4c)$$

$$\alpha_4 = \left(y_v^* + \frac{g_1}{W_c}\right) + \frac{1}{W_c}\left\{ n_p^*(y_r^* - u_c^*) - y_p^* n_r^* + \right.$$

$$\left. + \frac{y_p^*}{y_r^* - u_c^*}\left(\rho_p^*(y_r^* - u_c^*) - \rho_r^* y_p^*\right)\right\} \qquad (3.4d)$$

$$\beta_1 = \alpha_1 + \frac{g_1 \rho_r^*}{y_r^* - u_0^*} \qquad (3.4e)$$

$$\beta_2 = \alpha_2 + \frac{\rho_r^*(y_p^* + W_c) - \rho_p^*(y_r^* - u_c^*)}{y_r^* - u_0^*} \qquad (3.4f)$$

$$\beta_3 = \alpha_3 + \frac{W_c}{y_r^* - u_c^*}\left\{ \ell_v^*(y_r^* - u_c^*) - \ell_r^*(y_v^* + \frac{g_1}{W_c}) \right\} \qquad (3.4g)$$

$$\beta_4 = \alpha_4 + \frac{\ell_p^*(y_r^* - u_c^*) - \ell_r^* y_p^*}{y_r^* - u_c^*} \qquad (3.4h)$$

with
$$y_p^* = y_p'$$
$$y_r^* = y_r' - y_p' \tan\theta_c$$
$$u_0^* = u_0 + W_c \tan\theta_c = 1/u_1$$
$$\ell_v^* = \ell_v' + n_v' \tan\theta_c$$
$$n_v^* = n_v'$$
$$\ell_p^* = \ell_p' + n_p' \tan\theta_c$$
$$n_p^* = n_p'$$
$$\ell_r^* = \ell_r' - \ell_p' \tan\theta_c + (n_r' - n_p' \tan\ell_c) \tan\theta_c$$
$$n_r^* = n_r' - n_p' \tan\theta_c \qquad (3.5)$$

Now the partitional matrix in (3.3) is of the form,

$$C = \left[\begin{array}{c|c} C_{11} & C_{12} \\ \hline C_{21} & C_{22} \end{array}\right] \qquad (3.6)$$

and provided the conditions for weak coupling (see Chapter 2) between the sideways $\{v_c, \dot{v}_c\}$ and sideslip $\{v, \dot{v}\}$ modes are satisfied, then the eigenvalues of C of low modulus will be approximated by the characteristic equation,

$$\det\left[\lambda I - C_{11} + C_{12}\, C_{22}^{-1} C_{21}\right] = 0 \qquad (3.7)$$

and those of high modulus will be approximated by,

$$\det\left[\lambda I - C_{12}\right] = 0 \qquad (3.8)$$

In terms of the coefficients α_i , β_i (3.7) and (3.8) read, respectively,

$$\lambda^2 - \left(\alpha_2 - \frac{\beta_2 \alpha_3}{\beta_3}\right)\lambda - \left(\alpha_1 - \frac{\beta_1 \alpha_3}{\beta_3}\right) = 0 \qquad (3.9)$$

and $$\lambda^2 - \beta_4 \lambda - \beta_3 = 0 \qquad (3.10)$$

With y_r , y_p assumed to be zero the damping and stiffness expressions in (3.9), (3.10) are simplified and can be written in the form,

$$\alpha_2 - \frac{\beta_2 \alpha_3}{\beta_3} =$$

$$\frac{W_0 (n_r^* \ell_v^* - \ell_r^* n_v^*) + U_0^* (\ell_v^* n_p^* - n_v^* \ell_p^*) - g_1 \ell_v^* + \frac{\left(y_v^* + \frac{g_1}{W_0}\right)}{U_0^*}\left(-\ell_r^* g_1 + U_0^* (\eta_p^* \ell_r^* - \ell_p^* n_r^*)\right)}{W_0 \ell_v^* - n_v^* U_0^* + \frac{\left(y_v^* + \frac{g_1}{W_0}\right)}{U_0^*}\left(W_0 \ell_r^* - U_0^* n_r^*\right)} \qquad (3.11)$$

$$\alpha_1 - \frac{\beta_1 \alpha_2}{\beta_3} =$$

$$= \frac{g\left(n_r^* e_v^* - e_r^* n_v^*\right)}{W_c e_v^* - n_v^* U_c^* + \frac{\left(y_v^* + \frac{g_1}{W_c}\right)}{U_c^*}\left(W_c e_r^* - U_c^* n_r^*\right)} \qquad (3.12)$$

$$\beta_4 = e_p^* - \frac{n_p U_c^*}{W_c} + y_v^* + \frac{g_1}{W_c} \qquad (3.13)$$

$$\beta_3 = W_c e_v^* - n_v^* U_c^* + \frac{\left(y_v^* + \frac{g_1}{W_c}\right)}{U_c^*}\left(e_r^* W_c - n_r^* U_c^*\right) \qquad (3.14)$$

Of particular interest in the results derived is (3.13), the expression for the approximate damping of the sideslip oscillation. Pinsker (REF. 3.1) derives a corresponding result for this damping by assuming zero yaw in the motion and hence predicts that instability will occur in this mode, when, (REF. 3.1 p.18).

$$\frac{C_L}{2\sin\theta_c} > \frac{-e_{p3}}{i_{A_c}} \qquad (3.15)$$

Where C_L is the lift coefficient at incidence θ_c, e_{p3} and i_{A_c} are the damping in roll and normalized inertia moment about the principal axis of inertia along the fuselage. As shown in Appendix 1 the gravitational coefficient in the body axes system is $(C_L / 2\mu_z)\cos\theta_c$ and hence (3.15) approximates (3.13) when y_v^* and n_p^* are small. Although y_v^* is usually very small compared with e_p^* (except where e_p^* changes sign) the term $(-n_p^* U_c^* / W_c)$ can be significant and, of course, for $n_p^* < 0$, is destabilizing. The physical significance of the gravity term (g_1 / W_c) in (3.13) can be understood by observing that during the oscillation, zero sideslip $(v=0)$ does not coincide with zero roll angle $(\phi = 0)$. In fact when v passes through zero from positive to negative the aircraft is moving to starboard with a velocity V_0 and banked to port through the angle ϕ.

With the aircraft in this attitude the gravitational force acting along the banked wing opposes the damping moment due to roll rate. Note that although the 'v_c' modes have been partitioned from the mode in (3.3) we can still expect to find a contribution from 'v_c' in 'v' ($v = v_c + w_c \phi$) .

Before illustrating the foregoing approximation with some numerical examples we wish to derive an improved approximation for the high modulus subsystem characteristics. We require to do this because as it stands the approximate damping of the oscillatory 'v' mode given by (3.13) shows no dependence on the sideslip derivatives ℓ_v and n_v whereas the common practice of displaying the oscillatory and divergence stability boundaries on the (ℓ_v, n_v) plane (see for example REF. 3.5 p.424) is, in itself, evidence that, at least for more conventional configurations, the damping should depend on these derivatives. The extent to which the damping of the oscillation depends on ℓ_v and n_v is a reflection of the displacement of the oscillation axis relative to the body X axis, and hence of the amount that the oscillation is out of phase with the sideslip velocity V .

We can derive a second approximation to the oscillation damping and frequency by considering the coupling terms $\beta_1 v_c$ and $\beta_2 \dot{v}_c$ in (3.3) together with the damping term $\beta_4 \dot{v}$ as perturbations on the simple harmonic oscillator in v given by,

$$\ddot{v} + \beta_3 v = 0 \qquad (3.16)$$

The necessary analysis has, in fact, already been developed for the case of α_3 and β_3 having a dependence on V in section 2.5. With the nonlinear terms set to zero (2.57) and (2.58) have the same form as (3.3); (3.16) is then equivalent to (2.61) with ε set to zero. The required results for the damping and frequency correction are then given by (2.74) and (2.75) respectively with $\bar{\alpha}$ and $\bar{\beta}$ set to zero. With the oscillation of the form $e^{\mu^* t} \cos \omega^* t$, we can therefore write,

$$\mu^* \simeq \frac{1}{2}\left\{\beta_4 + \frac{\alpha_3(\beta_1\alpha_2 - \beta_2(\alpha_1 - \beta_3)) - \alpha_4(\beta_1(\alpha_1 - \beta_2) - \beta_2\beta_3\alpha_2}{(\alpha_1 - \beta_2)^2 - \beta_3\alpha_2^2}\right\} \qquad (3.17)$$

and $$w^* \simeq (-\beta_3)^{1/2} +$$

$$+\frac{1}{2(-\beta_3)^{1/2}}\left\{\frac{\alpha_3(\beta_1(\alpha_1-\beta_3)-\beta_2\beta_3\alpha_2)+\alpha_4(\beta_2\beta_3(\alpha_1-\beta_3)-\beta_1\alpha_2\beta_3)}{(\alpha_1-\beta_3)^2-\beta_3\alpha_2^2}\right\} \qquad (3.18)$$

Along with the damping and frequency, a quantity of significance in the oscillation is the ratio of roll angle ϕ to sideslip velocity v, commonly known as the 'dutch roll ratio' for conventional configurations. Now if the sideslip is due entirely to rolling so that

$$V = W_c \phi$$

then this ratio would reduce to $1/W_c$, a result arrived at by Pinsker (REF. 3.1 p.20). However, with our second approximation derived above, we can make a better estimate than this. We can write

$$\frac{\phi}{V} = \frac{(V-V_c)}{W_c V} = \frac{1}{W_0}\left(1-\left(\frac{V_c}{V}\right)\right) \qquad (3.19)$$

Now an approximation to the ratio (V_c/V) can be derived from the results of section 2.5. It is convenient to represent (V_c/V) as a complex number and hence using (2.70) and (2.71) we can write,

$$\frac{V_c}{V} = R_{V_c} + i I_{V_c} \qquad (3.20)$$

where $$R_{V_c} = -\left\{\frac{(\alpha_1-\beta_3)\alpha_3-\beta_3\alpha_2\alpha_4}{(\alpha_1-\beta_3)^2-\beta_3\alpha_2^2}\right\} \qquad (3.21a)$$

and $$I_{V_c} = -(-\beta_3)^{1/2}\left\{\frac{(\alpha_1-\beta_3)\alpha_4-\alpha_2\alpha_3}{(\alpha_1-\beta_3)^2-\beta_3\alpha_2^2}\right\} \qquad (3.21b)$$

Hence $$\left(\phi/v\right) \simeq \frac{1}{w_c}\left(1 - R_{v_c} + i\,I_{v_c}\right) \qquad (3.22)$$

We are now at an appropriate stage to apply the foregoing approximations to some particular aircraft to examine the utility of the technique. We will study the characteristics of three slender winged aircraft, the H.P.115, the B.A.C. 221 and the prototype Concorde, in the incidence range $12^\circ \leq \alpha \leq 26^\circ$.

EXAMPLE 1 - The H.P. 115

The Handley-Page H.P.115 aircraft was built for research purposes to examine the low speed stability characteristics and handling qualities of slender configurations. An interesting discussion of the flying qualities of this aircraft can be found in REF. 3.6. The relevant data for the calculations can be found in Table 3.1 and Fig. 3.1. All the data except for the C_L vs. α curve were taken from REF. 3.7. The aerodynamic derivatives in Fig. 3.1 are referred to a body axes system with X axis coincident with the fuselage datum. Note that the principal axis of inertia is located approximately 4° nose down from the fuselage datum. The C_L vs. α curve is taken from REF. 3.8, where there also can be found a detailed description of the aircraft in question. Since no explicit information was available to the contrary it was assumed in the calculations that the aircraft was able to maintain a straight and level flight condition at all incidences. It is pointed out later that this assumption is a probable source of discrepancy between calculated and actual flight characteristics.

The coefficients $\alpha_i, \beta_i, i = 1,\ldots 4$ for the H.P.115 over the incidence range are located in Table 3.2. The additional data ~~is~~ are relevant to the nonlinear study of the next section. Using the QR algorithm (NAG library subroutine F02AGF), the eigenvalues and eigenvectors of the system matrix in (3.3) were computed and are shown by the full lines in Figs. 3.2, 3.3, 3.4, In Fig. 3.2, the damping and frequency of the oscillation are shown in dimensional form as the real and imaginary parts of the complex eigenvalue. Instability is seen to occur when the damping passes through zero at $\simeq$ 23°, while the frequency increases steadily as the incidence increases. The two subsidence roots are shown in Fig. 3.3. The oscillatory roots are clearly well separated in modulus from the subsidence roots by virtue of the high frequency of the oscillation: Thus the first requirement for the application of the weakly coupled approximation is satisfied. The second condition relates to the modal content of eigenvectors associated with the eigenvalue sets. This information is given in Fig. 3.4. In particular the ratio (v/v_c) for the aperiodic modes and (v_c/v) for the oscillatory mode are small enough to validate the second assumption i.e. that the oscillatory mode is mainly in sideslip and the subsidences are mainly sideways motions. Both the assumptions on the root separation and modal content improve as the incidence increases.

The approximate characteristics using (3.9) and (3.10) are shown as the first approximation in Figs. 3.2 and 3.3. and can be seen to give very good agreement with the exact results. Application of the second approximation, (3.17) and (3.18), for the oscillatory damping and frequency achieves an excellent comparison, as shown in Fig. 3.2, over the incidence range considered. Using (3.22) the approximate dutch roll ratio (ϕ/v) , for the oscillation, can be obtained and compared with the exact ratio given by (3.19) where (v_0/v) is taken from Fig. 3.4. The comparison is shown in Fig. 3.4. as the second approximation. Note that the first approximation, given by $1/w_0$, would appear as a line on the real axis.

Flight experience with the H.P.115 revealed that the oscillatory mode became unstable at an incidence of approximately 19°, some 4° lower than the present predictions (REF. 3.6). It is thought that this discrepancy could be due in part to the assumption of constant height in the theory. There are indications (REF. 3.8 p.11) that the thrust available in the aircraft was not sufficient to maintain trimmed level flight at high incidence and hence a descent angle should be included in the analysis. The main effect of including this modification can be seen in the approximations derived. In the first approximation to the oscillation damping (3.13) it can be shown that, for a given flight incidence, the term (g_1/w_1) will increase with increasing descent angle and, since this term is destabilizing, the incidence at which the damping vanishes decreases. The approximation can therefore be used to explain the apparent discrepancy.

EXAMPLE 2 - The B.A.C. 221

This aircraft, with its ogee wing planform, was constructed with the aim of examining the aerodynamic and handling characteristics of slender aircraft at subsonic and supersonic speeds. The early part of the research programme was concerned with flight behaviour at low speeds. A general description of the low speed handling of the B.A.C. 221 can be found in REF. 3.9. The data appropriate to the present study are located in Table 3.3. and Fig. 3.5. together with a plan view of the wind tunnel model used to obtain the aerodynamic derivatives. The derivatives were extracted from REF. 3.10. and converted to a body axes system coincident with the principal axes of inertia. The C_L vs. α curve in Fig. 3.5. was taken from Fig. 1. of REF. 3.11. corresponding to trimmed elevator angles taken from REF. 3.12.

The α and β coefficients for the system matrix in (3.3) can be found in Table 3.4. The computed eigenvalues and eigenvectors in the dimensional form are displayed in Figs. 3.6 and 3.7. together with the weak coupling approximations. The approximation cannot be expected to give good results for $\alpha > 22^\circ$ since the requirement of root modulus separation is not satisfied and, indeed, the approximations become progressively worse at higher incidences. From Fig. 3.6. it can be see that at $\alpha \simeq 19^\circ$ a second oscillation, composed mainly of sideways motion (v_1) , forms and it is this oscillation which finally becomes unstable at $\alpha = 23.5^\circ$. The improvement in the approximation achieved by an application of the second approximation was insignificant at all values of incidence. Turning to the eigenvector

display, Fig. 3.7, again it can be see that the (V_c / V) ratio for the 'V' mode (top diagram) and the (V / V_c) ratio for the V_c mode (bottom diagram) are becoming large enough at $\alpha \simeq 22^0$ to deem the approximation invalid. Below this incidence the trend is predicted for the dutch roll ratio (middle diagram) by the second approximation although the out of phase component is somewhat lower than the exact values.

The peculiar characteristics of the B.A.C.221 at high incidence can be attributed to bursting of the concentrated vortex flow over the leeside wing surface predicted to occur at $\alpha \simeq 22^0$ (REF. 3.12). On the other hand observations in flight (REF. 3.13) indicate that vortex bursting does not occur on the H.P.115 wing until much higher incidences that are outside the range considered for this aircraft.

EXAMPLE 3 - The Prototype Concorde

The Concorde also has an ogee wing as shown in Fig. 3.8. although considerable design effort has achieved more satisfactory aerodynamic characteristics than the previous example, as will be seen. The relevant data located in Table 3.5. and Fig. 3.8. ~~was~~ were supplied to the author in the form of REF. 3.14. Included in the aerodynamic derivatives is the effect of the "moustaches" which are small foreplanes located on the underside of the nose. Also included in the data in Fig. 3.8. are estimates of the acceleration derivatives $\ell_{\dot v}$ and $n_{\dot v}$. It can be easily shown that the contribution from these derivatives merely affect the coefficients α_4 and β_4 in (3.3); in fact, the extra terms appear in exactly the same way as the ℓ_v and n_v terms appear in α_3 and β_3. Hence the additions to α_4 and β_4 become,

$$\delta\alpha_4 = Y_r^* \ell_{\dot v}^* + n_{\dot v}^* (Y_r^* - w_c^*) \qquad (3.22a)$$

$$\delta\beta_4 = \delta\alpha_4 + w_c \ell_{\dot v} \qquad (3.22b)$$

$$\ell_{\dot v}^* = \ell_{\dot v}' + n_{\dot v}' \tan\theta_c \quad ; \quad n_{\dot v}^* = n_{\dot v}'$$

where

$$\ell_{\dot v}' = \frac{\ell_{\dot v} + e_z n_{\dot v}}{\mu_2 i_{xx} (1 - e_x e_z)} \quad ; \quad n_{\dot v}' = \frac{n_{\dot v} + e_x \ell_{\dot v}}{\mu_2 i_{zz} (1 - e_x e_z)} \qquad (3.23)$$

The α and β coefficients for Concorde are tabulated in Table 3.6. The computed eigenvalues and eigenvectors for the system matrix in (3.3) are shown in Figs. 3.9 - 3.12. along with the approximation for comparison. The effect of the acceleration derivatives is exposed by including the eigenvalues for $\ell_{\dot v} = n_{\dot v} = 0$ (see Figs. 3.10, 3.11). The effect is seen to be quite small. Overall the approximations are less accurate than the previous examples particularly the second

approximation for the frequency of the oscillation (Fig. 3.9). The author has not been able to find a rational explanation for this situation. The magnitude of λ_1, as shown in Fig. 3.11. does make the assumption on the root modulus separation a little suspect and the ratios (v_c/v) for the oscillatory mode and (v/v_c) for the aperiodic modes in Fig. 3.12 are clearly not small compared to unity. However, the trends are predicted correctly and the reason for the improved stability of Concorde compared to the previous examples can be attributed directly to the relatively high and low magnitude of e_p and Ω_p respectively in the approximate damping given by (3.13).

We now consider the lateral motions of aircraft in more conventional low incidence flight situations.

3.3 Conventional Lateral Motions

We require to derive a form of (3.1) that is more suitable for approximating the classical spiral, dutch roll and roll subsidence modes. Let us assume that the oscillatory dutch roll mode is again dominated by the sideslip variables, $(v\ ;\ \dot{v})$ and that the roll mode is dominated by the roll rate p. As in the previous analysis for high incidence flight, we wish to separate the lateral velocity of the aircraft centre of gravity from the sideslip velocity except that for flight at low incidence any sideslip generated through rotary motions will arise mainly from yawing. In fact it is more appropriate to work in terms of 'stability axes' for the classical modes, in which case $w_c = 0$ and no sideslip is produced through rolling. The lateral acceleration (a more convenient variable to use) can then be written in the separated form,

$$\dot{v} = \dot{v}_0 - u_0 r \qquad (3.24)$$

Introducing (3.24) into (3.1) and eliminating the yaw rate r, the equations of motion can be fairly easily re-arranged in terms of the motion variables $\{\dot{v}_0, v, \dot{v}, p\}$. The system matrix can then be written in the three level, partitional form (REF. 3.15).

$$\begin{bmatrix} c_{11} & c_{12} & c_{13} \\ c_{21} & c_{22} & c_{23} \\ c_{31} & c_{32} & c_{33} \end{bmatrix} = \left[\begin{array}{c|c|c|c} y_r' n_r' + y_p' l_r' & y_r' n_v' + y_p' l_v' & y_v' - (y_r' n_r' + y_p' l_r') & g_1 + y_r' n_p' + y_p' l_p' \\ \hline 0 & 0 & 1 & 0 \\ -n_r' + y_r' n_r' + y_p' l_r' & -n_v' + y_r' n_v' + y_p' l_v' & y_v' + n_r' - (y_r' n_r' + y_p' l_r') & g_1 - n_p' + y_r' n_p' + y_p' l_p' \\ \hline l_r' & l_v' & -l_r' & l_p' \end{array}\right] \quad (3.25)$$

(Note - derivatives now in stability axes system)

As shown in (REF. 3.15) (for controlled longitudinal motions), the approximating polynomials for a three level partitional system (3.25) are given by,

$$\text{spiral mode} - \quad \det\left[\lambda I - C_{11} + \begin{bmatrix} C_{12} & C_{13} \end{bmatrix} \begin{bmatrix} C_{22} & C_{23} \\ C_{32} & C_{33} \end{bmatrix}^{-1} \begin{bmatrix} C_{21} \\ C_{31} \end{bmatrix}\right] = 0 \qquad (3.26)$$

$$\text{dutch roll mode} - \quad \det\left[\lambda I - C_{23} C_{33}^{-1} C_{32}\right] = 0 \qquad (3.27)$$

$$\text{roll subsidence mode} - \quad \det\left[\lambda I - C_{33}\right] = 0 \qquad (3.28)$$

With $y_p = y_r = 0$, the expanded forms of these approximate polynomials take the form,

$$\text{spiral mode} - \quad \lambda_1 = \frac{g_1 \left(n_r' e_v' - e_r' n_v'\right)}{n_v' e_p' + (g_1 - n_p') e_v'} \qquad (3.29)$$

$$\text{dutch roll mode} - \quad \lambda_{2,3}^2 - \left(y_v' + n_r' + \frac{e_r'}{e_p'}(g_1 - n_p')\right)\lambda_{2,3} + \left(n_v' + \frac{e_v'}{e_p'}(g_1 - n_p')\right) = 0 \qquad (3.30)$$

$$\text{roll subsidence mode} - \quad \lambda_4 = e_p' \qquad (3.31)$$

For cases where the dutch roll roots are of higher modulus than the roll subsidence root their relative position in the partitional system (3.25) can be reversed and the approximating polynomials become,

roll subsidence mode - $$\lambda_2 = e_{\rho}' + \frac{e_v'}{n_v'}(g_1 - n_{\rho}') \qquad (3.32)$$

dutch roll mode - $$\lambda_{3,4}^2 - (y_v + n_r)\lambda_{3,4} + n_v = 0 \qquad (3.33)$$

The expression for λ_1 remains unchanged.

We must expect that the dutch roll damping given by (3.30) and (3.33) will be in error except in special situations. Once again the error will be due to the assumption that this mode can be described in terms of the sideslip velocity of the aircraft referred to an axes system passing through the centre of gravity. The approximation to the small spiral root given by (3.29) and the roll subsidence root given by (3.31) are well established results (REF. 3.5 p.418) and do not require further comment.

We will now apply the foregoing analysis to two examples which serve to show the attributes and shortcomings of the approximation technique. The examples are taken from American texts and hence the notation is slightly different; details of the relevant conversion are given in Appendix A.

EXAMPLE 1 - North American X.B.-70.1 in horizontal flight

This example is taken from REF. 3.16, where detailed descriptions of the flight conditions are given at three Mach numbers. The relevant data for the present study can be found in Table 3.7. All three flight conditions are at low C_L values and although the aircraft in question has a slender delta wing we might expect the natural modes to resemble the classical form. The computed eigenvalues and corresponding approximations derived from (3.29), (3.30) and (3.31) are compared in Table (3.8).

The comparisons show fairly good agreement although the oscillation damping is, once again, not too well predicted. One could carry out a perturbation analysis, assuming small damping in this mode, to find the contribution to the damping force from the other approximate modes (V_c and p motion) but this improvement will not be pursued in this thesis.

EXAMPLE 2 - Hypothetical Jet Transport

This example forms the basis of the numerical studies in REF. 3.17, where full details of the geometric, inertia and aerodynamic characteristics are given. The data pertinent to the present study are located in Table 3.9. Following the presentation in REF. 3.17, we will investigate the stability characteristics of this aircraft over the speed range $250 < V < 800$ ft/s. In REF. 3.17(p.370) approximations are derived for these characteristics that correspond very closely to those given by (3.29), (3.32) and (3.33) though based on somewhat different physical and mathematical arguments.

The computed and approximate characteristics are shown in Figs.3.13 and 3.14 as the number of cycles to half amplitude ($N_{\frac{1}{2}}$) and the period T for the oscillation and the dimensional eigenvalues for the aperiodic modes. For the latter the agreement is seen to be excellent. The period of the oscillation is also predicted well but the damping (hence $N_{\frac{1}{2}}$) becomes progressively worse as the speed decreases. This error must be attributed to the inability of a purely sideslip motion to approximate the oscillatory mode. There is strong evidence (REF. 3.5 p.424), of course, that the derivatives C_v and n_v have a significant effect on the oscillatory stability boundary for conventional aircraft configurations whereas, as in the case of inertially slender configurations, the approximate damping given by (3.33) shows no dependence on these sideslip derivatives. To incorporate these effects one would have to derive a similar approximation with reference to an axis system that does not pass through the aircraft centre of gravity, or carry out a perturbation analysis on the full equation of motion to include the coupling with the sideways and roll mode. Neither of these possible improvements is attempted in this thesis.

Since the lower speeds of the present example correspond to quite high incidences it might be expected that the approximations derived for flight at high incidence, assuming a mainly rolling oscillation, would be more appropriate here. Converting the derivatives to geometric body axes and finding the approximate damping as given by (3.13) shows a hopeless comparison with instability being predicted at the lower speeds. It seems that this type of approximation should be retained for inertially slender aircraft.

The approximations developed in this section serve mainly to illustrate how the various aerodynamic derivatives (hence design features) inertial properties and gravitational components combine to produce the dynamic characteristics of the aircraft lateral motions. Armed with this, hopefully more wholesome, understanding of the linear problem we now embark on an investigation of nonlinear problems of lateral dynamics, in particular those associated with aerodynamic nonlinearity.

CHAPTER 4 - NONLINEAR SIDESLIP OSCILLATIONS AT HIGH INCIDENCE

4.1 Introduction

The results of the previous chapter indicate that for slender configurations flight at high incidence might be impaired by a reduction in the damping of the oscillatory mode. In the event that a high enough incidence is reached to cause instability in this mode it is of interest to know how the motion will develop. Generally speaking, we would like to know whether the stability boundary is safe in the sense that motions will be self limiting or dangerous where the instability persists with growing amplitudes. We also require to know how stable is flight at incidences lower than the critical value since a large enough disturbance may cause a divergent motion to develop. The linear theory is clearly inadequate in this respect and hence we need to consider any nonlinear effects that exist.

The predictions of the linear theory reveal that, at least for the H.P.115 aircraft, the oscillatory mode of interest involves mainly sideslip motion and therefore it is to be expected that any nonlinearity of the rolling and yawing moments with sideslip velocity will have a significant effect on the oscillation. Results from the data sources of all three slender aircraft considered indicate that both the static aerodynamic moments have a nonlinear variation with sideslip velocity at high incidence. These variations are primarily caused by the changes in position and strength of the vortices over the wing and those springing from the forebody. Any vortex bursting that occurs will add further substance to the nonlinear effect. Assuming that the aerodynamic moments are asymmetric functions of sideslip angle it is straightforward to incorporate these nonlinearities into the equations of motion developed in Appendix A. This is achieved by allowing the derivatives ℓ_v and n_v to depend on v in a symmetric fashion.

A second nonlinear effect will appear in the gravitational term in the sideforce equation and in the kinematic relations if the roll angle is not assumed small. To simplify the analysis we will neglect this effect which will in fact only begin to make its presence felt for roll angles greater than about 20°. The restrictions of the nonlinearity to one variable does give rise to far reaching simplifications in the analysis and with this in mind we make the further assumption that the inertial nonlinearities are negligible. This assumption is justifiable if the angular rates are small.

This leads us to the third assumption of constant incidence during the oscillation and this is perhaps the most significant. If we assume that the oscillation is a pure rolling motion about an axis coincident with the incidence datum line then the incidence will be related to the roll angle ϕ through the expression.

$$\tilde{N} = \sin\theta_c \cos\phi \qquad (4.1)$$

When θ_c is 25° and ϕ is 20° the incidence $\tilde{W}$ is reduced to about 23.4°. Now if the aerodynamic derivatives are changing significantly at high incidence then it could be argued that any effect that changes the incidence by only $1\frac{1}{2}^{\circ}$ should contribute to the development of the motion. Indeed, if the measured damping on a purely rolling wind tunnel model passes through zero at some incidence then the oscillatory motion could be self limiting due to the variation of the damping with roll angle through the mechanism described above. A real example having this characteristic will be described in the next chapter but for the case of an aircraft in flight we must also take into account the response in the longitudinal motion. Any incidence changes due to wing rolling will give rise to a response primarily in the short period mode with incidence changes of the same order as those initially caused by the lateral motion. The problem will thus grow considerably in complexity and therefore for the main part of the forthcoming analysis we will assume that the aerodynamic derivatives remain constant during the oscillation at the values appropriate to the trimmed flight state.

4.2 Approximations for the Nonlinear Theory

We therefore proceed to investigate the effect of the above mentioned aerodynamic nonlinearity on the lateral oscillation of slender aircraft. Assuming the aerodynamic moments to have a cubic variation with sideslip velocity we can write,

$$n_v(v) = n_{v_0} + n_{v_2} v^2 \qquad (4.2)$$

$$\ell_v(v) = \ell_{v_0} + \ell_{v_2} v^2 \qquad (4.3)$$

For this representation the equations of motion in the sideways/sideslip partioned form can be readily obtained simply by replacing the constant sideslip derivatives n_v, ℓ_v by their nonlinear counterparts given in (4.2), (4.3).

The equations therefore take the same basic form as (3.3) with α_3 and β_3 now functions of V. In fact, we can write,

$$\alpha_3(v) = \alpha_{3_0} + \alpha_{3_2} v^2 \qquad (4.4)$$

$$\beta_3(v) = \beta_{3_0} + \beta_{3_2} v^2 \qquad (4.5)$$

Where α_{3c}, β_{2c} are given by the linearised expression (3.4c) and (3.4g), and,

$$\alpha_{32} = y_p^* \rho_{v2}^* + n_{v2}^* (y_r^* - v_0^*) \qquad (4.6)$$

$$\beta_{32} = (y_p^* + w_c) \rho_{v2}^* + n_{v2} (y_r^* - v_c^*) \qquad (4.7)$$

Where ρ_{v2}^* and n_{v2}^* can be written in terms of ρ_{v2} and n_{v2} in exactly the same way as ρ_v and n_v given by (3.5), (A.10) and (A.11). The equations then take the same form as (2.57), (2.58) and we will therefore begin the analysis of the nonlinear problem by applying the approximations derived in Chapter 2 for these equations. We therefore assume that the coefficients β_1, β_2, β_4 and the combination $\beta_{32} v^2$ are small so that we can write the equations in the form (2.60), (2.61) suitable for application of the perturbation scheme.

A result of particular importance is the approximate amplitude envelope $a_0(\tau)$ given by (2.69), which can be written in the form,

$$\frac{da_0}{d\tau} = \frac{1}{2}\left\{ 2\mu^* + \frac{3}{4}\alpha_{32}\left(\frac{\beta_1\alpha_2 - \beta_2(\omega_c^2 + \alpha_1)}{(\omega_c^2 + \alpha_1)^2 + \alpha_2^2\omega_c^2} \right) a_0^2 \right\} a_0 \qquad (4.8)$$

where μ^* is the approximate linear damping given by (3.17). The limit cycles are therefore obtained by equating the right side of (4.8) to zero.

Assuming $\omega_c^2 >> \alpha_1$, which will generally be the case and writing,

$$\alpha_{32} = n_{v2} (j_1 + j_2 \gamma_2) \qquad (4.9)$$

$$\beta_{32} = n_{v2} (k_1 + k_2 \gamma_2) \qquad (4.10)$$

with

$$j_1 = \frac{y_p' e_x + (y_r' - \frac{i}{U_c})}{(1-e_x e_3)\mu_2 i_{zz}} \quad ; \quad j_2 = \frac{y_p' + e_z (y_r' - 1/U_c)}{(1-e_x e_z)\mu_2 \; i_{xx}}$$

$$k_1 = \frac{(y_p' + W_c) e_x + (y_r' - U_c)}{(1-e_x e_z)\mu_2 i_{zz}} \quad ; \quad k_2 = \frac{(y_p' + W_c) + e_z (y_r' - U_c)}{(1-e_x e_z)\mu_2 \; i_{xx}} \tag{4.11}$$

and $\gamma_2 = \rho_{v_2} / n_{v_2}$, we can express the limit cycles of (4.8) in the form,

$$\sigma_L = \frac{3}{4} n_{v_2} V_L^2 = \frac{2\mu^* (\alpha_2^2 - \beta_{3c})}{(j_1 + j_2 \gamma_2)(\frac{\beta_1 \alpha_2}{\beta_{3c}} + \beta_2)} \tag{4.12}$$

where V_L $(= a_c(\omega))$ is the sideslip amplitude in the limit cycle. The frequency of the limit cycle oscillation can be obtained from (2.70) and reduces to the form,

$$\omega_L = \omega^* - \frac{1}{2(-\beta_{3c})^{\gamma_2}} \left\{ k_1 + k_2 \gamma_2 - \frac{(j_1 + j_2 \gamma_2)}{\alpha_2^2 - \beta_{3c}} (\beta_1 + \beta_2 \alpha_2) \right\} \sigma_L \tag{4.13}$$

where ω^* is given by (3.18)

The limit cycle function σ_L , given by (4.12), for the H.P.115 described in the previous section, is displayed in Fig. 4.1. for various values of γ_2 . The nearly linear variation of σ_L with incidence can be attributed to the nearly linear variation of the Routhian for the H.P.115 in the vicinity of the critical incidence (α_c) . The close connection of the incidence dependent terms in (4.12) and the Routhian was revealed in Chapter 2 (cf. 2.72). An examination of Fig. 4.1. clearly shows where the present approximation predicts limit cycles. They can exist at incidences both above and below the critical value. Thus if Ω_{v_2} is negative, limit cycles can exist for $\alpha > \alpha_c$ only if ρ_{v_2} is positive; the situation is reversed for $\alpha < \alpha_c$. For Ω_{v_2} positive and $\alpha > \alpha_c$, limit cycles are possible for all positive values of ρ_{v_2} and a limited range of negative values; again the situation is reversed for $\alpha < \alpha_c$. It is intuitively clear that all limit cycles for $\alpha > \alpha_c$ represent stable periodic solutions and all limit cycles for $\alpha < \alpha_c$ represent unstable periodic solutions. This is because the asymptotic stability of the equilibrium trim state for $\alpha < \alpha_c$ and the instability of the trim state for $\alpha > \alpha_c$ are not effected by the nonlinear terms in the equations of motion.

An interesting feature of the present approximation is that it points directly to the nonlinear coupling term $\alpha_{32} v^2$, in the sideways motion equation, as the main cause of the limit cycle behaviour. According to (4.12)if α_{32} is zero then no limit cycles are possible. If we ignore the small derivatives $y_{p'}$ and $y_{r'}$ in the expressions for j_1 and j_2 in (4.11) then this condition is satisfied when,

$$\Omega_{v_2} + e_x \rho_{v_2} = 0 \qquad (4.14)$$

If this is the case, then providing the oscillation remains a primarily sideslip motion, there is no mechanism in the sideways equation to produce the phase change between sideslip and sideways motion to stabilise the oscillation.

Another result to be gleaned from (4.12) is that the limit cycle behaviour is a strong function of the product of inertia term e_x . In fact if the product of inertia is zero then the function σ_L is a very weak function of γ_2 indeed, indicating that, although yawing motion is practically absent, the yawing moment $\Omega_v(v)\, v$ can be large and have a significant effect on the damping of the motion. It should be noted that if (4.14) is satisfied at the critical incidence or, more correctly when μ^* vanishes, then the function σ_L becomes indeterminate indicating that the equilibrium in the $(v, \dot{v}')$ phase portrait remains a centre after the inclusion of the nonlinear cubic terms. The significance of this condition will be explored further following an application of the more extensive approximation method outlined in section 2.5.

The transient response characteristics of the nonlinear oscillation can be determined by solving (4.8). The solution to an equation of this type is given by (2.29), which, for (4.8) takes the form,

$$q_0(\tau) = \frac{e^{\mu\tau}}{\left(k_0 + \frac{e^{2\mu\tau}}{V_L^2}\right)^{1/2}} \qquad (4.15)$$

where k_0 is a constant depending on the initial conditions. Note that, from (4.12), V_L^2 can actually be negative, implying that V_L does not exist. Now (4.15) can be written in the simpler form,

$$\psi(\tau) = \frac{\chi(\tau)}{1+\chi(\tau)} \qquad (4.16)$$

where $\chi = e^{2\mu\tau}/k_0 V_L^2$, $\psi = \left(\frac{q_0(t)}{V_L}\right)^2$

The different types of transient behaviour depicted by (4.15) can be illustrated by the function ψ in (4.16) for three ranges of χ .

(a) $\chi > 0$ the oscillation grows up to or decays away from the stable or unstable limit cycle respectively, at $\psi = 1$; $k_0 V_L^2 > 0$

(b) $-1 < \chi < 0$ no limit cycle exists and the oscillation grows unbounded or decays to zero depending on the sign of M . $k_0 V_L^2 < 0$ since $V_L^2 < 0$

(c) $\chi < -1$ again limit cycles are at $\psi = 1$ and oscillation either grows away from or decays to steady value for initial values outside limit cycle. $k_0 V_L^2 < 0$ since $k_0 < 0$

We now turn to the application of the second approximation scheme developed in Chapter 2 whereby the system equations are transformed into a canonical form (2.73a), (2.73b) serving to separate the critical and non-critical variables of the equations. By setting to zero the contributions from the non-critical variables in the equation for the critical variables we attempt, as described in

Chapter 2, to deduce the periodic solutions that bifurcate off the linear oscillation $Ce^{s\omega t}$ by analysing the abbreviated two-dimensional critical subsystem (2.83). Again, by incorporating the slow time scale τ in the analysis we are able to determine the behaviour of trajectories close to the periodic solutions; in other words the transient response functions and associated limit cycles.

Since the nonlinearity appears only in the sideslip velocity V it is convenient to transform the equation of motion into the fourth order nonlinear companion form for which the analysis is presented in section 2.6. It is quite straightforward to obtain the required equation from the nonlinear form of (3.3) and this can be expressed in the same form as (2.95), i.e.

$$\frac{d^4V}{dt^4} + a_1\frac{d^3V}{dt^3} + \frac{d^2b(v)}{dt^2} + \frac{d\,c(v)}{dt} + d(v) = 0 \qquad (4.17)$$

The coefficient a_1 and the functions $b(v)$, $c(v)$, $d(v)$ can be written in terms of the α and β coefficients of (3.3) as follows,

$$a_1 = -(\alpha_2 + \beta_4) \qquad (4.18a)$$

$$b(v) = b_1V + b_3V^3 = (-\beta_{3c} - \alpha_1 + \alpha_2\beta_4 - \alpha_4\beta_2)V - \beta_{32}V^3 \qquad (4.18b)$$

$$c(v) = c_1V + c_3V^3 = (\beta_{3c}\alpha_2 - \alpha_{3c}\beta_2 + \alpha_1\beta_4 - \beta_1\alpha_4)V + (\beta_{32}\alpha_2 - \alpha_{32}\beta_2)V^3 \qquad (4.18c)$$

$$d(v) = d_1v + d_3V^3 = (\beta_{3c}\alpha_1 - \alpha_{3c}\beta_1)V + (\beta_{32}\alpha_1 - \alpha_{32}\beta_1)V^3 \qquad (4.18d)$$

Where the linear coefficients are given in (3.4) and the nonlinear coefficients α_{32}, β_{32} are given in (4.6), (4.7). In terms of the aerodynamic derivatives the coefficients b_1, b_3 etc. take the form,

$$a_1 = -y_v' - e_p' - n_r'$$

$$b_1 = e_p' y_v' + e_p' n_r' + y_v' n_r' - e_r' n_p' - e_{v_0}'(y_p' + w_0) - n_{v_0}'(y_r' - v_0)$$

$$c_1 = y_v'(e_r' n_p' - n_r' e_p') + (y_p' + w_0)(e_{v_0}' n_r' - e_r' n_{v_0}') + (y_r' - v_0)(e_p' n_{v_0}' - n_p' e_{v_0}') - g_1(e_{v_0}' + n_{v_0}' \tan\theta_0)$$

$$d_1 = -g_1(n_{v_0}'(e_r' - e_p' \tan\theta_0) - e_{v_0}'(n_r' - n_p' \tan\theta_0))$$

$$b_3 = -e_{v_2}'(y_p' + w_0) - n_{v_2}'(y_r' - v_0)$$

$$c_3 = e_{v_2}'(n_r'(y_p' + w_0) - n_p'(y_r' - v_0) - g_1) + n_{v_2}'(e_p'(y_r' - v_0) - e_r'(y_p' + w_0) - g_1 \tan\theta_0)$$

$$d_3 = -g_1(n_{v_2}(e_r' - e_p' \tan\theta_0) - e_{v_2}'(n_r' - n_p' \tan\theta_0)) \qquad (4.19)$$

The abbreviated critical system to be analysed takes the form of (2.108) with the amplitude envelope and frequency correction given by (2.110) and (2.116) respectively. To proceed with the analysis we require to determine the artificial values of a_1, b_1, c_1, d_1 necessary to maintain a zero Routhian over the whole incidence range of interest. We choose these coefficients so that the two non-critical eigenvalues (λ_1, λ_2) and the linear oscillation frequency (ω_c) are preserved correctly over the incidence range. Therefore, setting,

$$a_1 = a_{10} + \varepsilon a_{11} \qquad b_1 = b_{10} + \varepsilon b_{11}$$

$$c_1 = c_{10} + \varepsilon c_{11} \qquad d_1 = d_{10} + \varepsilon d_{11} \qquad (4.20)$$

we require that a_{1c}, b_{1c}, c_{10} and d_{10} satisfy the relations, (cf. 2.98).

$$a_{10} = -(\lambda_1 + \lambda_2) \qquad c_{10} = a_{10}\,\omega_0^2$$

$$b_{10} = \lambda_1\lambda_2 + \omega_0^2 \qquad d_{10} = \omega_0^2\,\lambda_1\lambda_2 \qquad (4.21)$$

so that,

$$a_{10}\,b_{10}\,c_{10} - c_{10}^2 - a_{10}^2\,d_{10} = 0 \qquad (4.22)$$

The appropriate values of the coefficients a_{10}, b_{10}, c_{10}, d_{10} for the H.P.115, satisfying (4.21) and (4.22) are given in Table 4.1. for the incidence range $20^\circ \leqslant \alpha \leqslant 26^\circ$.

The amplitude envelope for the present approximation is given by (2.110) and the steady state limit cycle amplitude by (2.115). The latter can be written in the form,

$$\sigma_L = \frac{3}{4}\,n_{v_2}V_L^2 = \frac{2\mu\Delta}{\ell_1 + \ell_2\,Y_2} \qquad (4.23)$$

Where V_L is the sideslip velocity amplitude in the limit cycle, μ is the damping in the oscillation (Real part of complex eigenvalue),

$$\Delta = a_{10}\,(b_{10}^2 + c_{10}a_{10} - 4d_{10}) \qquad (4.24)$$

$$Y_2 = \ell_{v_2}/n_{v_2} \qquad (4.25)$$

ℓ_1 and ℓ_2 are the coefficients of n_{v_2} and ℓ_{v_2} in the denominator R_2 of (2.115).

$$R_2 = a_{10} c_{10} b_3 + a_{10} b_{10} c_3 - a_{10}^2 d_3 - 2 c_{10} c_3 \qquad (4.26)$$

ℓ_1 and ℓ_2 are thus obtained from (4.19) in conjunction with (A.9), (A.10) and (A.11), and are included in Table (4.1.) for the H.P.115 example, along with μ and Δ .

The sideslip limit cycle function σ_L can be computed with the data of Table 4.1. and is shown by the full lines in Fig.4.2. for various values of γ_2 (bifurcation theory approximation). In general the agreement with the previous approximation (Fig.4.1.) is seen to be fairly good. The frequency correction is given by (2.117) and hence the frequency ratio in the limit cycle can be written in the form

$$\left(\frac{\omega}{\omega_c}\right)^2 = 1 + \frac{C_3(\alpha, \gamma_2)}{c_{10}\, n_{v_2}} \sigma_L \qquad (4.27)$$

where ω_c is the linear oscillation frequency. The results for the frequency ratio corresponding to the computed values of σ_L are shown in Fig. 4.3. as the full lines.

The results of the present approximation indicate that the vanishing of the denominator in (4.23) is again closely approximated by (4.14) i.e. when the effective value of the nonlinear sideslip derivative, $\bar{n}_{v_2} = n_{v_2} + \ell_4 \ell_{v_2}$, vanishes. Again, if this occurs at the critical incidence when μ vanishes then the equilibrium at this incidence remains a centre in the third approximation. That this is actually the case for any values of the coefficients b_3 , c_3 , and d_3 can be seen if we search for periodic solutions of the non-linear companion problem given by (4.49) in terms of Jacobian Elliptic functions.

Setting

$$V(t) = a\, C_n(\omega t, k) \qquad (4.28)$$

we can write,

$$\frac{dV}{dt} = -\omega a\, S_n(\omega t, k)\, D_n(\omega t, k) \qquad (4.29)$$

$$\frac{d^2V}{dt^2} = -w^2(1-2k^2)V - \frac{2w^2k^2}{a^2}V^3 \qquad (4.30)$$

$$\frac{d^3V}{dt^3} = -w^2(1-2k^2)\frac{dV}{dt} - \frac{6w^2k^2}{a^2}V^2\left(\frac{dV}{dt}\right) \qquad (4.31)$$

$$\frac{d^4V}{dt^4} = -w^2(1-2k^2)\frac{d^2V}{dt^2} - \frac{6w^2k^2}{a^2}\left(V^2\frac{d^2V}{dt^2} + 2V\left(\frac{dV}{dt}\right)^2\right) \qquad (4.32)$$

Multiply (4.30) by an arbitrary constant δ_2 and (4.31) by δ_1, by adding (4.30), (4.31) and (4.32), we obtain

$$\frac{d^4V}{dt^4} + \delta_1\frac{d^3V}{dt^3} + \frac{d^2}{dt^2}\left[\left(\delta_2 + w^2(1-2k^2)\right)V + \frac{2w^2k^2}{a^2}V^3\right] +$$

$$+ \frac{d}{dt}\left[\delta_1\left(w^2(1-2k^2)V + \frac{2w^2k^2}{a^2}w^3\right)\right] +$$

$$+ \delta_2\left[w^2(1-2k^2)V + \frac{2w^2k^2}{a^2}V^3\right] = 0 \qquad (4.33)$$

If we now associate the coefficients in (4.33) with the coefficients a_1, b_1, c_1, d_1, b_3 etc. given by (4.18), then two of the necessary conditions for (4.28) to be an exact solution of (4.17) can be written in the form,

$$a_1b_1c_1 - c_1^2 - a_1^2d_1 = 0$$

$$a_1b_1c_3 + a_1c_1b_2 - d_3a_1^2 - 2c_1c_3 = 0 \qquad (4.34)$$

The first of these conditions is easily recognised as the vanishing of the Routhian while the second corresponds to the vanishing of R_2 in (4.26). The amplitude a is of course arbitrary and hence this oscillation will have the character of a centre in the $(v, \dot{v})$ plane.

The use of Elliptic functions for fourth order problems such as the companion problem described above does seem to have some potential. A perturbation procedure based on these functions could be developed but the author has found difficulties in the selecting of the periodicity conditions for the higher order approximation. As a result of this these ideas will not be pursued any further in this thesis.

Returning to the main theme of the Chapter it is appropriate, before comparing the results obtained with numerically integrated solutions, to examine a third approximate technique mentioned in Chapter 2. Assuming a Fourier Series expansion for the sideslip limit cycle oscillation, we write, as a first approximation to a symmetric oscillation,

$$V(t) = V_L \cos \omega t \tag{4.35}$$

Substituting (4.35) and its time derivatives into (4.17) and equating the components of $\cos \omega t$ and $\sin \omega t$ to zero, we obtain the two relations,

$$a_1 \left(b_1 + \tfrac{3}{4} b_3 V_L^2\right)\left(c_1 + \tfrac{3}{4} c_3 V_L^2\right) - \left(c_1 + \tfrac{3}{4} c_3 V_L^2\right)^2 - a_1^2 \left(d_1 + \tfrac{3}{4} d_3 V_L^2\right) = 0 \tag{4.36}$$

$$\omega^2 = \frac{c_1 + \frac{3}{4} c_3 V_L^2}{a_1} \tag{4.37}$$

These relations are simply the nonlinear Routhian and frequency obtained by adding to the linear coefficients b_1, c_1, d_1 the nonlinear coefficients $\frac{3}{4} b_3 V_L^2$, $\frac{3}{4} c_3 V_L^2$, $\frac{3}{4} d_3 V_L^2$. Now (4.36) is a bi-quadratic in V_L^2 and can be written as,

$$\frac{9}{16}\left(a_1 b_3 c_3 - c_3^2\right) V_L^4 + \frac{3}{4}\left(a_1 b_1 c_3 + a_1 c_1 b_3 - 2 c_1 c_3 - a_1^2 d_3\right) V_L^2 + a_1 b_1 c_1 - c_1^2 - a_1^2 d_1 = 0 \tag{4.38}$$

The constant term in (4.38) is recognised as the linear Routhian R_0 .

Introducing the limit cycle amplitude function σ_L and the parameter γ_2 as defined in (4.23) and (4.25) respectively, we can write (4.38) in the convenient form,

$$(m_2\gamma_2^2 + m_1\gamma_2 + m_0)\sigma_L^2 + (n_1\gamma_2 + n_0)\sigma_L + R_0 = 0 \qquad (4.39)$$

Now (4.39) will admit, for a given value of γ_2 , either two real values of σ_L or a complex conjugate pair. The significance of the two solutions can be understood in the following terms. Since the quantities $\frac{3}{4} n_{v_2} v_L^2$ and $\frac{3}{4} \ell_{v_2} v_L^2$ can be regarded as increments in the sideslip derivatives n_{v_0} and ℓ_{v_0} then (4.39) can be interpreted as an equation defining the locus of points on the (n_v, ℓ_v) plane for which the Routhian vanishes. Such stability diagrams are familiar in stability and control work and examples can be found in most text books (REF. 3.5 p.424). The two real solutions to (4.39) have the following meaning. The Routhian for a fourth order system vanishes when two roots of the characteristic equation (eigenvalues of the system matrix) are equal in magnitude but opposite in sign. This situation occurs when the real part of a complex conjugate pair vanishes or when two real roots of equal modulus have opposite signs. For the linear problem the two cases are distinguished by the sign of the ratio of the coefficients c_1 and a_1 i.e. the coefficients of λ and λ^3 in the characteristic equation. If c_1 and a_1 have the same sign then a vanishing Routhian corresponds to a complex pair crossing the imaginary axis in the complex plane, whereas if c_1 and a_1 are of opposite sign a vanishing Routhian signifies that two equal and opposite real roots exist. For the case of (4.39) then, only the former case is of interest so that when two real solutions for σ_L exist, the one corresponding to the real frequency, given by (4.37), is the correct limit cycle value.

The numerical values for the coefficients m_0 , m_1 , m_2 etc. in (4.39) for the H.P.115 over the incidence range of interest are given in Table 4.2. The computed values of σ_L for various values of γ_2 are displayed, along with the previous approximation, as the broken lines in Fig. 4.2. (denoted Nonlinear Routhian approximation). The frequency ratio, computed from (4.37) are compared in Fig. 4.3. The similar trends produced by all three approximations is certainly encouraging. Some numerically integrated solutions using Merson's Method are shown in these figures. Only the stable limit cycles for $\alpha > 23\frac{1}{2}^0$ were investigated numerically and the agreement is seen to be very good indeed. Fig. 4.4. is a portion of the numerically integrated limit cycle response for the H.P.115 at 26^0 incidence with $\gamma_2 = 0$ and $n_{v_2} = 20\, n_{v_0}$ which serves to illustrate the main characteristics of the oscillatory motion. We see that the normalized yaw rate $\bar{r}$ is small enough for our previous assumptions

regarding sideslip generated by yaw to be valid. The roll rate $\bar{p}$ can thus be assumed to be 90^{o} out of phase with the roll angle ϕ. The motion can therefore be seen as a primarily rolling oscillation with a small component of sideways velocity $\bar{v}_c$. The roll angle in the limit cycle is about 17^{o} maximum. When $\bar{p}$ is a maximum, corresponding to zero roll angle then $\bar{v} = \bar{v}_c$. Therefore as the aircraft passes through zero roll angle, in rolling from port to starboard, it also has a residual sideways velocity $\bar{v}_c$ to port. The oscillation can be described as an 'inside the barrel' roll. The phase angle between $\bar{v}$ and $\bar{v}_c$ is crucial to the development of the limit cycle. From Fig. 3.4. we see that linear theory predicts a phase angle of approximately 76^{o} between sideslip velocity $\bar{v}$ and sideways velocity $\bar{v}_c$. The maximum amplitude ratio is about 0.24. The phase angle in the limit cycle can be estimated from Fig. 4.4. to be about 66^{o} with the amplitude ratio $(\bar{v}_c/\bar{v})$ remains about 0.24. This change in phase angle of about 10^{o} takes place as the oscillation is growing and finally results in a 'stabilisation' of the motion.

4.3 Assessment of the Various Approximations and Review of Assumptions.

It is appropriate at this stage to discuss to some extent the relative merits of the foregoing approximations for the nonlinear oscillations of slender aircraft at high incidence. It is not intended to enter into a detailed value analysis of the different methods but instead the main attributes and weaknesses are exposed.

The use of the sideslip/sideways weak coupling analysis relies on a fairly good ~~instructive~~ *intuitive* understanding of the problem at hand. A correct choice of motion variables for the partioned form of the system equations obviously depends on a knowledge of the physical nature of the aircraft motions. If the assumed physical basis for the approximation scheme yields successful results then it is clear that the use of this technique will substantially add to our understanding of the problem. This is certainly the case in the application to the H.P.115 aircraft. The sideslip coefficient n_{v_2}, associated with a conservative force in purely sideslip motion, gives rise to what are essentially non-conservative forces when sideslip and sideways motions are coupled. If we consider, instead of the geometric body axis sideslip v, a more general sideslip velocity associated with an axes displaced from the aircraft centre of gravity, then the actual manner in which the derivative n_v enters the damping of the oscillation, can be clearly seen. To simplify the analysis we will assume that all the derivatives due to roll and yaw rates and the sideslip derivative y_v are zero. The sideforce, rolling and yawing moment equations then take the form,

$$\dot{v} - W_o p + U_o r - g_1 \phi = 0 \qquad (4.40)$$

$$\dot{p} - e_v^* v = 0 \qquad (4.41)$$

$$\dot{r} - n_v^* v = 0 \qquad (4.42)$$

Differentiating (4.40) with respect to time and combining with (4.42), the three equations above can be reduced to two in the variables V and ϕ .

$$\ddot{V} - W_0 \dot{\phi} + U_0 n_v^* \dot{V} - g_1 \phi = 0 \qquad (4.43)$$

$$\dot{\phi} - \rho_v^* V = 0 \qquad (4.44)$$

We now introduce a new sideslip velocity V_1 referred to an axis displaced a normalised distance z_c along the body z axis from the aircraft centre of gravity. Let,

$$V_1 = V + z_c \phi$$

Eliminating V from (4.43), (4.44) we can write,

$$\ddot{V}_1 - z_0 \rho_v^* (\dot{V}_1 - z_0 \dot{\phi}) - W_0 \dot{\phi} + U_0 n_v^* (V_1 - z_c \phi) - g_1 \phi = 0 \qquad (4.45)$$

$$\dot{\phi} - \rho_v^* (V_1 - z_0 \phi) = 0 \qquad (4.46)$$

If we assume that the roll rate ϕ is approximately equal to the rate of change of the Euler angle ϕ , the sideways velocity can be introduced with the relation,

$$\phi = \frac{\dot{V}_1 - \dot{V}_0}{W_c \gamma_1} \qquad (4.47)$$

where $\gamma_1 = 1 + \frac{z_c}{W_c}$

Substituting for ϕ and $\dot{\phi}$ in (4.45) and (4.46) using (4.47) the equation can be written in the form,

$$\nu_2 \ddot{V}_c + (1-\nu_2)\ddot{V}_1 + \left(\frac{g_1 + U_c n_{v^*} z_c}{W_c \nu_1}\right)\dot{V}_c -$$

$$-\left[\frac{g_1 + U_c n_{v^*} z_c}{W_c \nu_1} + z_c \rho_{v^*}\right]\dot{V}_1 + U_c n_{v^*} V_1 = 0 \qquad (4.48)$$

$$\ddot{V}_1 - \ddot{V}_c - W_c \nu_1 \rho_{v^*} V_1 + \rho_{v^*} z_c (\dot{V}_1 - \dot{V}_c) = 0 \qquad (4.49)$$

where $$\nu_2 = \frac{W_c - z_c^2 \rho_{v^*}}{W_c \nu_1}$$

Eliminating the $\ddot{V}_1$ term in (4.48) and the $\ddot{V}_c$ term in (4.49) we can write the equation in the first order form given by (3.3). The expression for the damping in the V_1 mode corresponds to the coefficient β_4 in (3.3) and we denote this by β_4^*. Hence we obtain,

$$\beta_4^* = \frac{(g_1 + U_c n_{v^*} z_c)}{W_c \nu_1} + z_c \rho_{v^*} - \nu_2 \rho_{v^*} z_c \qquad (4.50)$$

If we now assume that z_c is small enough to warrant neglecting terms involving powers of z_c higher than the first, (4.50) reduces to,

$$\beta_4^* \simeq \frac{g_1}{W_0}\left(1 - \frac{z_c}{z_2}\right) + \frac{U_c}{W_0} z_c n_{v^*} \qquad (4.51)$$

With z_c equal to zero, β_4^* reduces to β_4 in (3.4h) with the aerodynamic derivatives set to zero. The expression for β_4^* illustrates how the derivative n_v, at least for the simplified model considered, effects the damping of the oscillation. Thus if z_c is negative, implying an oscillation axis positioned above the aircraft, the contribution from a positive n_{v^*} to the damping is stabilising. The same line of reasoning can be applied to the nonlinear case when n_v depends on V in a quadratic fashion i.e. a positive n_{v_2} is stabilising and a negative n_{v_2} is destabilising.

Generally speaking the oscillatory lateral motion of an aircraft can be defined as a sideslip motion about some axis displaced and rotated about the body X axis. Along with the frequency and damping of the oscillation, the position of this oscillation axis could serve as a useful guide in characterising the oscillatory mode and hence in defining suitable handling qualities. Without intending to discuss aspects of handling qualities in any detail it is interesting to examine a particularly useful quantity of paramount importance in aircraft lateral motions, the dutch roll ratio. For slender aircraft configurations this ratio is most conveniently expressed as the ratio of roll angle ϕ to sideslip velocity v. For the linear theory, the sideslip/sideways mode coupling approximation gave very accurate predictions for this ratio as indicated in Fig. (3.4.). The theory is also capable of predicting the variation of the dutch roll ratio with amplitude and in particular the steady state value at the limit cycle. Referring to (3.22) we can see that the values of R_{vc} and I_{vc} at the limit cycle condition can be written as,

$$R_{v_0} = R_{v_{cL}} - \frac{3}{4}\alpha_{32}\frac{(\alpha_1 - \beta_{3c})}{(\alpha_1-\beta_{3c})^2 - \beta_{3c}\alpha_2^2}\sqrt{}_L^2 \qquad (4.52)$$

$$I_{v_0} = I_{v_{cL}} + \frac{3}{4}\frac{(-\beta_{3c})^{1/2}\alpha_2}{(\alpha_1-\beta_{3c})^2 - \beta_{3c}\alpha_2^2}\alpha_{32}\sqrt{}_L^2 \qquad (4.53)$$

where $R_{v_{cL}}$ and $I_{v_{cL}}$ are given by (3.21a) and (3.21b) respectively. Using (4.12) the expressions for R_{vc} and I_{vc} can be reduced to the approximate form,

$$R_{v_0} = R_{v_{cL}} - \frac{2\mu^*}{\frac{\beta_1\alpha_2}{\beta_{3c}} + \beta_2} \qquad (4.54)$$

$$I_{v_c} = I_{v_{cL}} + \frac{\alpha_2}{(-\beta_{3c})^{1/2}}\frac{2\mu^*}{\frac{\beta_1\alpha_2}{\beta_{3c}} + \beta_2} \qquad (4.55)$$

The approximate dutch roll ratio follows from (3.22), i.e.

$$\left(\frac{\phi}{v}\right)_{\substack{\text{Limit}\\ \text{cycle}}} \simeq \frac{1}{v_0}\left(1 - R_{vc} + iI_{vc}\right) \qquad (4.56)$$

The variation of (ϕ/v) at the limit cycle predicted by (4.56) for the H.P.115 aircraft is shown in Fig. (4.5) as the amplitude and phase angle between roll and sideslip. The results are depicted for the incidence range $20^{\circ} \leq \alpha \leq 26^{\circ}$ and are compared with the approximate results from the linear theory. Of most significance in Fig. (4.5) is the reversal in the trend of the phase angle variation with incidence. The small amplitude linear theory predicts a decreasing phase angle while the nonlinear limit cycle analysis predicts an increasing phase angle variation. At an angle of incidence of, say 26°, it is the increase in the phase angle of about $1\frac{1}{2}^{\circ}$ that serves to limit the amplitude of the oscillation. One of the attributes of the sideslip/sideways mode coupling approximation is its ability to readily predict such variations.

The second approximate technique, referred to as the bifurcation approximation, involves a transformation of the system into non-critical and critical motion variables. This decomposition requires an a priori knowledge of the linear system eigenvalues and eigenvectors involving substantial computations. Of course, for the companion matrix, the eigenvectors follow directly from the eigenvalues are shown in (2.101). The required knowledge of the linear system characteristics obviously makes this approximation the most extensive to apply. The most attractive feature of the bifurcation method lies in the quality of the perturbation method i.e. a rational and systematic approach to the problem. The path to take in order to make improvements in the solutions is clearly indicated by the ordering scheme adopted. The technique can be extended to cases in which the nonlinearity occurs in more than one variable. Thus if the nonlinear terms in the roll angle ϕ appearing in the gravitational term $g_1 \sin\phi$, the normalised velocity $We\cos\phi$ and the kinematic relation $\dot{\psi} = p + r\tan\theta_e \sec\phi$ were included in the equations then it would be appropriate to recast the equations in terms of the motion variables $\{\phi, \dot{\phi}, v, \dot{v}\}$. With such a state vector the eigenvectors can again be easily expressed in terms of the eigenvalues and hence the analysis would not be much more complicated. For more general nonlinear systems the eigenvectors of the system matrix would also have to be computed.

For the case of a single real root of the linear system crossing the imaginary axis the approximation locates any equilibrium points and their stability characteristic in the following manner. Applying the perturbation scheme directly to the fourth order equation (4.17) and setting the required periodic solution of the zeroth order problem to a single function of the slow time $\tilde{\tau}$, enables us to determine the approximate growth characteristics of this 'zero' mode by setting to zero the terms independent of the fast time η (or t) on the right side of the first order perturbation equation. It is a fairly straightforward exercise to show that the bifurcation equation in this case takes the form

$$\frac{da_0}{d\tilde{\tau}} + \frac{d_1}{c_1} a_0 + \frac{d_3}{c_1} a_0^3 = 0 \qquad (4.57)$$

The zero frequency limit cycles are of course the 'trivial' equilibrium points given by,

$$a_c^2 = -d_1/d_3 \qquad (4.58)$$

According to (4.57) as initially subsident motion for the case $d_1 > 0$ $c_1 > 0$ can diverge due to a large amplitude disturbance if $d_3 < 0$.

The case of two critical modes in the linear system is also amenable to the present approximation. The complexity of the case of a pair of critical oscillatory modes will generally require a computer solution of the bifurcation equations in any parametric analysis. Aspects of the stability of the critical cases of two pairs of imaginary eigenvalues and of one pair of imaginary eigenvalues and one vanishing real root are discussed in some detail by Malkin (REF. 4.1, Chapter 6.D.).

We turn now to the final approximation utilized whereby the limit cycles are predicted by setting to zero the nonlinear Routhian given by (4.36). Of the three techniques employed this gives the best comparison with the numerically integrated and since it is quite simple to apply it certainly has a lot in its favour. The sideslip limit cycle amplitude can be obtained by a novel graphical method. Since the nonlinear terms $3/4\ n_{v_2} v_L^2$ and $3/4\ e_{v_2} v_L^2$ appearing in the nonlinear Routhian given by (4.36) can be regarded as perturbations in the derivatives n_{v_c} and e_{v_c} respectively then they are also a measure of the distance to the oscillatory stability boundary from the point (n_{v_c}, e_{v_c}) in the (n_v, e_v) plane. Fig.4.6. shows the stability boundaries for the H.P.115 at 24° of incidence. Point A represents the point (n_{v_c}, e_{v_c}) and is of course on the unstable side of the oscillatory boundary. For any line from the point A to the stability boundary, such as ABC, there is a corresponding value of γ_2 (e_{v_2} / n_{v_2}) and hence for a given value of n_{v_2} the value of v_L^2 can easily be determined. The divergence boundary, given by $d_1 = 0$, is also shown on the diagram and provided this remains to the right of the oscillatory stability boundary the stable limit cycle motions will characterise the response. If the point A lies between the two boundaries, i.e. the equilibrium has asymptotic stability, then the characters of the response, as indicated by Fig. 4.6, will depend on which boundary the point A is closer to.

One of the shortcomings of the nonlinear Routhian techniques is that it only predicts the limit cycle condition of the oscillation. However, in REF. 4.2. a method is proposed for determining the amplitude envelope of the oscillation, that assumes a slowly varying amplitude and frequency, so that the averaging principle can be exploited. For an oscillation of the form,

$$v(t) = a \cos \omega t \qquad (4.59)$$

the equation for a given in REF. 4.2. takes the form,

$$\dot{a} = \lambda a$$

$$\text{with} \qquad \lambda = \lambda_c \left(1 - \left(\frac{a}{a_L}\right)^2\right) \tag{4.60}$$

where λ_c is the linear damping of the oscillation and a_L the limit cycle amplitude. Not surprisingly, there is a close resemblance of (4.60) with (2.110) derived from bifurcation theory.

The technique described above was developed in REF. 4.2. for application to the lateral oscillation of the H.P.115 aircraft described earlier in this chapter. Flight experience with this aircraft indicated that with the loss in damping of the oscillatory mode there developed a motion that appeared to have all the features of a limit cycle. With a view to reproducing this motion a dynamic wind tunnel simulation was carried out at the Royal Aircraft Establishment (REF. 4.3). A similar type of motion was discovered in the wind tunnel test although the loss of damping appeared at an incidence of about 11° as opposed to 19° in flight. With the data from REF. 4.3. the theoretical analysis of REF. 4.2 was used to obtain approximate results for comparison with the simulation study. As indicated in REF. 4.2. and later in REF. 4.4. the trends of the nonlinear oscillation are predicted correctly by including a nonlinear variation of yawing moment with sideslip velocity. The sideslip amplitudes, however, are overestimated by a substantial amount (25% - 40%). Clearly there are other nonlinear effects involved in the oscillation absent from the theoretical model and it is appropirate at this stage to review some of the assumptions made in the construction of the model that leads to the fourth order equation (4.17).

Results from numerical integration of the equations of motion with the gravity term allowed to vary as $g_1 \sin\phi$ and the kinematic relation between roll rate and the rate of change of ϕ with time to vary as $\dot{\phi} = p + r\tan\theta_c \sec\phi$, show that the response is essentially of the same character as with linear ϕ terms. The response levels in the limit cycle condition are only some 5%-7% lower with the nonlinear ϕ terms included. The assumption of constant incidence during the oscillation can only be satisfactorily tested by obtaining some numerical solutions to the full equations of motion of the aircraft although it is probably valid to assume that changes in flight speed can be neglected. Adding the heave and pitch equations of motion to the lateral subset will thus allow the short period oscillation to respond naturally and hence the incidence to vary with the correct phase with respect to sideslip. The five degrees of freedom system is described by the equations, (in dimensional form),

$$\dot{v} + r U_o - p(w_o + w) =$$

$$= \frac{\rho S V_R^2}{m}\left(y_\beta \beta + y_p\left(\frac{bs}{V_R}\right) + y_r\left(\frac{rs}{V_R}\right)\right) + g_y \qquad (4.61)$$

$$\dot{w} + pv - q U_o = \frac{\rho S V_R^2}{m} Z_\alpha \alpha' + g_z. \qquad (4.62)$$

$$\dot{p} - e_x(\dot{r} + pq) - \left(\frac{i_{yy}\left(\frac{\bar{c}}{s}\right)^2 - i_{zz}}{i_{xx}}\right) qr =$$

$$= \frac{\rho S V_R^2}{I_{xx}}\left(\ell_\beta(\beta)\beta + \ell_p\left(\frac{ps}{V_R}\right) + \ell_r\left(\frac{rs}{V_R}\right)\right) \qquad (4.63)$$

$$\dot{q} - e_y(r^2 - p^2) - \left(\frac{s}{\bar{c}}\right)^2\left(\frac{i_{zz} - i_{xx}}{i_{yy}}\right) rp =$$

$$= \frac{\rho S V_R^2 \bar{c}}{I_{yy}}\left(m_\alpha \alpha' + m_q\left(\frac{q\bar{c}}{V_R}\right)\right) \qquad (4.64)$$

$$\dot{r} - e_z(\dot{p} - qr) - \left(\frac{i_{xx} - \left(\frac{\bar{c}}{s}\right)^2 i_{yy}}{i_{zz}}\right) pq =$$

$$= \frac{\rho S V_R^2 s}{I_{zz}}\left(n_\beta(\beta)\beta + n_p\left(\frac{bs}{V_R}\right) + n_r\left(\frac{rs}{V_R}\right)\right) \qquad (4.65)$$

with the kinematic relations

$$\dot{\phi} = p + (q \sin\phi + r\cos\phi)\tan\theta \qquad (4.66)$$

$$\dot{\theta} = q\cos\phi - r\sin\phi \qquad (4.67)$$

where,

$$g_y = g \sin\phi \cos\theta \tag{4.68}$$

$$g_z = g(\cos\phi\cos\theta - \cos\theta_c) \tag{4.69}$$

and,

$$\beta = \tan^{-1}\frac{v}{V_R \cos\theta_c} \tag{4.70}$$

$$\alpha' = \tan^{-1}\frac{w}{V_R \cos\theta_c} \tag{4.71}$$

w is the perturbation heave velocity along the body z axis, q the pitch rate, α' the perturbation incidence defined by (4.71). Z_α, m_α and m_q are the normalised longitudinal derivatives defined as,

$$Z_\alpha = \frac{\partial(Z/\rho S V_R^2)}{\partial\alpha} \qquad m_\alpha = \frac{\partial(M/\rho S V_R^2 \bar{c})}{\partial\alpha}$$

$$m_q = \frac{\partial(M/\rho S V_R^2 \bar{c})}{\partial(q\bar{c}/V_R)} \tag{4.72}$$

We also have, $i_{yy} = I_{yy}/m\bar{c}^2$, the normalised moment of inertia about the body y axis, and $e_y = I_{xz}/I_{yy}$.

V_R is the reference flight velocity. For purposes of the numerical integration of (4.61) to (4.67) the lateral derivatives y_v, ℓ_p, n_r etc. are functions of $(\theta_c + \alpha')$ as displayed in Fig.(3.1). Some results from a sample numerical solution are shown in Fig. 4.7. The trim flight incidence is 25° with a flight speed of 40.08 m/sec (V_R). Values for the longitudinal derivatives were taken from REF. 4.5. and for the case displayed in Fig. 4.7. are,

$$Z_\alpha = -1.11, \quad m_\alpha = -0.016, \quad m_q = -0.64$$

The results shown are at the limit cycle condition and are compared with numerical results obtained for the restricted lateral equations. The appropriate nonlinearity in the moment variations with sideslip are,

$$n_{v_2} = 20\, n_{v_c} \qquad \ell_{v_2} = 0$$

The variation of both sideslip and roll angle are seen to be very well predicted by the restricted lateral equations. Heave velocity (w) varies, as expected, with twice the frequency of the roll oscillation. For a restricted rolling motion w would vary as

$$w = -W_c (1 - \cos\phi) \tag{4.73}$$

With W_c = 17 m/sec and ϕ = .21 rads. w works out at about .37 m/s, a result which compares well with the level of short period response shown in Fig. 4.7. We can only conclude that for the particular case studied the effect of the short period mode on the lateral oscillation is negligible. Numerical solutions computed with both ℓ_{v_2} and n_{v_2} equal to zero indicate that the responses will still be limited in amplitude with the overall levels about doubled.

CHAPTER 5 - ASPECTS OF SYSTEM IDENTIFICATION

5.1 Introduction

For our purposes the term system identification refers to the synthetic construction of a dynamic model of a system based on the known behaviour of the system when excited with particular inputs. The experimental determination of the aerodynamic forces on a moving body, either in a wind tunnel or in flight, is generally based on this type of synthesis. The starting point here is the assumption of a certain representation of the aerodynamic forces in terms of the motion of the body. Such a representation clearly has to be established on both physical and mathematical grounds and it will not always be obvious at the outset what form this representation should take. A well established and now almost habitual formulation involves expressing the forces and moments as linear functions of the aircraft's velocities and accelerations and hence defining the group of parameters known as stability derivatives. The estimation of these derivatives from flight records using numerical and statistical techniques is becoming increasingly popular; an excellent review of the subject is given in (REF. 5.1). For a great many flight situations this type of representation is adequate in providing information on the behaviour of aircraft following a disturbance as exemplified by the studies in Chapter 3 of this thesis. There are, however, essentially two deficiencies in this formulation that make it invalid for a number of applications.

Even within the linearity assumption a more general representation of the aerodynamic forces would have to include the effect of the past history of the motion. Such effects are particularly important in rapid manoeuvering situations where the disturbed air will continue to effect aircraft motion for a short time after leaving the vicinity of the aircraft. When the velocity perturbations are not small or when the flow field around the aircraft changes rapidly with flight condition then the problem must be treated as a nonlinear one. It is not too difficult to imagine both the time history and nonlinear effects being present at the same time and in such cases the issue of modelling for system identification becomes extremely difficult unless there is strong physical evidence for an initial representation.

For the most part this chapter will be concerned with a seemingly straightforward problem, i.e. the representations for and the determination of the aerodynamic moment on a single degree of freedom hypothetical wind tunnel model. When the aerodynamic moment can be written as an instantaneous nonlinear function of the model motion it is shown that the damping moment can be synthesised from measurements of the logarithmic decrement for oscillatory motions. The synthesis is carried out in an approximate manner with the aid of the analytic techniques of Chapter 2. Later in this chapter we will discuss and review aspects of time history effects but this section will be of a rather more conjectural nature than the previous one.

We begin by outlining the sort of wind tunnel test situation that might be used to predict the linear and nonlinear contributions to the aerodynamic forces and moments when these are represented as instantaneous functions of the model motion.

5.2 Measurement of aerodynamic forces and moments

A typical set up for a wind tunnel free oscillation test is shown in Fig. 5.1. The model is located on an arm which can be rotated about A to change the incidence α ; the length of the arm $O'A$ is assumed to be adjustable. A mechanical spring (a selection of stiffnesses will be available) and bearing assembly links the arm from the pivot point at P to the rotating sting and model. The inclination of the whole unit (θ) can be adjusted by rotation about P so that the axis PO' can be inclined to the axis Ac through various angles for a given incidence. All the required measurement transducers are located on the arm PO' outboard of the spring unit. Referring to Fig. 5.1, for a given incidence α there are four adjustable physical properties, viz. the arm length k_o , the model centre of gravity position Ac , the inclination δ $(\alpha-\theta)$ and the spring stiffness.

Let u, v, w be the translational velocities, p and r the rotational velocities, Y the sideforce and L, N the rolling and yawing moments respectively of a model fixed axes system centred at the model centre of gravity and with the X axis aligned along the incidence datum of the model. Denoting the motion of the sting axes $O'x'z'$ by primed quantities, the model motion can be written in the form (REF. 5.2. p.666).

$$u = V_R\,(\cos\theta\cos\delta - \sin\theta\cos\phi\sin\delta) \tag{5.1}$$

$$v = V_R\,\sin\theta\sin\phi + \Delta p' \tag{5.2}$$

$$w = V_R\,(\cos\theta\sin\delta + \sin\theta\cos\phi\cos\delta) \tag{5.3}$$

$$p = p'\cos\delta \qquad r = p'\sin\delta \tag{5.4}$$

where (Fig. 5.1) $$\Delta = h\sin\delta - k\cos\delta = h_c\sin\delta - k_o \tag{5.5}$$

$\delta = \alpha-\theta$, ϕ is the roll angle about the axis $O'x'$

The rolling moment about the sting axis $O'X'$ can be expressed in terms of the sideforce and rolling and yawing moments about the model axes OXZ with the relation,

$$L' = Y\Delta + L\cos\delta + N\sin\delta \qquad (5.6)$$

Now the issue of system identification for the present problem is resolved, as pointed out earlier, by finding a suitable representation for the force Y and moments L and N in terms of the motion of the model. The required representation, for measurements about the rolling sting axis $O'X'$, is then given by (5.6) together with (5.1) - (5.5). If, for example, a linear representation in terms of the sideslip velocity (v) and roll and yaw rates (p) and (r) is assumed, so that,

$$Y = Y_v v + Y_p p + Y_r r \qquad (5.7)$$

$$L = L_v v + L_p p + L_r r \qquad (5.8)$$

$$N = N_v v + N_p p + N_r r \qquad (5.9)$$

then the rolling moment L' can be written in the form (REF. 5.2, p.669)

$$L' = L'_{p'}p' + L'_{v'}v' \qquad (5.10)$$

where $v' = VR \sin\Theta \sin\phi$

and
$$L'_{v'} = L_v\cos\delta + N_v\sin\delta + Y_v\Delta \qquad (5.11)$$

$$L'_{p'} = L_p\cos^2\delta + (L_r + N_p)\sin\delta\cos\delta + N_r\sin^2\delta + [(Y_p + L_v)\cos\delta + (Y_r + N_v)\sin\delta]\Delta + Y_v\Delta^2 \qquad (5.12)$$

Assuming that L'_v and L'_p can be measured from a free oscillation test, the complete set of derivatives $Y_v - N_r$ can be estimated at a given α by varying δ and Δ .

In order to determine the aerodynamic characteristics of the model for large amplitude oscillations it is clearly necessary to replace (5.7) - (5.9) by a more general nonlinear representation that includes higher order terms in v , p and perhaps r , $\dot{v}$, $\dot{p}$ and $\dot{r}$; the effect of a changing incidence during the oscillation could also appear in the more general representation. The mathematical form of the force and moment expansions in terms of the motion variable can always be defined in a purely formal sense. The task of determining, on physical grounds, which nonlinearities have a significant effect on the motion, will however, be quite a formidable task.

Let us assume that this problem is reduced to the determination of a form for the rolling moment about the sting axis $O'x'$, L' , in terms of the rolling motion. Now the equation of spring restrained motion of the model about the sting axis $O'x'$ will take the general form,

$$\frac{d^2\phi'}{dt^2} + c(\phi') + h\left(\phi', \frac{d\phi'}{dt}, \frac{d^2\phi'}{dt^2}, \ldots\right) = 0 \qquad (5.13)$$

The 'stiffness' $c(\phi')$ will contain contributions of mechanical (spring), gravitational ($\sim \sin\phi$) , and aerodynamic origin. Presumably, estimates of the contribution of the latter can be made from static tests for comparison with measurements from free oscillation tests. Since it has been assumed that the aerodynamic moment is an instantaneous function of the motion then the 'damping' moment $h\left(\phi', \frac{d\phi'}{dt}, \ldots\right)$ must be, for small rates, proportional to $d\phi/dt$. Even for large oscillation rates the aerodynamic moment, when $d\phi'/dt$ is zero, must reduce to the contribution in $c(\phi')$ if $d^2\phi'/dt^2$ is small.

In general the only satisfactory way of determining, at least qualitatively, the internal structure of the function $h(\phi', d\phi'/dt, \ldots)$ would be to actually measure the damping moment. One method of achieving this would be to measure the acceleration $d^2\phi'/dt^2$, subtract the statically measured stiffness $c(\phi')$ and finally examine in detail the remaining moment as a function of the motion. In this way the function $h(\phi', d\phi'/dt, \ldots)$ could be gradually built up and a tentative representation proposed for the system identification scheme. It is not proposed to dwell on this particular synthesis issue here but instead a method is constructed for estimating the parameters of a 'small' nonlinear damping moment, such as the one described above, i.e. when the model motion is close to the oscillatory stability boundary. To this end we develop an expression for a nonlinear logarithmic decrement.

5.3 A Logarithmic Decrement for Nonlinear Oscillations

The logarithmic decrement of the free response of a dynamical system is a familiar concept in linear mechanics and within the framework of the linear theory, assuming that the different modes of motion can be isolated, provides an estimate of the direct damping coefficients of the system modes. When the dynamic model of a system is a nonlinear differential equation, the logarithmic decrement is still a meaningful quantity but we must expect that, in general, it will be a function of the oscillation amplitude.

In this section a method is proposed whereby the damping coefficients, appropriate to an adopted dynamic model, can be estimated from measurements of the logarithmic decrement of the experimental oscillation records. This is achieved by matching these measurements to an approximate functional relationship between the logarithmic decrement and the oscillation amplitude envelope which is, in turn, derived from an approximate analytic solution of the describing equation. The method is restricted to cases in which the damping is small in the sense that the damping force in the equation of motion is multiplied by a small parameter. The undamped system is assumed to exhibit a known, periodic oscillation and the differential equation generating this solution can and will in general be nonlinear. With a small amount of damping in the system it is clear that the logarithmic decrement will differ by a small amount from zero and can therefore be approximately represented by the first term of an asymptotic expansion in terms of the small parameter. The approximation is constructed in the spirit of the perturbation technique developed for strongly nonlinear second order differential equations in Chapter 2.

The type of equation to be considered has the form given by (5.13) although we revert to the notation of Chapter 2 and consider (2.37), i.e.

$$\ddot{y} + c(y) + \varepsilon h(y, \dot{y}; \varepsilon) = 0 \qquad (5.14)$$

The inclusion of higher order derivatives of y in the function $h(y, \dot{y}; \varepsilon)$ does not modify the form of analysis which follows. A result we require from Chapter 2 is the periodicity relation or bifurcation equation for the first order term in the asymptotic expansion of $y(t;\varepsilon) \equiv Z(\eta, \tau; \varepsilon)$ in powers of ε. This relation is given by (2.42), i.e.

$$\frac{\partial}{\partial \tau} \phi(A_c(\tau)) = -q(A_c(\tau)) \qquad (5.15)$$

where
$$\phi(A_0) = \int_0^{T_\eta} \omega_0 \left(\frac{\partial z_0}{\partial \eta}\right)^2 d\eta \tag{5.16}$$

$$q(A_0) = \int_0^{T_\eta} h\left(z_0, \omega_0 \frac{\partial z_0}{\partial \eta}; 0\right) \frac{\partial z_0}{\partial \eta}\, d\eta \tag{5.17}$$

and
$$\frac{d\eta}{dt} = \omega_0 + \varepsilon\omega_1 \tag{5.18}$$

$A_0(\tau)$ is the amplitude function defining the envelope of the oscillations, T_η is the period of the oscillation in η and $z_0(\eta, \tau)$ is the zeroth order approximation to $x(\eta, \tau; \varepsilon)$ satisfying the equation,

$$\omega_0^2 \frac{\partial^2 z_0}{\partial \eta^2} + C(z_0) = 0 \tag{5.19}$$

Now (5.15) can be written in the alternative form given by (2.43),

$$\frac{dA_0}{d\tau} = -q(A_0) \Big/ d\phi/dA_0 \tag{5.20}$$

An expression for the derivative $d\phi/dA_0$ can be obtained using (5.19). Multiplying (5.19) by $2\,\partial z_0/\partial \eta$, we obtain,

$$\omega_0^2 \frac{\partial}{\partial \eta}\left(\frac{\partial z_0}{\partial \eta}\right)^2 = -2\frac{\partial z_0}{\partial \eta} C(z_0) \tag{5.21}$$

Integrating (5.21) from a cycle point where $(dz_c/d\eta) = 0$, $z_c = A_o$, to a general cycle point we obtain,

$$\left(\frac{dz_c}{d\eta}\right)^2 w_c^2 = -2\int_{A_o}^{z_o} C(z_c)\,dz_o = 2\left(F(A_o) - F(z_o)\right) \qquad (5.22)$$

X

where $F(x) = \int_0 C(x)\,dx$

so that,

$$w_o \frac{dz_o}{d\eta} = \sqrt{2}\sqrt{\left(F(A_o) - F(z_o)\right)} \qquad (5.23)$$

Now the function $\phi(A_2)$ can be written in the approximate form,

$$\phi(A_2(H)) = \int_0^{T_\eta} w_o\left(\frac{dz_c}{d\eta}\right)^2 d\eta = \int_{y_n}^{y_{n+1}} w_o\left(\frac{dz_c}{d\eta}\right) dz_o \qquad (5.24)$$

where y_n , y_{n+1} are two adjacent maximum (or minimum) points of the oscillation. Hence using (5.23) we can write,

$$\phi(A_o) = \sqrt{2}\int_{y_n}^{y_{n+1}} \sqrt{F(A_2) - F(z_o)}\,dz_o \qquad (5.25)$$

Differentiating (5.25) with respect to A_o we obtain, using (5.23)

$$\frac{d\phi}{dA_o} = \frac{1}{\sqrt{2}}\int_{y_n}^{y_{n+1}} \frac{F'(A_o)\,dz_o}{\sqrt{F(A_2) - f(z_c)}} = \frac{F'(A_o)}{w_c}\Delta\eta = \frac{c(A_o)}{w_o}\Delta\eta \qquad (5.26)$$

where $\Delta\eta$ is the interval (period) in η between adjacent maximum points y_n , y_{n+1} . Considering the two adjacent maximum (or minimum) points y_n , y_{n+1} measured from an experimental record we can define the logarithmic decrement of the oscillation in the usual way and expand this as an asymptotic sequence in powers of ε . Thus,

$$\log_e \left| \frac{y_{n+1}}{y_n} \right| = \varepsilon \sigma_m + O(\varepsilon^2) \tag{5.27}$$

where $$\left| \frac{y_{n+1}}{y_n} \right| = \delta_m = 1 + \varepsilon \sigma_m + O(\varepsilon^2) \tag{5.28}$$

An expression for the first order term σ_m can be derived using (5.20) in conjunction with (5.26). We prefer to work in terms of A_0^2 rather than A_0 and hence (5.20) can be written as,

$$\frac{\partial (A_0^2)}{\partial \tau} = - \frac{2 A_0 q(A_0) \omega_0}{c(A_0) \Delta \eta} \tag{5.29}$$

Now if we assume that the function A_0^2 varies linearly over the interval $\Delta\eta$ ($\Delta\tau$) , (5.29) takes the form

$$\frac{\Delta A_0^2}{\Delta \tau} = \frac{y_{n+1}^2 - y_n^2}{\Delta \tau} = - \frac{2 y_m q(y_m) \omega_0}{c(y_m) \Delta \eta} \tag{5.30}$$

where $$y_m^2 = \frac{y_{n+1}^2 + y_n^2}{2} \tag{5.31}$$

From (5.28) we can also write

$$y_n^2 = \frac{2 y_m^2}{1+\delta_m^2} = y_m^2 (1 - \varepsilon \delta_m) + O(\varepsilon^2) \qquad (5.32a)$$

$$y_{n+1}^2 = \frac{2 \delta_m^2 y_m^2}{1+\delta_m^2} = y_m^2 (1 + \varepsilon \sigma_m) + O(\varepsilon^2) \qquad (5.32b)$$

Also, assuming a linear variation of η with t over the interval between maximum points, (5.18) gives

$$\varepsilon \Delta\eta = \Delta\tau (\omega_0 + \varepsilon \omega_1) \qquad (5.33)$$

Combining (5.33) and (5.32a), (5.32b) with (5.30) the expression for the approximate logarithmic decrement can be written in the form,

$$\log_e \left| \frac{y_n}{y_m} \right| = \varepsilon \sigma_m + O(\varepsilon^2) = - \frac{\varepsilon \, q(y_m)}{2 c(y_m) y_m \left(1 + \varepsilon \frac{\omega_1}{\omega_0}\right)} \qquad (5.34)$$

The nature and utility of the above approximation for the logarithmic decrement are best illustrated with a few examples.

Example 1 - Referring to (5.14), consider the case of a linear stiffness and a damping function proportional to velocity and symmetrically nonlinear in displacement, so that,

$$c(y) = \omega_0^2 y \qquad (5.35)$$

$$h(y, \dot{y}; \varepsilon) = (h_0 + h_2 y^2 + h_4 y^4 + O(y^6)) \dot{y} \qquad (5.36)$$

The zeroth order solution of (5.19) then takes the form,

$$z_0(\eta,\tau) = A_0(\tau)\cos\eta \tag{5.37}$$

with $$\frac{\partial z_0}{\partial \eta} = -A_0(\tau)\sin\eta \tag{5.38}$$

The function $q(y_m)$ can therefore be written as (cf. 5.17),

$$q(y_m) = \int_0^{2\pi} \omega_0 y_m^2 \left(h_0 + h_2 y_m^2\cos^2\eta + h_4 y_m^4\cos^4\eta + O(y_m^6)\right)\sin^2\eta\, d\eta$$

$$= \pi y_m^2 \omega_c \left(h_0 + \frac{h_2}{4} y_m^2 + \frac{h_4}{16} y_m^4 + O(y_m^6)\right) \tag{5.39}$$

The function σ_m can finally be written as, (note $\omega_1 = 0$)

$$\sigma_m = \frac{-\pi}{2\omega_c}\left(h_0 + \frac{h_2}{4} y_m^2 + \frac{h_4}{16} y_m^4 + O(y_m^6)\right) \tag{5.40}$$

The damping parameters h_0, h_2, h_4 etc. can thus be estimated from a set of displacement oscillation records. Plotting the measured values of $\log|\delta_m|$ against y_m^2 and performing a least squares fit will yield h_0, h_2, h_4 . It should be noted that the actual amplitude dependence of the damping function need not be specified before hand; the least squares solution can be used to determine the most appropriate form of this dependence for any given range of amplitude,

In connection with the use of trigonometric functions for parameter estimation in nonlinear oscillation problems it is appropriate to mention the work of Tobak (REF. 5.3) who tackles the problem of deducing the actual form of nonlinear elements from a set of experimental records. Tobak considers the equation,

$$\ddot{y} + \dot{y} f(y) + \omega_0^2 y + k(y) = 0 \qquad (5.41)$$

where $f(y)$ is even and $k(y)$ is odd.

With the aim of deducing the forms of $f(y)$ and $k(y)$ Tobak proceeds as follows. The solution $y(t)$ and its first derivative are assigned the forms,

$$y(t) = A(t) \sin \psi(t)$$

$$\psi(t) = \omega_0 t + \phi(t)$$

$$\dot{y}(t) = \omega_0 A_0(t) \cos \psi(t) \qquad (5.42)$$

Using (5.42) and (5.41), a pair of first order differential equations can be derived for $A(t)$ and $\psi(t)$

$$\frac{d(A^2)}{dt} = -2A^2 f(A\sin\psi)\cos^2\psi - \frac{2A}{\omega_0} k(A\sin\psi)\cos\psi \qquad (5.43)$$

$$A^2 \omega_0 (\dot{\psi} - \omega_0) = A^2 \omega_0 f(A\sin\psi)\cos\psi\sin\psi + A k(A\sin\psi)\sin\psi \qquad (5.44)$$

Integrating over a period in ψ, (5.43) and (5.44) reduce to,

$$\frac{1}{2\pi}\int_0^{2\pi} \dot{A}^2(A^2,\psi)\,d\psi = F(A^2) = -\frac{1}{\pi}\int_0^{2\pi} A^2 f(A\sin\psi)\cos^2\psi\,d\psi \qquad (5.45)$$

$$\frac{A^2\omega_0}{2\pi}\int_0^{2\pi} [\dot{\psi}(A^2,\psi) - \omega_0]\,d\psi = K(A^2) = \frac{1}{2\pi}\int_0^{2\pi} A\,k(A\sin\psi)\sin\psi\,d\psi \qquad (5.46)$$

The similarity of (5.45) with (5.15) should be noted; in (5.15) $\dot{A}_0^2$ was assumed constant over a period in η .

Now it is assumed that the functions $F(A^2)$ and $k(A^2)$ can be obtained from the experimental records and hence (5.45), (5.46) are of the form of a pair of integral equations for the functions $f(A\sin\psi)$ and $k(A\sin\psi)$. With the change of variables $A^2=\theta$, $\theta\sin^2\psi=\xi$ these equations can be written in the form,

$$F'(\theta) = -\frac{1}{\pi}\int_0^{\theta} \xi^{-1/2} f(\xi^{1/2})(\theta-\xi)^{-1/2} d\xi \qquad (5.47)$$

$$k(\theta) = \frac{1}{\pi}\int_0^{\theta} k(\xi^{1/2})(\theta-\xi)^{-1/2} d\xi \qquad (5.48)$$

Inversion of these Abel integral equations leads to, (REF. 5.3),

$$\theta^{-1/2} f(\theta^{1/2}) = -\frac{d}{d\theta}\int_0^{\theta} F'(\xi)(\theta-\xi)^{-1/2} d\xi \qquad (5.49)$$

$$k(\theta^{1/2}) = \frac{d}{d\theta}\int_0^{\theta} k(\xi)(\theta-\xi)^{-1/2} d\xi \qquad (5.50)$$

The main attribute of Tobak's analysis is the exact nature of (5.49) and (5.50) although in a particular application the construction of the functions $F(A^2)$, $k(A^2)$ could involve lengthy data analysis.

Returning to the main theme of this section we now consider the example given in Chapter 2 where the zeroth order solution can be written in terms of Jacobian elliptic functions.

Example 2 - The approximation for the logarithmic decrement is well illustrated with an application to the equation,

$$\ddot{y} + \varepsilon(h_0 + h_2 y^2)\dot{y} + c_1 y + c_3 y^3 = 0 \qquad (5.51)$$

As shown in Chapter 2, the zeroth order approximation to (5.51) satisfies the equation,

$$\omega_0^2 \frac{\partial^2 z_0}{\partial \eta^2} + c_1 z_0 + c_3 z_0^3 = 0 \qquad (5.52)$$

and can therefore be written in terms of Jacobian elliptic functions, with period $4K(\mu)$ in η where $K(\mu)$ is the complete elliptic integral of the first kind. The integration constants and of course the modulus μ will be functions of the slow time τ. Now the oscillatory solutions of (5.52) (or (5.51) when $\varepsilon = 0$) can be classed as four different types depending on the values of c_1 and c_3 and the initial trajectory. These are shown for the case $\varepsilon = 0$ as phase plane portraits in Fig. 5.2. Since the function $K(\mu)$ is usually tabulated for $0 \leq \mu \leq 1$ we choose to use, for each type of oscillation, that particular form of elliptic function giving μ in the stated range (REF. 5.4. Appendix 1). In all cases we make use of the quantity γ defined as,

$$\gamma = \frac{c_3}{2c_1}(y_{n+1}^2 + y_n^2) = \frac{c_3}{c_1} y_m^2 \qquad (5.53)$$

For the present example an integral from zero to $4(K(\mu))$ can be replaced by twice the integral from zero to $2(K(\mu))$ for symmetric oscillations. For the asymmetric oscillation to be studied (case (iv)) the period is actually $2K(\mu)$. Replacing $4K(\mu)$ by $2K(\mu)$ throughout the following analysis affects only the symmetric oscillations in that y_n and y_{n+1} now denote adjacent maximum and minimum points of the oscillation.

Case (i) $c_1 \geq 0$ $c_3 \geq 0$ $\gamma \geq 0$ The appropriate solution of (5.52) is the elliptic cosine function (REF. 5.5. ex. 213.00),

$$z_0(\eta, \tau) = A_0(\tau)\, C_n(\eta, \mu_0(\tau)) \qquad (5.54)$$

The functions A_0, ω_0 and μ_c are related by the expressions,

$$\omega_c^2 = c_1 + c_3 A_0^2 \qquad \mu_c^2 = \frac{\frac{1}{2} c_2 A_0^2}{c_1 + c_3 A_0^2} \tag{5.55}$$

The derivative of $z_c(\eta, \tau)$ w.r.t. η is given by,

$$\frac{\partial z_c}{\partial \eta} = -A_0(t)\, Sn(\eta, \mu_c)\, Dn(\eta, \mu_c) \tag{5.56}$$

Hence we can write, from (5.16) and (5.17), (REF. 5.5. p.212)

$$p(A_c) = \frac{2\omega_0 A_c^2}{3\mu_c^2}\left\{(2\mu_c^2 - 1)E(\mu_c) + (1-\mu_c^2)K(\mu_c)\right\} \tag{5.57}$$

and

$$q(A_c) = h_0 p(A_c) + \frac{2h_2\omega_0 A_c^4}{15\mu_c^4}\left\{(1-\mu_c^2)(\mu_c^2-2)K(\mu_c) + 2(\mu_c^4 + 1 - \mu_c^2)E(\mu_c)\right\} \tag{5.58}$$

where $E(\mu_c)$ is the complete elliptic integral of the second kind with modulus μ_c.

Let

$$p_0^{(1)} = (2\mu_c^2 - 1)E(\mu_c) + (1-\mu_c^2)K(\mu_c) \tag{5.59a}$$

$$q_0^{(1)} = (1-\mu_c^2)(\mu_c^2 - 2)K(\mu_c) + 2(\mu_c^4 + 1 - \mu_c^2)E(\mu_c) \tag{5.59b}$$

Then from (5.34), after some reduction, we obtain,

$$\delta_m(y_m) = \frac{-4\, h_0(1+\gamma)}{3\gamma\, c_1^{1/2}} \left\{ p_0^{(1)} + \lambda \frac{8}{5}(1+\gamma) q_0^{(1)} \right\} \qquad (5.60)$$

where $$\lambda = \frac{h_2}{4h_0}\left|\frac{c_1}{c_3}\right|$$

The asymptotic approximation for the logarithmic decrement can therefore be written in the form,

$$2\log_e|\rho_m|\frac{c_1^{1/2}}{\pi\varepsilon h_0} = -\frac{8(1+\gamma)}{3\gamma\pi}\left\{ p_0^{(1)} + \frac{8\lambda(1+\gamma)}{5} q_0^{(1)} \right\} + O(\varepsilon)$$

$$= -\psi_0^{(1)}(\gamma) + O(\varepsilon) \qquad (5.61)$$

The function $\psi_0^{(1)}(\gamma)$ is plotted against $|\gamma|^{1/2}$ in Fig. 5.3 for several values of the parameter λ. The occurrence of a zero logarithmic decrement implies the existence of a periodic approximate solution and this must be interpreted here as a limit cycle oscillation.

Case (ii) $c_1 \geq 0$ $c_3 \leq 0$ $-1 \leq \gamma \leq 0$. Note that outside this interval in γ the effective stiffness $c_1 + c_3 y^2$ becomes negative and the solution loses its oscillatory character. The appropriate solution of (5.52) for this case is the elliptic sine function (REF. 5.5. ex. 219.00).

$$z_0(\eta,\tau) = A_0(\tau)\, S_n(\eta, \mu_0(\tau)) \qquad (5.62)$$

where

$$w_0^2 = c_1 + \frac{1}{2} c_3 A_0^2 \qquad \mu_0^2 = \frac{-\frac{1}{2} c_3 A_0^2}{c_1 + \frac{1}{2} c_3 A_0^2} \qquad (5.63)$$

The derivative of $z_c(\eta, \tau)$ w.r.t. η is given by,

$$\frac{\partial z_c}{\partial \eta} = A_0 C_n(\eta, \mu_c) D_n(\eta, \mu_c) \qquad (5.64)$$

Hence the corresponding functions $p(A_0)$, $q(A_0)$ become (REF. 5.5. p.212),

$$p(A_0) = \frac{2\omega_c A_0^2}{3\mu_c^2}\left\{(1+\mu_c^2)E(\mu_c) - (1-\mu_c^2)K(\mu_c)\right\} = \frac{2\omega_0 A_0^2}{3\mu_c^2} p_0^{(11)} \qquad (5.65)$$

$$q(A_0) = h_0 p(A_0) + \frac{2\omega_0 A_0^4}{15\mu_0^4} h_2 q_0^{(11)}, \quad q_0^{(11)} = q_0^{(11)} \qquad (5.66)$$

Passing directly to the approximate expression for the logarithmic decrement, we obtain, after some reduction,

$$2\log_e|\delta_m|\frac{C_1}{\pi\varepsilon h_c}^{1/2} = \frac{\delta(1+\gamma/2)^{3/2}}{3\gamma(1+\gamma)\pi}\left\{p_0^{(11)} + \frac{\lambda\delta(1+\gamma/2)}{5} q_0^{(11)}\right\} + O(\varepsilon)$$

$$= -\Psi_c^{(11)} + O(\varepsilon) \qquad (5.67)$$

The function $\Psi_c^{(11)}(\gamma)$ is plotted in Fig. 5.4. Note again that limit cycles are possible for this case.

<u>Case (iii)</u> $C_1 \leqslant 0 \quad C_3 \geqslant 0 \quad \gamma \leqslant -2$ The phase plane portrait for this system when $\varepsilon = 0$ is shown in the lower diagram of Fig. 5.2. Three equilibrium points exist at $y = 0, \pm(-C_1/C_3)^{1/2}$ and the separatrix cuts the y axis at the points $y = 0, \pm(-2C_1/C_3)^{1/2}$

The solution of (5.52) for this case can again be expressed as,

$$z_0(\eta,\tau) = A_0(\tau)\, C_n(\eta,\mu_0) \qquad (5.68)$$

with

$$\omega_0^2 = c_1 + c_3 A_0^2 \qquad \mu_0^2 = \frac{\frac{1}{2} c_3 A_0^2}{c_1 + c_2 A_0^2} \qquad (5.69)$$

The functions $p(A_0)$ and $q(A_0)$ take a similar form to (5.57), (5.58) and the logarithmic decrement takes the slightly different form,

$$2 p_{ege} |\delta_m| \frac{|c_1|^{1/2}}{\pi \varepsilon h_0} = \frac{8|1+\gamma|^{1/2}}{3\gamma\pi} \left\{ p_0^{(iii)} - \frac{\lambda 8(1+\gamma)}{5} q_0^{(iii)} \right\} + O(\varepsilon)$$

$$= -\psi_0^{(iii)}(\gamma) + O(\varepsilon) \qquad (5.70)$$

where $p_0^{(iii)} = p_0^{(i)}$ and $q_0^{(iii)} = q_0^{(i)}$

The function $\psi_0^{(iii)}(\gamma)$ is shown plotted in Fig. 5.5.

Case (iv) $c_1 \leq 0$ $c_3 \geq 0$ $-2 \leq \gamma \leq 0$ In this case the solution represents an oscillation growing or decaying about the focus equilibrium point at $y = \pm (-c_1/c_3)^{1/2}$ and as such will be asymmetric in character. This asymmetry is reflected in the different forms of solution required for maximum and minimum peaks and troughs.

a) for maximum peaks $-2 \leq \gamma \leq -1$. The required solution of (5.52) takes the form, (REF. 5.5. ex.218.00)

$$z_0(\eta,\tau) = A_0(\tau)\, D_n(\eta, \mu_0(\tau)) \qquad (5.71)$$

with $$\omega_0^2 = \frac{1}{2} c_3 A_0^2 \qquad \mu_0^2 = \frac{c_1 + c_3 A_0^2}{\frac{1}{2} e_3 A^2} \tag{5.72}$$

The derivative $\partial \chi_0 / \partial \eta$ is given by,

$$\frac{\partial \chi_0}{\partial \eta} = -\mu_0^2 S_n(\eta, \mu_0) C_n(\eta, \mu_0) \tag{5.73}$$

Hence the functions $p(A_0)$ and $q(A_0)$ take the form (REF. 5.5, p.212).

$$p(A_0) = \frac{A_0^2 \omega_0}{3}\left\{(2-\mu_0^2)E(\mu_0) - 2(1-\mu_0^2)K(\mu_0)\right\} = \frac{A_0^2 \omega_0}{3} p_0^{(iv)} \tag{5.74}$$

$$q(A_0) = h_0 p(A_0) + \frac{h_2 A_0^4 \omega_0}{15} q_0^{(iv)} \tag{5.75}$$

where $q_0^{(iv)} = q_0^{(i)}$

The logarithmic decrement therefore takes the form,

$$2 \log_e |\varrho_m| \frac{|c_1|^{1/2}}{\pi \varepsilon h_0} = \frac{2\sqrt{2}\,|\gamma|^{1/2}}{3\pi(1+\gamma)}\left\{p_0^{(iv)} - \frac{4\lambda}{5}\gamma\, q_0^{(iv)}\right\} + O(\varepsilon)$$

$$= -\Psi_0^{(iv)}(\gamma) + O(\varepsilon) \tag{5.76}$$

b) for minimum troughs $-i \leq \gamma \leq 0$, the appropriate solution takes the form (REF. 5.5. ex 217.00)

$$z_c(\eta,\tau) = A_2(\tau)\, N_d(\eta, \mu_c(\tau)) \tag{5.77}$$

with $$\omega_c^2 = c_1 + \tfrac{1}{2} c_3 A_0^2 \qquad \mu_0^2 = \frac{c_1 + c_3 A_0^2}{c_1 + \frac{1}{2} c_3 A_0^2} \tag{5.78}$$

and $$\frac{\partial z_c}{\partial \eta} = \mu_0^2\, S_d(\eta, \mu_0)\, C_d(\eta, \mu_c) \tag{5.79}$$

Hence, (REF. 5.5 pp. 213, 214)

$$\beta(A_2) = \frac{A_2^2 \omega_0}{3(1-\mu_c^2)} \left\{ (2-\mu_c^2)E(\mu_c) - 2(1-\mu_c^2)K(\mu_c) \right\}$$
$$= \frac{A_c^2 \omega_0}{3(1-\mu_c^2)}\, \beta_0^{(v)} \tag{5.80}$$

$$q(A_2) = h_0 \beta(A_2) + \frac{h_2 A_2^4 \omega_0}{15(1-\mu_0^2)}\, q_0^{(v)} \tag{5.81}$$

where $q_0^{(v)} = q_0^{(1)}$, $\beta_0^{(v)} = \beta_0^{(iv)}$

The logarithmic decrement is then given by,

$$2 \log_e |\rho_m| \frac{|c_1|^{1/2}}{\pi \varepsilon h_c} = -\frac{\varepsilon(1+\gamma/2)}{\gamma(1+\gamma)\pi} \left\{ \beta_0^{(v)} + \frac{2\lambda}{5}(1+\gamma/2) q_0^{(v)} \right\} + O(\varepsilon)$$

$$= -\Psi_c^{(v)}(\gamma) + O(\varepsilon) \tag{5.82}$$

The functions $\psi_0^{(iv)}(\gamma)$ and $\psi_0^{(v)}(\gamma)$ are shown plotted in Fig. 5.6.

Note that $\psi_0^{(iv)} \to \psi_0^{(v)} \to 0$ as $\gamma \to -1$. Also, from (5.72) and (5.69), $\mu_0^2 \to 1$ as $\gamma \to -2$ and since $E(1) = 1$ and $K(1) = \infty$ it is fairly straightforward to show that $\psi_0^{(iii)} \to \psi_0^{(v)}$ as $\gamma \to -2$.

Together, Figs. 5.3 - 5.6, form a complete picture of the approximate logarithmic decrement for oscillatory solutions of (5.51). Rasmussen (REF. 5.6) has obtained a similar set of curves for the logarithmic decrement using his own technique to generate a uniformly valid asymptotic approximation. Where comparison is possible (for symmetric oscillations only) the agreement between the present method and that of Rasmussen is excellent. Details of Rasmussen's method for determining a multiple scales approximation can be found in(REF. 5.7 and 5.8.)

The function $\psi_0(\gamma)$ can be used, in conjunction with a least squares approach, to estimate the damping parameters, h_0 and h_2, of an adopted dynamic model. A set of e measurements of the quantities $\log_e |\rho_m|$ and γ_m from a series of oscillation records would yield a set of approximate relations of the general form,

$$W_j = U_{0j}(\gamma_j)\,\varepsilon h_0 + U_{2j}(\gamma_j)\,\varepsilon h_0 \lambda \qquad (5.83)$$

$$j = 1, 2, \ldots e$$

or $\underset{\sim}{W} = \mathrm{U}\,\underset{\sim}{V}$ where $\underset{\sim}{V} = \varepsilon \begin{bmatrix} h_0 \\ \lambda h_0 \end{bmatrix}$

Hence the least squares solution for $\underset{\sim}{V}$ is given by,

$$\underset{\sim}{V}^* = (\mathrm{U}^T\mathrm{U})^{-1}\mathrm{U}^T\underset{\sim}{W} \qquad (5.84)$$

We now apply the estimation technique described above to four distinct oscillations, selected to cover the range of possible oscillations described in cases (i) - (iv). The particular examples studied are somewhat artificial in that the measurements of ρ_m and γ_m are taken from a set of numerically integrated solutions of (5.51). In this sense the results serve only as a demonstration of the technique and have no physical meaning in themselves.

Typical phase plane portraits of the four oscillations studied are shown in Fig. 5.7 and in Table 5.1 are listed the parameter values for these cases. In all but case (iv) the trajectories spiral outwards to a stable limit cycle (h_0 negative) and are in fact symmetric

oscillations. Although h_c is also negative for trajectory (iv), at the equilibrium point $\gamma = -1$, the effective damping $(h_c + h_2 y^2)$ is positive and hence the trajectory will spiral into this equilibrium point. A trajectory, of which (iv) is typical, will include all values of $\gamma < 0$.

Corresponding measurements and least squares approximations are shown in Fig. 5.8 and in the associated table 5.2 are listed the least squares estimates of the damping parameters h_0 and h_2. The results are clearly encouraging. In the case of the asymmetric oscillation (iv) it was found that every equation of the form (5.83) for $2 < \gamma < 0$ (i.e. when $D_n(\gamma, \mu)$ and $N_d(\gamma, \mu)$ were the approximate solutions) was, to the accuracy of measurement, practically the same. Hence, using a large number of such results led to numerical problems in the form of ill-conditioning. However, the measurements of this oscillation for $\gamma < -2$ were not susceptible to this problem and hence an estimate for h_0 and h_2 could still be made.

Although in the foregoing analysis the coefficients c_1 and c_3 were assumed to be known, these can also be determined from the oscillation records. The required relation is (5.18), i.e.

$$\frac{d\gamma}{dt} = \omega_c + \varepsilon\omega_1$$

Hence, assuming a linear variation of γ with t over one period, we have,

$$\frac{\Delta\gamma}{\Delta t} = \omega_0 + \varepsilon\omega_1 \qquad (5.85)$$

For the case $C(y) = c_1 y + \varepsilon c_3 y^3$, the frequency correction ω_1 is given by (2.28) and hence (5.85) can be written as,

$$\frac{\pi^2}{(t_{n+1}-t_n)^2} = c_1\left(1 + \varepsilon\frac{3}{4}\frac{c_3}{c_1}y_m^2\right) \qquad (5.86)$$

where t_{n+1} corresponds to the peak (trough) y_{n+1} and t_n corresponds to y_n. Measurements of $(\pi/\Delta t)^2$ plotted against y_m^2 will thus yield the coefficients c_1 and c_3. For the strongly nonlinear oscillation ($c_3 y_m^2/c_1 = O(1)$) the half period in γ is $2k(\mu)$ and the relation corresponding to (5.86) now takes the form,

$$\left(\frac{\pi}{\Delta t}\right)^2 = \frac{\pi^2 c_1}{4(1-2\mu_c^2)k^2(\mu_c)} \quad , \quad \mu_c^2 = \frac{\frac{1}{2}c_3 y_m^2}{c_1 + c_3 y_m^2} \qquad (5.87)$$

Having estimated c_1 , the value of μ_c for a given y_m can be obtained from the first relation in (5.87) and hence c_3 follows from the second expression. The estimated values of the stiffness coefficients from the oscillation records can be compared with estimates obtained from static tests.

The use of the logarithmic decrement concept for nonlinear oscillations does seem to have considerable potential and the idea of cataloguing this function of amplitude for different damping and stiffness functions suggests itself as a useful exercise. It is worth re-emphasising, however, that the form of the damping function should be supported by physical evidence since two quite different damping functions can lead to the same form of logarithmic decrement variation with amplitude. To illustrate this point we need only look at a single example with linear stiffness. Let us compare the result for the two damping moments,

$$\text{a)} \quad h(y,\dot{y}) = (h_0 + h_2 y^2)\dot{y} \qquad (5.88a)$$

$$\text{b)} \quad h(y,\dot{y}) = (h_0 + h_2 \dot{y}^2)\dot{y} \qquad (5.88b)$$

For these two cases the function δ_m (cf. 5.34) is given by,

$$\text{a)} \quad \delta_m = \frac{-\pi}{2w_0}\left(h_0 + \frac{h_2}{4} y_m^2\right) \qquad (5.89a)$$

$$\text{b)} \quad \delta_m = \frac{-\pi}{2w_0}\left(h_0 + \frac{3}{4} h_2 w_0^2 y_m^2\right) \qquad (5.89b)$$

Hence if the damping moment actually behaved as (5.88b), but was assumed to be of the form (5.88a), estimates for h_0 and h_2 could still be realized leading to erroneous conclusions with regard to the physical model.

An example that could be susceptible to the above incorrect physical modelling is afforded by the work in (REF. 5.9). Here a model gothic wing was tested on an oscillation rig similar to the one described in Section 5.2 with $\beta = 0$ and $k_c = 0$. The rolling oscillations were observed to grow into a limit cycle motion at high incidence and measurements of the logarithmic decrement (assuming a linear model) indicated that the derivative L_p became positive at a high incidence. The limit cycle behaviour could be explained by assuming that the damping varies with roll angle on account of the kinematic relation between roll angle and incidence. The mathematical representation of the damping moment would then take the form (5.88a) with φ interpreted as the roll angle. However, for such motions, it might be expected that the derivative L_p will also depend on the roll rate $\dot{\varphi}$ and a model such as (5.88b) could equally well explain the limit cycle behaviour. In actuality, a damping moment depending nonlinearly on both roll angle and rate would probably be more appropriate and, as pointed out earlier, measurements of the damping moment itself would be necessary to clear this issue.

The same gothic wing model of (REF. 5.9) was tested earlier on a forced oscillation rig (REF. 5.10) to determine the effect of frequency parameter on the aerodynamic roll damping and stiffness. Some results of these tests, taken from (REF. 5.10) are shown in Fig. 5.9. and clearly there is a substantial variation in both the stiffness moment (in phase with angular displacement) and damping moment (in phase with angular velocity) with frequency parameter. Such a frequency dependence is at variance with the representation of the aerodynamic moment as an instantaneous function of the wing motion and brings us naturally to the issue of memory effects in this context.

5.4 Memory effects in the representation of aerodynamic forces and moments.

The results displayed in Fig. 5.9. indicate that, even when the assumption of linearity is invoked, a more substantial formulation for the aerodynamic rolling moment is required when the motion is other than simple harmonic. For the latter case of a mono frequency oscillation a moment representation as two terms, one proportional to displacement, the other proportional to velocity, would, of course, be exact. For more general motions the linear moment response function can be reconstituted from oscillatory measurements provided the frequency range of the test is high enough to allow sensible assumptions to be made with regard to the asymptotic values.

Let $C_\ell(t)$ be an aerodynamic moment and $V(t)$ a motion variable. For a linear stationary system the moment response to a general variation in $V(t)$ can be expressed in terms of the moment impulse response function $h(t)$ i.e.

$$C_\ell(t) = \int_0^t h(t-\tau)\, V(\tau)\, d\tau \qquad (5.90)$$

If the motion is simple harmonic so that,

$$V(t) = V_0 \cos \nu t \tag{5.91}$$

then the moment response is also harmonic and can be written as,

$$\frac{C_\ell(t)}{V_0} = H_e(\nu)\cos\nu t - H_o(\nu)\sin\nu t \tag{5.92}$$

where $H_e(\nu)$, $H_o(\nu)$ are the in phase and quadrature components and are also given by the Fourier transform of $h(t)$, i.e.

$$H(\nu) = H_e(\nu) + i H_o(\nu) = \int_0^\infty h(t)\, e^{-i\nu t}\, dt \tag{5.93}$$

From (5.92) and (5.93) we can therefore write,

$$H_e(\nu) = \frac{1}{V_0}\int_0^\infty h(t)\cos\nu t\, dt \quad , \quad H_o(\nu) = -\frac{1}{V_0}\int_0^\infty h(t)\sin\nu t\, dt \tag{5.94}$$

The above relations can then be inverted to yield an equivalence class of impulse functions,

$$h(t) = V_0 \frac{1_+(t)}{\pi}\int_{-\infty}^{\infty} H_e(\nu)\, e^{i\nu t}\, d\nu = -V_0 \frac{1_+(t)}{\pi}\int_{-\infty}^{\infty} H_o(\nu)\, e^{i\nu t}\, d\nu \tag{5.95}$$

where $1_+(t)$ is the unit step function which guarantees that $h(t) = 0$ for $t < 0$. The particular member of the equivalence class can be established for a particular problem by fixing, for example, the zero value of $H_e(\nu)$. Thus if $H_e(\nu)$ and $H_o(\nu)$ are measured, as in Fig. 5.9, the corresponding impulse response function can be obtained from the quadratures in (5.95). Having determined $h(t)$,

we can compute the moment response to an arbitrary variation of $V(t)$ from the convolution form (5.90). The time history or memory effects for this type of problem are embodied in the function $h(t)$. From (5.90) it can be seen that if $h(t)$ is made up of a contribution from the delta function and its first derivative then the moment will reduce to the form,

$$C_e(t) = \int_0^t (a_1 \delta(t-\tau) + a_2 \dot{\delta}(t-\tau)) V(\tau) d\tau = a_1 V(t) + a_2 \dot{V}(t) \qquad (5.96)$$

In general such a simple representation will not be adequate but it is often desirable to find the simplest possible representation for a wide range of motions. Now the extent of the function $h(t)$ is a measure of the time it takes for the flow conditions to adjust themselves to the appropriate 'steady' values commensurate with the particular motion variable. For example, the rolling moment on a wing depends on a varying sideslip velocity in such a way that it does not reach the values predicted by steady state tests until some short time has elapsed. This phase lag should not be confused with the one produced by, for example, the addition of a roll rate motion. If this characteristic time is small compared with the characteristic time of the motion itself then a first approximation is obtained by assuming that only the very recent past effects the present. This approximation can be expressed quantitatively by expanding the function $V(t-\tau)$ in a Taylor series about the present time t .

$$V(t-\tau) = V(t) - \tau \dot{V}(t) + \frac{\tau^2}{2!} \ddot{V}(t) - \frac{\tau^3}{3!} \dddot{V} + \ldots \qquad (5.97)$$

Substituting (5.97) into (5.90) we obtain,

$$C_e(t) = \int_0^t h(t-\tau) V(\tau) d\tau = \int_0^\infty h(\tau) V(t-\tau) d\tau$$

(since $h(t) = 0$, $t < 0$)

$$= V(t) \int_0^\infty h(\tau) d\tau - \dot{V}(t) \int_0^\infty \tau h(\tau) d\tau + \frac{\ddot{V}(t)}{2} \int_0^\infty \tau^2 h(\tau) d\tau - \ldots \qquad (5.98)$$

If the function $h(\tau)$ is of 'short' duration compared with characteristic motion times then the higher moments of this function will be small numbers and the resultant aerodynamic moment can be approximated by a finite linear combination of the motion variable and its derivatives evaluated at time t . When $v(t)$ takes the form (5.91), the approximate form (5.98) reads,

$$C_{\ell}(t) = H_e(\nu)\cos\nu t - H_o(\nu)\sin\nu t$$

$$\overline{v_o} = \left\{ \int_0^\infty h(\tau)\,d\tau - \frac{\nu^2}{2}\int_0^\infty \tau^2 h(\tau)\,d\tau + \dots \right\} \cos\nu t$$

$$- \nu\left\{ - \int_0^\infty \tau\, h(\tau)\,d\tau + \frac{\nu^2}{3!}\int_0^\infty \tau^3 h(\tau)\,d\tau - \dots \right\} \sin\nu t \qquad (5.99)$$

The above result can also be obtained by expanding the functions $H_e(\nu)$ and $H_o(\nu)$ as a Taylor series about $\nu = 0$. From (5.94) we can therefore write, (note that $H_e(\nu)$ is even and $H_o(\nu)$ is odd)

$$H_e(0) = \int_0^\infty h(\tau)\,d\tau \quad , \quad \frac{d^2 H_e(0)}{d\nu^2} = -\int_0^\infty \tau^2 h(\tau)\,d\tau \quad , \text{ etc.}$$

$$\frac{d\,H_o(0)}{d\nu} = -\int_0^\infty \tau\, h(\tau)\,d\tau \quad , \quad \frac{d^3 H_e(0)}{d\nu^3} = \int_0^\infty \tau^3 h(\tau)\,d\tau \quad , \text{ etc.} \qquad (5.100)$$

Hence the coefficients in the 'memory' expansion (5.98) can also be obtained from the frequency response characteristics at zero frequency as given by (5.100). The approximation corresponding to the ordinary stability derivatives can be readily obtained from (5.98) and (5.100). Thus if $C_\ell(t)$ is the rolling moment and $v(t)$ the sideslip velocity we would write,

$$C_\ell(t) = L_v\, v(t) + L_{\dot v}\, \dot v(t) \qquad (5.101)$$

where the derivative L_v is given by the zero frequency value of $H_c(\nu)$ and $L_{\dot{v}}$ by the slope of the quadrature component $iH_c(\nu)$ at $\nu = 0$. Such a coarse representation has formed the basis of many years successful stability and control work where aircraft motions are slow compared with characteristic flow adjustment times.

Perhaps the first efforts to include the more complicated unsteady flow effects in the formulation were addressed to the problem of extending two and three dimensional unsteady, inviscid flow, wing theories to the calculation of damping and stiffness coefficients for dynamic stability applications. As early as 1949 Miles (REF. 5.11) noted that, 'unsteady flow effects, particularly the complex sidewash correction, may be expected to exercise a pronounced effect on the lateral damping characteristics of a vertical fin, as implied by the tendency of many high speed, jet aircraft (with fins designed on the basis of steady flow theory) to "snake".' It is also pointed out in (REF. 5.11) that the quadrature components (in phase with velocity) of aerodynamic moments can behave in ways other than the simple analytic form of (5.99) as $\nu \rightarrow 0$ (e.g. $\nu \log_e \nu$) and that aspect ratio and Mach number effects in general modify this behaviour. In (REF. 5.12) Goland derives 'least squares' equivalent, low frequency, power series variations for two dimensional unsteady forces and moments on a pitching aerofoil. Brune (REF. 5.13) defines a range of valid application, in terms of aspect ratio and Mach number, of the first order in frequency approximation from lifting surface theory for both subsonic and supersonic flight conditions. Rodden and Giesing (REF. 5.14) apply the doublet lattice lifting surface method to the calculation of higher order lift and pitching moment derivatives for a typical jet transport wing but they conclude that "perhaps the only mathematically rigorous approach to the inclusion of three dimensional oscillatory aerodynamic theory is to adapt Fourier Transform techniques to meet the requirements of Stability and Control Analyses since oscillatory aerodynamic solutions are to be regarded as Fourier Transforms of transient aerodynamic solutions."

One of the few systematic and rigorous approximations to the response of systems including memory effects is developed by Milne (REF. 5.15) who uses a method of analytic continuation to derive large time asymptotic solutions from a knowledge of the system's frequency response characteristics. The technique is applicable to both stable and unstable systems. For stable systems, Milne points out that approximations to the function $h(t)$, based on numerical evaluation of the integrals in (5.95), are probably more accurate for intermediate ranges of time since numerical problems effect large time response and unreliable high frequency aerodynamic data deteriorate the small time response. Such an approximation, using inverse Fourier transform techniques, forms the basis for the work of (REF. 5.16) where the lateral response of a delta aircraft is computed using frequency dependent aerodynamic 'derivatives'. A comparison of the transient response at a trimmed incidence of 20° computed with frequency dependent 'derivatives' and constant derivatives (both zero frequency and dutch roll frequency) reveals large differences and the authors conclude 'that the frequency effects of the stability derivatives can cause considerable changes in predicted airplane motions.

An additional effect revealed by the data in (REF. 5.16) is a significant variation in the aerodynamic 'derivatives' with the amplitude of oscillation (the data was obtained from a forced oscillation test). For example, the quadrature component in a rolling test, designated C_{e_p} is practically doubled when the oscillation amplitude is increased from 5^o to 10^o at a reduced lateral frequency of 0.08. Without giving any clue to the actual cause, this type of result is an indication that non-linear effects are present. An amplitude effect can also be observed in the quadrature component in Fig. 5.9. The methods of linear analysis described above are not applicable to such cases and clearly there is a requirement for a more general formulation of the aerodynamic forces and moments when both memory and nonlinear effects are present.

This requirement has been fulfilled, to a certain extent, by the formulation due to Tobak, a full account of which can be found in (REF. 5.17). The basic postulate of Tobak is that the aerodynamic forces and moments are functionals of the motion variables. Restricting the analysis to one moment $C_e(t)$ and one motion variable $v(t)$, the functional representation takes the form,

$$C_e(t) = C_e[v(\xi)] \qquad \xi \in (-\infty, t] \tag{5.102}$$

i.e. the value of C_e at time t depends on the complete history of $v(t)$ or on the function $v(\xi)$.

The form (5.102) reduces to (5.90) if the assumptions of linearity and stationarity are invoked. With the emphasis on obtaining a practical form of (5.102) Tobak systematically reduces the generality of the functional by making a series of simplifying assumptions. Thus indicial moments are introduced to give an integral representation that is further simplified by assuming that a first order in frequency approximation is valid for the relatively low frequency oscillations characteristic of aircraft motions. With the additional assumption of a nearly rectilinear flight path, Tobak's final form for non planar motions in his body axes system can be written (REF. 5.17, p. 56),

$$\begin{aligned} C_k(t) = {} & C_k\left(\hat{\alpha}, \hat{\beta}, \frac{p_B}{\hat{V}}\right) + \\ & + \frac{1}{\hat{V}} \frac{\dot{\hat{\alpha}}\, \ell}{V_R}\left\{C_{k q_B}\left(\hat{\alpha}, \hat{\beta}, \frac{p_B}{\hat{V}}\right) + \hat{V} C_{k\dot{\alpha}}\left(\hat{\alpha}, \hat{\beta}, \frac{p_B}{\hat{V}}\right)\right\} - \\ & - \frac{1}{\hat{V}} \frac{\dot{\hat{\beta}}\, \ell}{V_R}\left\{C_{k r_B}\left(\hat{\alpha}, \hat{\beta}, \frac{p_B}{\hat{V}}\right) - \hat{V} C_{k\dot{\beta}}\left(\hat{\alpha}, \hat{\beta}, \frac{p_B}{\hat{V}}\right)\right\} \end{aligned} \tag{5.103}$$

where V_R is the flight speed (assumed constant), ℓ a representative length; $\hat{\alpha}$, $\hat{\beta}$ are incidence and sideslip angles defined as,

$$\hat{\alpha} = \frac{W_B}{V_R} \quad , \quad \hat{\beta} = \frac{V_B}{V_R} \quad , \quad \hat{Y} = \frac{U_B}{V_R} \qquad (5.104)$$

where (U_B , V_B , W_B) are the velocity components along the body axes system and (q_B , p_B , r_B) are the angular velocities of the body axes system. The first term in (5.103) is the coefficient that would be measured in a steady coning motion at fixed $\hat{\alpha}$ and $\hat{\beta}$; the second coefficient is directly related to the damping in pitch that would be measured from small oscillations in $\hat{\alpha}$ about $\hat{\beta}$ and coning rate constant. Similarly, the third coefficient is related to the damping in yaw obtained from small oscillations in $\hat{\beta}$ about $\hat{\alpha}$ and coning rate constant. The three required motions are illustrated in Fig. 5.10 (from REF. 5.17). Tobak argues that the form of (5.103) might be adequate for representing the aerodynamic characteristics of slender aircraft manoeuvring at high angle of attack e.g. in the stall and post stall conditions, when the spin radius is small and constant. The three contributions to the right side of (5.103) can be measured, in a wind tunnel, with the same coning apparatus and Tobak points out that the second two contributions need not be measured in the presence of coning rate (equivalent p_B) if no nonlinear dependence on p_B is evident.

An important aspect of the Tobak formulation is its ability to cater for complex flight manoeuvres and in the way it suggests the wind tunnel testing required. The idea of trying to approximately reproduce free flight behaviour on a constrained wind tunnel model seems to offer a satisfying solution to this difficult problem. Of course, a different aerodynamic force and moment representation will then be required for each distinct motion but at least the results will be meaningful and capable to extrapolation to free flight motions, unlike much of the data obtained on simple forced and free oscillation tests.

The coefficients in a representation such as (5.103) can be estimated from free response measurements either by the standard numerical techniques (REF. 5.1) or by approximate analytical techniques such as the method described in this chapter. The memory effects in the representation given by (5.103) are embodied in the dependence on the rates $\dot{\hat{\alpha}}$, $\dot{\hat{\beta}}$ and p_B and for aircraft motions slow compared with the memory time, as Tobak asserts, this is probably a sensible approximation. In a new test situation it will, however, be advisable to measure (indirectly or directly) the actual aerodynamic forces and moments during the unsteady motion in order to estimate the extent of the memory effects. Even when the forces and moments are measured indirectly (e.g. accelerometers) the addition knowledge gained from a study of selective pressure measurements will add considerable weight to a proposed presentation. It is sometimes argued that an understanding of

the fine inner structure of the aerodynamics is not essential if the behaviour corresponding to a class of inputs is known. This viewpoint is not at all in accordance with the philosphy of the aerodynamicist to whom an understanding of the physical mechanisms involved is of paramount importance.

It has been pointed out by Milne (REF. 5.18) that the search for aerodynamic force end moment representations is analogous to the deduction of constitutive relations in continuum mechanics. Considerable effort has been expended on this problem over the last fifteen years e.g. Pipkin (REF. 5.19) discusses the different integral formulations required for small, short and slow motions of materials with fading memory. Pipkin concludes,

> "Constitutive equations of simple useful forms should not be expected to provide accurate descriptions of the behaviour of fluids over the full range of flow conditions implied in the term viscoelastic. The physical properties of most direct importance in a given type of flow may have little or no bearing on the behaviour of the material under other conditions. One fluid may be described under various circumstances by many different narrow range approximations. If a simple narrow range approximation is required in order to make solution of a problem feasible, then the particular approximation to be used should be determined in the course of solving the problem. There is no reason to believe that an approximation valid in one type of motion will also be valid in other types, and there is no reason to require that every narrow range approximation should exhibit the self-consistency desired in the definition of an idealised material."

These conclusions are also germane to the present problem and add substance to the argument that, where complex aircraft motions are involved, suitable force and moment representations should be chosen to fit the problem (narrow range approximations) rather than trying to find general wide range representations that will either be too complicated to apply or too simple to be of any use.

CHAPTER 6 - GENERAL DISCUSSION

The material in the preceeding three chapters is largely concerned with uncontrolled aircraft lateral motions and in particular with the dynamic behaviour of slender configurations at high incidence where the oscillatory mode is prone to instability. To an extent these chapters are autonomous, enjoying their own introductions and discussions; however, the analyses rely heavily on the preliminary mathematical material in Chapter 2. In this chapter some of the important results will be re-stated, the limitations emphasised and possible extensions to other problem areas discussed.

One of the main shortcomings of the mathematical techniques as developed in Chapter 2 is the restriction to one critical mode. For the situation where two or more of the 'whole' aircraft modes are close to the critical condition it will probably be necessary to relax this restriction. There is no essential difficulty in extending the analysis to cater for this type of problem although the periodicity conditions will in general take the form of coupled nonlinear equations requiring a computer solution.

In Chapter 3 approximations were determined for the lateral modes of aircraft motion, as predicted by linear theory, based on a consideration of the aircraft as a weakly coupled system. For slender configurations at high incidence the approximations were achieved by partitioning the complete system into sideways motion and sideslip motion sub-systems with the oscillatory mode corresponding to the latter. The results for the three slender aircraft studied show, in general, a good comparison with exact results. Although it is not possible to draw any strictly general conclusions from those results the indications are that the following tenative conclusions should hold good in other examples, with, of course, the additional proviso that the conditions for weak coupling are satisfied. For configurations that are free from vortex breakdown effects in the incidence range of interest an instability of the oscillatory mode will be accompanied by, at some nearby incidence, a vanishing of the approximate damping given by (3.13) (e.g. H.P.115). A more accurate estimate of the critical incidence can then be found by determining where the second approximation to the damping, given by (3.17), passes through zero. If vortex breakdown does occur in the incidence range of interest then it is unlikely that the approximations will then be valid, as demonstrated by the results for the B.A.C.221. For such cases a different form of partitioning of the system matrix must be sought for a weakly coupled analysis to be valid.

For both slender and conventional configurations the results indicate that the lateral oscillation takes place about some axis displaced and rotated with respect to the aircraft fuselage axis. It was pointed out in Chapter 3 that the location of this axis could serve as a useful parameter in the definition of suitable lateral handling qualities of aircraft. The analysis of Chapter 2 relates to a basically straight and level flight trim state but an extension to the case of descending or climbing flight or the steady banked turn would present no great difficulty.

Chapter 4 is concerned with the effect of a nonlinear yawing and rolling moment with sideslip velocity on the lateral oscillation of slender aircraft. Three different approximation schemes are applied to this problem and while they all reveal the same basic trends they each have particular attributes that are discussed in full at the end of Chapter 4. From the results for the H.P.115 aircraft two important points can be made regarding flight behaviour in the vicinity of an oscillatory stability boundary. Referring to Fig. 4.2, the first point concerns flight above the critical incidence. We see that for a range of values of n_{v_2} and γ_2 the motion can be self limiting, reducing the instability to a mild form with possibly no serious consequences on the overall flight conditions. Secondly, with regard to flight at incidences lower than critical, we deduce that instability is possible for a range of n_{v_2}, γ_2, for large enough disturbances. These two situations cannot co-exist for the same configuration and the one that is realised for a particular case essentially depends upon the effect of the nonlinearities at the critical incidence. It is clearly necessary to base a perturbation scheme on an artificial critical system over the incidence range of interest in order to determine the limit cycle motions on both sides of the critical incidence.

For the example studied in Chapter 4 the effect of the longitudinal motion on the lateral oscillation was shown to be quite small. In a general motion analysis where, say, the aircraft is responding to disturbances in both the longitudinal and lateral sense, then there will probably be a more pronounced aerodynamic coupling effect. The whole question of response to control application and gusts has not been investigated in this thesis but the perturbation methods are also well suited to the response problem and such a study would be a natural step from the free motion analysis of Chapter 4.

The main result of Chapter 5 is the approximate analytic expression derived for the logarithmic decrement of a nonlinear oscillation. It was shown how this approximation can be used to obtain estimates of damping parameters by obtaining a least squares fit of experimental measurements with the approximate logarithmic decrement. Particular examples were studied to illustrate the technique using ordinary trigonometric and Jacobian elliptic functions to model the basic oscillation. The method is restricted to oscillations with small damping functions and is ideally suited to the analysis of wind tunnel model motions having marginal stability. Such situations often require large amplitude tests to be performed and clearly any nonlinearities present will have a significant effect on the results.

The question of incorporating fading memory effects in the representation of aerodynamic forces and moments is also discussed in Chapter 5. For aircraft motions where the memory time is short and the motion relatively slow compared with the memory time then the formulation of Tobak seems to offer the most suitable framework for force and moment representations in oscillatory modes. In the simplest form the memory effects appear in the first order rate terms. It seems unlikely, however, that a single formulation will be adequate for a wide range of complex aircraft motions and the best efforts would probably be directed towards

constructing a set of narrow range approximate representations each pertaining to a particular class of aircraft motion. Such representations should be soundly based on both physical and mathematical grounds.

ACKNOWLEDGEMENTS

I would like to express my thanks to my supervisor, Dr. P.A.T. Christopher, for his continuing encouragement and for providing the opportunity for me to teach Aircraft Stability and Control to short course students at Cranfield, an experience that indirectly contributed to the content of this thesis. I am especially grateful to Professor Maurice Rasmussen of the University of Oklahoma for the countless stimulating discussions during his stay at Cranfield during the year 1973/74 and for suggesting several aspects of the work in this thesis including the method of multiple scales and the nonlinear logarithmic decrement. For valuable discussions on the effect of aerodynamic nonlinearity on aircraft lateral motions I am grateful to Dr. A. Jean Ross of the Royal Aircraft Establishment, Farnborough. Thanks also to Hewitt Phillips of NASA, Langley, who during his stay at Cranfield in 1975, was a source of considerable inspiration and novel ideas. For a few short discussions on the representation of aerodynamic forces in the presence of nonlinear and memory effects I am indebted to Murray Tobak of NASA, Ames.

I am very grateful to Malcolm Goodridge of the Aerodynamics Division at Cranfield for preparing the figures to such a very high standard and to Mrs. J. Betteridge who typed the thesis from manuscript.

Special thanks are due to my wife Joey and son Jude who, with their gifted ways, made it all so clearly possible.

Finally, I would like to thank the Science Research Council for the essential financial support.

REFERENCES

CHAPTER 1

1.1 STERNFIELD, L. — Some effects of nonlinear variation in the directional stability and damping in yawing derivatives on the lateral stability of an airplane. NACA report 1042,1952

1.2 RHOADS, D.W. SCHULER, T.M. — A theoretical and experimental study of airplane dynamics in large disturbance maneouvres. Journal of the Aeronautical Sciences, July 1957, pp. 507-526 (532).

1.3 HACKER, T. OPRISIU, C. — A discussion of the roll-coupling problem. Progress in Aerospace Sciences, Vol. 15, pp.151-180, Pergamon Press Ltd., 1974.

1.4 WILEY, H.G. — The significance of nonlinear damping trends determined for current aircraft configurations. AGARD-CP-17, 1966.

1.5 THOMAS, H.H.B.M. COLLINGBOURNE, Joan — Longitudinal motions of aircraft involving high angles of attack. A.R.C. R. & M. 3753 (1973).

1.6 ROSS, A. Jean BEECHAM, L.J. — An approximate analysis of the nonlinear lateral motion of a slender aircraft (H.P.115) at low speeds. A.R.C. R. & M. 3674 (1971).

CHAPTER 2

2.1 STRUBLE, R.A. — Nonlinear Differential Equations. McGraw-Hill Book Company, 1962.

2.2 KUZMAK, G.E. — Asymptotic solutions of nonlinear second order differential equations with variable coefficients. P.M.M., VOL. 23, No. 3, 1959, pp. 515-526.

2.3 NAYFEH, A.H. — Perturbation Methods. John Wiley, 1973.

2.4 HAHN, W.
Stability of Motion.
Springer Verlag, 1967.

2.5 PADFIELD, G.D.
On the use of approximate solutions for nonlinear oscillation problems.
Cranfield Aero. Note 3/74,
August 1974.

2.6 BYRD, P.F.
FRIEDMAN, M.D.
Handbook of Elliptic Integrals for Engineers and Physicists.
Springer Verlag, 1954.

2.7 BARKHAM, P.
SOUDACK, A.
International Journal of Control
Vol. 10, No. 4, 1969, pp.377-392.
Vol. 11, No. 1, 1970, pp.101-114.
Vol. 12, No. 5, 1970, pp.763-767.
Vol. 13, No. 4, 1971, pp.767-770.

2.8 CHRISTOPHER, P.A.T.
(with BROCKLEHURST, A.)
International Journal of Control
Vol. 17, No. 3, 1973, pp.597-608.
Vol. 19, No. 4, 1974, pp.831-839.

2.9 RASMUSSEN, M.L.
Uniformly valid approximations for nonlinear oscillations with small damping.
Int. J. Nonlinear Mechanics, Vol. 5, 1970, pp.687-696.

2.10 MILNE, R.D.
The analysis of weakly coupled dynamical systems.
Int. J. Control, Vol. 2, 2, 1965, pp. 171-199.

2.11 MALKIN, I.G.
Theory of Stability of Motion (translated from Russian).
United States Atomic Energy Commission (translation series)
AEC-tr. 3352.

2.12 As Ref. (1.6)

CHAPTER 3

3.1 PINSKER, W.J.G.
The lateral motion of aircraft, and in particular of inertially slender configurations.
A.R.C. R. & M. 3334 (1963)

3.2 THOMAS, H.H.B.M.
NEUMARK, S.
Interim note on stability and response characteristics of supersonic aircraft.
A.R.C. 18,263 (1955)
R.A.E. T.N. Aero. 2412 (1955)

3.3	ROSS, A. Jean	The lateral oscillation of slender aircraft. A.R.C. C.P. 845 (1966)
3.4	As Ref. (2.10)	
3.5	BABISTER, A.W.	Aircraft Stability and Control. Pergamon Press 1961.
3.6	HENDERSON, J.M.	Low speed handling of a slender delta (H.P.115). Journal of the R.Ae.S. May 1965.
3.7	As Ref. (1.6)	
3.8	BISGOOD, P.L. POULTER, R.L.	Flight measurements of the lateral stability and control characteristics of a slender wing research aircraft (H.P.115) and comparison with wind tunnel results. R.A.E. Tech. Rpt. 72186 (1972).
3.9	BARNES, C.S. NICHOLES, O.P.	Preliminary flight assessment of the low speed handling of the B.A.C. 221 ogee wing research aircraft. A.R.C. C.P. 1102 (Nov. 1967).
3.10	PINSKER, W.J.G.	Directional stability in flight with bank angle constraint as a condition defining a minimum acceptable value for n_v . A.R.C. R. & M. 3556 (1968).
3.11	HOLFORD, Dorothy M.	Aerodynamic data for the B.A.C. 221 up to a mach number of 0.955 as measured in wind tunnel tests. A.R.C. C.P. No. 1230 (1972).
3.12	O'LEARY, C.O.	Low speed wind tunnel measurements of the oscillatory lateral aerodynamic derivatives of a B.A.C.221 model and comparison with similar Concorde and H.P.115 data. A.R.C. R. & M. 3671 (1971).
3.13	FENNELL, L.J.	Vortex breakdown - some observations in flight on the H.P.115 aircraft. R.A.E. Tech. Rpt. 71177 (Sept. 1971).
3.14		Unpublished Sud-Aviation, British Aircraft Corporation Data Sheets, Series 1.15, 1.16, 2.5.

3.15 MILNE, R.D.
PADFIELD, G.D.
The strongly controlled aircraft.
Aeronautical Quarterly, May 1971, pp. 146-168.

3.16 ASHLEY, HOLT
Engineering Analysis of Flight Vehicles.
Addison Wesley, 1974.

3.17 ETKIN, Bernard
Dynamics of Atmospheric Flight.
John Wiley 1972.

CHAPTER 4

4.1 As Ref. (2.11)

4.2 As Ref. (1.6)

4.3 PARTRIDGE, D.W.
PECOVER, B.E.
An application of the RAE wind tunnel/flight dynamics simulator to the low speed dynamics of a slender delta aircraft (H.P.115).
A.R.C. R. & M. 3669 (1969).

4.4 ROSS, A. Jean
An experimental and analytical study of nonlinear motion experienced on a slender wing research aircraft.
R.A.E. Tech. Memo.Aero. 1386 (1972).

4.5 KLEIN, V.
Longitudinal aerodynamic derivatives of a slender delta wing research aircraft extracted from flight data.
Cranfield Rpt. Aero. No. 27, January 1975.

CHAPTER 5

5.1 KLEIN, V.
System parameter identification in aircraft dynamics.
'Aircraft Stability and Control'.
Von Karman Institute Lecture series 80, May 1975.

5.2 As Ref. (3.5)

5.3 TOBAK, Murray
An inverse problem for a class of non-linear differential equations.
J. Mathematical Analysis and Applications, Vol. 15, No. 2, Aug. 1966.

5.4 As Ref. (2.5)

5.5 As Ref. (2.6)

5.6 RASMUSSEN, M.L. Unpublished Notes. Cranfield, Aero. Div. 1974.

5.7 As Ref. (2.9)

5.8 RASMUSSEN, M.L. Nonlinear oscillations with small speed dependent damping. Developments in Mechanics, Vo. 7. University of Pittsburg Engr. School, 1973, pp.437-448.

5.9 HAYNES, T.L. Development of a Rig to Measure Lp and Investigation at High Incidence. College of Aeronautics (Aerodynamics Div.) M.Sc. Thesis 1974.

5.10 OWEN, T.B. Low speed wind tunnel measurements of oscillatory rolling derivations on a sharp edged slender wing. Effects of frequency parameter and of ground. A.R.C. R. & M. 3617 (1968).

5.11 MILES, John W. Unsteady flow theory in dynamic stability. Journal of the Aeronautical Sciences, Vol. 17. January 1950, pp.62-63.

5.12 GOLAND, Martin The quasi steady air forces for use in low frequency stability calculations. Journal of the Aeronautical Sciences, Vol. 17, No. 10. October 1950, pp. 601-608 (672).

5.13 BRUNE, Gunter W. Low Frequency approximations to unsteady aerodynamics. Journal of Aircraft, Vol. 6, No. 5. (Oct. 1969). pp.478-480.

5.14 RODDEN, W.P. GIESING, J.P. Application of oscillatory aerodynamic theory to estimation of dynamic stability derivatives. Journal of Aircraft. Vol. 7, No. 3. (May-June 1970), pp. 272-275.

5.15 MILNE, R.D. Asymptotic solutions of linear stationary integro-differential equations. A.R.C. R. & M. 3548 (1966).

5.16 BROWN, A.E. SCHY, A.A. Analysis of the dynamic lateral stability of a delta wing airplane with frequency dependent stability derivatives. NASA-TN-D-113 Nov. 1959.

5.17 TOBAK, Murray
SCHIFF, L.B.
On the formulation of the aerodynamic characteristics in aircraft dynamics. NASA-TR-R-456 (1975).

5.18 MILNE, R.D.
Private communication.

5.19 PIPKIN, A.C.
Approximate Constitutive Equations. Modern Developments in the Mechanics of Continua. pp.89-108. Academic Press (1966).

APPENDIX A - THE LINEARISED EQUATIONS OF AIRCRAFT LATERAL MOTION

Within the framework of the linear theory the equations of motion referred to geometric body axes (axes fixed in the body, irrespective of flight condition), origin at the centre of gravity, are written in the form,

$$\frac{dV}{dt} - W_c p + U_c r - g\cos\theta_c \phi = \frac{\rho S V_R^2}{m}\left(Y_v\left(\frac{V}{V_R}\right) + Y_p\left(\frac{pS}{V_R}\right) + Y_r\left(\frac{rS}{V_R}\right)\right) \qquad (A.1)$$

$$\frac{dp}{dt} - \frac{I_{xz}}{I_{xx}}\frac{dr}{dt} = \frac{\rho S V_R^2}{I_{xx}}\left(\ell_v\left(\frac{V}{V_R}\right) + \ell_p\left(\frac{pS}{V_R}\right) + \ell_r\left(\frac{rS}{V_R}\right)\right) \qquad (A.2)$$

$$\frac{dr}{dt} - \frac{I_{xz}}{I_{zz}}\frac{dp}{dt} = \frac{\rho S V_R^2}{I_{zz}}\left(n_v\left(\frac{V}{V_R}\right) + n_p\left(\frac{pS}{V_R}\right) + n_r\left(\frac{rS}{V_R}\right)\right) \qquad (A.3)$$

$$\frac{d\phi}{dt} = p + r\tan\theta_c \qquad (A.4)$$

where v, p, r are the sideslip velocity, roll rate and yaw rate referred to the body axes system respectively. ϕ is the Euler 'roll angle' when the Euler angles (ψ , θ , ϕ) are the rotations required to take the aircraft into its disturbed state from a 'horizontal' reference condition (as opposed to the trim state reference).

θ_c is the trim incidence for straight and level flight; w_c and u_c are the velocity components along the body z and x axes respectively. I_{xx} and I_{zz} are the moments of inertia about the x and z axes and I_{xz} is the product of inertia about the x and z axes. V_R is the trim flight speed, ρ the air density, S the reference wing area, s the semi span. The coefficients y_v, ℓ_p, n_r etc. are normalised aerodynamic derivatives representing the linearised terms in the expansion of the aerodynamic force in terms of the aircraft motion. These derivatives are normalised as follows:

$$y_v = \frac{\partial(Y/\rho V_R^2 S)}{\partial(V/V_R)} \quad , \quad y_p = \frac{\partial(Y/\rho V_R^2 S)}{\partial(pS/V_R)} \quad , \quad y_r = \frac{\partial(Y/\rho V_R^2 S)}{\partial(rS/V_R)}$$

$$\ell_v = \frac{\partial(L/\rho V_R^2 S)}{\partial(V/V_R)} \quad , \quad \ell_p = \frac{\partial(L/\rho V_R^2 S)}{\partial(pS/V_R)} \qquad \ell_r = \frac{\partial(L/\rho V_R^2 S)}{\partial(rS/V_R)}$$

similarly for n_v , n_p and n_r .

We choose to normalize (A.1) - (A.4) according to the following scheme:

$$\text{let} \quad \bar{V} = V/V_R \quad , \quad \bar{p} = \frac{pS}{V_R} \quad , \quad \bar{r} = \frac{rS}{V_R}$$

$$\bar{W}_0 = W_0/V_R \quad , \quad \bar{U}_0 = U_0/V_R .$$

$$\hat{t} = \frac{V_R}{S} t \quad , \quad \mu_2 = m/\rho S s \quad , \quad g_1 = \frac{g S \cos\theta_0}{V_R^2}$$

$$i_{xx} = \frac{I_{xx}}{m s^2} \quad , \quad i_{zz} = \frac{I_{zz}}{m s^2} \quad , \quad i_{xz} = \frac{I_{xz}}{m s^2}$$

$$e_x = i_{xz}/i_{xx} \qquad e_z = i_{xz}/i_{zz}$$

The normalized equation therefore take the form,

$$\frac{d\bar{v}}{d\hat{t}} - \bar{w}_o \bar{p} + \bar{U}_o \bar{r} - g_1 \phi = \frac{1}{\mu_2}\left(y_v \bar{v} + y_p \bar{p} + y_r \bar{r} \right) \qquad (A.5)$$

$$\frac{d\bar{p}}{d\hat{t}} - e_x \frac{d\bar{r}}{d\hat{t}} = \frac{1}{\mu_2}\left(\ell_v \bar{v} + \ell_p \bar{p} + \ell_r \bar{r} \right) \qquad (A.6)$$

$$\frac{d\bar{r}}{d\hat{t}} - e_z \frac{d\bar{p}}{d\hat{t}} = \frac{1}{\mu_2}\left(n_v \bar{v} + n_p \bar{p} + n_r \bar{r} \right) \qquad (A.7)$$

$$\frac{d\phi}{d\hat{t}} = \bar{p} + \bar{r} \tan\theta_c \qquad (A.8)$$

If the body X axes coincides with the flight direction in all flight conditions then it is referred to as the stability axes system. All the kinematic variables, aerodynamic derivatives and inertias will then be referred to this new system and (A.5) - (A.8) are modified since we have.

$$\theta_c = \bar{w}_o = 0 \quad , \quad \bar{U}_o = 1 \qquad \text{(straight and level)}$$

The concise derivatives appearing in (3.1) for the above normalising scheme can be written,

$$y_v' = \frac{y_v}{\mu_2} \quad ; \quad y_p' = \frac{y_p}{\mu_2} \quad ; \quad y_r' = \frac{y_r}{\mu_2} \qquad (A.9)$$

$$n_v' = \frac{n_v + e_x \rho_v}{\mu_2 i_{zz}(1-e_x e_z)} \qquad n_p' = \frac{n_p + e_x \rho_p}{\mu_2 i_{zz}(1-e_x e_z)} \qquad n_r' = \frac{n_r + e_x \rho_r}{\mu_2 i_{zz}(1-e_x e_z)} \tag{A.10}$$

$$\rho_v' = \frac{\rho_v + e_z n_v}{\mu_2 i_{xx}(1-e_x e_z)} \qquad \rho_p' = \frac{\rho_p + e_z n_p}{\mu_2 i_{xx}(1-e_x e_z)} \qquad \rho_r' = \frac{\rho_r + e_z n_r}{\mu_2 i_{xx}(1-e_x e_z)} \tag{A.11}$$

Also $$g_1 = C_L \cos\theta_0 / 2\mu_2$$

To convert (3.1) into the form given by (3.3) we proceed as follows, From (A.8) we can write,

$$\bar{p} = \frac{d\phi}{d\hat{t}} - \bar{r} \tan\theta_c \tag{A.12}$$

The rolling moment equation in (3.1) gives, using (A.12)

$$\bar{r} = \frac{1}{\rho_r^*} \int \frac{d^2\phi}{d\hat{t}^2} - \rho_v^* \bar{v} - \rho_p^* \frac{d\phi}{d\hat{t}} \Big\} \tag{A.13}$$

where the new concise derivatives ρ_r^*, ρ_v^*, ρ_p^* are given by (3.5).

The sideforce equation in (3.1) can be written, using (A.13), (A.12),

$$\frac{d\bar{v}}{d\hat{t}} - y_v^* \bar{v} - (y_p^* + w_c)\frac{d\phi}{d\hat{t}} - \frac{(y_r^* - v_c^*)}{\rho_r^*} \int \frac{d^2\phi}{d\hat{t}^2} - \rho_v^* \bar{v} - \rho_p^* \frac{d\phi}{d\hat{t}} \Big\} - g_1 \phi = 0 \tag{A.14}$$

Differentiating the sideforce equation in its original form and substituting for $d\bar{r}/d\hat{t}$ from the yawing moment equation gives,

$$\frac{d^2\bar{v}}{d\hat{t}^2} - y_v^* \frac{d\bar{v}}{d\hat{t}} - (y_p^* + \bar{w}_c)\frac{d^2\phi}{d\hat{t}^2} -$$

$$-(y_r^* - \bar{u}_c^*)\left\{ n_v^* \bar{v} + n_p^* \frac{d\phi}{d\hat{t}} + \frac{n_r^*}{e_r^*}\left(\frac{d^2\phi}{d\hat{t}^2} - e_v^* \bar{v} - e_p^* \frac{d\phi}{d\hat{t}} \right) \right\} \qquad (A.15)$$

$$- g_1 \frac{d\phi}{d\hat{t}} = 0$$

We now use the relation defined in (3.2) to eliminate ϕ, i.e.

$$\phi = \frac{(\bar{v} - \bar{v}_c)}{\bar{w}_c} \qquad (A.16)$$

Substituting (A.16) into (A.14) and (A.15) we obtain the two second order equations in $\bar{v}_c$ and $\bar{v}$.

$$\begin{bmatrix} (y_p^* + \bar{w}_c) e_r^* + (y_r^* - \bar{u}_c^*) n_r^* & -(y_p^* e_r^* + (y_r^* - \bar{u}_c^*) n_r^*) \\ (y_r^* - \bar{u}_c^*) & -(y_r^* - \bar{u}_c^*) \end{bmatrix} \begin{bmatrix} \ddot{\bar{v}}_c \\ \ddot{\bar{v}} \end{bmatrix} +$$

$$+ \begin{bmatrix} (y_r^* - \bar{u}_c^*)(n_p^* e_r^* - n_r^* e_p^*) + g_1 e_r^* & -\left(y_v^* + \frac{g_1}{\bar{w}_c} + \frac{(y_r^* - \bar{u}_c^*)}{\bar{w}_c e_r^*}(n_p^* e_r^* - n_r^* e_p^*) \right) \bar{w}_c e_r^* \\ (y_p^* + \bar{w}_c) e_r^* - (y_r^* - \bar{u}_c^*) e_p^* & -y_p^* e_r^* + (y_r^* - \bar{u}_c^*) e_p^* \end{bmatrix} \begin{bmatrix} \dot{\bar{v}}_c \\ \dot{\bar{v}} \end{bmatrix} +$$

$$+ \begin{bmatrix} 0 & -\bar{w}_c (y_r^* - \bar{u}_c^*)(n_v^* e_r^* - n_r^* e_v^*) \\ g_1 e_r^* & -\bar{w}_c e_r^* \left(y_v^* + \frac{g_1}{\bar{w}_c} - \frac{(y_r^* - \bar{u}_c^*)}{e_r^*} e_v^* \right) \end{bmatrix} \begin{bmatrix} \bar{v}_c \\ \bar{v} \end{bmatrix} = 0 \qquad (A.17)$$

The equation can be finally brought to the form given by (4.3) by pre-multiplying (A.17) by the inverse of the coefficient matrix of $\{\ddot{v}_o, \ddot{\gamma}\}$.

Concise derivatives in American Notation

The examples used in Chapter 3 to illustrate the linearised approximation to the classical modes of motion are taken from American texts (REF. 3.16 and REF. 3.17). In the notation of these texts, the concise derivatives in (3.1) can be written in the form,

$$Y_v' = \frac{C_{y\beta}}{2\mu_2}, \quad Y_p' = \frac{C_{yp}}{2\mu_2}, \quad Y_r' = \frac{C_{yr}}{2\mu_2}$$

$$\ell_v' = \frac{C_{\ell\beta}}{\bar{i}_{xx}} + e_x \frac{C_{n\beta}}{\bar{i}_{zz}}, \quad \ell_p' = \frac{C_{\ell p}}{\bar{i}_{xx}} + e_x \frac{C_{np}}{\bar{i}_{zz}}, \quad \ell_r' = \frac{C_{\ell r}}{\bar{i}_{xx}} + \frac{C_{nr} e_x}{\bar{i}_{zz}}$$

$$n_v' = \frac{C_{n\beta}}{\bar{i}_{zz}} + e_z \frac{C_{\ell\beta}}{\bar{i}_{xx}}, \quad n_p' = \frac{C_{np}}{\bar{i}_{zz}} + e_z \frac{C_{\ell p}}{\bar{i}_{xx}}, \quad n_r' = \frac{C_{nr}}{\bar{i}_{zz}} + e_z \frac{C_{\ell r}}{\bar{i}_{xx}}$$

where $\bar{i}_{xx} = I_{xx}/\rho S(s)^3 \qquad \bar{i}_{zz} = I_{zz}/\rho S(s)^3$

and $g_1 = C_L/2\mu_2$

It can be seen that the only observable difference in the equation of motion will be the $\frac{1}{2}$ multiplying the derivatives in the sideforce equation.

TABLE 3.1 - H.P.115 DATA (REF.3.7)

Mass	m	2154 kg	
Moment of inertia about X axis	I_{xx}	2182 kg m^2	$i_{xx} = 0.109$
Moment of inertia about Z axis	I_{zz}	25430 kg m^2	$i_{zz} = 1.27$
Product of inertia about XZ axis	I_{xz}	1615 kg m^2	$i_{xz} = 0.0806$
Moment of inertia about Y axis	I_{yy}	23517 kg m^2	
Wing semi span	s	3.05 m	
Mean chord	$\bar{c}$	12.2 m	
Wing area	S	40.18 m^2	
Relative density	μ_2	20.0	

TABLE 3.2 - H.P.115 α and β COEFFICIENTS FOR LATERAL EQUATION OF MOTION.

α°	α_1	α_2	α_3	α_4
12	-0.00036	-0.06782	-0.00129	0.0492
14	-0.00036	-0.0682	-0.00099	0.0505
16	-0.00034	-0.0686	-0.0007	0.0518
18	-0.00032	-0.0685	-0.00041	0.0528
20	-0.00029	-0.0693	-0.00012	0.05464
22	-0.00026	-0.0697	0.00017	0.0563
24	-0.00022	-0.0702	0.00046	0.0582
26	-0.00018	-0.0707	0.00069	0.0597

α°	β_1	β_2	β_3	β_4
12	-0.00073	-0.02166	-0.01257	-0.0083
14	-0.0009	-0.0269	-0.0165	-0.0064
16	-0.00109	-0.03268	-0.0212	-0.00453
18	-0.00128	-0.0384	-0.0265	-0.00313
20	-0.0015	-0.0453	-0.0325	-0.00106
22	-0.00175	-0.0521	-0.0391	0.00063
24	-0.002	-0.0593	-0.0463	0.00238
26	-0.0022	-0.065	-0.0521	0.00367

TABLE 3.3 - B.A.C. 221 DATA

Moment of inertia about X axis	i_{xx}	=	0.106	} principal moments of inertia
Moment of inertia about Z axis	i_{zz}	=	0.634	
Wing semi-span	s	=	3.84 m	
Wing area	S	=	45.5 m^2	
Relative density	μ_2	=	83.27	

TABLE 3.4 - BAC.221 α and β COEFFICIENTS FOR LATERAL EQUATIONS OF MOTION.

α°	α_1	α_2	α_3	α_4
12	-0.00007	-0.0204	-0.00089	0.01205
14	-0.00007	-0.01971	-0.00068	0.0115
16	-0.00007	-0.0194	-0.00052	0.0111
18	-0.00008	-0.0193	-0.00037	0.0106
20	-0.00009	-0.0181	0.00044	0.00869
22	-0.00011	-0.0157	0.00107	0.00448
24	-0.00022	-0.0127	0.00432	-0.00768
26	-0.00021	-0.00974	0.00382	-0.0442

α°	β_1	β_2	β_3	β_4
12	-0.00009	0.00724	-0.0047	-0.0172
14	-0.00011	0.00819	-0.00525	-0.0191
16	-0.00012	0.00982	-0.00574	-0.022
18	-0.00015	0.0109	-0.00586	-0.0251
20	-0.0002	0.0108	-0.00483	-0.0284
22	-0.00028	0.00461	-0.00399	-0.0281
24	-0.00052	-0.00156	-0.00036	-0.0426
26	-0.00056	-0.00544	-0.00182	-0.0442

TABLE 3.5 - PROTOTYPE CONCORDE DATA (REF.3.14)
(approach configuration - nose droop $17\frac{1}{2}^{\circ}$)

Moment of inertia about X axis	i_{xx}	= 0.0817
Moment of inertia about Z axis	i_{zz}	= 0.735
Wing semi-span	s	= 12.8 m
Relative density	μ_2	= 16.14

TABLE 3.6 - α and β COEFFICIENTS FOR THE PROTOTYPE CONCORDE.

α°	α_1	α_2	α_3	α_4	α_4'*
12	-0.00251	-0.1182	-0.00754	0.07308	0.06303
14	-0.00291	-0.1234	-0.00804	0.0744	0.0632
16	-0.00326	-0.1271	-0.0079	0.07429	0.06197
18	-0.00367	-0.1319	-0.00638	0.0738	0.0603
20	-0.00398	-0.1354	-0.00397	C.0724	0.0577
21	-0.00417	-0.1377	-0.0024	0.07165	0.0563

α°	β_1	β_2	β_3	β_4	β_4'*
12	-0.00445	0.0489	-0.0297	-0.1178	-0.1337
14	-0.00569	0.03541	-0.0369	-0.1173	-0.1364
16	-0.007	0.0219	-0.0442	-0.1181	-0.1407
18	-0.00831	0.00598	-0.0511	-0.1171	-0.1435
20	-0.00944	-0.00676	-0.058	-0.1179	-0.1467
21	-0.0103	-0.0157	-0.061	-0.1189	-0.1507

* The coefficients α_4' and β_4' include the effect of the derivatives $\ell\dot{v}$ and $n\dot{v}$.

TABLE 3.7 - N.A. XB.70-1 DATA (REF. 3.16)

M = 0.79	M = 1.2	M = 2.1
V = 802.7 ft/s	V = 1161.6 ft/s	V = 2032.8 ft/s
C_L = 0.174	C_L = 0.158	C_L = 0.077
μ_2 = 33.51	μ_2 = 63.28	μ_2 = 95.01
$\bar{i_{xy}}$ = 2.038	$\bar{i_{xy}}$ = 3.645	$\bar{i_{xx}}$ = 5.271
$\bar{i_{zz}}$ = 22.646	$\bar{i_{zz}}$ = 41.687	$\bar{i_{zz}}$ = 61.634
e_x = -0.394	e_x = -0.436	e_x = -0.437
e_z = -0.0355	e_z = -0.0381	e_z = -0.0374

Aerodynamic derivatives

M = 0.79	M = 1.2	M = 2.1
Ce_β -0.091	-0.057	0.011
$C_{n\beta}$ 0.074	0.092	0.057
Ce_p -0.175	-0.24	-0.1
C_{np} 0.0	-0.13	-0.09
Ce_r -0.15	-0.47	0.0
C_{nr} -0.1	-0.55	-0.38
$C_{y\beta}$ -0.315	-0.344	-0.309
C_{yr} 0.109	0.19	0.22

TABLE 3.8 - COMPARISON OF EXACT AND APPROXIMATE EIGENVALUES FOR XB.70-1

M		Spiral Mode (λ_1)	Dutch Roll Mode ($\lambda_{2,3}$)	Roll Subsidence Mode λ_4
0.79	Exact	-0.00296	$-0.00421 \pm 0.0688\,i$	-0.0823
	Approximate	-0.00283	$-0.00344 \pm 0.0678\,i$	-0.086
1.2	Exact	-0.00298	$-0.00208 \pm 0.0549\,i$	-0.0696
	Approximate	-0.00285	$-0.00374 \pm 0.0571\,i$	-0.0645
2.1	Exact	0.000363	$-0.00497 \pm 0.0289\,i$	-0.017
	Approximate	0.000381	$-0.00399 \pm 0.0276\,i$	-0.0183

TABLE 3.9 - DATA FOR ETKIN'S SUBSONIC JET TRANSPORT (REF. 3.17)

Weight	W	= 100,000 lb.
Moment of inertia about X_p axis	$\bar{i}_{x_p x_p}$	= 3.664 (X_p, Z_p - principal axes of inertia)
Moment of inertia about Z_p axis	$\bar{i}_{z_p z_p}$	= 9.256
Angle between X_p axis and X axis in stability axes system	ε	$= -(0.019 + (C_L / 4.88))$
Relative density	μ_2	= 38.807
Wing semi-span	S = 54 ft	Wing area S = 1667 ft^2

Aerodynamic Derivatives (functions of C_L)

$C_{y_\beta} = -0.168$	$C_{y_p} = 0$	$C_{y_r} = 0.192$
$C_{\ell_\beta} = -(0.022+0.1 C_L)$	$C_{\ell_p} = -0.43$	$C_{\ell_r} = 0.0077+0.25 C_L$
$C_{n_\beta} = 0.036+0.04 C_L^2$	$C_{n_p} = 0.008-0.1 C_L$	$C_{n_r} = -(0.116+0.02 C_L^2)$

NOTE:

$$\bar{i}_{x_s x_s} = \bar{i}_{x_p x_p} \cos^2\varepsilon + \bar{i}_{z_p z_p} \sin^2\varepsilon$$

$$\bar{i}_{z_s z_s} = \bar{i}_{z_p z_p} \cos^2\varepsilon + \bar{i}_{x_p x_p} \sin^2\varepsilon$$

$$\bar{i}_{x_s z_s} = \frac{1}{2}(\bar{i}_{z_p z_p} - \bar{i}_{x_p x_p}) \sin 2\varepsilon$$

TABLE 4.1 - DATA FOR H.P.115 SIDESLIP LIMIT CYCLES FROM BIFURCATION THEORY.

α°	20	22	23	24	25	26
a_1	.07033	.06905	.06844	.06784	.06727	.06671
a_{10}	.0668	.06756	.06801	.06842	.06876	.0692
b_1	.0353	.0422	.0459	.04977	.05379	.05797
b_{10}	.03506	.0421	.0459	.0498	.05389	.05815
c_1	.002325	.002828	.003104	.003392	.003691	.00401
c_{10}	.002324	.002828	.003104	.003393	.003692	.00401
$d_1 \times 10^5$	.936	1.04	1.076	1.097	1.097	1.079
$d_{10} \times 10^5$	.936	1.04	1.076	1.097	1.097	1.079
μ	-.00176	-0.000745	-0.000216	.000289	.000744	.001245
Δ	.00009	.00013	.000155	.000183	.00024	.00025
$\rho_1 \times 10^5$	.47	.67	.79	.929	1.06	1.23
$\rho_2 \times 10^5$	.41	.555	.637	.734	.834	.955

TABLE 4.2 - NONLINEAR ROUTHIAN COEFFICIENTS FOR THE H.P.115

α°	20	22	23	24	25	26
$m_o \times 10^5$	-0.007	-0.105	-0.166	-0.238	-0.316	-0.41
$m_1 \times 10^4$	-0.221	-0.291	-0.333	-0.38	-0.43	-0.49
$m_2 \times 10^5$	-0.130	-0.205	-0.251	-0.302	-0.356	-0.425
$n_o \times 10^5$	0.496	0.680	0.793	0.926	1.06	1.23
$n_1 \times 10^5$	0.147	0.406	0.589	0.807	1.06	1.38
$R_o \times 10^6$	0.3185	0.1938	0.0667	-0.1052	-0.3177	-0.6213

TABLE 5.1 - PARAMETER VALUES FOR OSCILLATORY SOLUTIONS OF (5.51)

Case	i	ii	iii	iv
c_1	1.0	1.0	-1.0	-1.0
c_3	10.0	-2.0	10.0	2.0
h_0	-0.5	-0.5	-0.5	-0.5
h_2	2.0	6.0	2.0	2.0
ε	1.0	1.0	1.0	1.0

TABLE 5.2 - LEAST SQUARES ESTIMATES OF DAMPING PARAMETERS h_0, h_2

Case	i	ii	iii	iv
h_0^*	-0.513	-0.499	-0.504	-0.49
h_2^*	2.035	6.063	2.03	2.09

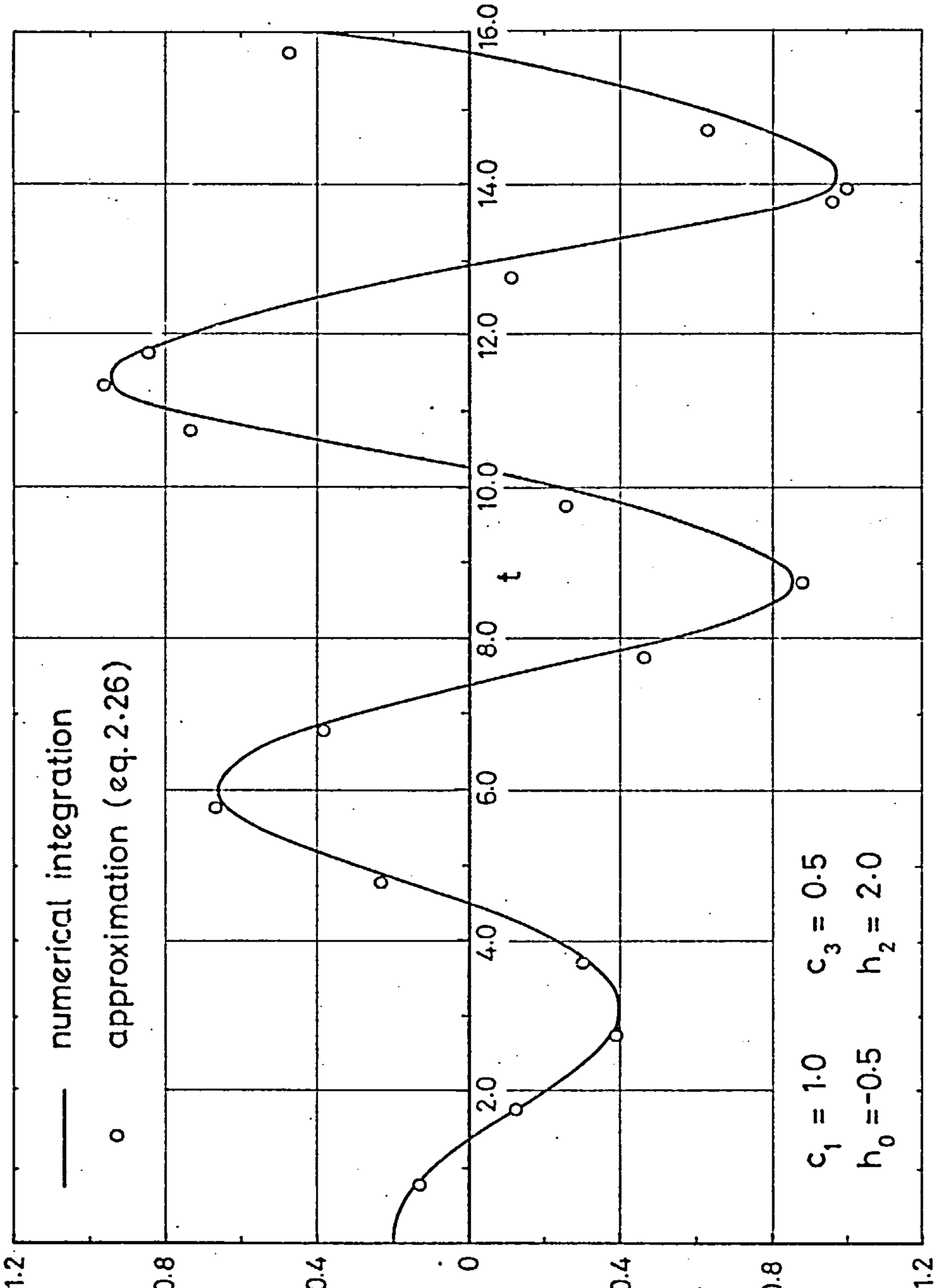

Fig.2.1 Comparison of approximate and exact numerical solution for a weakly non-linear second order system.

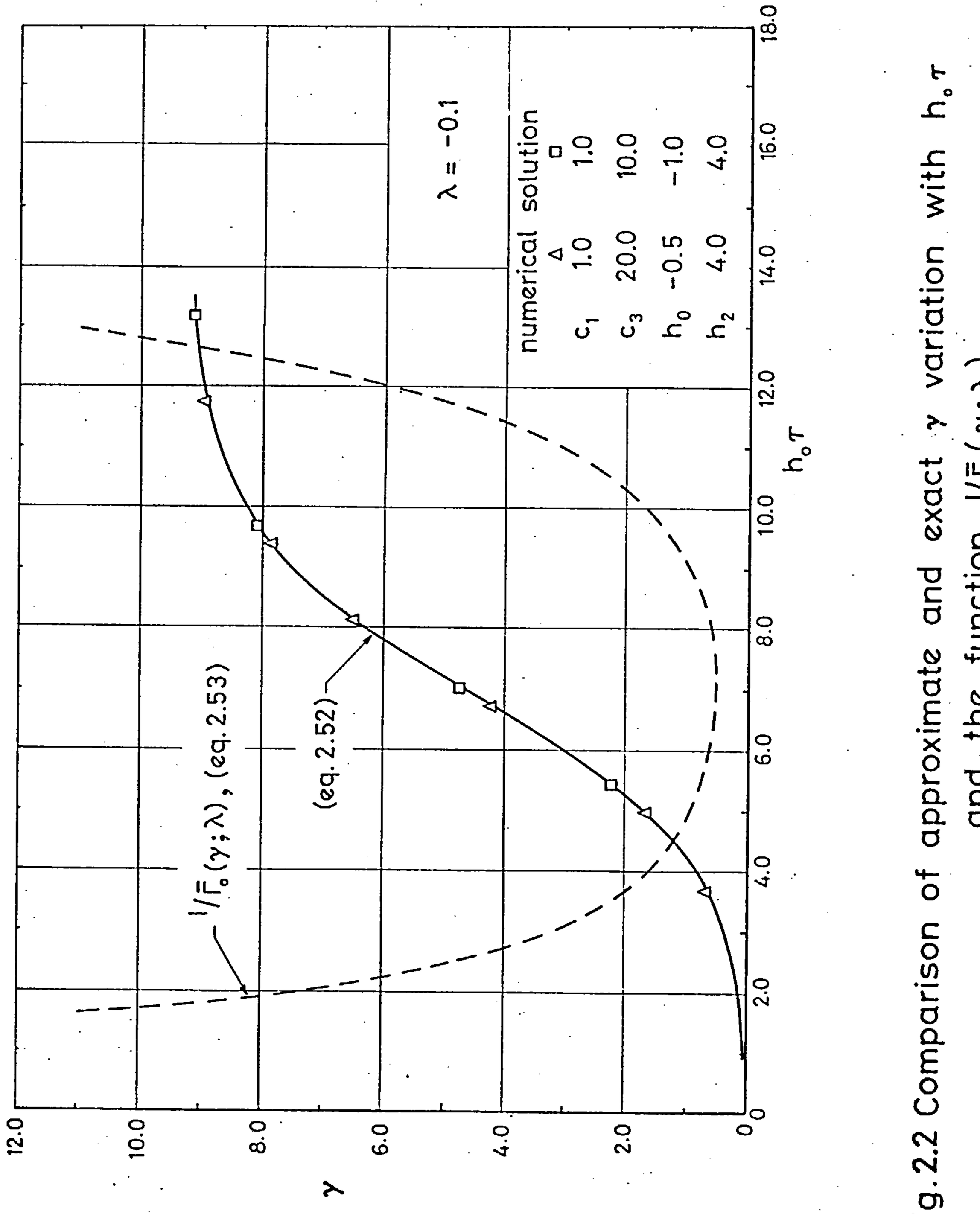

Fig. 2.2 Comparison of approximate and exact γ variation with $h_0\tau$ and the function $1/\bar{F}_0(\gamma;\lambda)$.

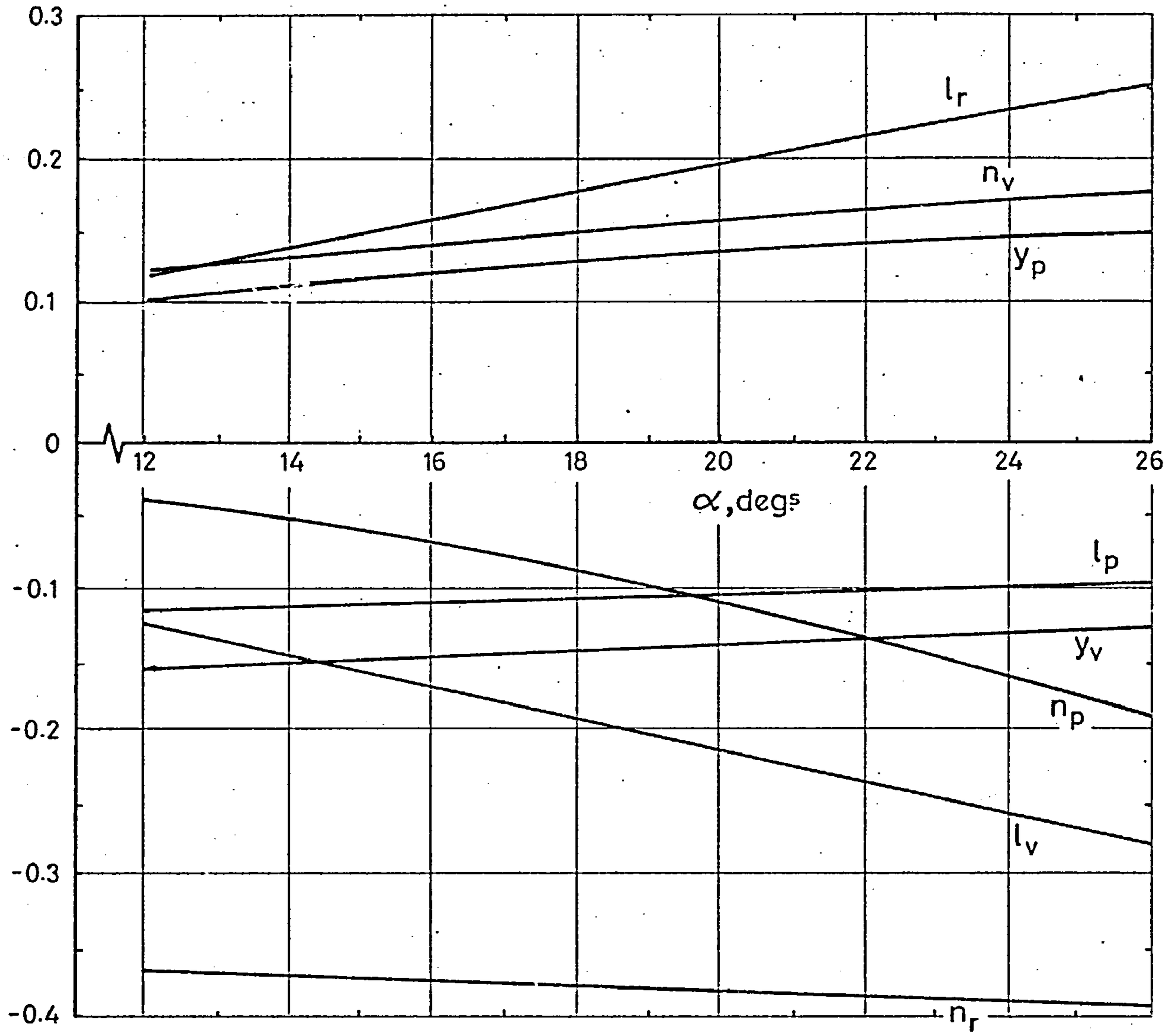

Variation of HP 115 aerodynamic derivatives with incidence.

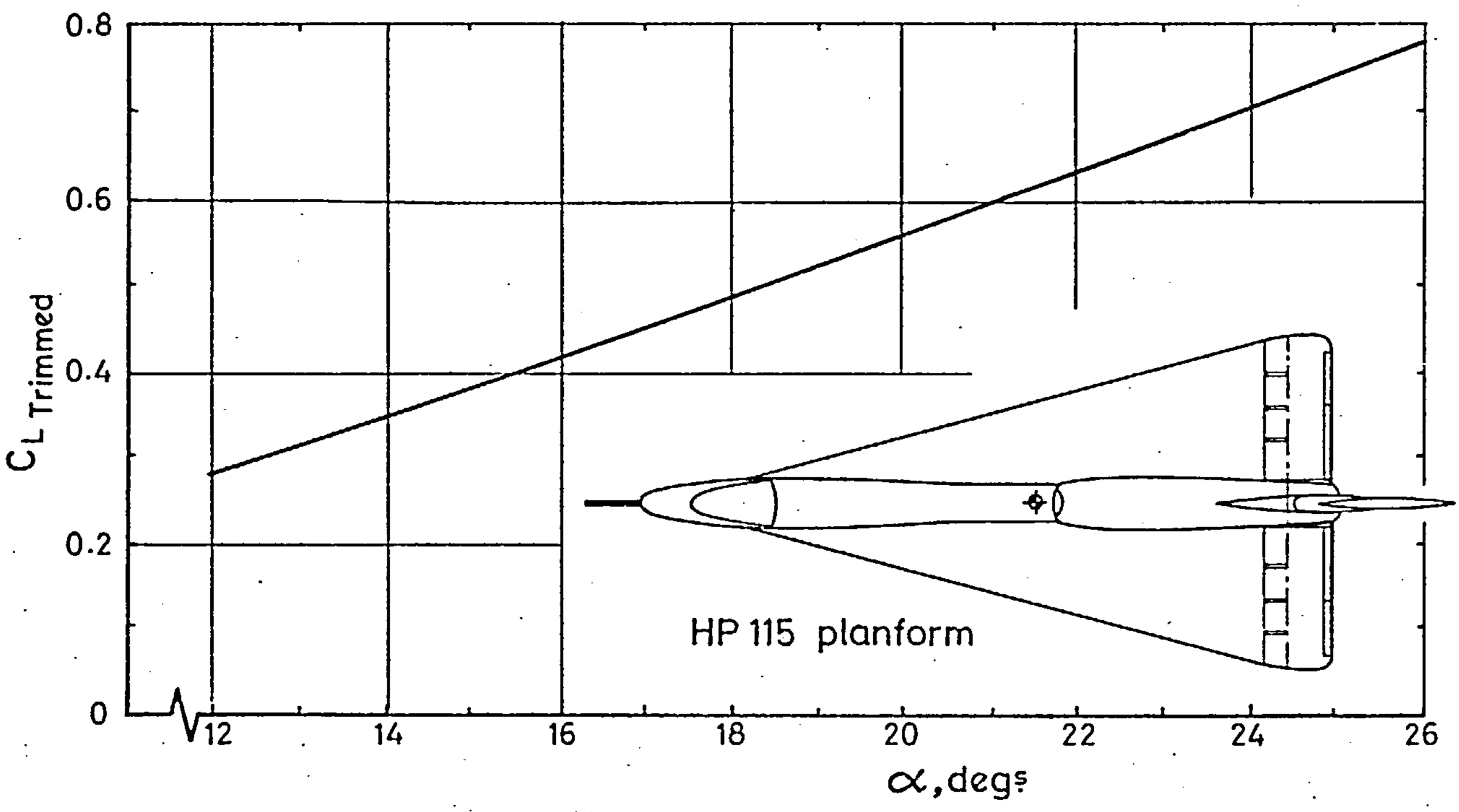

Fig.3.1 Variation of C_L with incidence for HP 115.

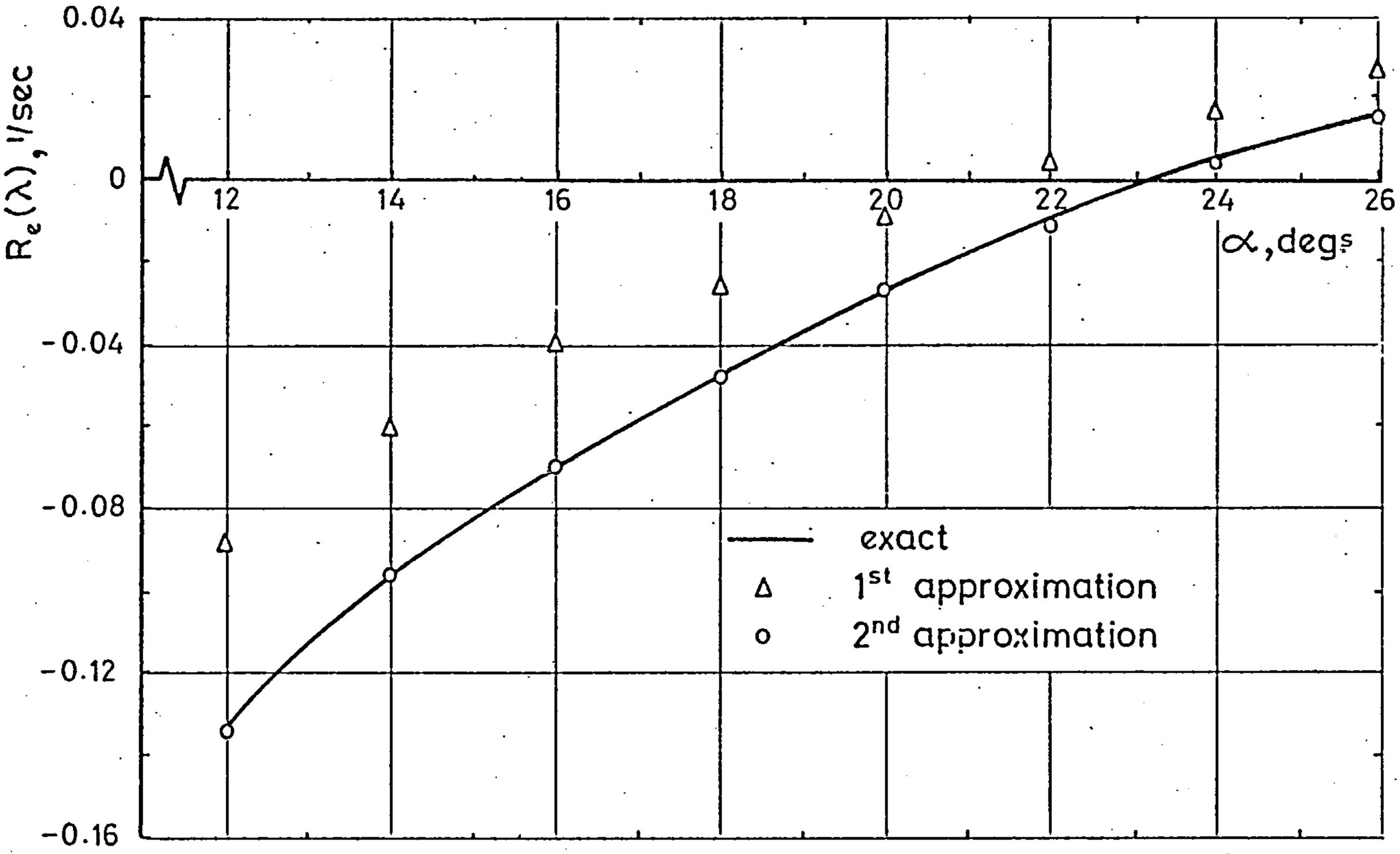

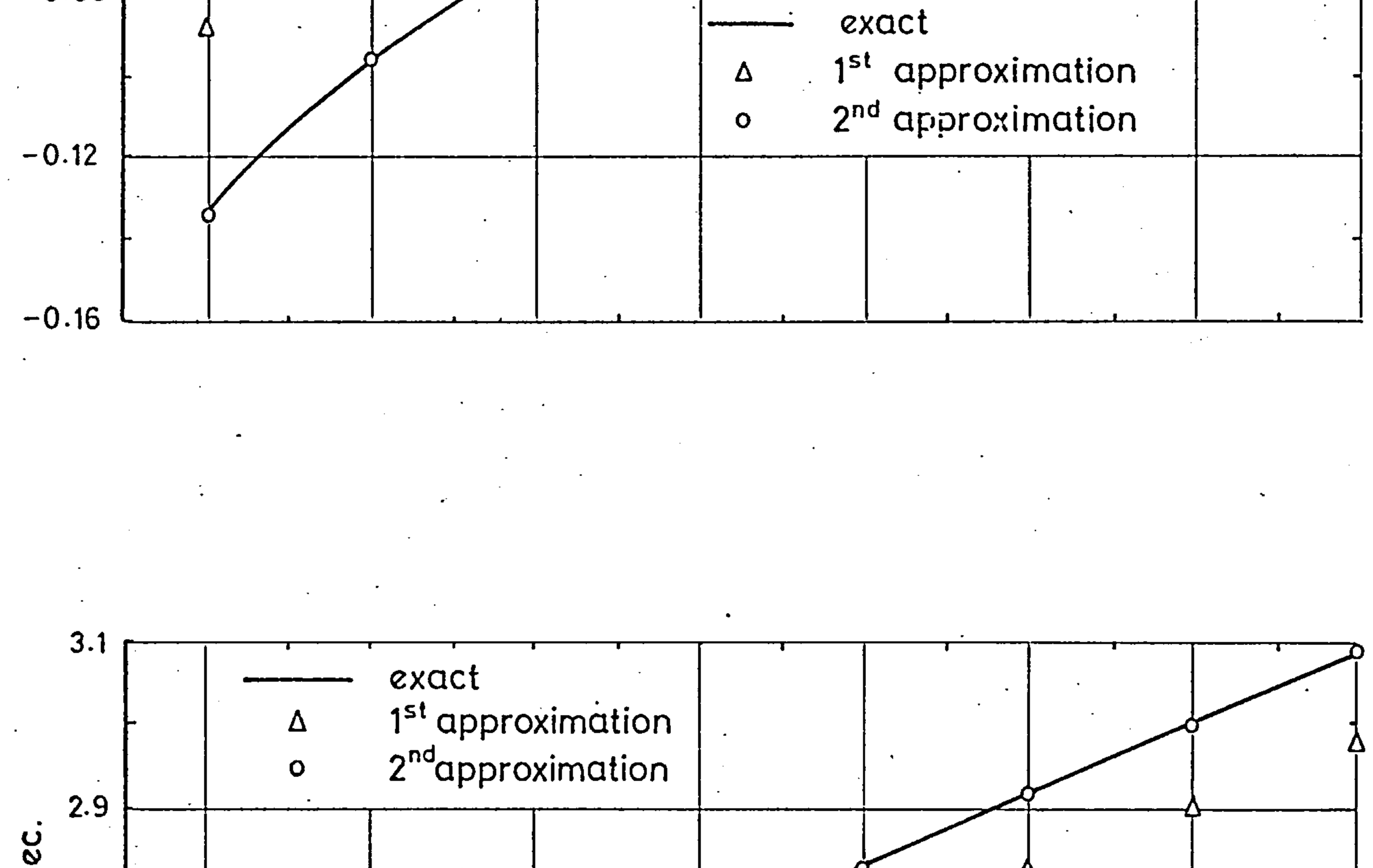

Fig. 3.2 Comparison of exact and approximate Eigenvalues for the HP 115

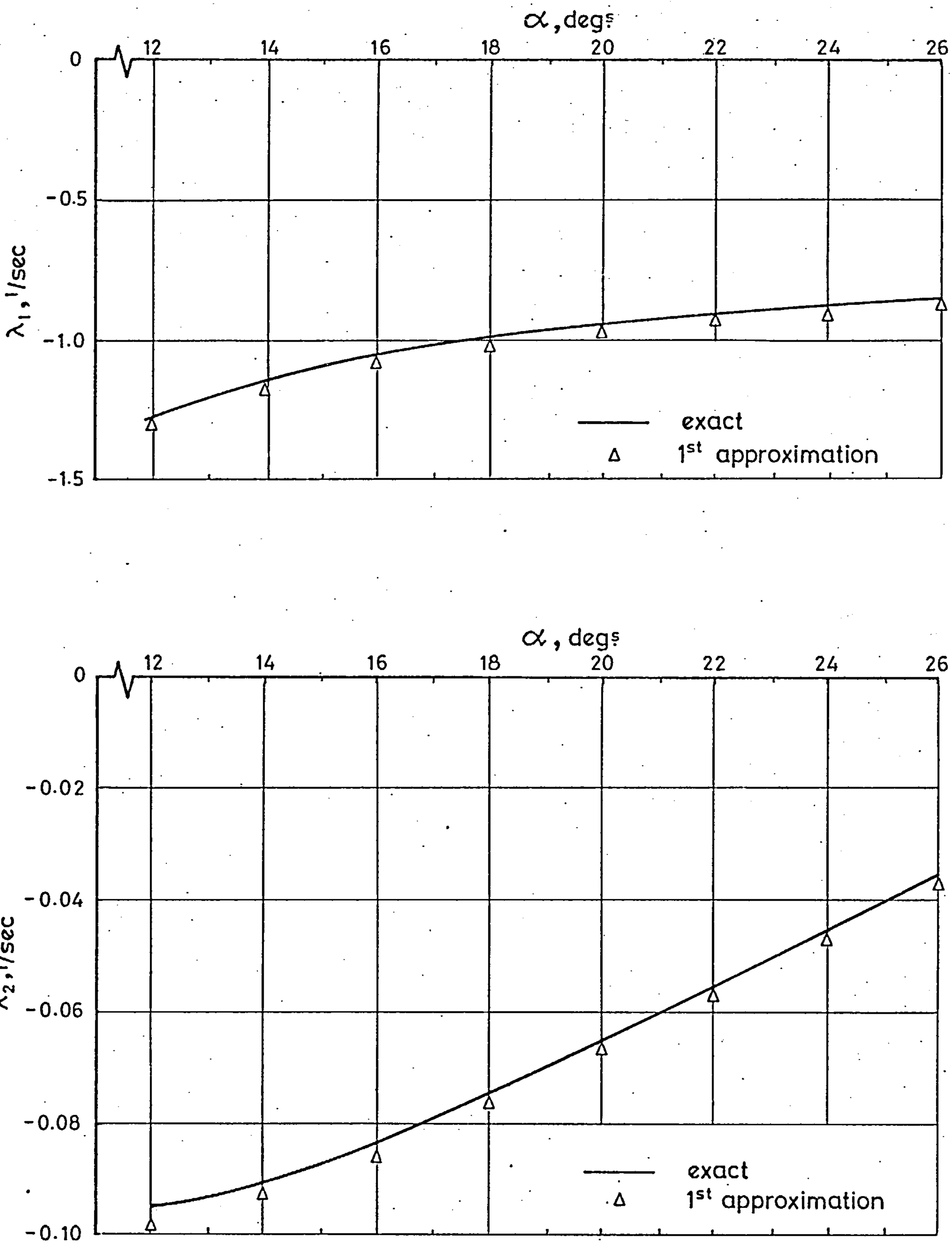

Fig. 3.3 Comparison of exact and approximate Eigenvalues for the HP 115.

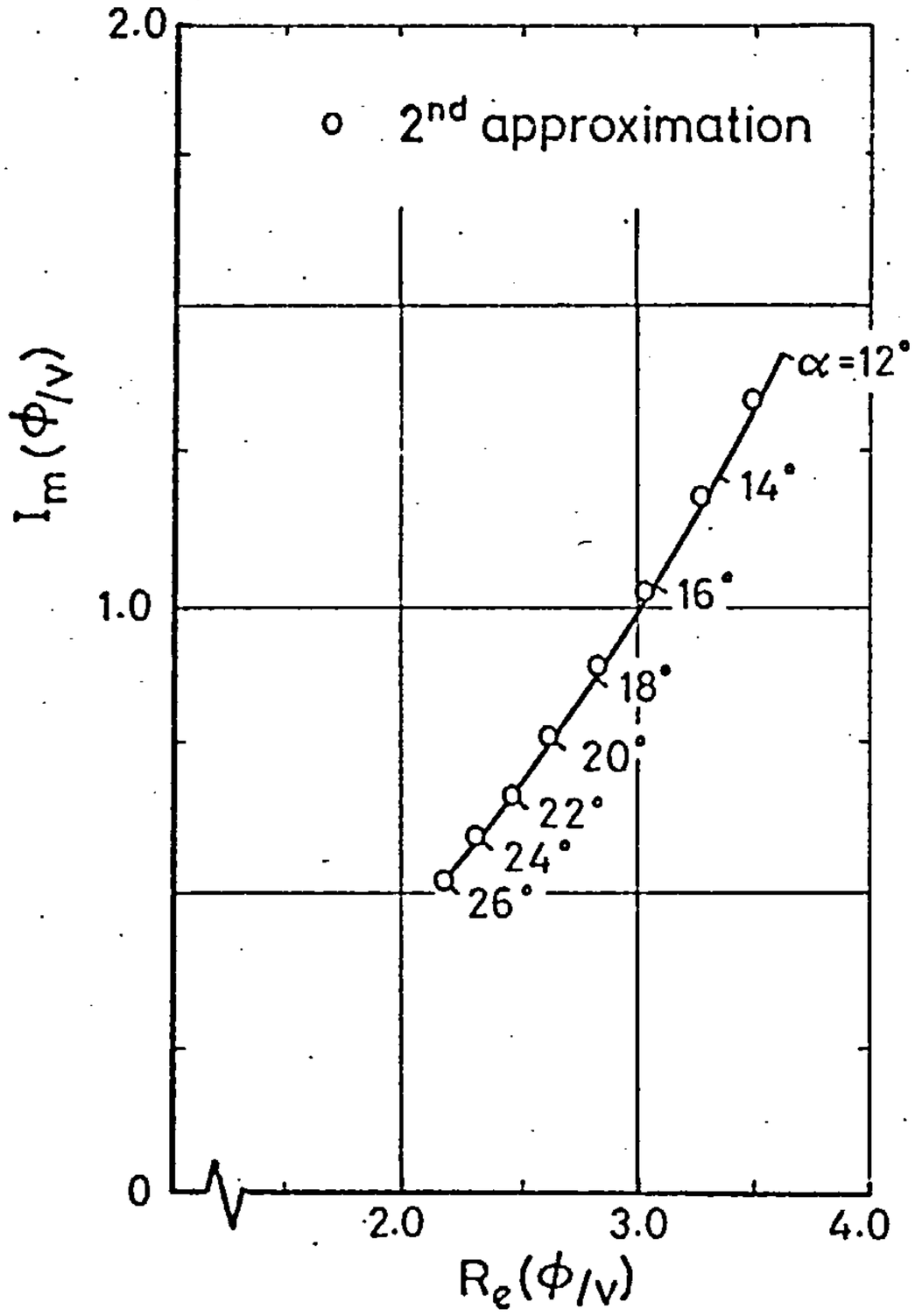

($\phi_{/V}$) RATIO FOR THE OSCILLATORY MODE.

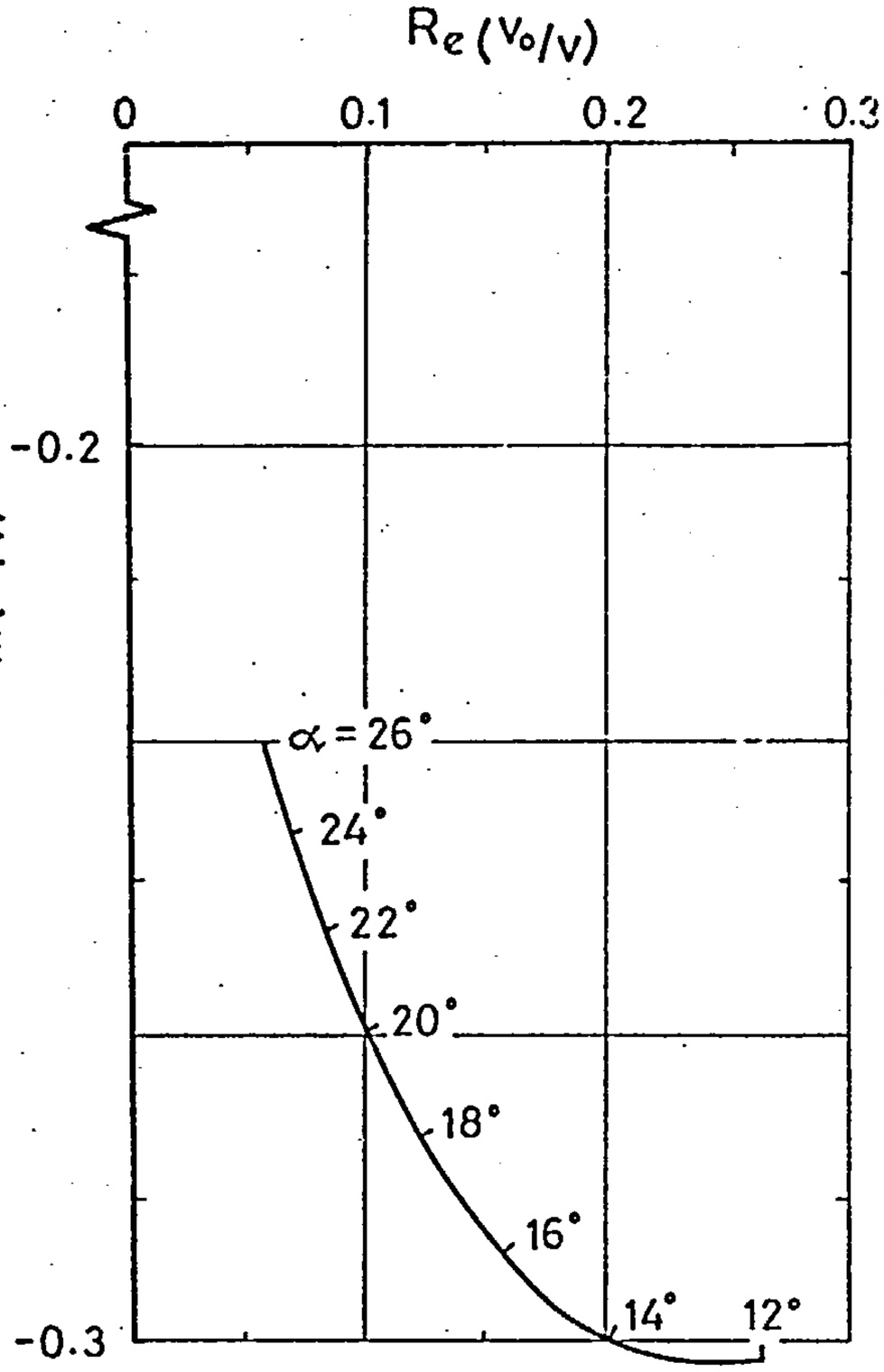

(V_o/V) RATIO FOR THE OSCILLATORY MODE

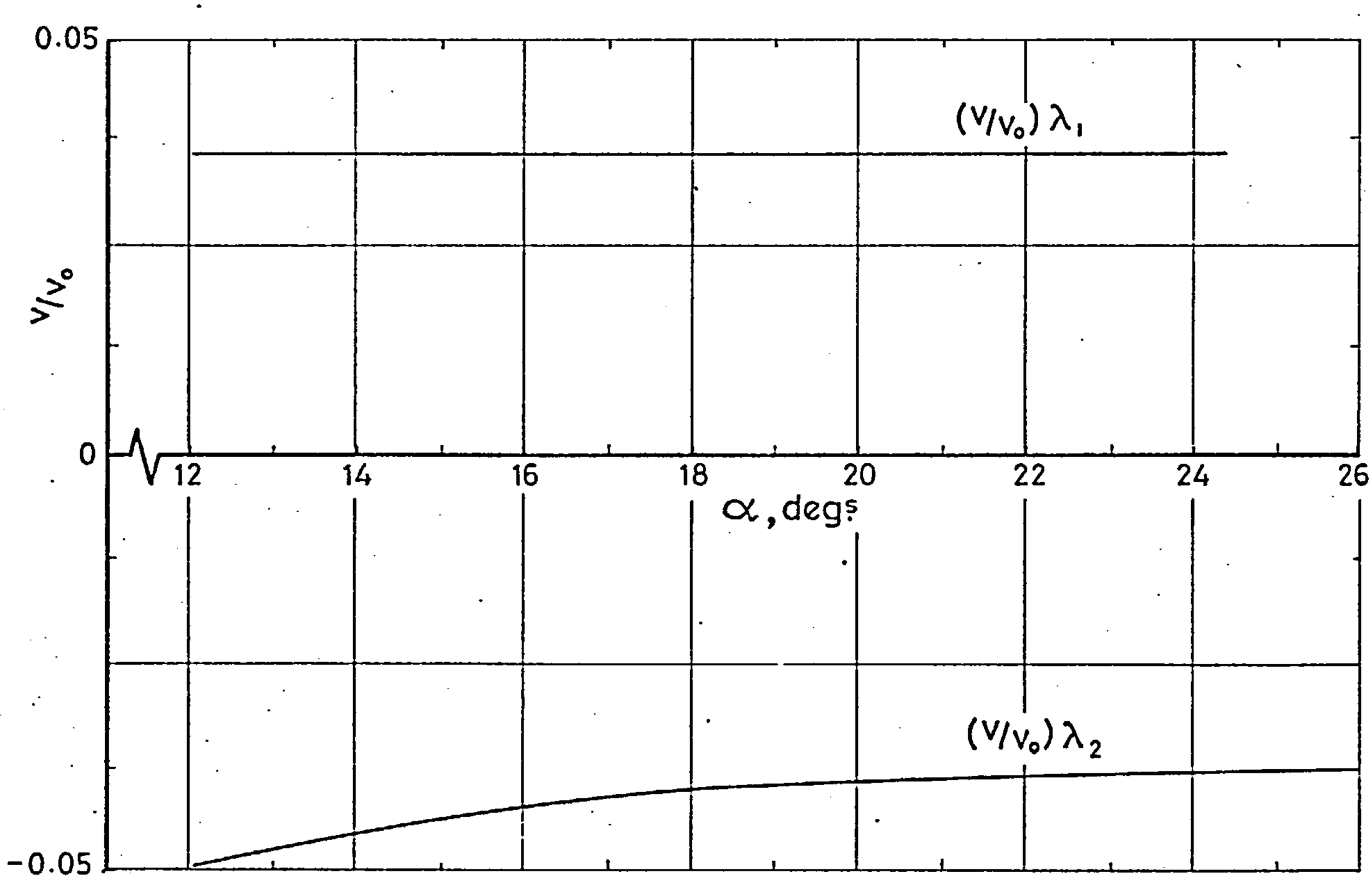

VARIATION OF (V/V_o) FOR APERIODIC MODES

Fig.3.4 Eigenvector display for the HP 115

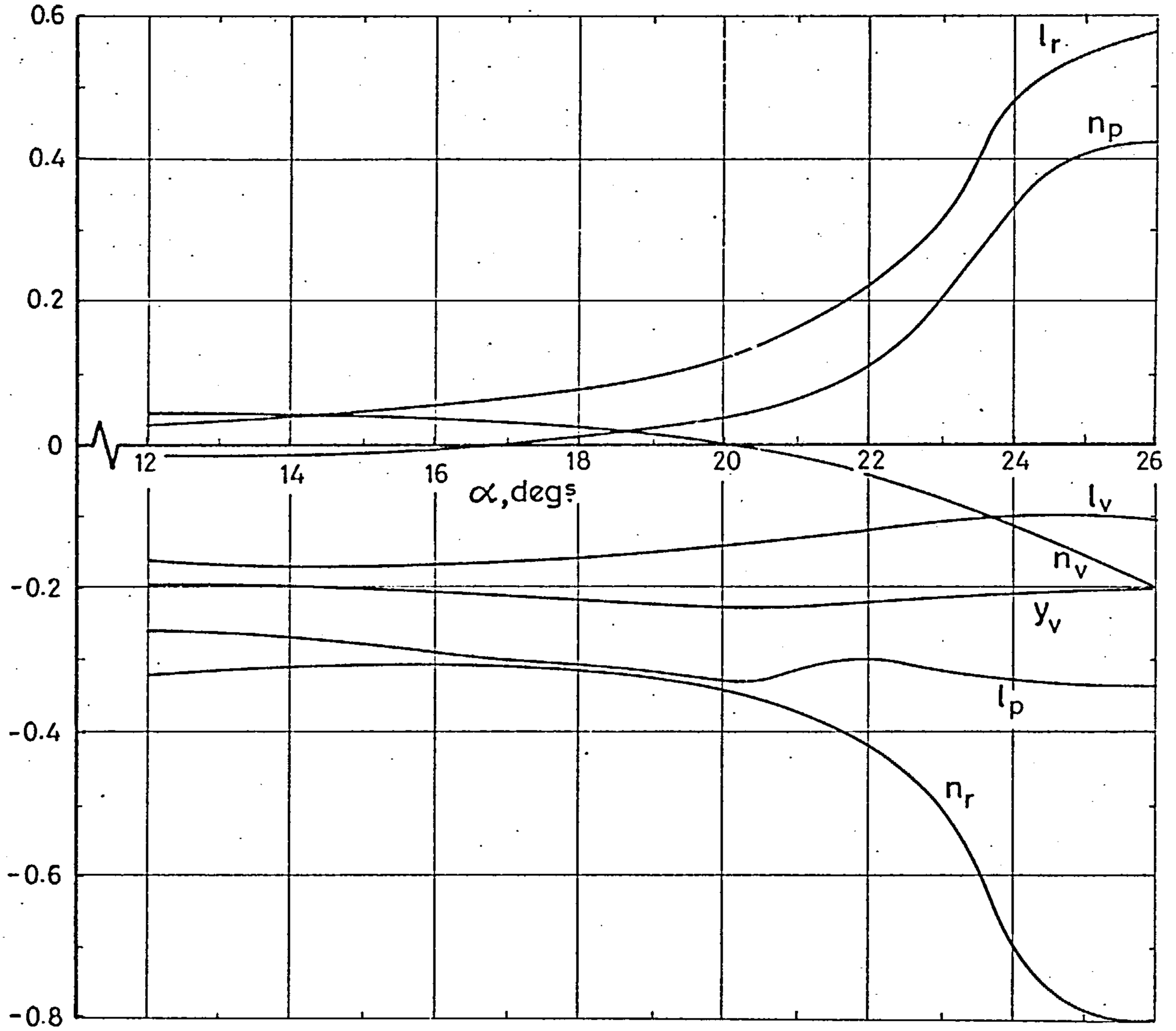

Variation of BAC 221 aerodynamic derivatives with incidence.

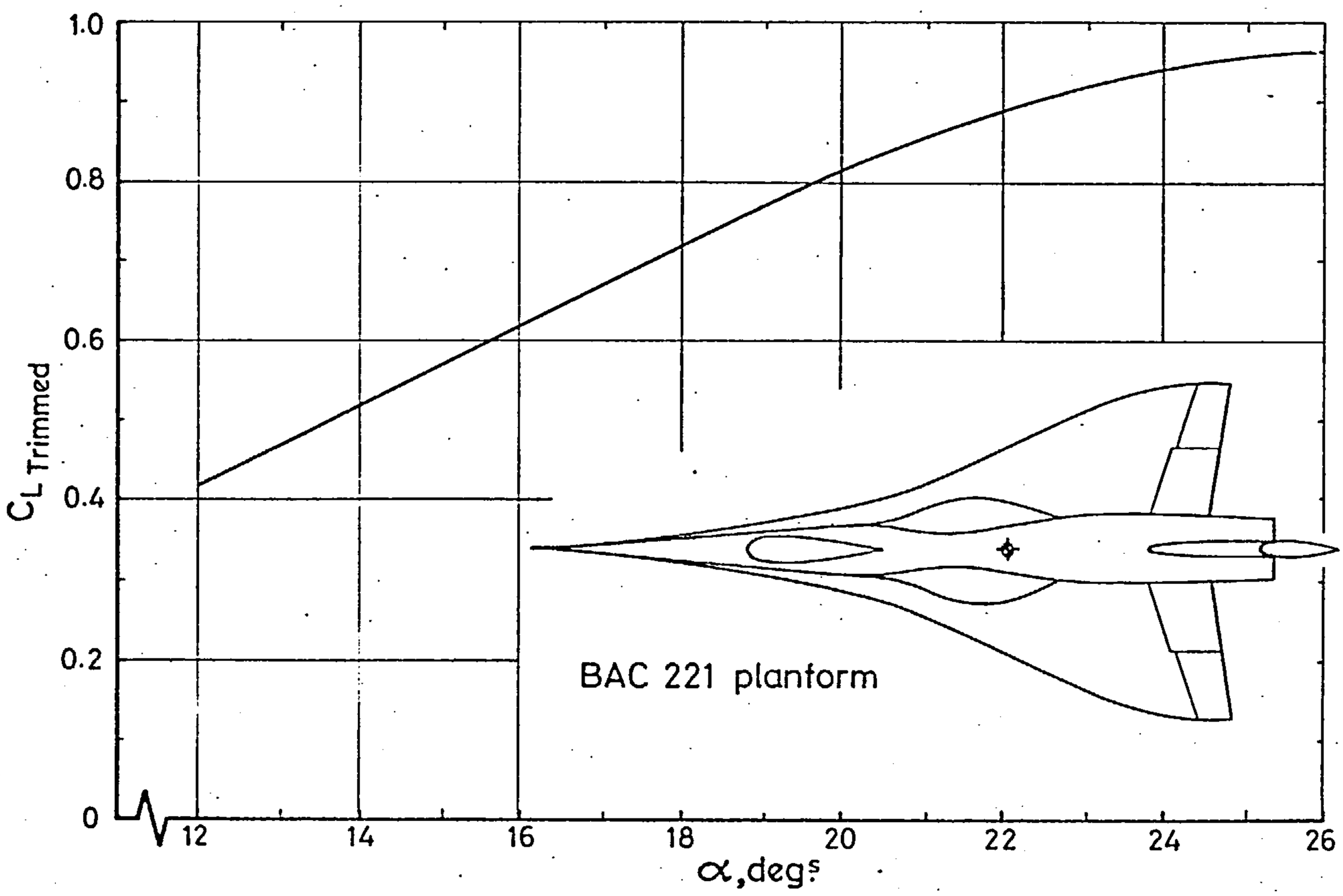

Fig. 3.5 Variation of C_L with incidence for the BAC 221

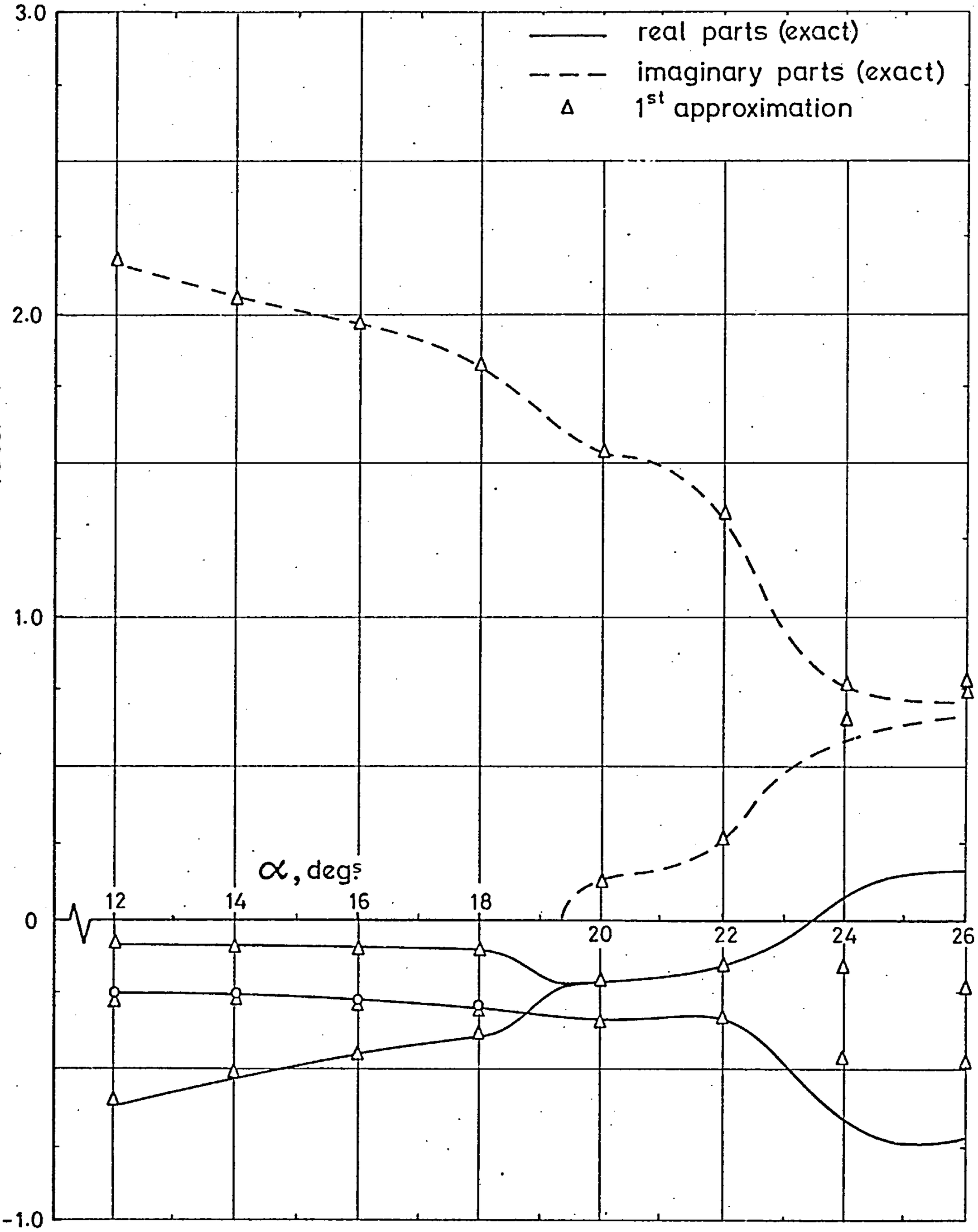

Fig. 3.6 Comparison of exact and approximate Eigenvalues for the BAC 221.

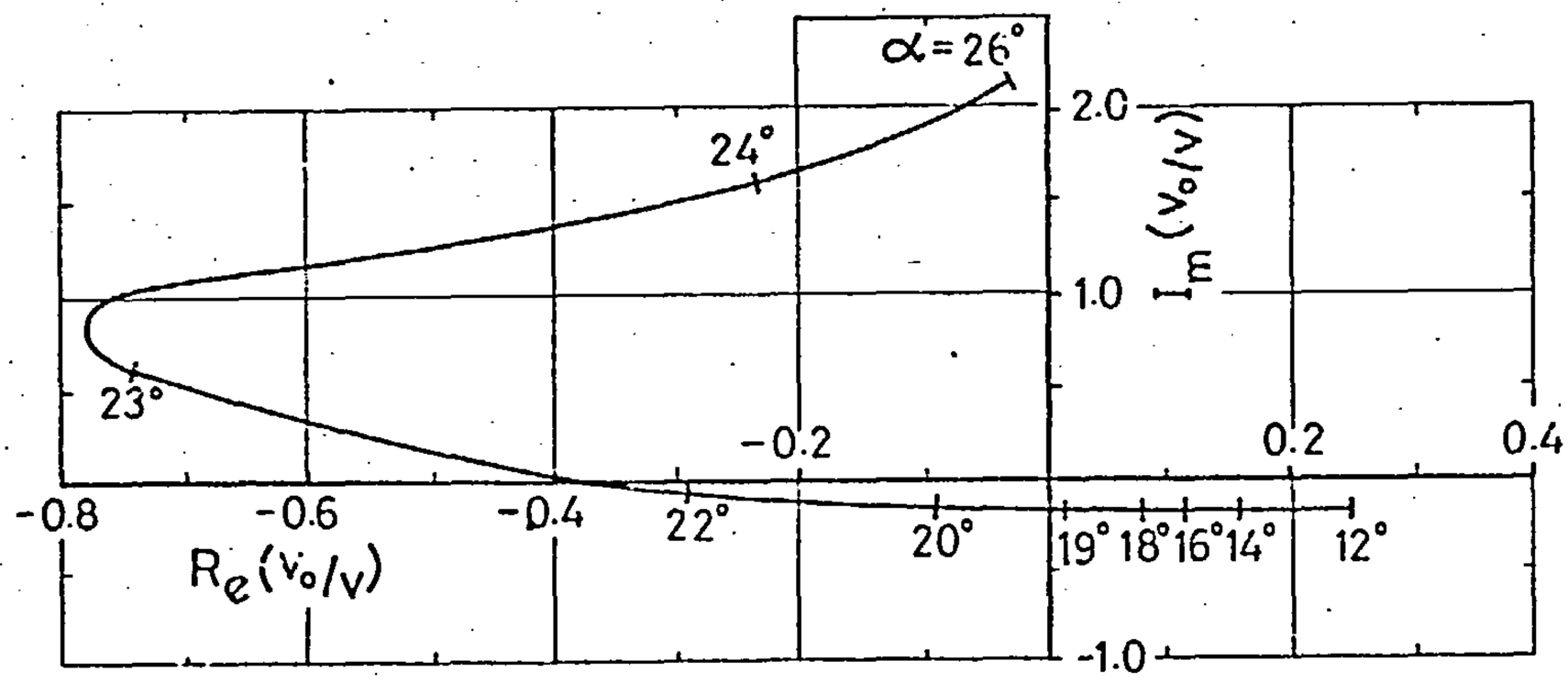

(V_o/V) RATIO FOR THE OSCILLATORY 'v' MODE.

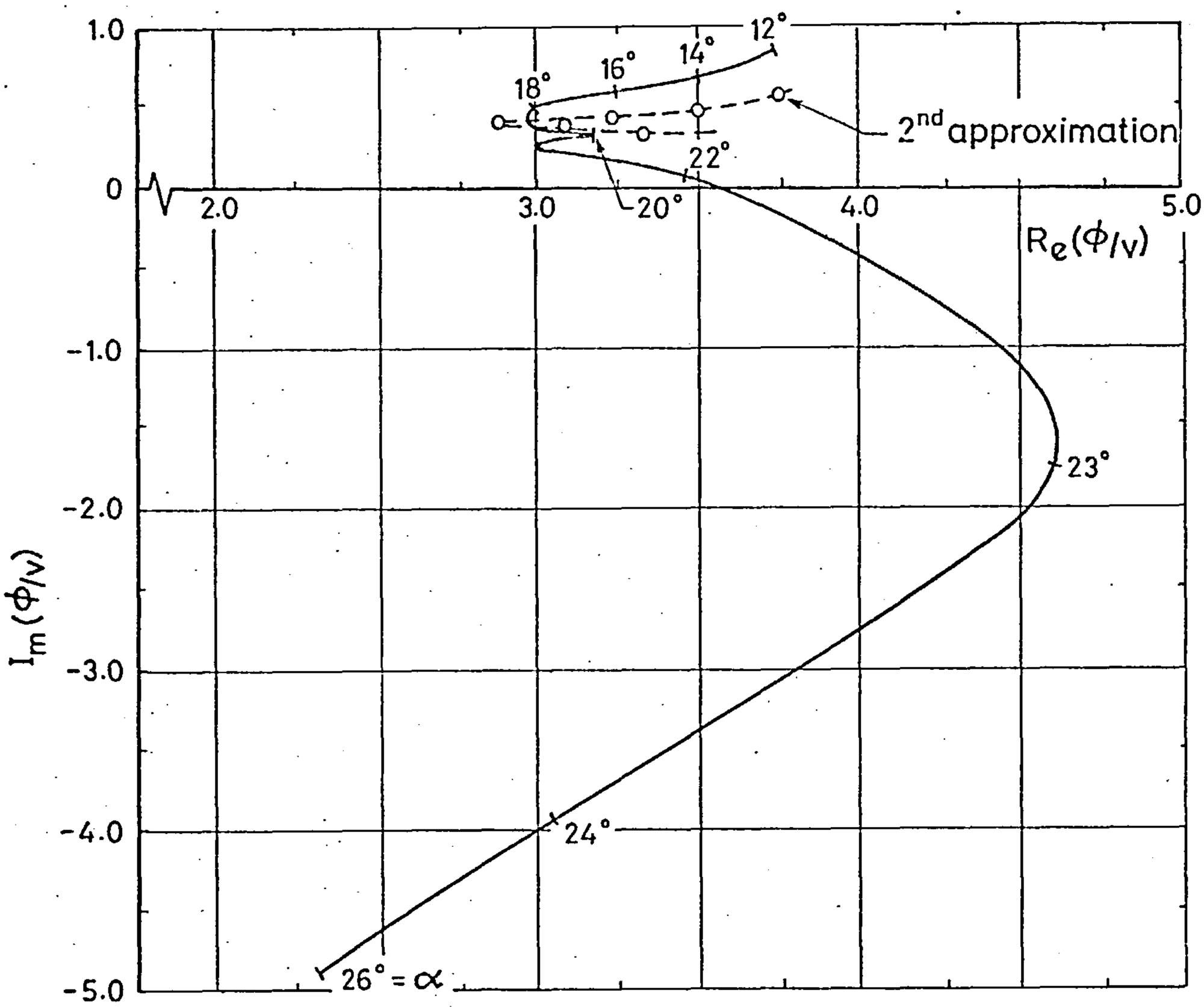

(Φ/V) RATIO FOR THE OSCILLATORY 'v' MODE.

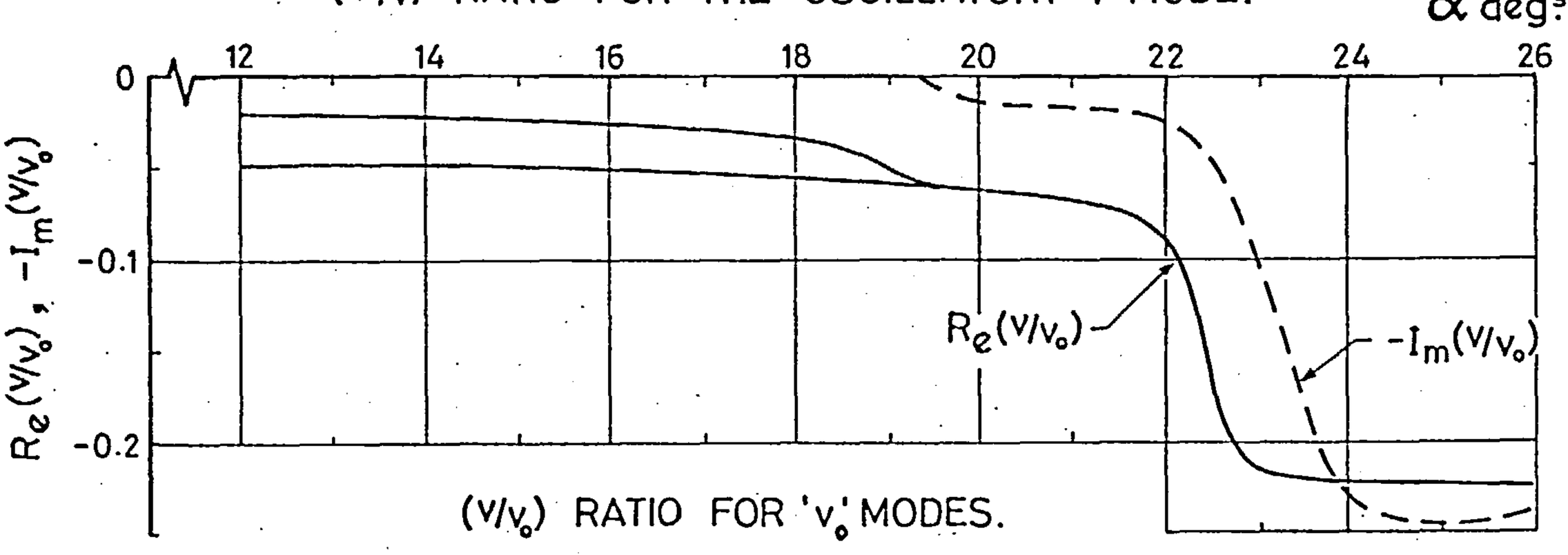

(V/V_o) RATIO FOR 'v_o' MODES.

Fig.3.7 Eigenvector display for the RAC 221

Text cut off in original

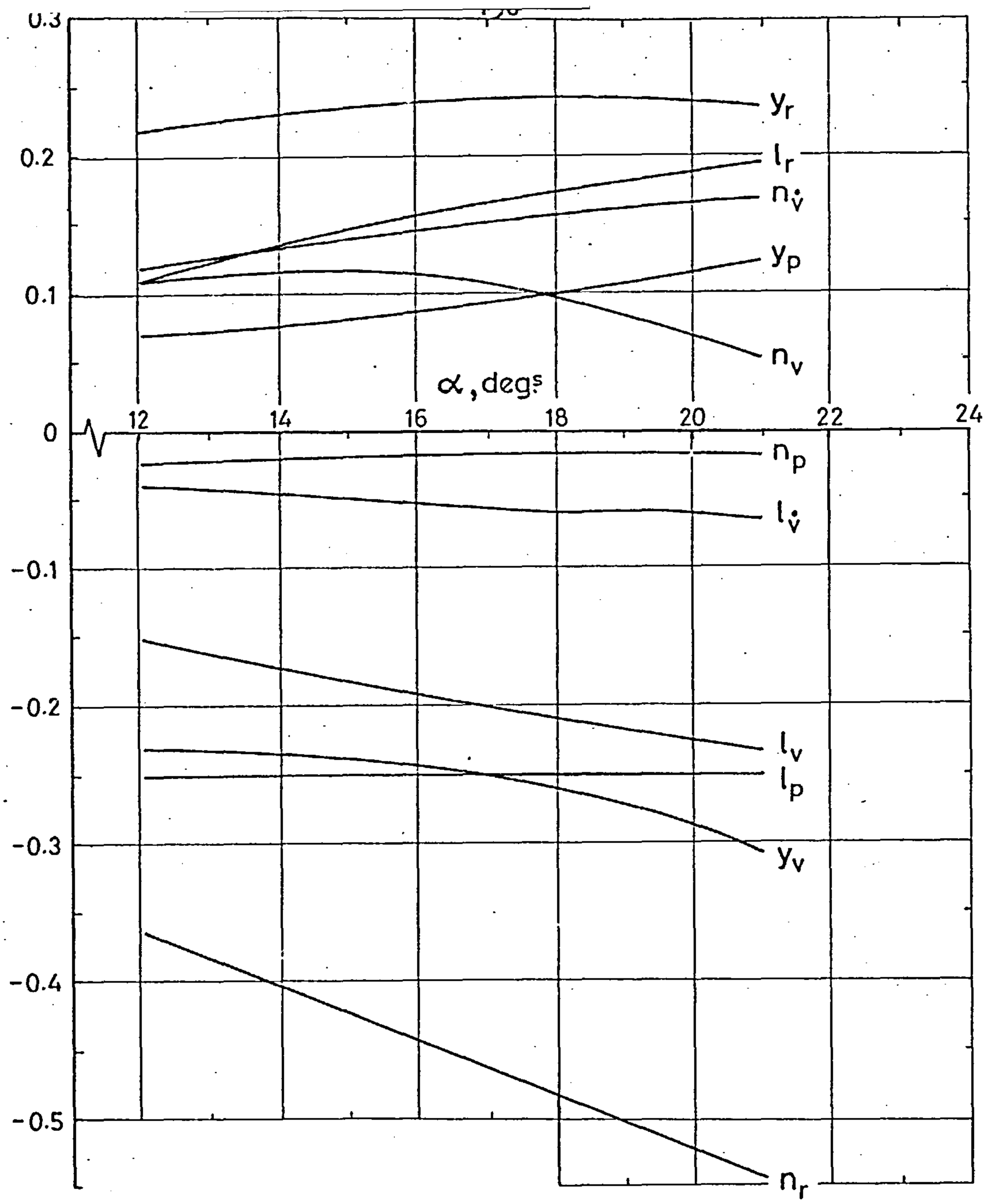

Variation of Concorde aerodynamic derivatives with incidence. (approach configuration)

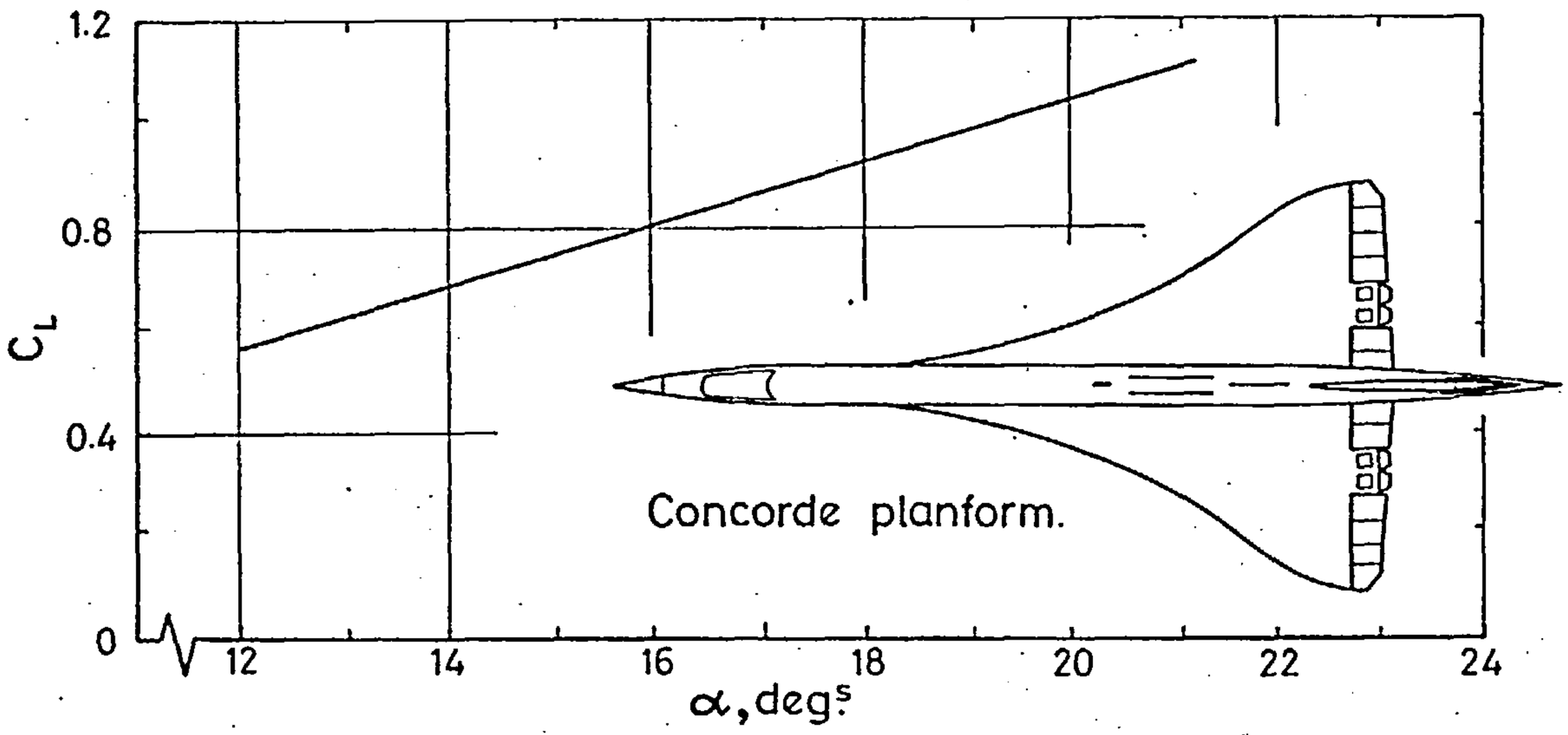

Fig. 3.8 Variation of C_L with incidence for Concorde.

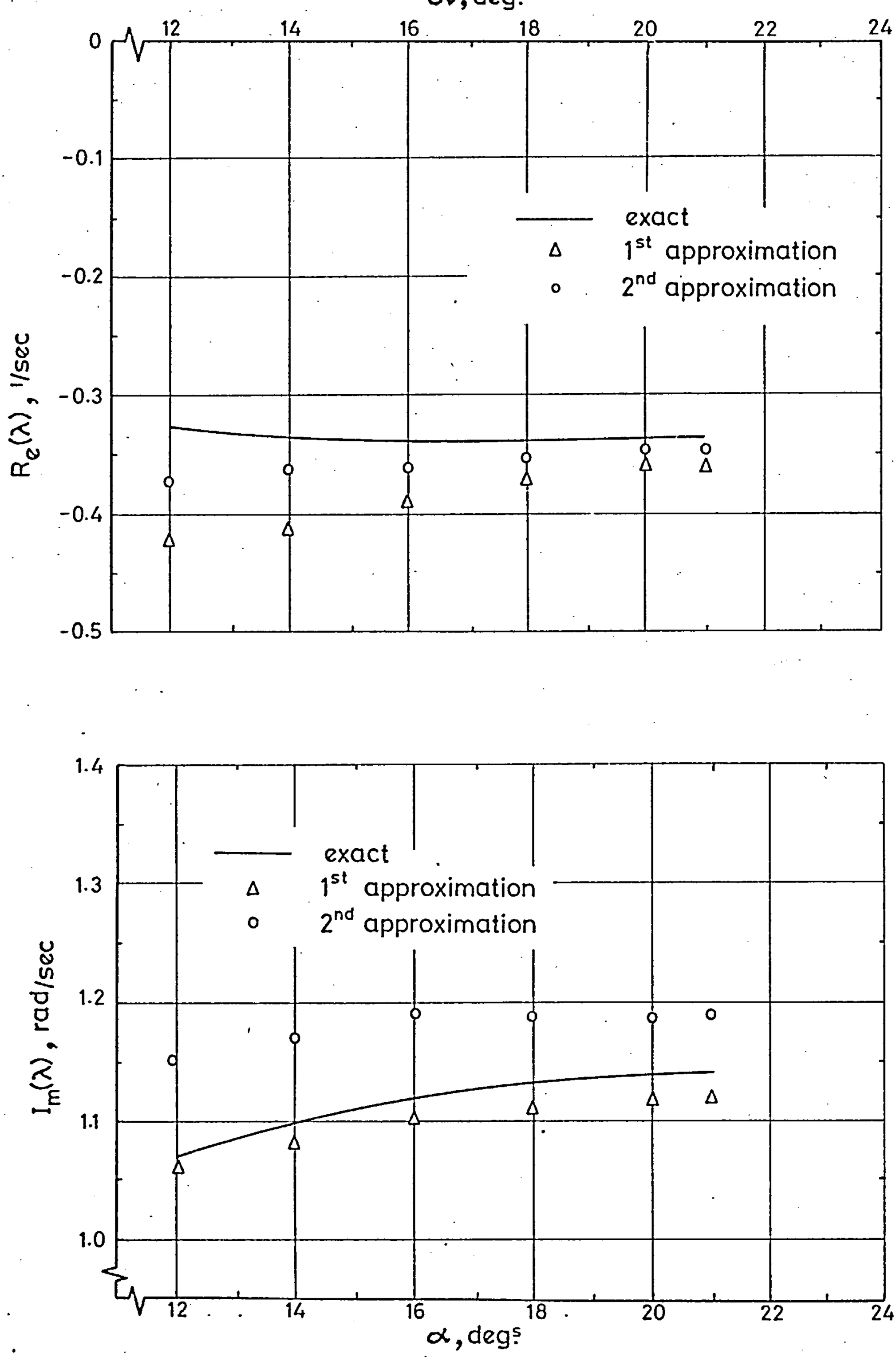

Fig. 3.9 Comparison of exact and approximate Eigenvalues for Concorde. ($l_v, n_v \neq 0$)

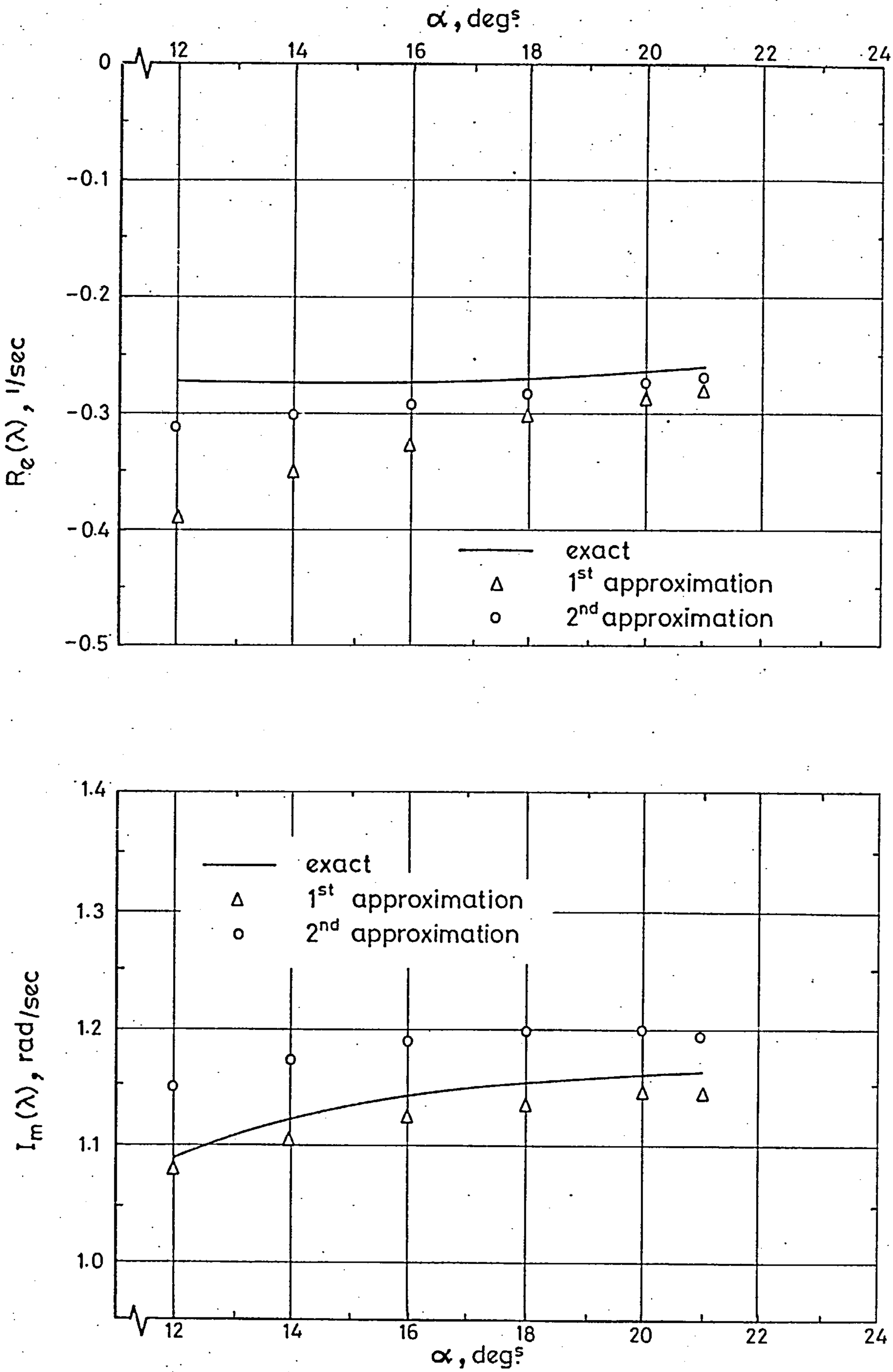

Fig. 3.10 Comparison of exact and approximate Eigenvalues for Concorde. ($l_{\dot{v}}, n_{\dot{v}} = 0$)

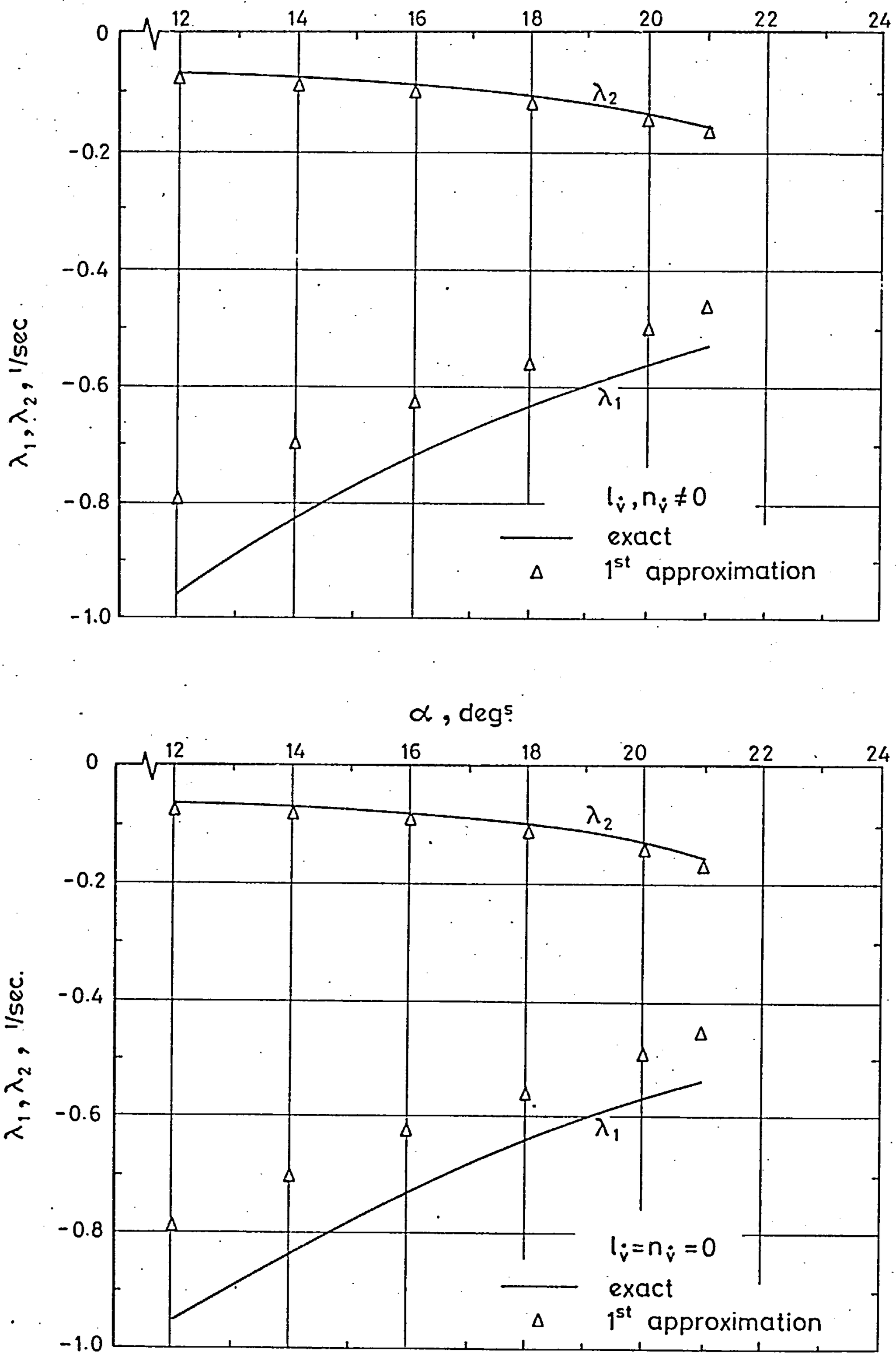

Fig. 3.11 Comparison of exact and approximate Eigenvalues for Concorde.

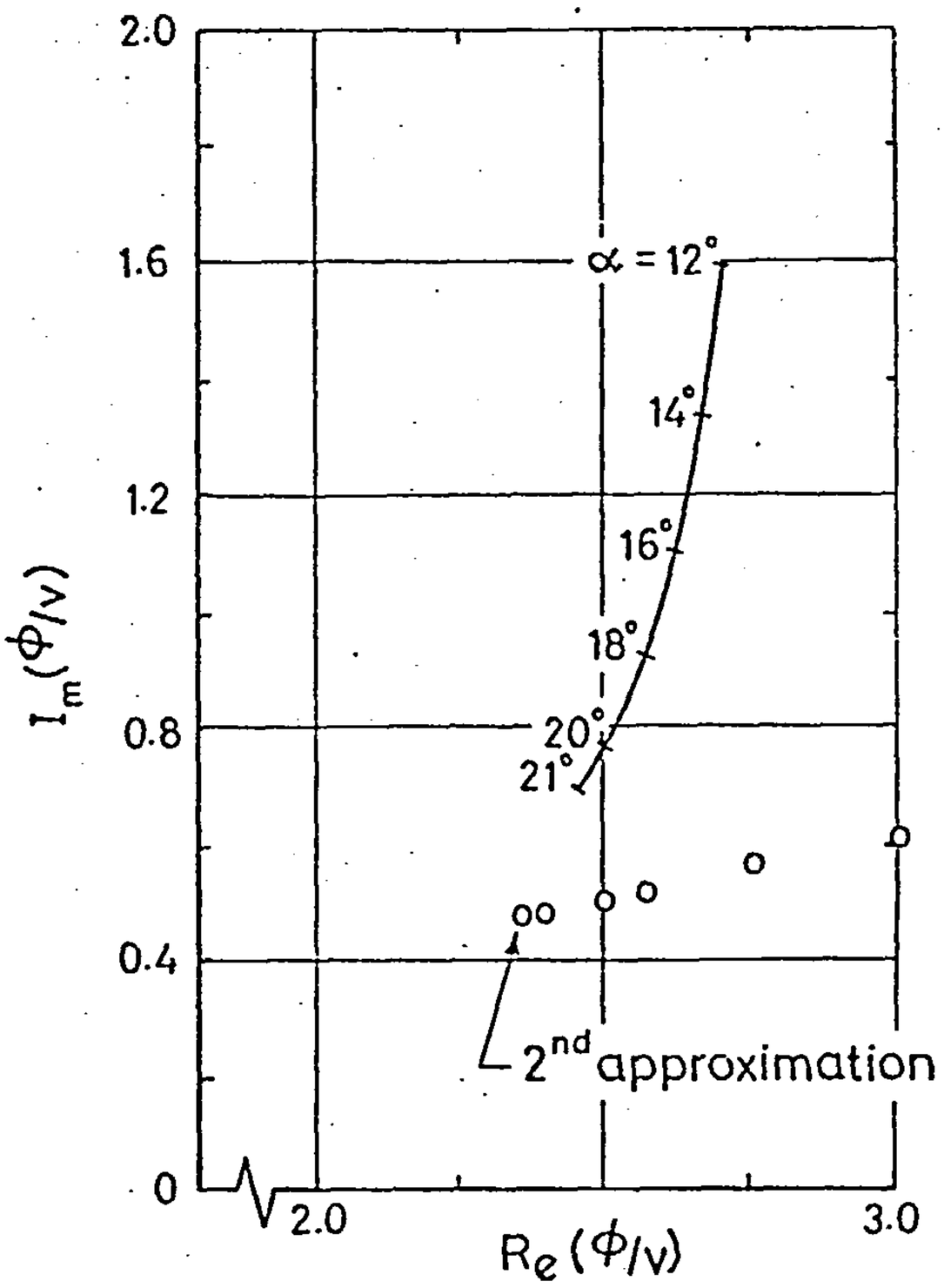

(Φ/v) RATIO FOR THE OSCILLATORY MODE.

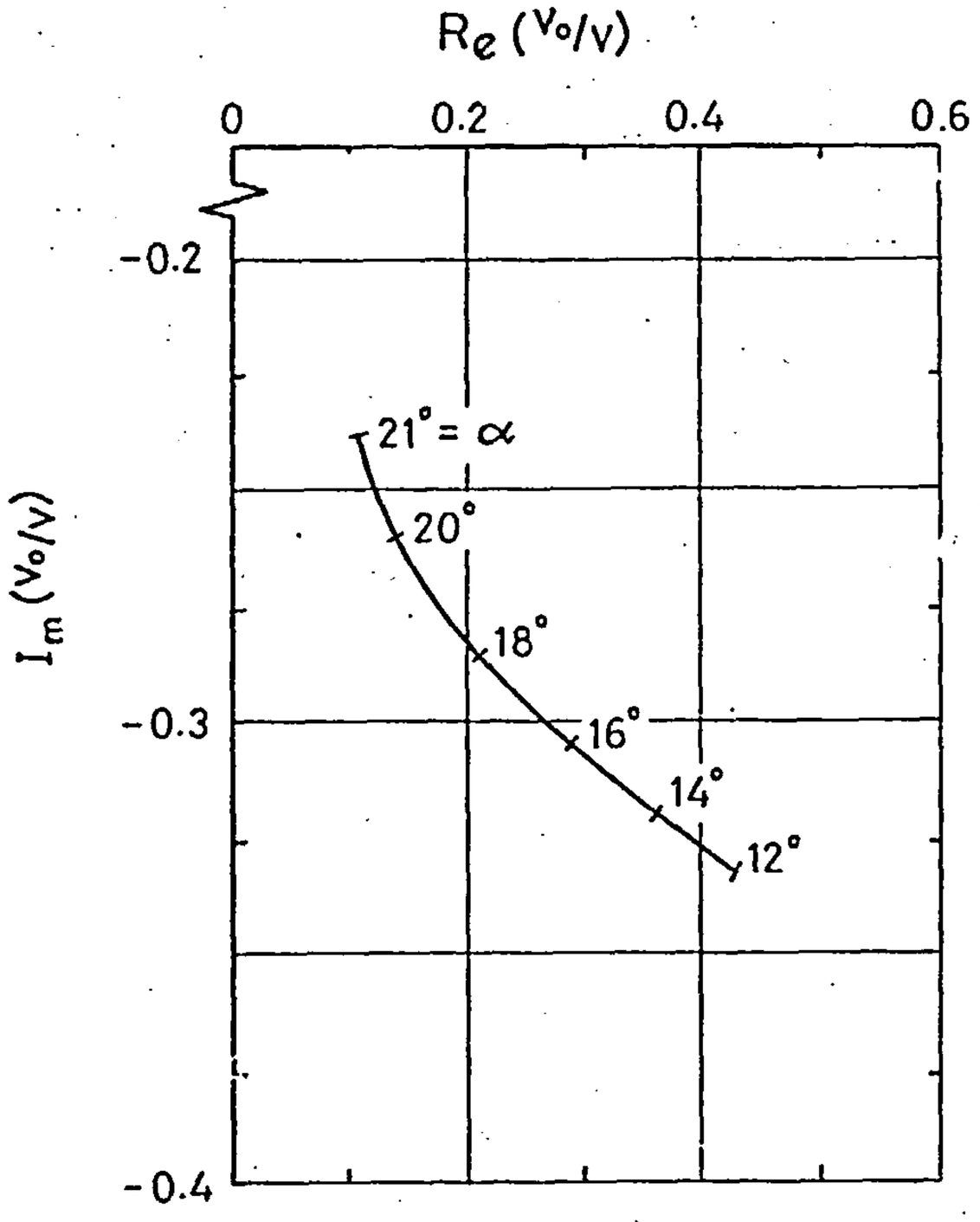

(V_o/v) RATIO FOR THE OSCILLATORY MODE.

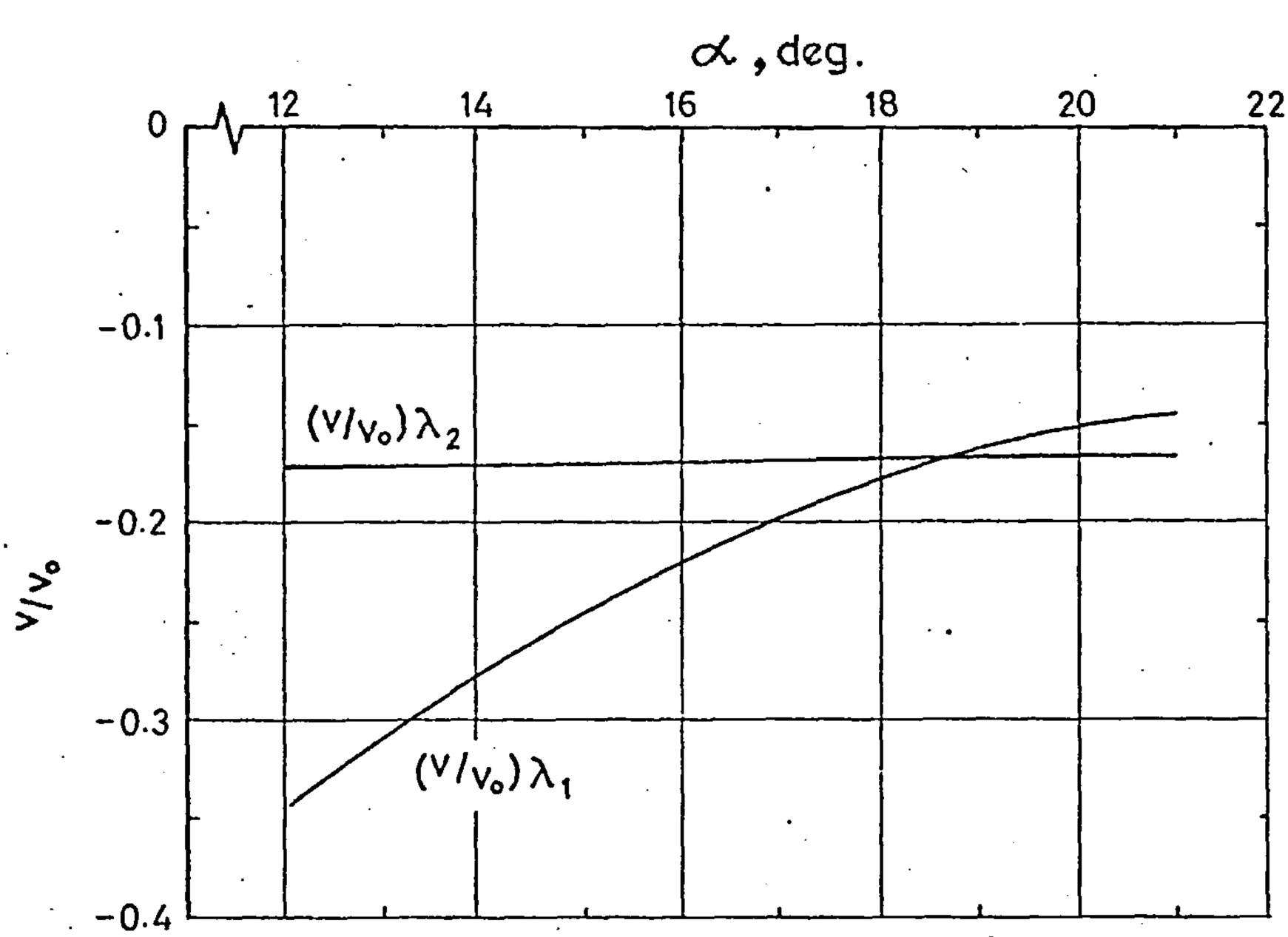

VARIATION OF (V/V_o) FOR APERIODIC MODES

Fig.3.12 Eigenvector display for Concorde.
($l_{\dot{v}}, n_{\dot{v}} \neq 0$)

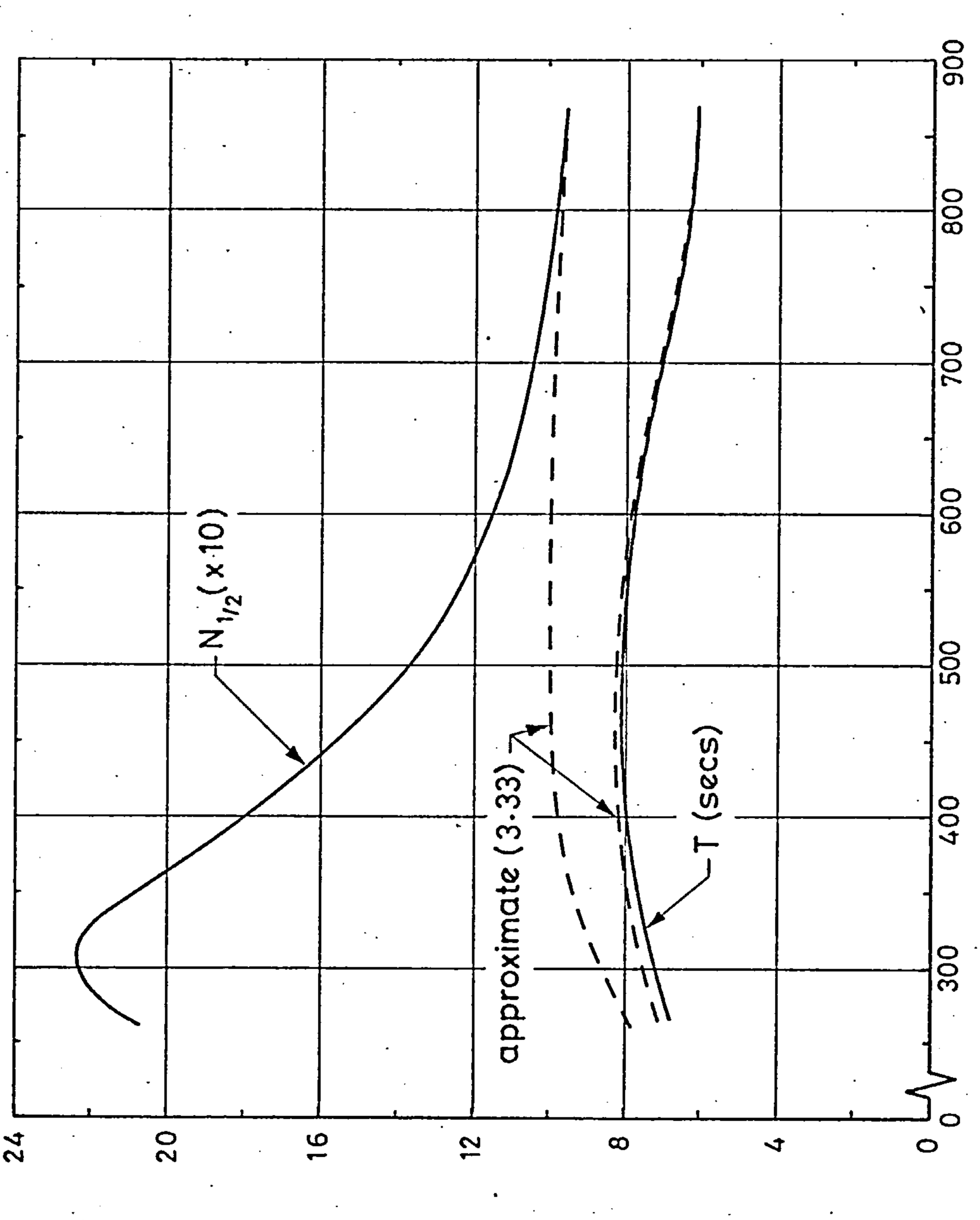

Variation of $N_{1/2}$ and period (T) with speed - a comparison of approximate and exact results.

Fig.3.13

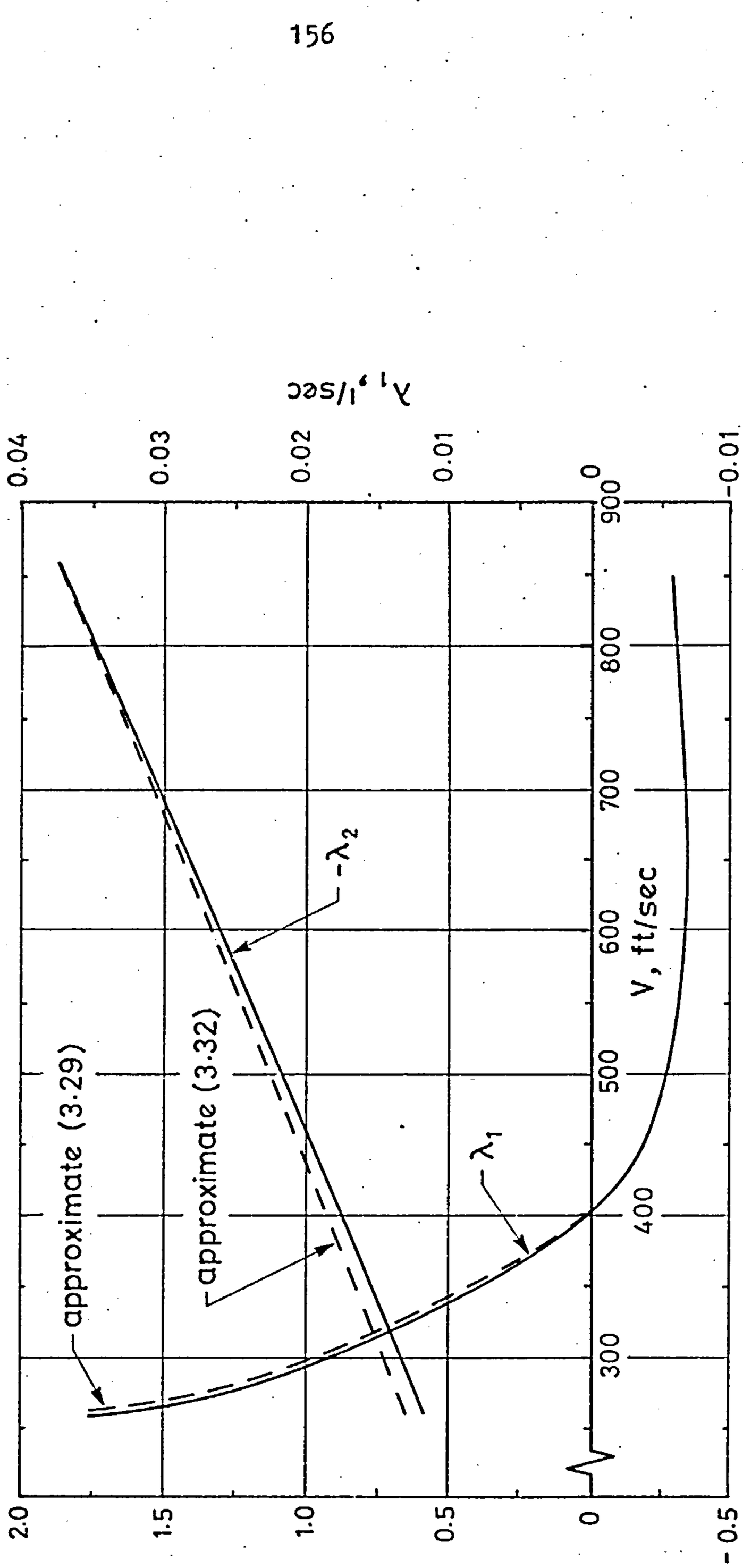

Fig.3.14 Comparison of exact and approximate spiral (λ_1) and roll subsidence (λ_2) roots.

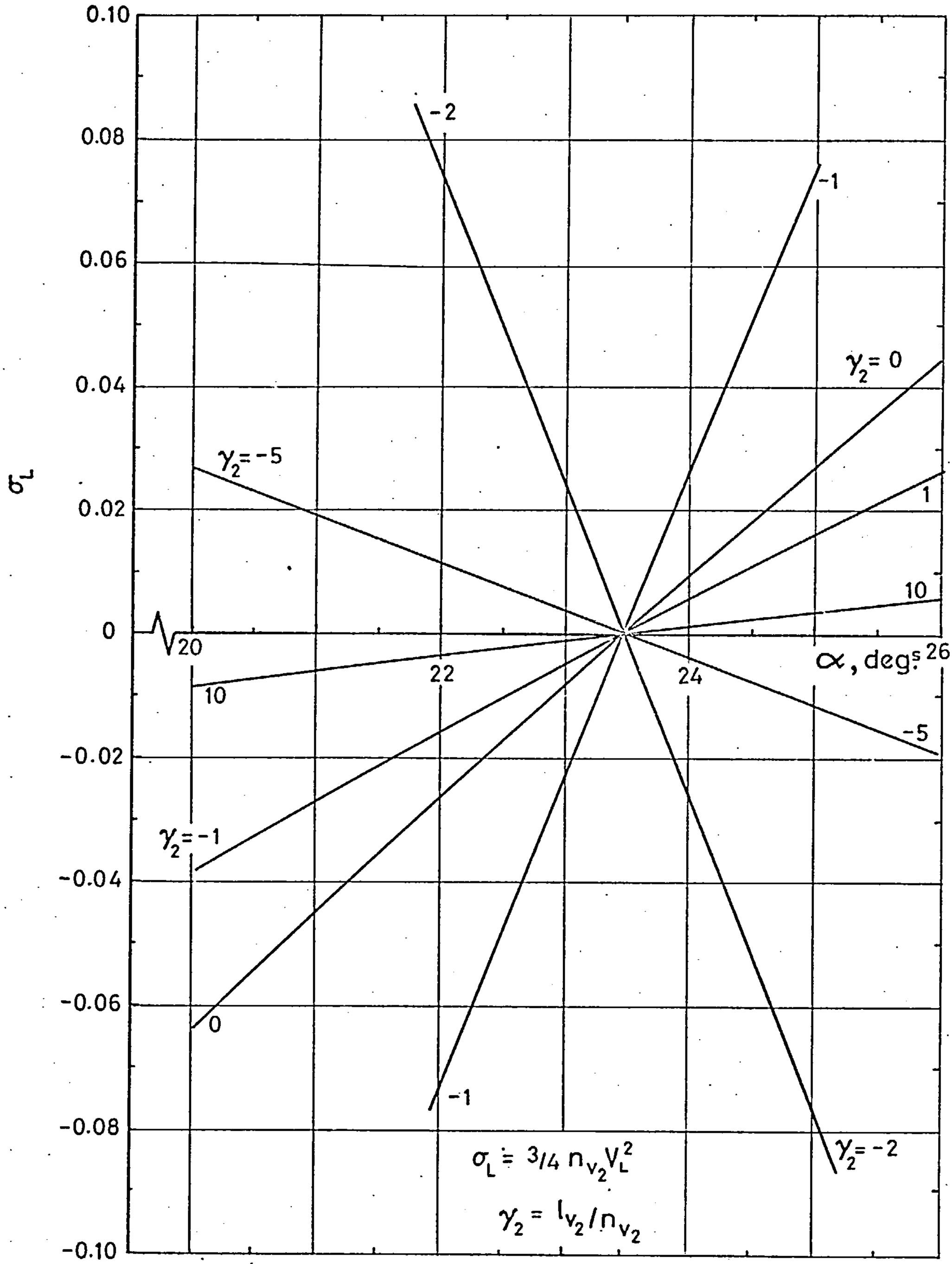

Fig. 4.1 Sideslip limit cycles for HP 115 using sideslip/sideways mode coupling approximation.

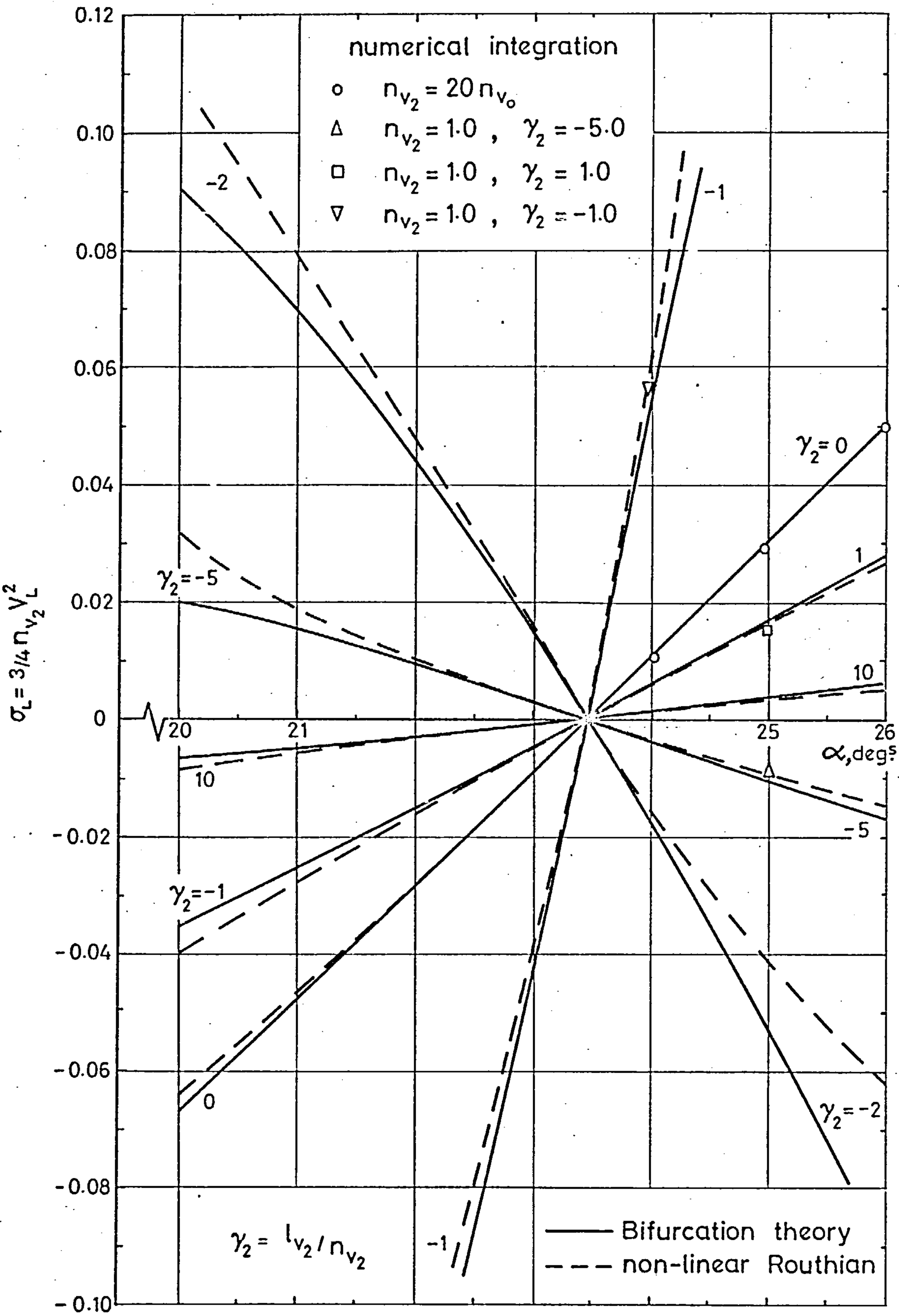

Fig. 4.2 Sideslip limit cycles for HP 115.

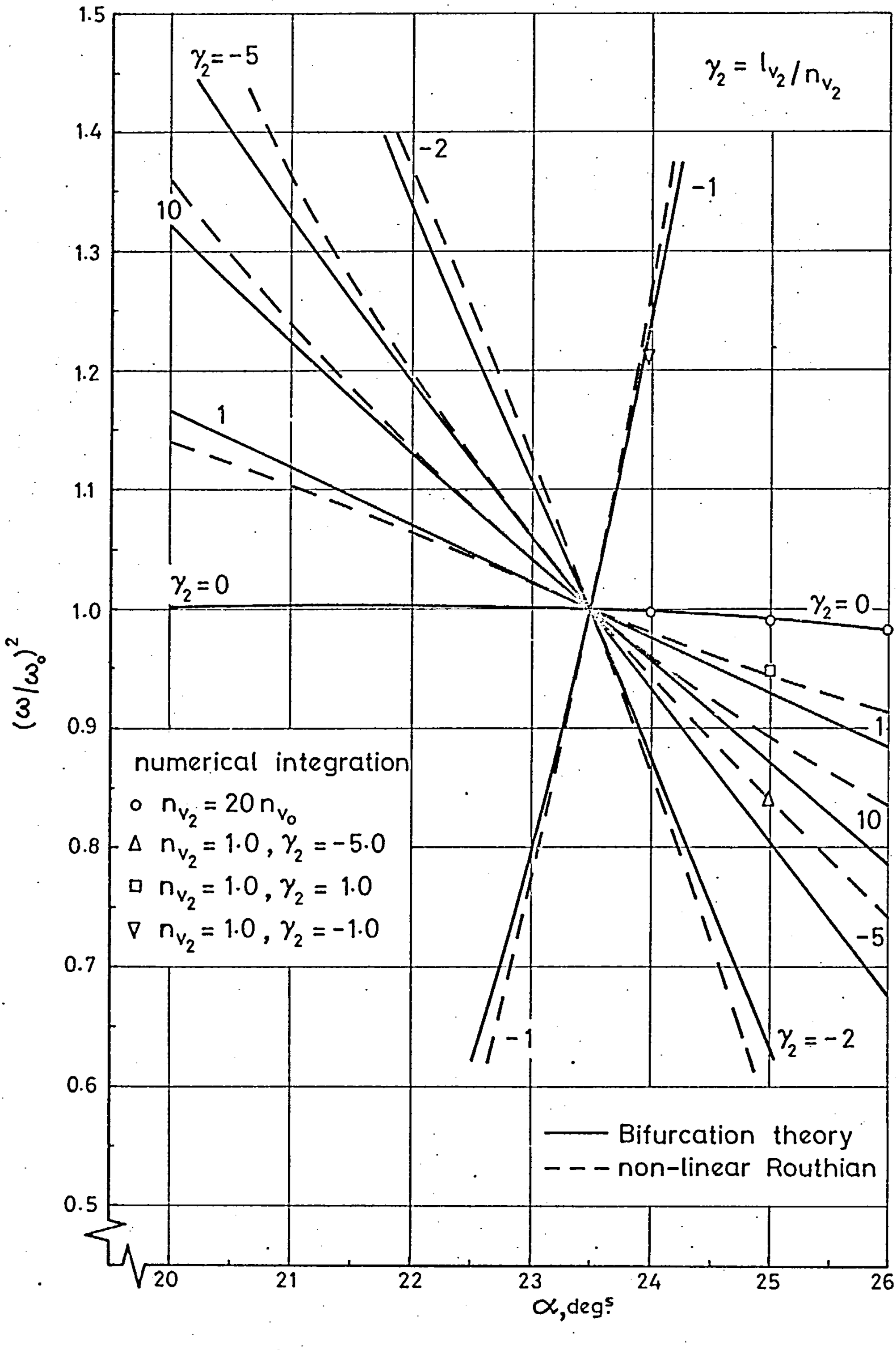

Fig. 4.3 Variation of limit cycle frequency ratio $(\omega/\omega_o)^2$ with incidence for HP 115.

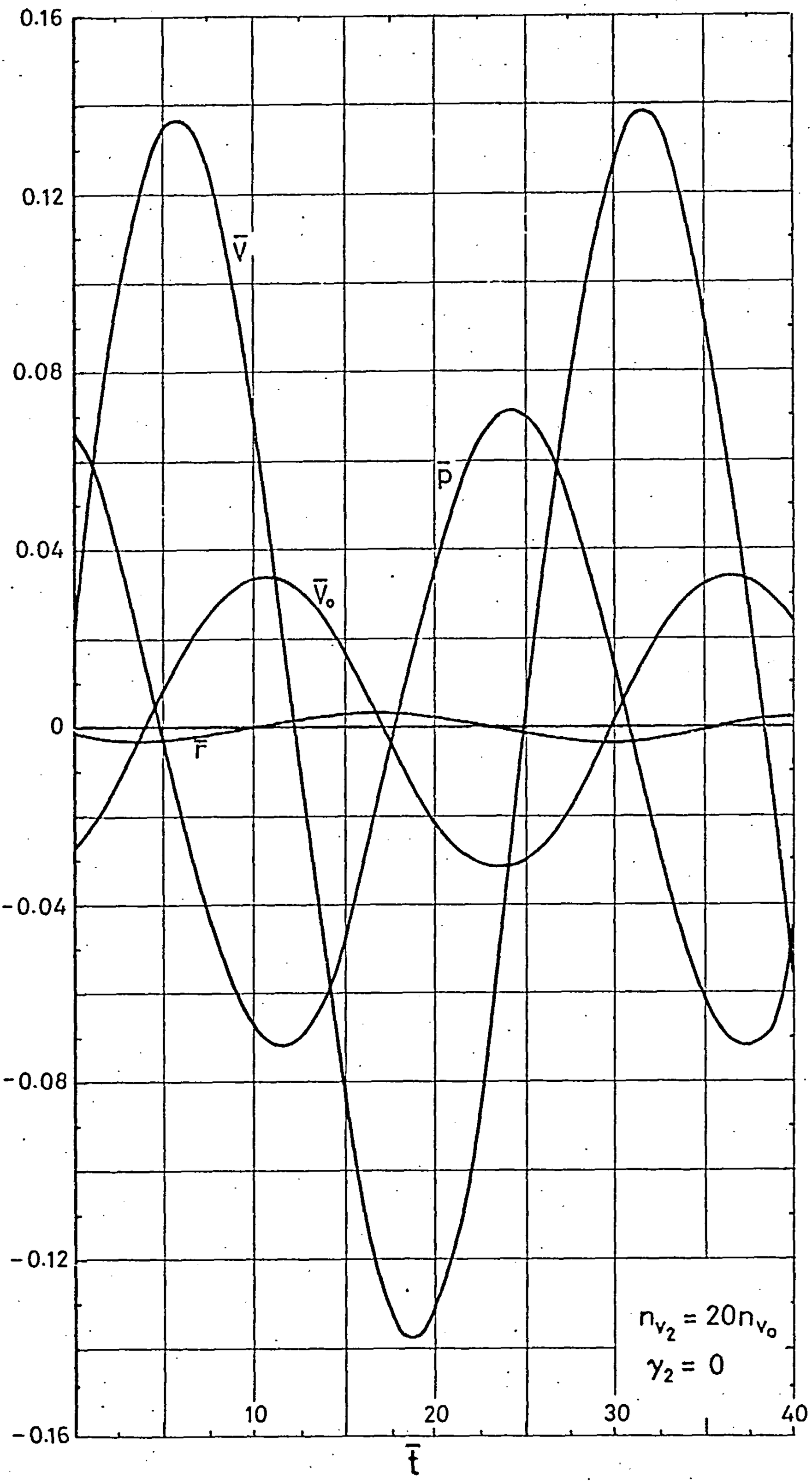

Fig. 4.4 Limit cycle response for HP 115. $\alpha = 26°$.
$(t = 0{\cdot}078\,\bar{t})$

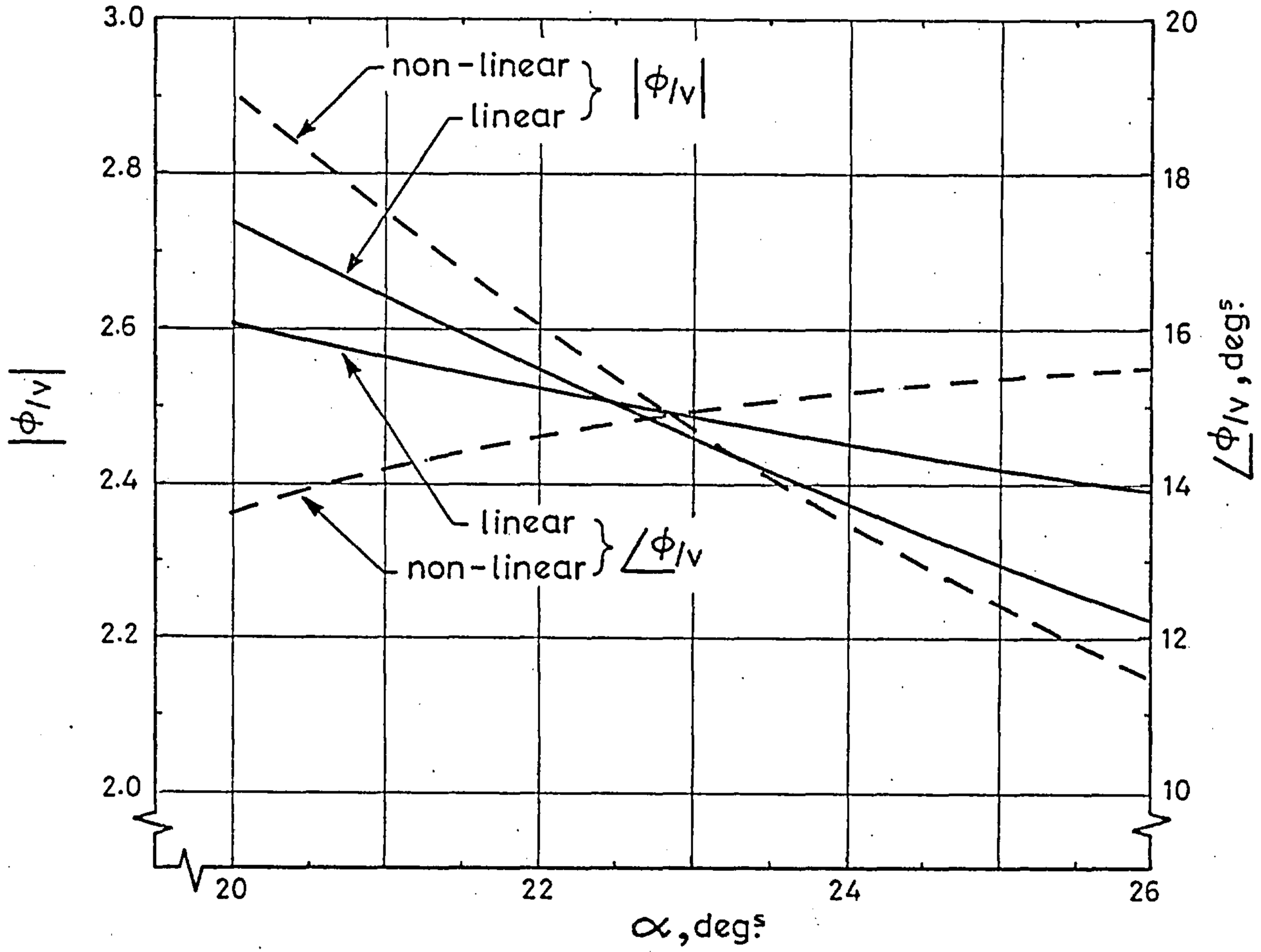

Fig. 4.5 Approximate Dutch Roll ratio for HP 115.

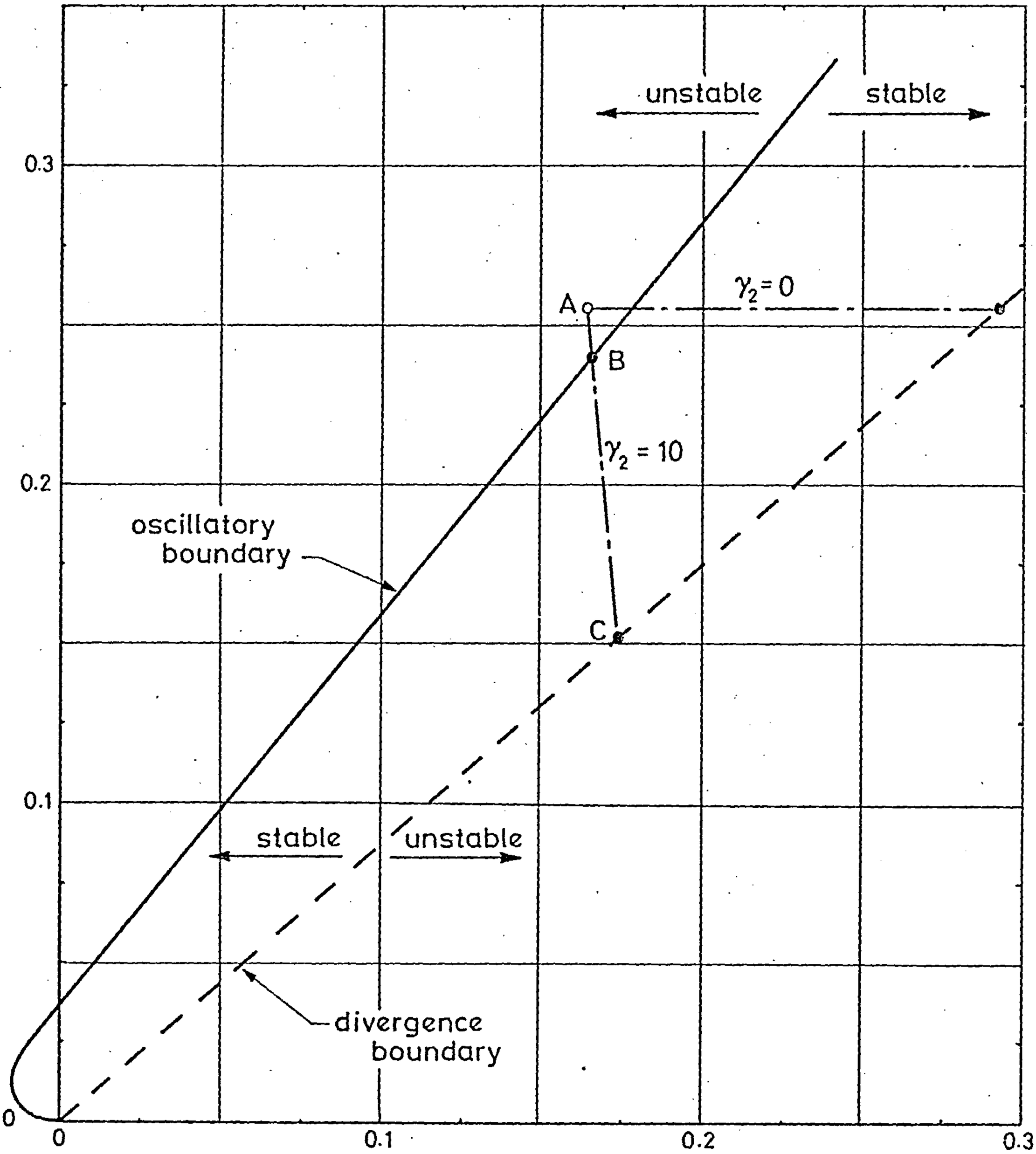

Fig. 4.6 Oscillatory and divergence boundaries for HP 115 at $\alpha = 24°$.

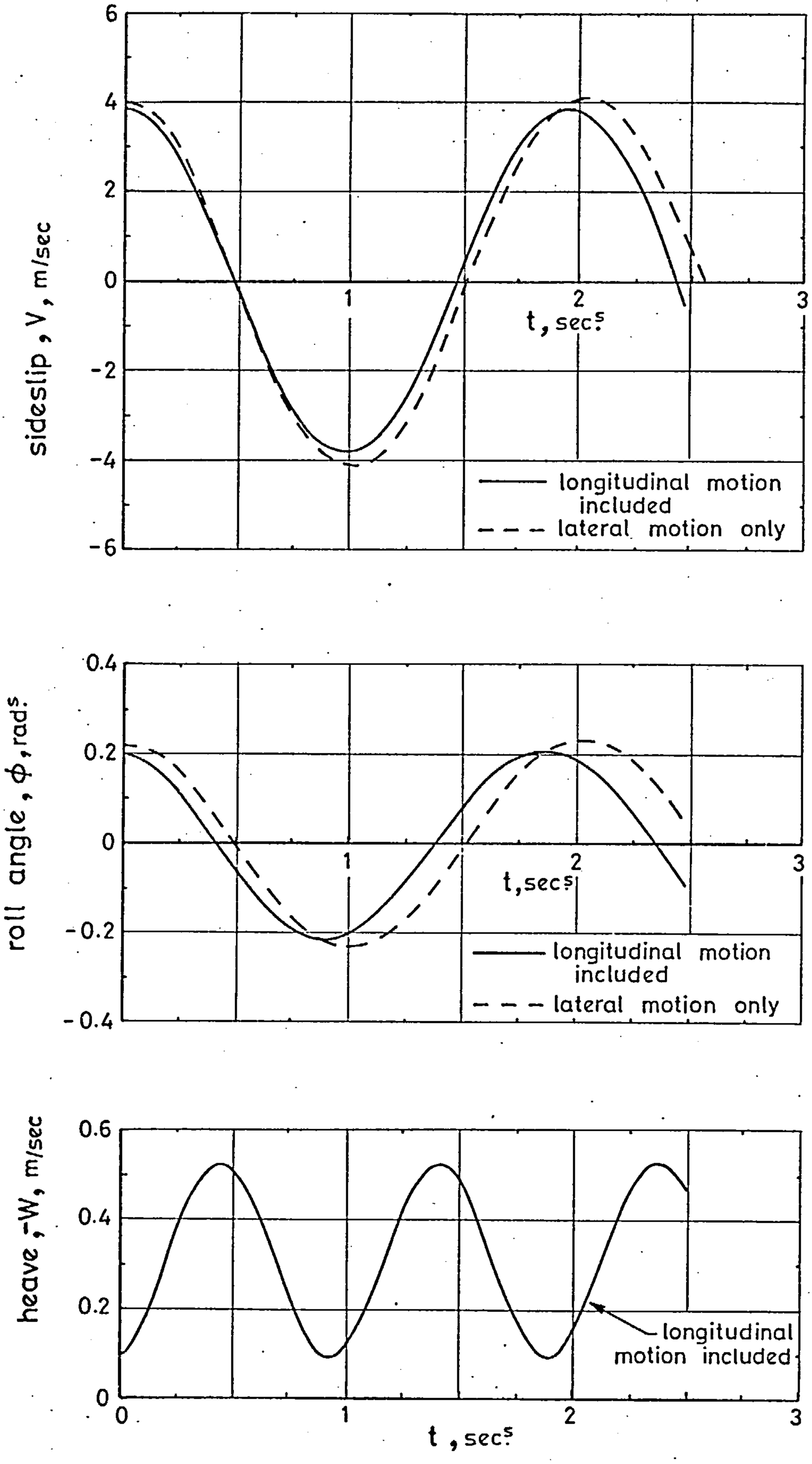

Fig. 4.7 Comparison of numerical solutions for restricted lateral motion and lateral + heave and pitch motions.
($\alpha = 25^\circ$, $V_R = 40.68$ m/sec, $n_{v_2} = 20 \times n_{v_o}$)

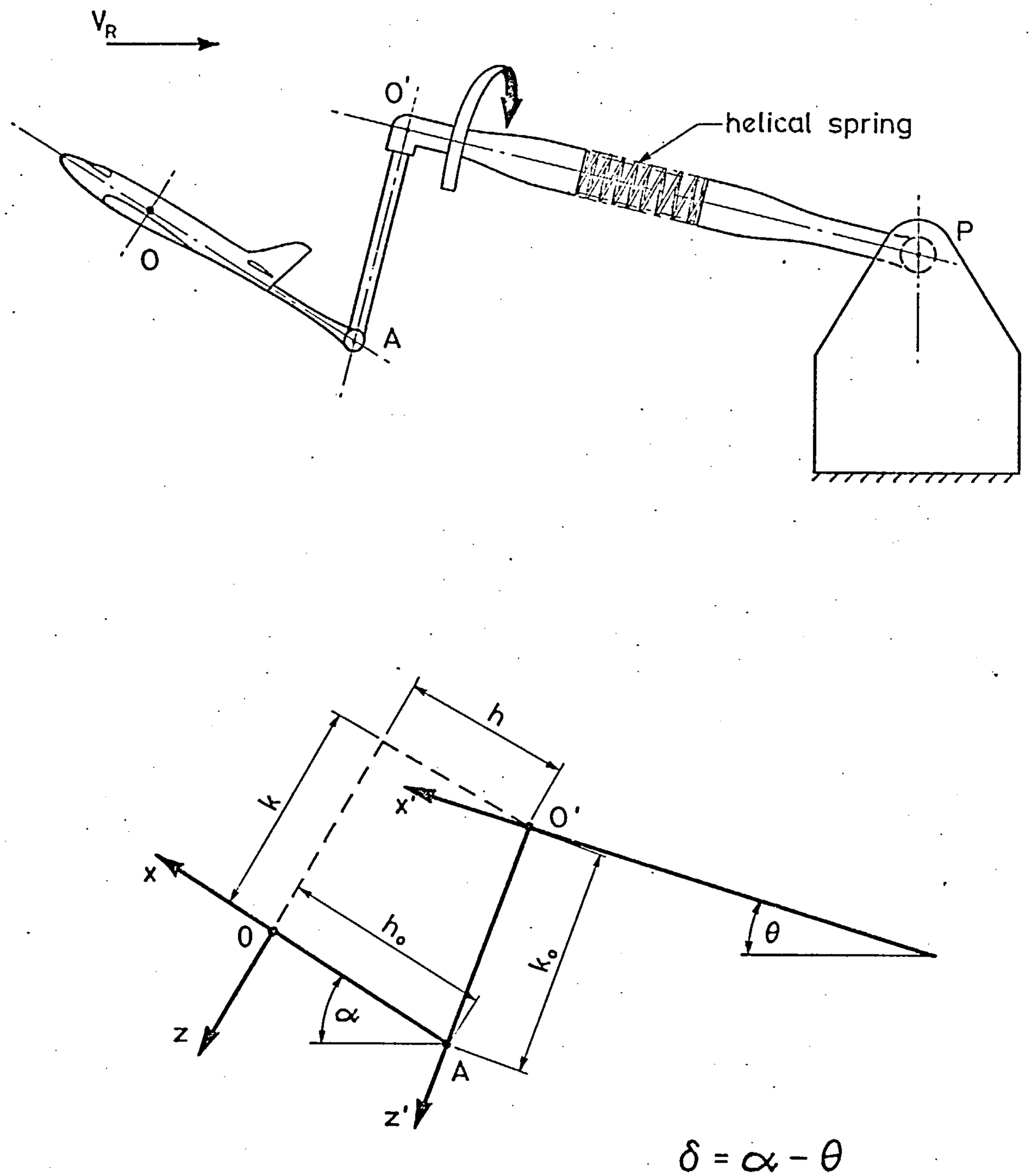

Fig. 5.1 Possible wind tunnel test set up for measuring aerodynamic forces.

Fig. 5.2 Phase plane portraits for the conservative equation $\ddot{y} + c_1 y + c_3 y^3 = 0$

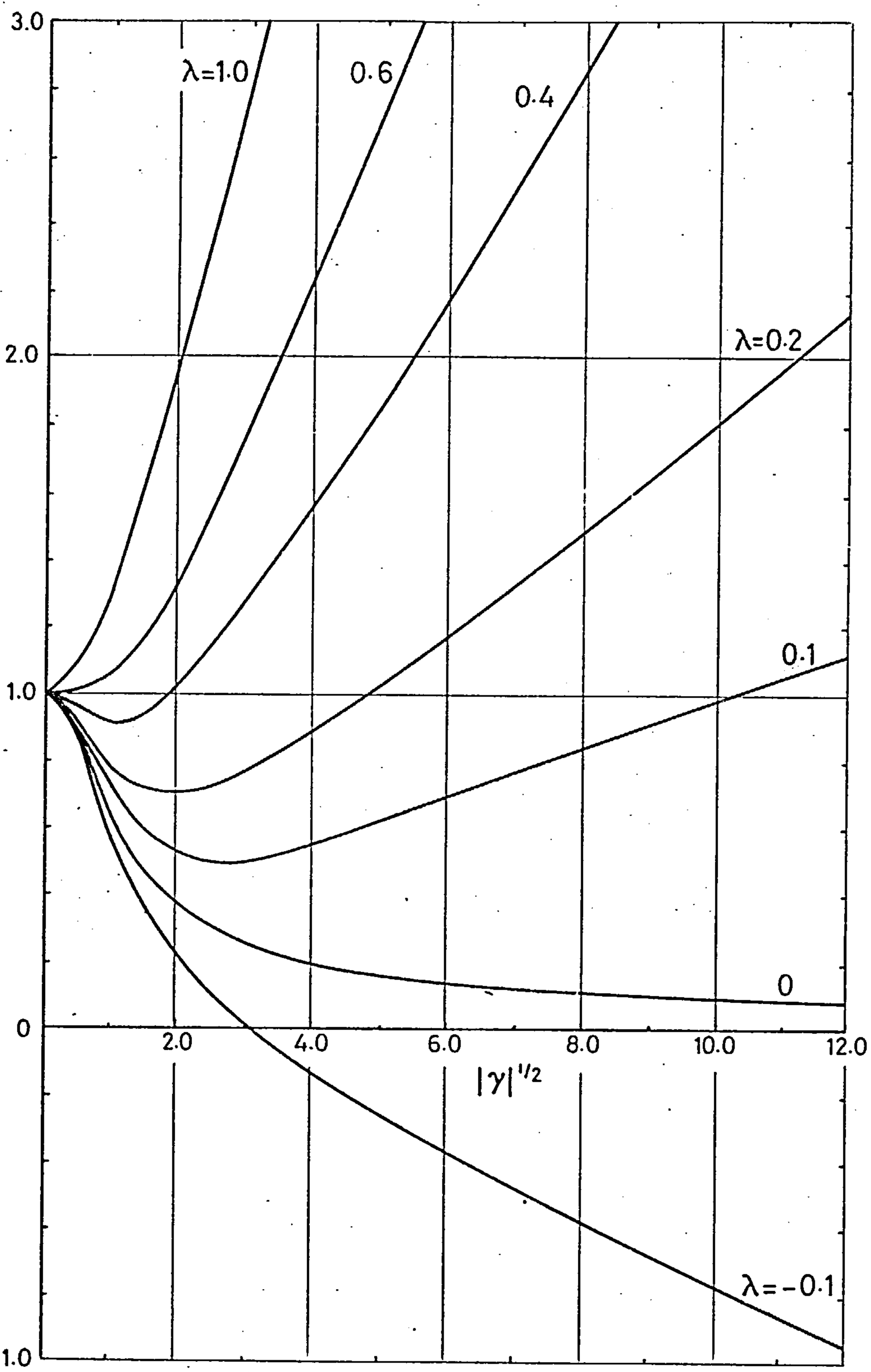

Fig. 5.3 Approximate variation of logarithmic decrement with amplitude according to (5.61). $\left[\gamma = 1/2 . c_3/c_1 (x_{n+1}^2 + x_n^2)\ ;\ \lambda = h_2/4h_0 \left|c_1/c_3\right|\right]$

Case (i) $c_1 > 0\ ;\ c_3 > 0$

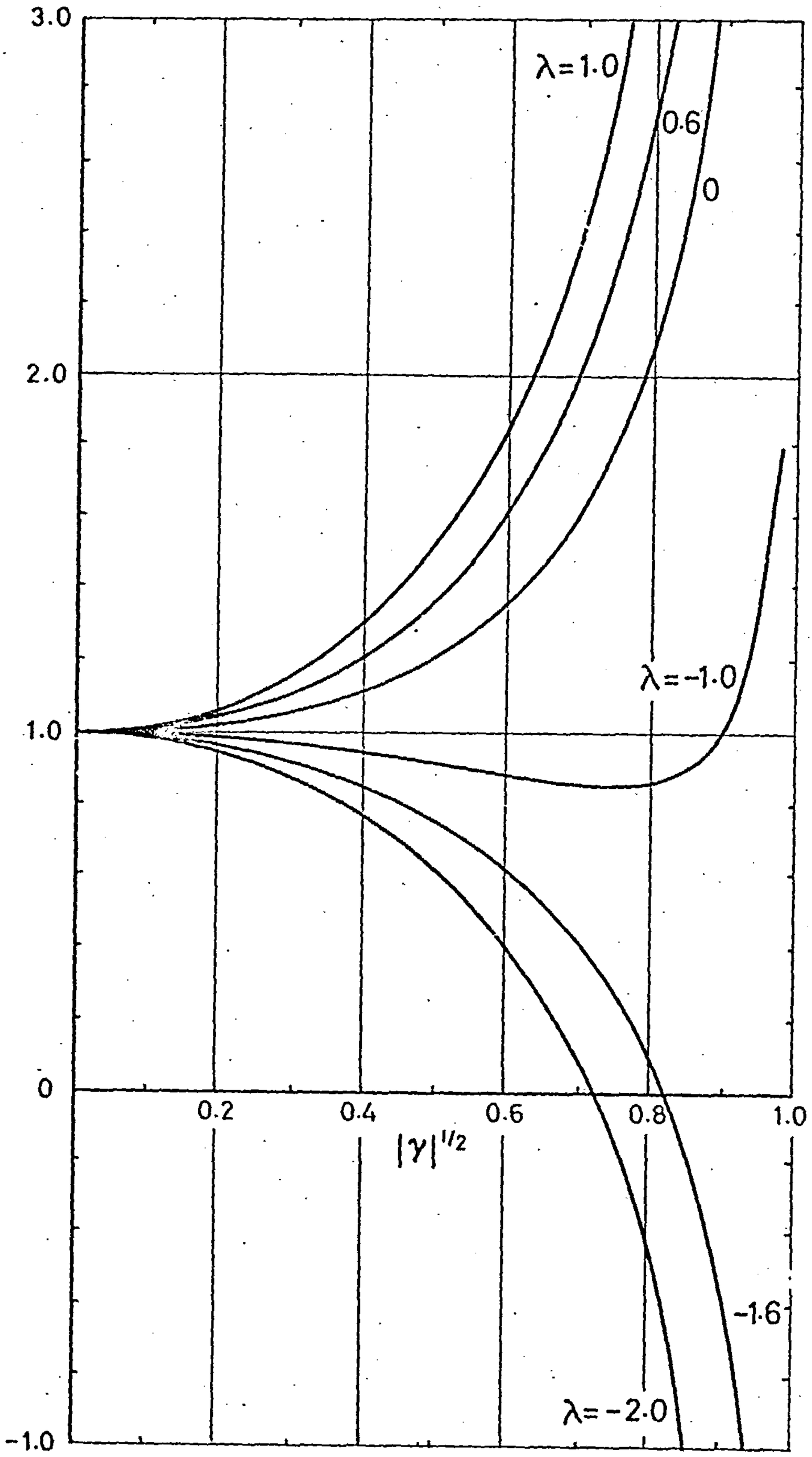

Fig 5·4 Approximate logarithmic decrement for case (ii)
$c_1 \geqslant 0$, $c_3 \leqslant 0$, $-1 \leqslant \gamma \leqslant 0$

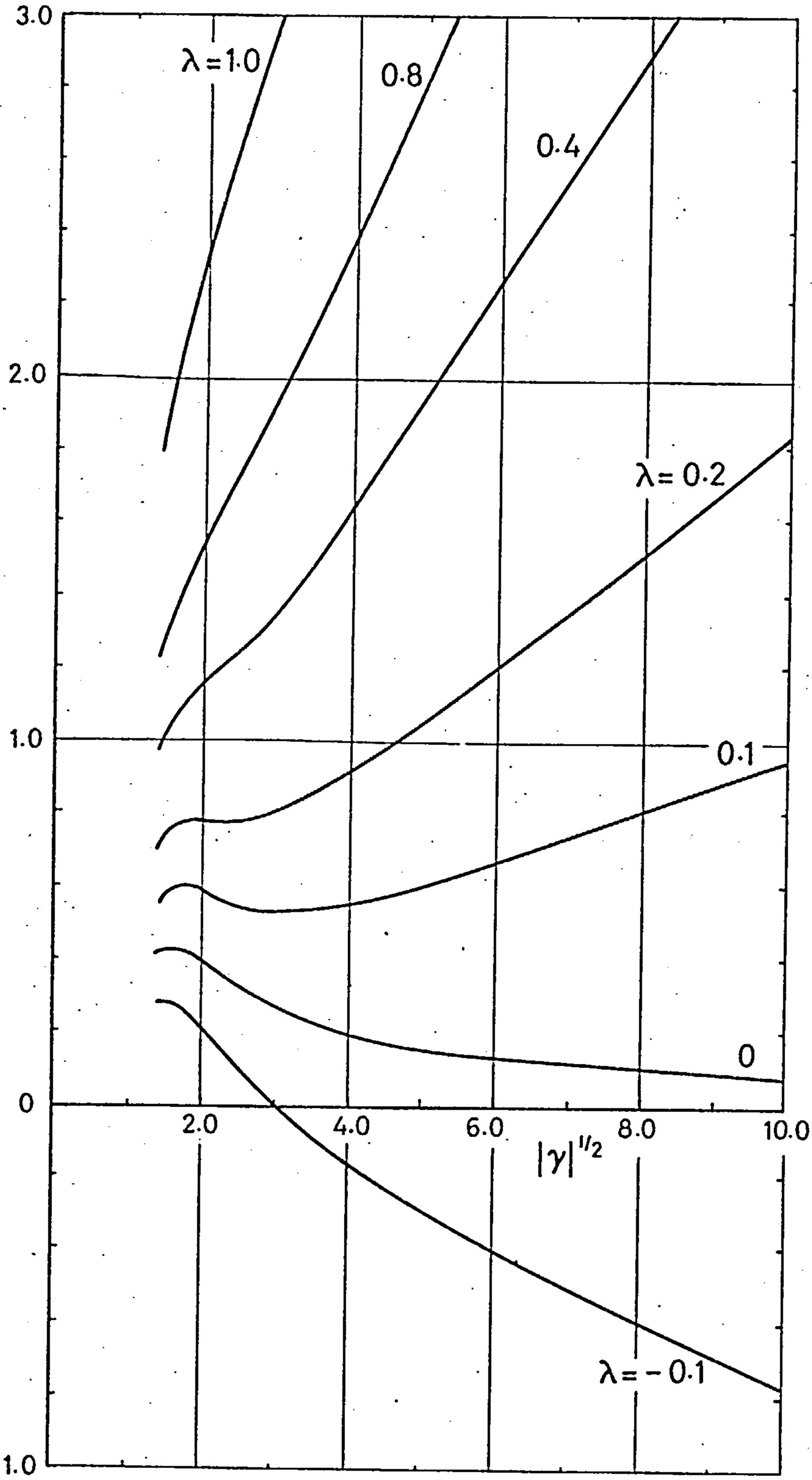

Fig. 5.5 Approximate logarithmic decrement for case (iii)
$c_1 \leqslant 0$, $c_3 \geqslant 0$, $\gamma \leqslant -2$

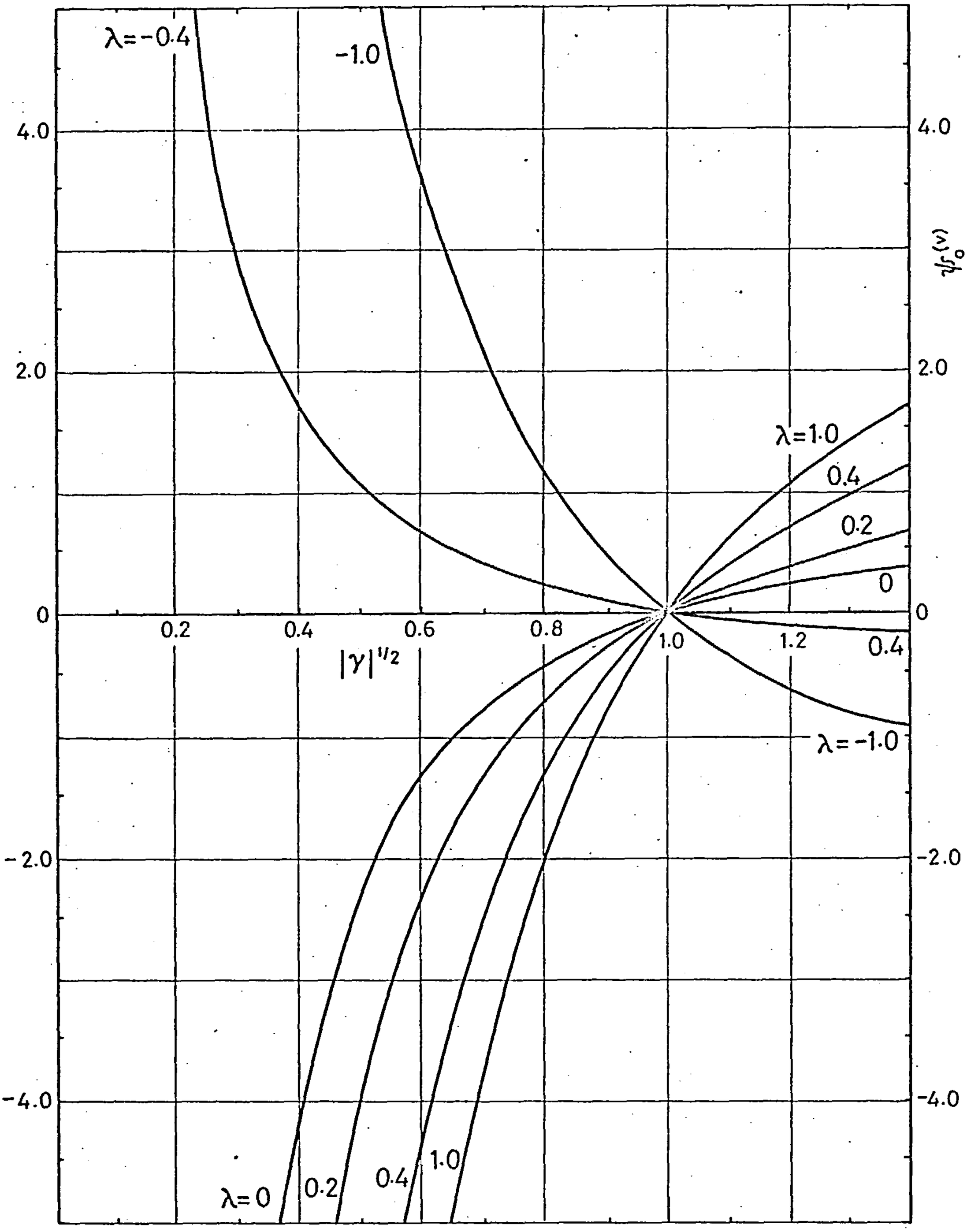

Fig. 5.6 Approximate logarithmic decrement for case (iv)
$c_1 \leqslant 0$, $c_3 \geqslant 0$, $-2 \leqslant \gamma \leqslant 0$

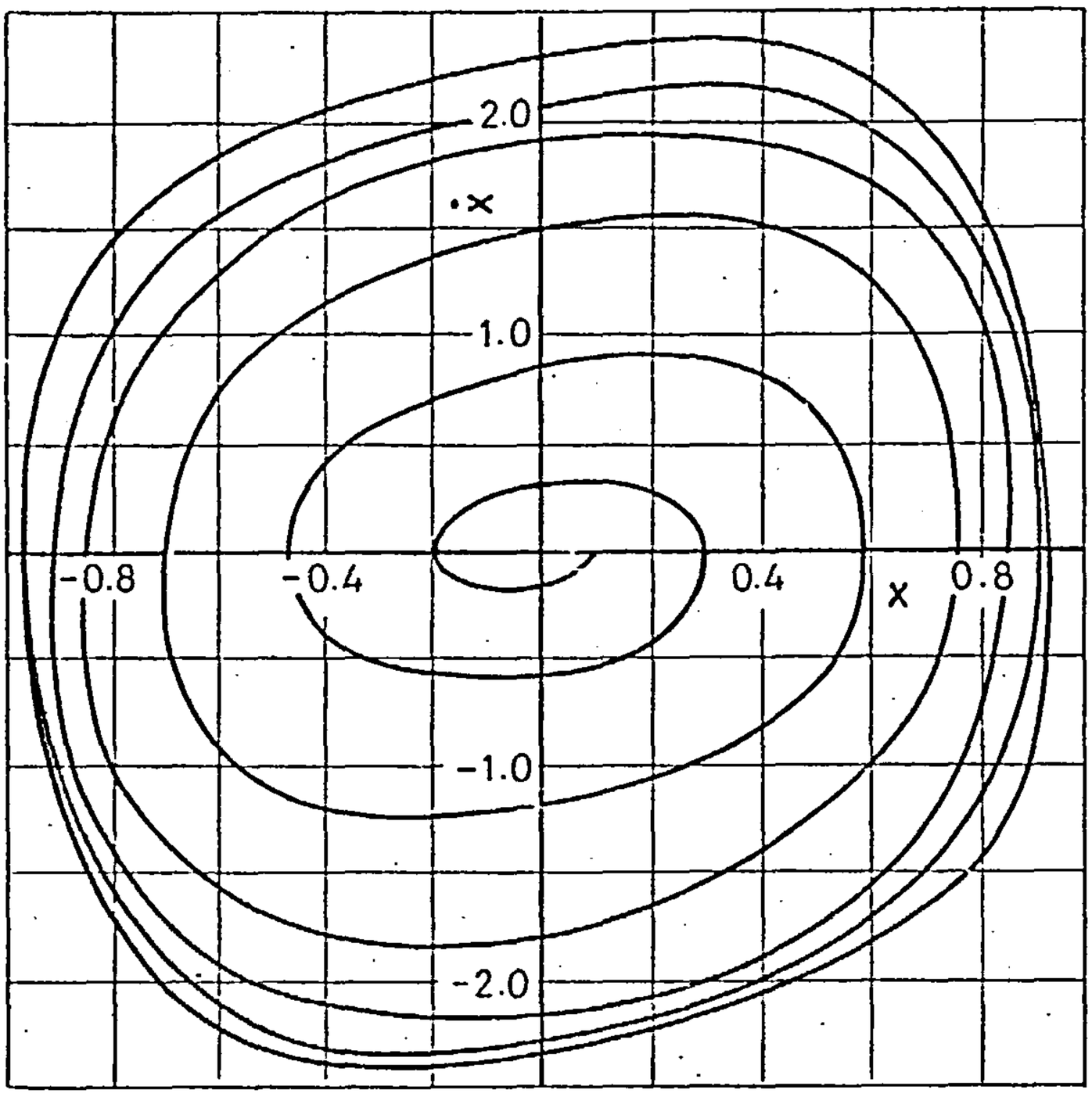

Case (i)

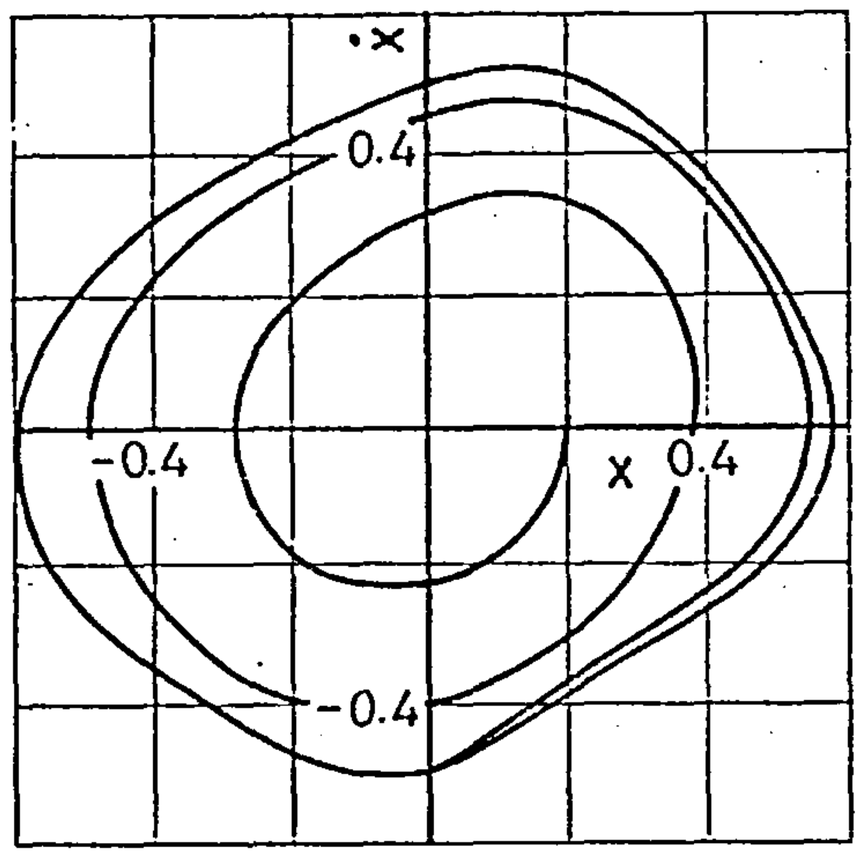

Case (ii)

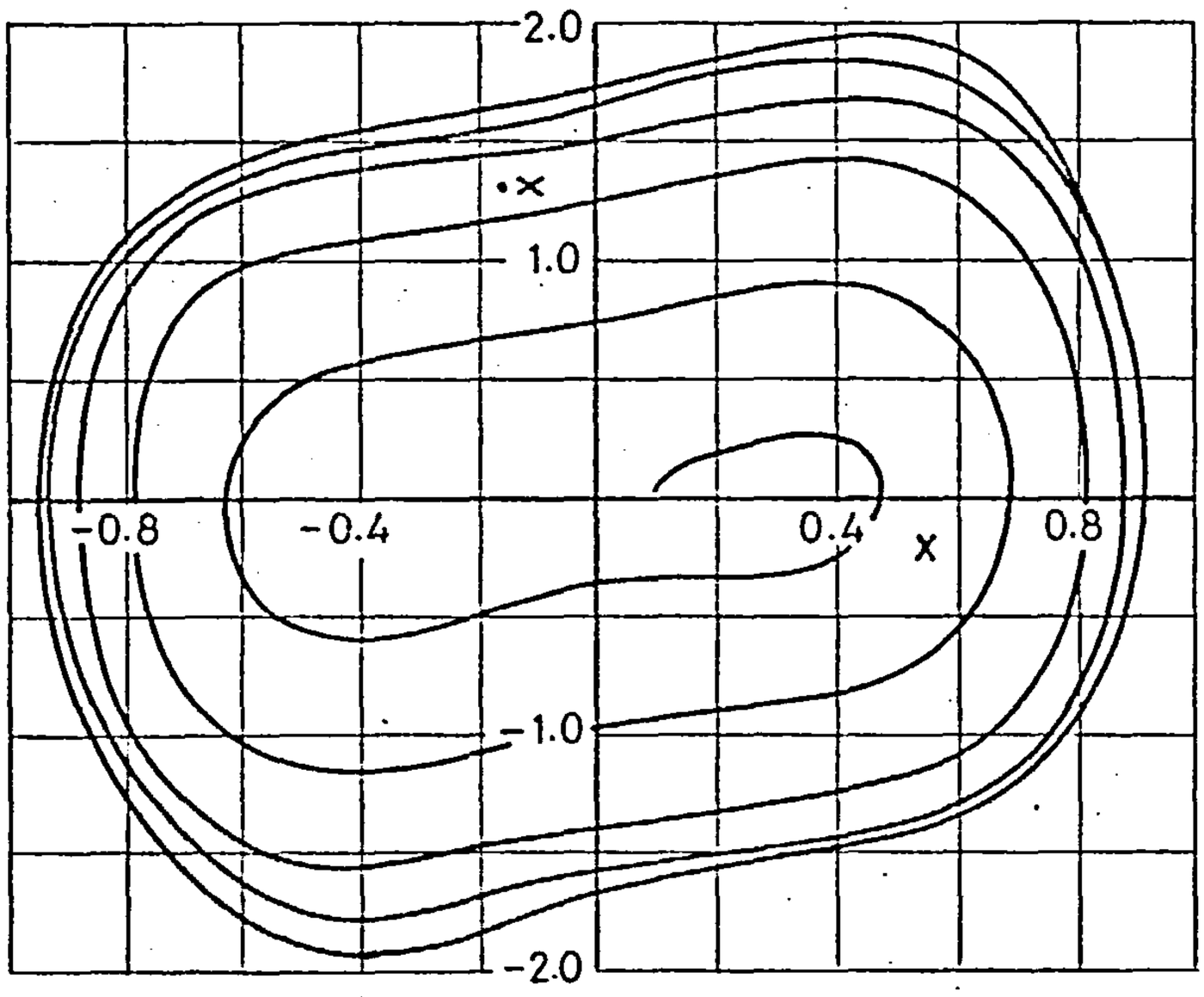

Case (iii)

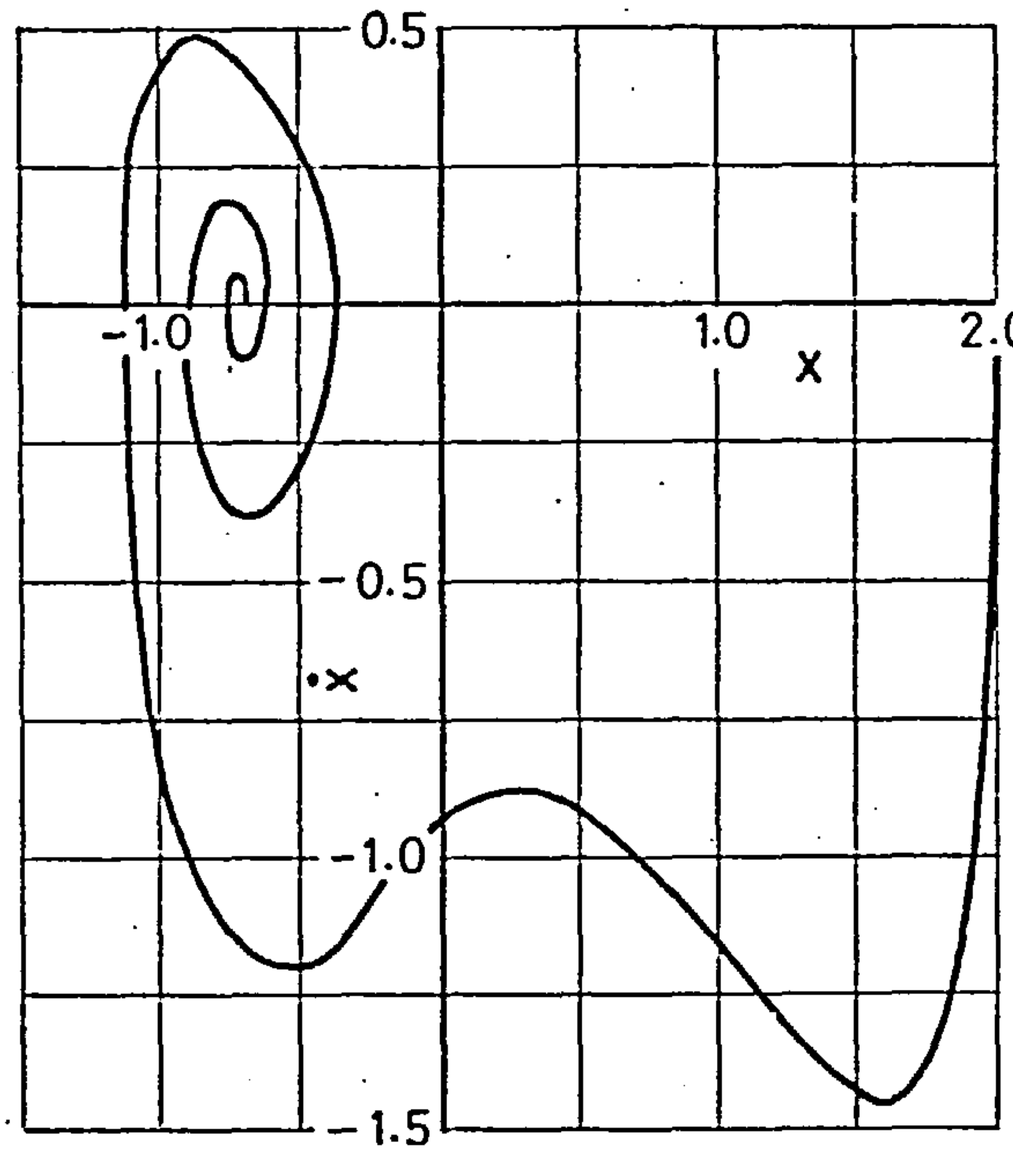

Case (iv)

Fig. 5.7 Phase plane portraits of numerically integrated solutions of (5.51) for the parameter cases shown in Table 5.1

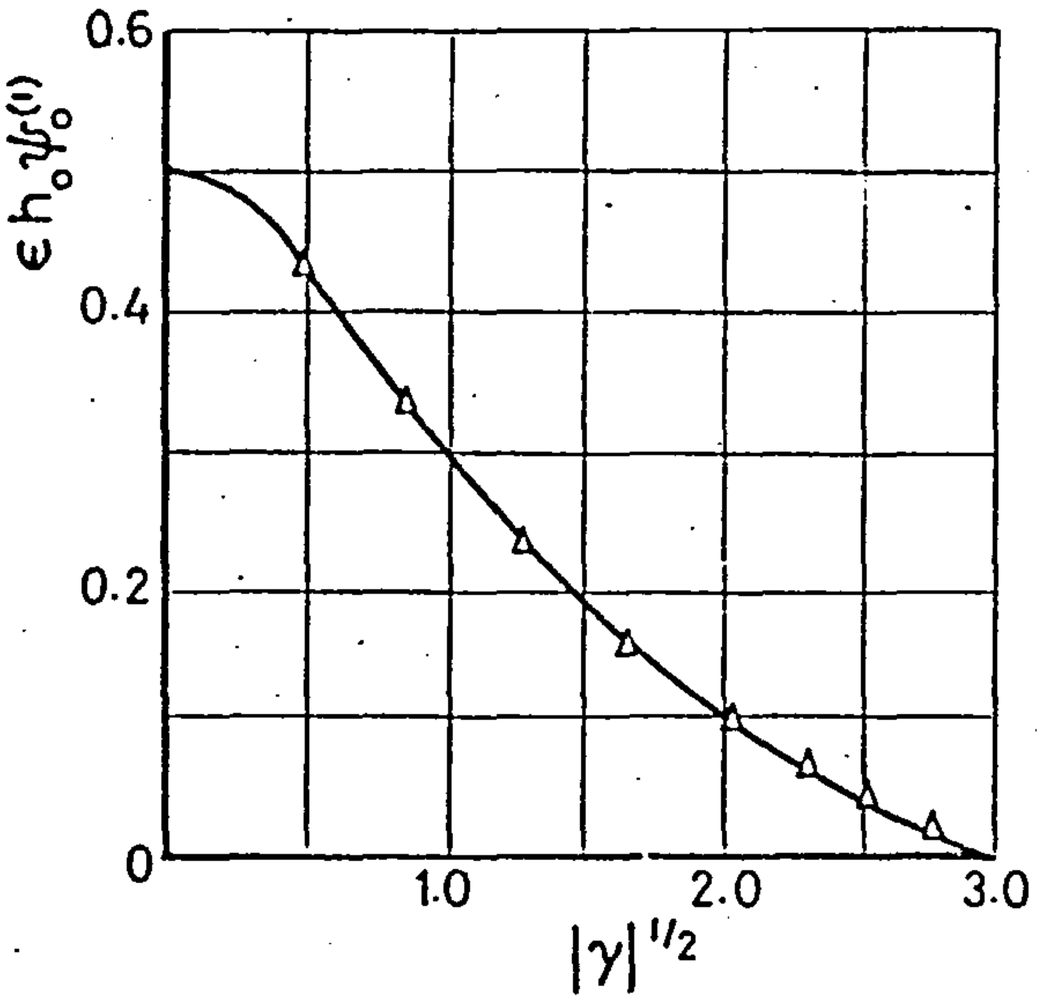

Case (i)

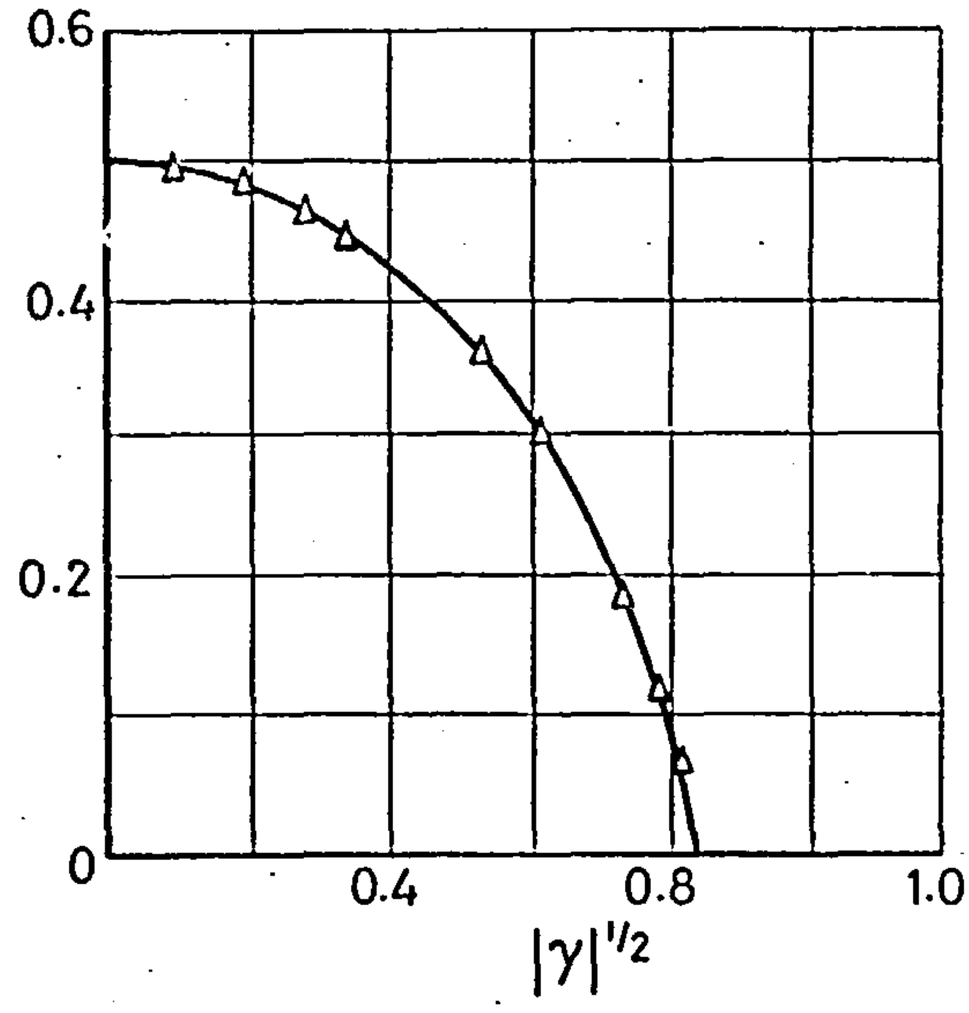

Case (ii)

——— first order approximations

Δ measurements of $2 \log_e |\delta| \frac{|c_1|^{1/2}}{\pi}$

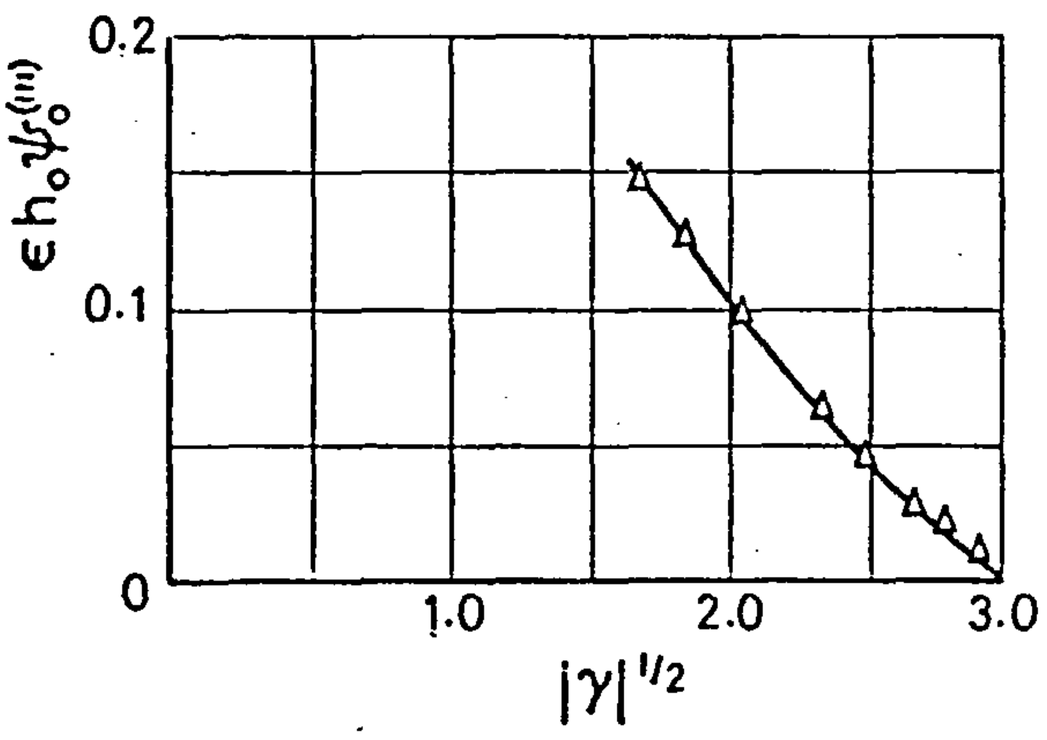

Case (iii)

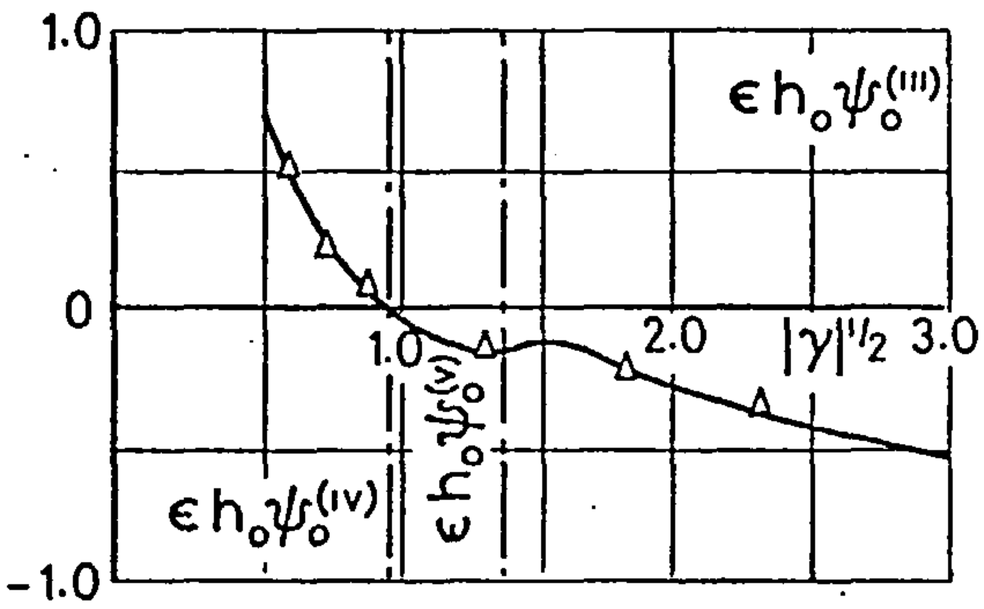

Case (iv)

Fig 5.8 Comparison of measured logarithmic decrement and least squares approximation for cases (i)-(iv) (Fig. 5.7 Table 5.1) respectively.

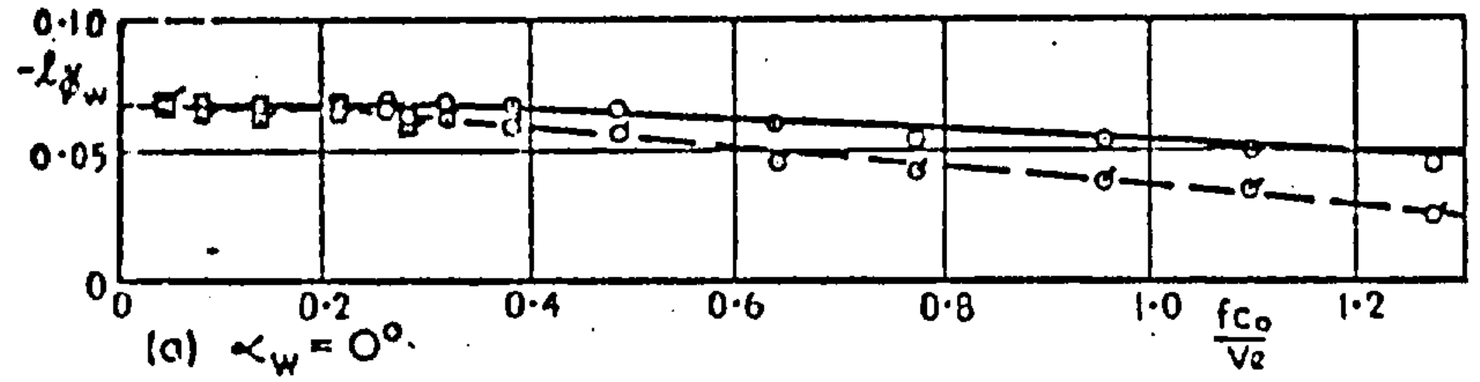

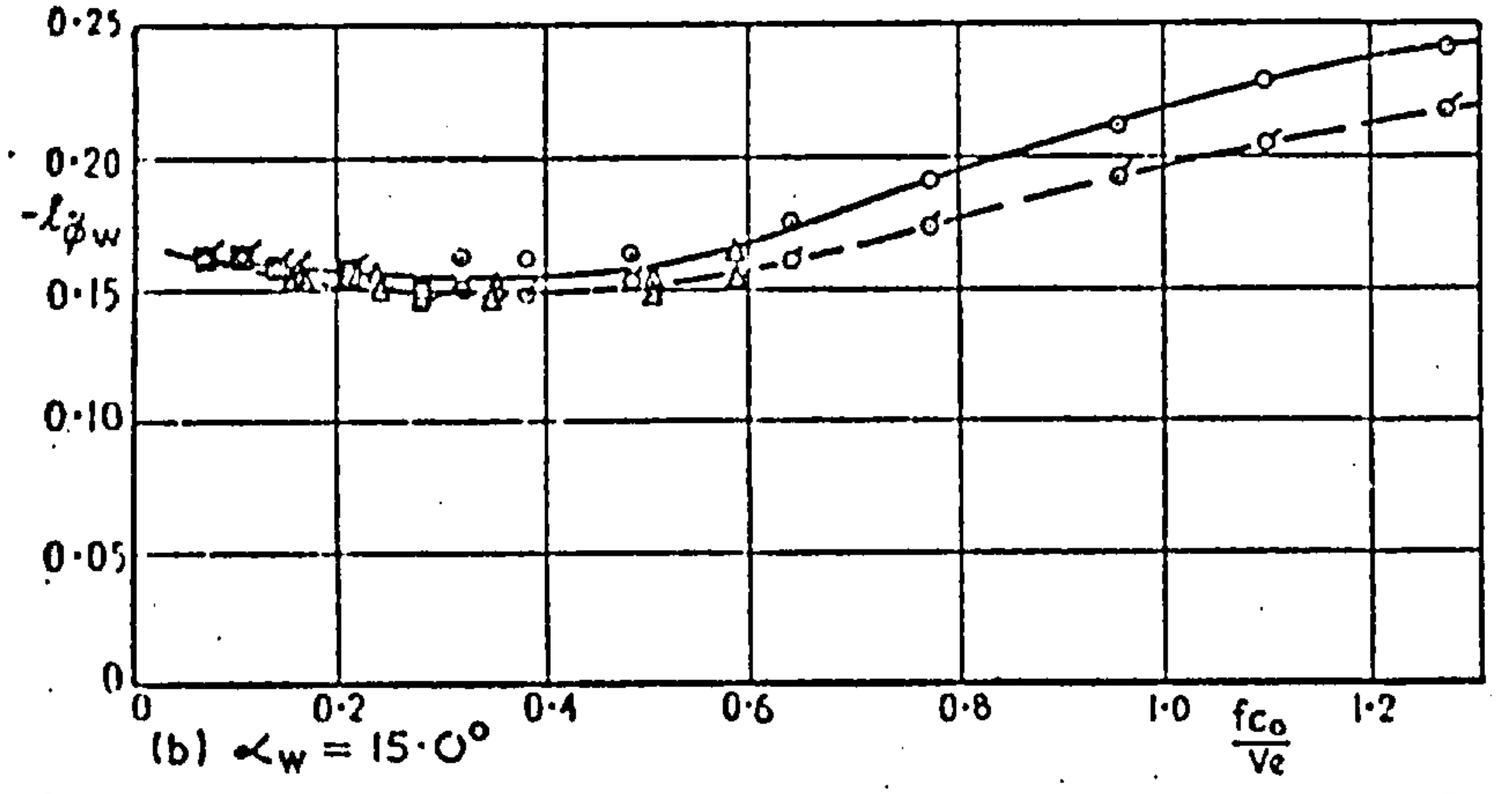

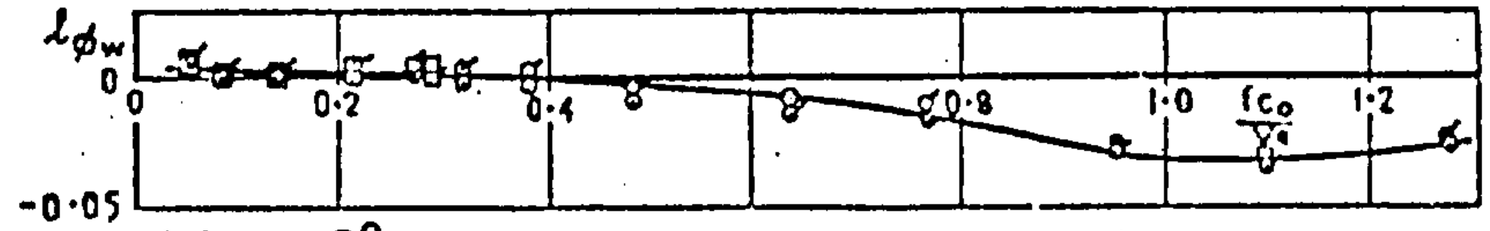

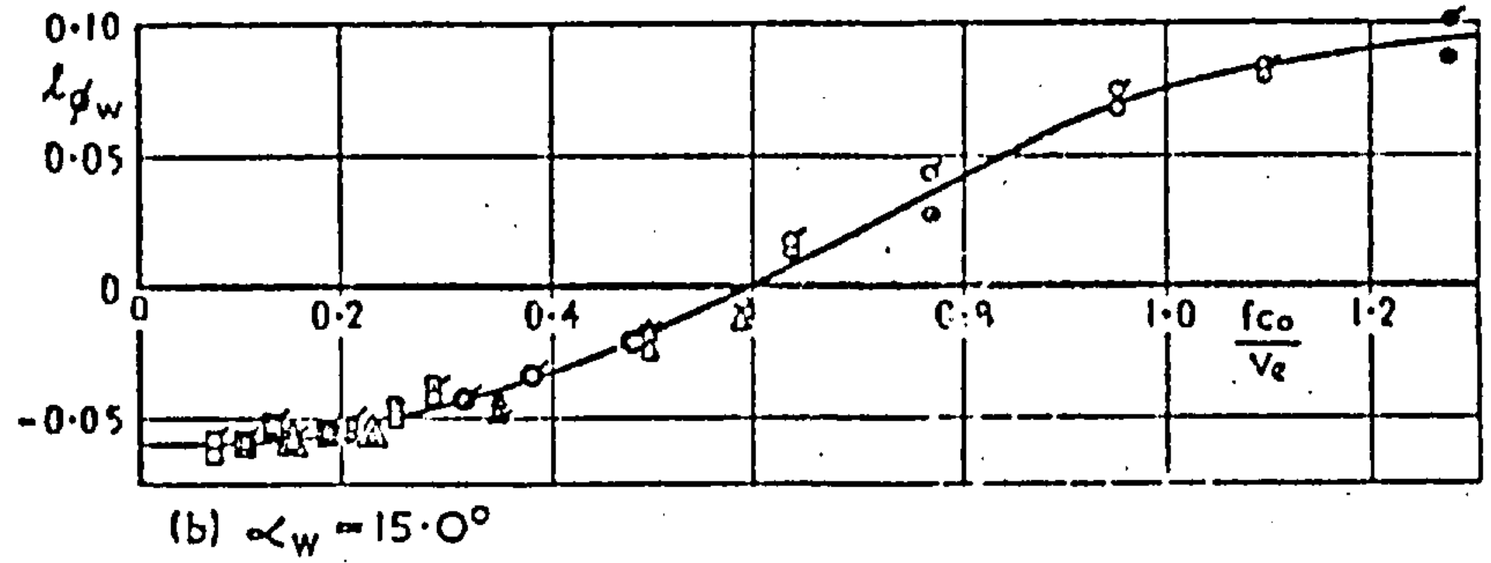

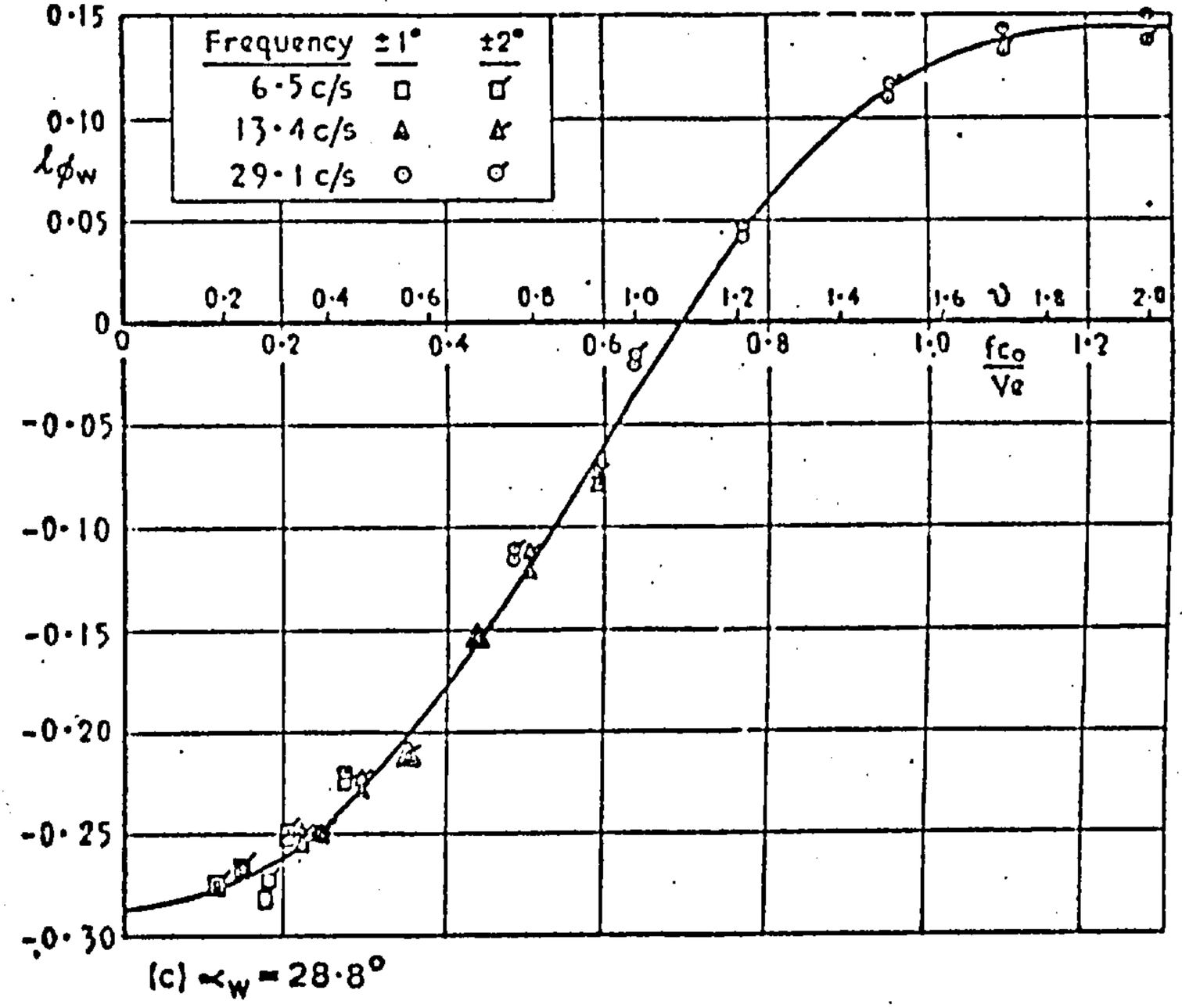

Fig. 5.9 Variation of in phase (l_{ϕ_w}) and quadrature ($l_{\dot{\phi}_w}$) rolling moment components with frequency parameter. (ref. 5.11).

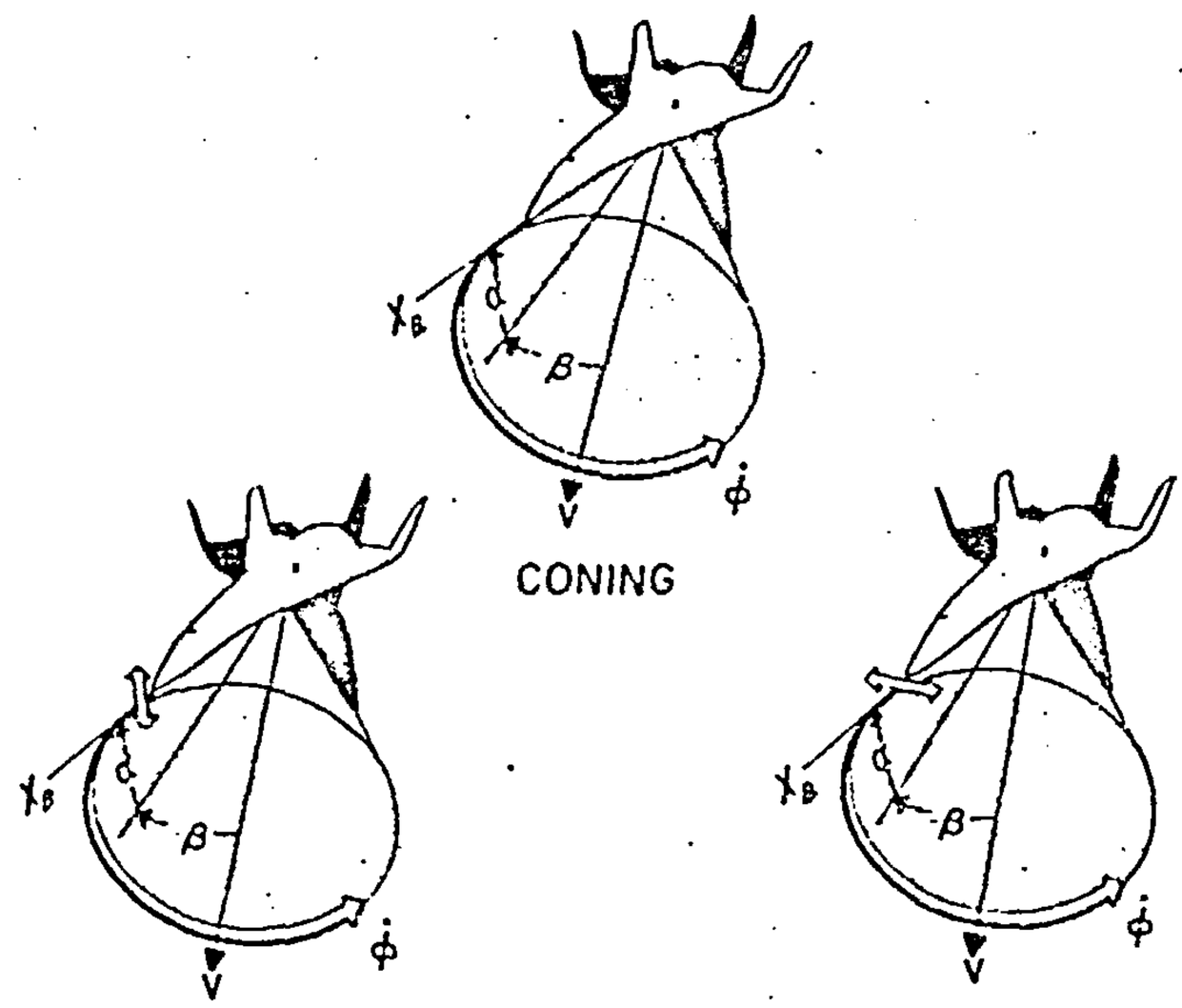

Fig. 5.10 Characteristic motions in the body axis system. Nonlinear dependence on coning rate. (after Tobak ref. 5.17)